UNIVERSIDAD DE GRANADA

IN-USE STABILITY OF THE THERAPEUTIC MONOCLONAL ANTIBODIES TOCILIZUMAB, NIVOLUMAB AND PEMBROLIZUMAB: COMPREHENSIVE ANALYSIS OF PHYSICOCHEMICAL PARAMETERS AND FUNCTIONALITY

TESIS DOCTORAL

Programa de Doctorado en Farmacia

Facultad de Ciencias

Departamento de Química Analítica

Anabel Torrente López

Granada 2023

Editor: Universidad de Granada. Tesis Doctorales
Autor: Anabel Torrente López
ISBN: 978-84-1195-110-4
URI: https://hdl.handle.net/10481/85770

UNIVERSIDAD DE GRANADA

Dpto. de Química Analítica
Prof. Fermín Capitán García

IN-USE STABILITY OF THE THERAPEUTIC MONOCLONAL ANTIBODIES TOCILIZUMAB, NIVOLUMAB AND PEMBROLIZUMAB: COMPREHENSIVE ANALYSIS OF PHYSICOCHEMICAL PARAMETERS AND FUNCTIONALITY

ESTABILIDAD EN USO DE LOS ANTICUERPOS MONOCLONALES TERAPÉUTICOS TOCILIZUMAB, NIVOLUMAB Y PEMBROLIZUMAB: ANÁLISIS COMPRENSIVO DE PARÁMETROS FISICOQUÍMICOS Y FUNCIONALIDAD

Memoria presentada por Anabel Torrente López, Graduada en Farmacia, para optar al título de Doctora por la Universidad de Granada dentro del Programa de Doctorado en Farmacia

Granada, noviembre 2023

Fdo. Anabel Torrente López
Dpto. de Química Analítica. Facultad de Ciencias.
Universidad de Granada

Vº Bº de las directoras

Fdo. Dra. Natalia África Navas Iglesias

Catedrática del Dpto. de Química Analítica
Facultad de Ciencias
Universidad de Granada

Fdo. Dra. Adolfina Ruiz Martínez

Catedrática del Dpto. de Farmacia y Tecnología Farmacéutica
Facultad de Farmacia
Universidad de Granada

UNIVERSIDAD DE GRANADA

Dpto. de Química Analítica
Prof. Fermín Capitán García

La doctoranda / The doctoral candidate **Anabel Torrente López** y las directoras de la Tesis / and the Thesis supervisors **Natalia África Navas Iglesias** y / and **Adolfina Ruiz Martínez**.

Garantizamos, al firmar esta Tesis doctoral, que el trabajo ha sido realizado por la doctoranda bajo la dirección de las directoras de la tesis y hasta donde nuestro conocimiento alcanza, en la realización del trabajo, se han respetado los derechos de otros autores a ser citados, cuando se han utilizado sus resultados o publicaciones.

Guarantee, by signing this doctoral thesis, that the work has been done by the doctoral candidate under the direction of the thesis supervisors and, as far as our knowledge reaches, in the performance of the work, the right of other authors has been respected by citing their results or publications when they have been used.

Granada, septiembre 2023

Dra. Natalia A. Navas Iglesias	Dra. Adolfina Ruiz Martínez	Anabel Torrente López
Thesis supervisor	*Thesis supervisor*	*Doctoral candidate*

Part of this PhD Thesis has been developed during an international research stay period (3 months) in **Coriolis Pharma Research GmbH, Martinsried, Munich, Germany**. The name of the project carried out is 'Optimization of the ReFOLD Assay for Protein Stability Prediction', and the results are shown in the *Chapter 6* of this PhD Thesis. This international research stay was funded by an **EMBO Scientific Exchange Grant** (number 9629).

Supervisors of the International Research Stay

Dr. Andrea Hawe and Dr. Constanze Helbig

Coriolis Pharma Research GmbH

Martinsried, Munich, Germany

ÍNDICE

ACRÓNIMOS

ACRÓNIMOS

ACG	Arteritis de células gigantes
ADN	Ácido desoxirribonucleico
AEMPS	Agencia Española de Medicamentos y Productos Sanitarios
AIJp	Artritis idiopática juvenil poliarticular
AIJs	Artritis idiopática juvenil sistémica
AINEs	Antiinflamatorios no esteroideos
AR	Artritis reumatoide
Asn	Asparagina
Asp	Aspartato
ATP	Adenosín trifosfato
AXC	Cromatografía de intercambio aniónico (*anionic exchange chromatography*)
CD	Dicroísmo circular (*circular dichroism*)
CDR	Región determinante complementaria (*Complementary Determining Region*)
CFG	Consorcio de glicómica funcional
CH_1	Región constante de la cadena pesada (primer dominio)
CH_2	Región constante de la cadena pesada (segundo dominio)
CH_3	Región constante de la cadena pesada (tercer dominio)
CHO	Células de ovario de hámster chino (*Chinese hamster ovary*)
CL	Región constante de la cadena ligera
COVID-19	Enfermedad por coronavirus 2019
CQA	Atributo crítico de la calidad (*Critical Quality Attribute*)
CTLA-4	Antígeno 4 de linfocitos T citotóxicos
CXC	Cromatografía de intercambio catiónico (*cationic exchange chromatography*)
DLS	Dispersión de luz dinámica (*dynamic light scattering*)

ELISA	Ensayo por inmunoadsorción ligado a enzimas (*enzyme linked immunosorbent assay*)
EMA	Agencia Europea de Medicamentos (*European Medicines Agency*)
FA	Ácido fórmico (*formic acid*)
Fab	Región de reconocimiento y unión a antígenos
FAMEs	Fármacos antirreumáticos modificadores de la enfermedad
Fc	Región cristalizable
FDA	Administración de Alimentos y Medicamentos de Estados Unidos (*Food and Drug Administration*)
GalNAc	N-acetilgalactosamina
Gla	ɣ-carboxiglutamato
Gln	Glutamina
Glu	Glutamato
HPLC	Cromatografía líquida de alta resolución (h*igh performance liquid chromatography*)
ICH	Conferencia Internacional de Armonización (*International Conference on Harmonization*)
ICI	Inhibidores de puntos de control inmunitario
IgG	Inmunoglobulina de tipo G
IL	Interleucina
INN	Denominación común internacional (*International Nonproprietary Name*)
IT-FS	Fluorescencia intrínseca de triptófanos (i*ntrinsic tryptophan fluorescence spectroscopy*)
IXC	Cromatografía de intercambio iónico (*ionic exchange chromatography*)
JCR	*Journal Citation Reports*
Lys	Lisina
mAb	Anticuerpo monoclonal (*monoclonal antibody*)
Met	Metionina
MS	Espectrometría de masas (*mass spectrometry*)

NRMSD	Raíz de la desviación cuadrática media normalizada (*normalised root mean squared deviation*)
OMS	Organización Mundial de la Salud
OPD	Dihidrocloruro de o-fenilendiamina
PD-1	Proteína-1 de muerte celular programada (p*rogrammed cell death protein-1*)
PD-L	Ligando de muerte celular programada (*Programmed death ligand-1*)
Pro	Prolina
PTM	Modificación postraduccional (*post-translational modification*)
QbD	Diseño de calidad farmacéutica (*quality by design*)
RPC	Cromatografía de fase inversa (*reverse phase chromatography*)
SARS-CoV-2	Síndrome respiratorio agudo severo por coronavirus 2
SEC	Cromatografía de exclusión molecular (*size exclusion chromatography*)
Ser	Serina
TCZ	Tocilizumab
TFA	Ácido trifluoroacético (*trifluoroacetic acid*)
Thr	Treonina
TNF	Factor de necrosis tumoral (*tumor necrosis factor*)
Tyr	Tirosina
UHPLC	Cromatografía líquida de ultra alta resolución (*ultra high performance liquid chromatography*)
UV/Vis	Ultravioleta/Visible
VH	Región variable de la cadena pesada
VL	Región variable de la cadena ligera

HIPÓTESIS Y OBJETIVOS/ HYPOTHESIS AND AIMS

HIPÓTESIS Y OBJETIVOS

Los anticuerpos monoclonales (mAbs) son biofármacos ampliamente utilizados en terapias oncológicas y autoinmunes. Estos han supuesto un avance en el ámbito farmacéutico y han permitido reducir la mortalidad y morbilidad de los pacientes. La mayor parte del consumo de los mAbs terapéuticos tiene lugar en el ámbito hospitalario. Estos medicamentos de origen proteico se degradan fácilmente. Dependiendo del cambio producido, este puede afectar o no a su eficacia y seguridad como medicamento. La manipulación rutinaria hospitalaria de los mismos puede comprometer esta estabilidad, produciéndose cambios estructurales que pueden quedar inadvertidos afectando a dicha seguridad y eficacia en sus correspondientes preparaciones farmacéuticas de uso clínico.

Por tanto, existe una gran demanda de herramientas de análisis que permitan evaluar la estabilidad de este tipo de medicamentos biotecnológicos en condiciones rutinarias de uso clínico. Este tipo de datos son de gran interés actualmente para los sistemas sanitarios de salud, tanto públicos como privados. De este modo, la puesta a punto de métodos y estrategias de análisis para la caracterización fisicoquímica y funcional de mAbs terapéuticos permitirá abordar estudios de estabilidad de los mismos con robustez y garantía de seguridad y eficacia

HYPOTHESIS AND AIMS

Monoclonal antibodies (mAbs) are biopharmaceuticals widely used in oncology and autoimmune therapies. They have been a breakthrough in the pharmaceutical field and have led to a reduction in patient mortality and morbidity. Most of the consumption of therapeutic mAbs takes place in the hospital setting. These protein-based drugs are easily degraded. Depending on the change that occurs, this may or may not affect their efficacy and safety as a medicine. Routine hospital handling of these drugs can compromise this stability, leading to structural changes that may go unnoticed and affect the safety and efficacy of their corresponding pharmaceutical preparations for clinical use.

Therefore, there is a great demand for analytical tools to assess the stability of these types of biotechnological medicinal products under routine clinical use conditions. This type of data is currently of great interest to both public and private health care systems. Thus, the development of analytical methods and strategies for the physicochemical and functional characterisation of therapeutic mAbs will make it possible to carry out stability studies of these drugs with robustness and a guarantee of safety and efficacy for the patient, in terms of their routine handling in hospitals.

para el paciente, en cuanto a la manipulación rutinaria de los mismos en los hospitales.

La hipótesis que sustenta los estudios realizados se basa en que el empleo de tecnologías avanzadas de análisis, involucrando técnicas espectroscópicas, cromatografía de líquidos de ultra altas prestaciones y espectrometría de masas de alta resolución y masa exacta, permitirán un estudio en profundidad de las características químicas y estructurales de mAbs terapéuticos, que unido a estudios de funcionalidad de los mismos, posibilitaran evaluar rigurosamente la seguridad y eficacia de estos complejos medicamentos biotecnológicos en las condones de su uso clínico en hospitales, donde son administrados.

Los objetivos de esta Tesis Doctoral se enmarcan dentro de los objetivos de los siguientes proyectos de investigación: “Estudios de estabilidad en el tiempo de sobrantes de medicamentos biotecnológicos –anticuerpos monoclonales y proteínas de fusión–. Estudios conformacionales comprensivos” (FEDER/Ministerio de Ciencia e Innovación-Instituto de Salud Carlos III, Fondos de Investigación en Salud, Proyecto **FIS PI17-00547**) y “Estabilidad de anticuerpos monoclonales terapéuticos antineoplásicos en condiciones de uso clínico: evaluación de parámetros fisicoquímicos y funcionalidad biológica en el tiempo y durante su manipulación y administración. Potenciales fuentes de

The hypothesis supporting the studies carried out in this Thesis is that the use of advanced analytical technologies, involving spectroscopic techniques, ultra-high performance liquid chromatography and high-resolution mass spectrometry and accurate mass spectrometry, will allow an in-depth study of the chemical and structural characteristics of therapeutic mAbs. This, together with studies of their functionality, will make it possible to rigorously evaluate the safety and efficacy of these complex biotechnological drugs in the context of their clinical use in hospitals, where they are administered.

The objectives of this Doctoral Thesis are framed within the objectives of the following research projects: "Studies of stability over time of biotechnological drug leftovers -monoclonal antibodies and fusion proteins-. Comprehensive conformational studies" (FEDER/Ministerio de Ciencia e Innovación-Instituto de Salud Carlos III, Fondos de Investigación en Salud, Project **FIS PI17-00547**) and "Stability of therapeutic antineoplastic monoclonal antibodies under conditions of clinical use: evaluation of physicochemical parameters and biological functionality over time and during handling and administration. Potential sources of instability" (FEDER/Junta de Andalucía-Consejería de Transformación Económica, Industria, Conocimiento y Universidades, Project

inestabilidad" (FEDER/Junta de Andalucía-Consejería de Transformación Económica, Industria, Conocimiento y Universidades, Proyecto **P20-01029** y FEDER/Junta de Andalucía-Consejería de Transformación Económica, Industria, Conocimiento y Universidades, Proyecto **B-FQM-308-UGR20**). Estos proyectos tienen como objetivos estudios de estabilidad en condiciones de uso hospitalario de mAbs terapéuticos. En concreto, en esta Tesis Doctoral los mAbs estudiados han sido tocilizumab, nivolumab y pembrolizumab en sus medicamentos originales RoActemra® (20 mg/mL (IV) o 162 mg/0,9 mL (SC), Roche Registration GmbH, Alemania), Opdivo® (10 mg/mL, Bristol-Myers Squibb Pharma EEIG, Irlanda) y Keytruda® (25 mg/mL, Merck Sharp & Dohme B.V., Países Bajos). Sin embargo, cabe destacar que los estudios llevados a cabo con tocilizumab derivan de la necesidad de dar respuesta a cuestiones hospitalarias referentes a este medicamento como consecuencia del inicio de la pandemia por COVID-19.

Por tanto, el **objetivo general** de esta Tesis Doctoral es estudiar la estabilidad en condiciones de uso hospitalario de mAbs innovadores inhibidores de la interleucina-6 (tocilizumab) e inhibidores de punto de control inmunitario (nivolumab y pembrolizumab), en aspectos relacionados con su manipulación en la práctica clínica diaria. Para ello, se lleva a cabo el desarrollo y validación de metodologías analíticas comprensivas, mediante la determinación

P20-01029 and FEDER/Junta de Andalucía-Consejería de Transformación Económica, Industria, Conocimiento y Universidades, Project **B-FQM-308-UGR20**). The objectives of these projects are to study the stability of therapeutic mAbs under hospital conditions. Specifically, in this Doctoral Thesis, the mAbs studied were tocilizumab, nivolumab and pembrolizumab in their original medicines RoActemra® (20 mg/mL (IV) or 162 mg/0.9 mL (SC), Roche Registration GmbH, Germany), Opdivo® (10 mg/mL, Bristol-Myers Squibb Pharma EEIG, Ireland) and Keytruda® (25 mg/mL, Merck Sharp & Dohme B.V., The Netherlands). However, it should be noted that the studies conducted with tocilizumab arise from the need to respond to hospital questions regarding this drug as a consequence of the onset of the COVID-19 pandemic.

Therefore, the **general aim** of this Doctoral Thesis is to study the stability under hospital use conditions of innovative mAbs interleukin-6 inhibitors (tocilizumab) and immune checkpoint inhibitors (nivolumab and pembrolizumab), in aspects related to their handling in daily clinical practice. To this end, comprehensive analytical methodologies were developed and validated, through the determination of the stability indicator profile, which allow the physicochemical and functional characterisation of the mAbs under study

del perfil indicador de estabilidad, que permitan la caracterización fisicoquímica y funcional de los mAbs en estudio bajo condiciones de uso hospitalario. Esto permitirá evaluar el impacto de la manipulación hospitalaria sobre los mAbs estudiados y obtener información dirigida a dar una mayor seguridad y eficacia a la manipulación en hospital de estos caros medicamentos biotecnológicos. Estas metodologías se centran en el empleo de técnicas espectroscópicas, cromatográficas y de espectrometría de masas de alta de resolución y masa exacta, así como de técnicas de inmunoanálisis para evaluar la funcionalidad. De este objetivo general se derivan los siguientes **objetivos específicos**:

1. Revisión bibliográfica de los mAbs empleados en el tratamiento de la enfermedad causada por el coronavirus SARS-CoV-2 (COVID-19) y diferenciación entre mAbs no específicos y específicos de dicho coronavirus (*Capítulo 1*).

2. Realizar un estudio analítico comparativo de los atributos de calidad fisicoquímicos de las formas farmacéuticas intravenosa y subcutánea del medicamento RoActemra® (tocilizumab), con la finalidad de utilizar la forma farmacéutica subcutánea para preparar las disoluciones de uso intravenoso (*Capítulo 2*).

3. Desarrollar y validar un método analítico indicador de la estabilidad para la cuantificación de nivolumab (Opdivo®) bajo condiciones de uso hospitalario. Esto permitirá evaluar el impacto de la manipulación hospitalaria sobre los mAbs estudiados y obtener información dirigida a dar una mayor seguridad y eficacia a la manipulación en hospital de estos caros medicamentos biotecnológicos. Estas metodologías se centran en el empleo de técnicas espectroscópicas, cromatográficas y de espectrometría de masas de alta de resolución y masa exacta, así como de técnicas de inmunoanálisis para evaluar la funcionalidad. De este objetivo general se derivan los siguientes **specific aims** are derived from this general aim:

1. Literature review of the mAbs used in the treatment of the disease caused by the SARS-CoV-2 coronavirus (COVID-19) and differentiation between non-specific and specific mAbs for this coronavirus (*Chapter 1*).

2. Conduct a comparative analytical study of the physicochemical quality attributes of the intravenous and subcutaneous dosage forms of the medicine RoActemra® (tocilizumab), with the aim of using the subcutaneous dosage form to prepare solutions for intravenous use (*Chapter 2*).

3. Develop and validate an analytical stability indicator method for the quantification of intact nivolumab (Opdivo®) by ultraviolet detection and mass spectrometry, and the determination of its isoform profile (*Chapter 3*).

intacto mediante detección ultravioleta y por espectrometría de masas, y la determinación de su perfil de isoformas (*Capítulo 3*).

4. Análisis comprensivo de las características fisicoquímicas y funcionales de nivolumab (Opdivo®) mediante el empleo de técnicas espectroscópicas, cromatografía de líquidos y espectrometría de masas, así como técnicas de inmunoanálisis, todo ello con el consiguiente desarrollo y validación de las metodologías requeridas. Estudios de degradación forzada (*Capítulo 4*).

5. Análisis comprensivo de las características fisicoquímicas y funcionales de pembrolizumab (Keytruda®) mediante el empleo de técnicas espectroscópicas, cromatografía de líquidos y espectrometría de masas, así como técnicas de inmunoanálisis, todo ello con el consiguiente desarrollo y validación de las metodologías requeridas. Estudios de degradación forzada (*Capítulo 5*).

6. Optimización del ensayo *ReFOLD* para la predicción de la estabilidad de mAbs terapéuticos durante su almacenamiento a largo plazo, empleando técnicas analíticas cromatográficas (*Capítulo 6*).

4. Comprehensive analysis of the physicochemical and functional characteristics of nivolumab (Opdivo®) using spectroscopic techniques, liquid chromatography and mass spectrometry, as well as immunoassay techniques, with the subsequent development and validation of the required methodologies. Forced degradation studies (*Chapter 4*).

5. Comprehensive analysis of the physicochemical and functional characteristics of pembrolizumab (Keytruda®) using spectroscopic techniques, liquid chromatography and mass spectrometry, as well as immunoassay techniques, with the subsequent development and validation of the required methodologies. Forced degradation studies (*Chapter 5*).

6. Optimisation of the ReFOLD assay for predicting the stability of therapeutic mAbs during long-term storage, using chromatographic analytical techniques (*Chapter 6*).

RESUMEN / ABSTRACT

RESUMEN

En la presente Tesis Doctoral se han desarrollado, puesto a punto y validado estrategias analíticas comprensivas para evaluar distintos atributos críticos de la calidad de anticuerpos monoclonales terapéuticos (mAbs) comerciales. Con la finalidad de alcanzar los objetivos propuestos, estas estrategias se han empleado posteriormente en estudios de caracterización (fisicoquímica y funcional) y estabilidad de los mismas en condiciones de uso hospitalario, los cuales se recogen en los distintos capítulos que conforman esta Tesis Doctoral. Los principales mAbs estudiados han sido tocilizumab, nivolumab y pembrolizumab, aunque también se ha realizado un estudio que recoge una amplia selección de mAbs terapéuticos.

Los trabajos recogidos en esta Tesis Doctoral se pueden dividir en tres grandes secciones. La primera sección recoge dos trabajos relacionados con mAbs empleados en el tratamiento de la COVID-19. Esto se debe a que el inicio de esta Tesis coincidió con el inicio de la pandemia causada por el coronavirus SARS-CoV-2, en octubre de 2019. En el primer capítulo se presenta un trabajo de revisión bibliográfica de los mAbs empleados en el tratamiento de la COVID-19, en el que se ha hecho una diferenciación entre los mAbs no específicos y específicos del SARS-CoV-2. El primer grupo recoge aquellos mAbs que bloquean la acción de la interleucina-6 (IL-6), la cual provoca una

ABSTRACT

In this Doctoral Thesis, comprehensive analytical strategies have been developed and validated to evaluate different critical quality attributes of commercial therapeutic monoclonal antibodies (mAbs). In order to achieve the proposed objectives, these strategies have subsequently been used in characterisation studies (physicochemical and functional) and stability studies under hospital use conditions, which are included in the different chapters of this Doctoral Thesis. The main mAbs studied were tocilizumab, nivolumab and pembrolizumab, although a study was also carried out on a wide selection of therapeutic mAbs.

The works included in this doctoral thesis can be divided into three main sections. The first section includes two scientific contributions related to mAbs used in the treatment of COVID-19. This is because the start of this Thesis coincided with the beginning of the pandemic caused by the SARS-CoV-2 coronavirus, in October 2019. The first chapter presents a review of the mAbs used in the treatment of COVID-19, in which a differentiation has been made between non-specific and specific mAbs for SARS-CoV-2. The first group includes mAbs that block the action of interleukin-6 (IL-6), which causes an exaggerated immune response in patients with the disease, so these mAbs are aimed at blocking a key point in the immune system response of infected patients. In contrast,

respuesta inmune exagerada en los pacientes con dicha enfermedad, por lo que estos mAbs van dirigidos a bloquear un punto clave de la respuesta del sistema inmune de los pacientes infectados. En cambio, el segundo grupo contempla aquellos mAbs que son capaces de neutralizar directamente la estructura proteica del virus, donde se recogen, además, los mAbs que recibieron una autorización de uso de emergencia.

El segundo capítulo recoge un trabajo en el que se han estudiado los atributos fisicoquímicos de la calidad de un mAb empleado en el tratamiento de la COVID-19, tocilizumab (RoActemra®, Roche Registration GmbH, Alemania), el cual se trata de un inhibidor de la IL-6. En este estudio se comparan los principales atributos fisicoquímicos de las formas farmacéuticas intravenosa (IV) y subcutánea (SC) de dicho medicamento, con el objetivo de averiguar si la forma farmacéutica SC podía ser administrada de manera IV como consecuencia del desabastecimiento hospitalario de la forma IV. Para ello se utilizaron una amplia variedad de técnicas analíticas: dispersión de luz dinámica (DLS), fluorescencia intrínseca de triptófanos (IT-FS), cromatografía de exclusión molecular (SEC) y cromatografía de intercambio catiónico (CEX). Estas técnicas permitieron comparar ambas formas medicamentosas a las concentraciones de disolución clínica de 6 y 4 mg/mL de tocilizumab. Además, también se llevaron a cabo estudios de

the second group includes mAbs that are capable of directly neutralising the protein structure of the virus, including mAbs that have received emergency use authorisation.

The second chapter is a study of the physicochemical quality attributes of a mAb used in the treatment of COVID-19, tocilizumab (RoActemra®, Roche Registration GmbH, Germany), which is an IL-6 inhibitor. This study compares the main physicochemical attributes of the intravenous (IV) and subcutaneous (SC) dosage forms of the medicine, with the aim of finding out whether the SC dosage form could be administered as IV because of hospital shortage of the IV form. A wide variety of analytical techniques were used: dynamic light scattering (DLS), intrinsic tryptophan fluorescence (IT-FS), molecular exclusion chromatography (SEC) and cation exchange chromatography (CEX). These techniques allowed comparison of both drug forms at clinical dilution concentrations of 6 and 4 mg/mL of tocilizumab. In addition, controlled degradation studies were also performed to corroborate the stability of all methods used and to assess the comparability of the IV and SC clinical dilutions.

The second section of this Thesis is composed of three studies carried out with immune checkpoint inhibitor mAbs, specifically these mAbs have the capacity to block the action of the PD-1 receptor. Firstly, the third chapter includes a study

degradación controlada con el objetivo de corroborar la estabilidad de todos los métodos utilizados y para evaluar la comparabilidad de las disoluciones clínicas IV y SC.

La segunda sección de esta Tesis está compuesta por tres trabajos llevados a cabo con mAbs inhibidores de puntos de control inmunitario, concretamente estos mAbs tienen la capacidad de bloquear la acción del receptor PD-1. En primer lugar, el tercer capítulo recoge un trabajo realizado con nivolumab (Opdivo®, Bristol-Myers Squibb Pharma EEIG, Irlanda) en el que se ha desarrollado y validado un método cromatográfico de fase inversa con detección ultravioleta y por espectrometría de masas ((RP)UHPLC/UV-(HESI/Orbitrap™)MS) para la cuantificación del contenido proteico de dicho medicamento. Este se trata de un método indicador de la estabilidad capaz de analizar el fármaco en presencia de sus productos degradados. Tanto el método de detección por absorción en el ultravioleta como el método utilizando espectrometría de masas han sido validados mediante el estudio de determinados parámetros de calidad del método, tales como linealidad, límites de detección y cuantificación, precisión, exactitud, especificidad, robustez y test de la adecuación al sistema (system suitability test). La especificidad del método ha sido evaluada mediante ensayos de degradación forzada en muestas de Opdivo®. Este trabajo también recoge la identificación del perfil de

carried out with nivolumab (Opdivo®, Bristol-Myers Squibb Pharma EEIG, Ireland) in which a reverse-phase chromatographic method with ultraviolet detection and mass spectrometry ((RP)UHPLC/UV-(HESI/Orbitrap™)MS) has been developed and validated for the quantification of the protein content of this drug. This is a stability indicator method capable of analysing the drug in the presence of its degraded products. Both the ultraviolet absorption detection method and the method using mass spectrometry have been validated by studying certain method quality parameters, such as linearity, detection and quantification limits, precision, accuracy, specificity, robustness and system suitability test. The specificity of the method has been evaluated by forced degradation tests on Opdivo® samples. This work also includes the identification of the nivolumab isoform profile thanks to the signal obtained by high-resolution and accurate mass spectrometry. In addition, a 15-day medicine stability study was performed to assess the applicability of the method.

The fourth chapter contains a comprehensive analysis of the physicochemical and functional characteristics of nivolumab (Opdivo®). To this end, various complementary analytical techniques were used to provide information on different physicochemical aspects of the protein, such as its secondary and tertiary structure,

isoformas de nivolumab gracias a la señal obtenida por espectrometría de masas de alta resolución y masa exacta. Además, se realizó un estudio de estabilidad del medicamento durante 15 días para evaluar la aplicabilidad del método.

En cuanto al cuarto capítulo, este recoge un análisis comprensivo de las características fisicoquímicas y funcionales de nivolumab (Opdivo®). Para ello, se utilizaron diversas y complementarias técnicas analíticas que aportan información sobre distintos aspectos fisicoquímicos de la proteína, tales como su estructura secundaria y terciaria, el perfil de agregación o el estudio de sus isoformas. Las técnicas utilizadas se pueden agrupar en técnicas espectrofotométricas (dicroísmo circular (CD), IT-FS y DLS), cromatográficas (SEC) y espectrometría de masas. La evaluación de la funcionalidad se llevó a cabo utilizando la técnica ELISA. También se llevaron a cabo estudios de degradación forzada para estudiar en profundidad las propiedades del medicamento, para lo que se sometieron muestras de Opdivo® a distintas condiciones estresantes, tales como elevada temperatura, ciclos de congelación/descongelación, agitación, exposición a la luz y exposición a una alta concentración salina. Los métodos fueron desarrollados *ad hoc* y validados.

El último capítulo de esta sección, el capítulo 5, recoge un trabajo de estructura similar al del capítulo 4, en este caso llevado a cabo con pembrolizumab (Keytruda®, Merck

aggregation profile or the study of isoforms. The techniques used can be grouped into spectrophotometric (circular dichroism (CD), IT-FS and DLS), chromatographic (SEC) and mass spectrometric techniques. Functionality assessment was carried out using the ELISA technique. Forced degradation studies were also carried out to study in depth the properties of the medicine by subjecting Opdivo® samples to different stressful conditions such as high temperature, freeze/thaw cycles, agitation, exposure to light and exposure to high salt concentration. The methods were developed ad hoc and validated.

The last chapter of this section, chapter 5, contains a study with a similar structure to chapter 4, in this case carried out with pembrolizumab (Keytruda®, Merck Sharp & Dohme B.V., The Netherlands). A comprehensive analysis of pembrolizumab has been carried out by physicochemical and functional characterisation using different complementary analytical techniques. Techniques used include CD, IT-FS, DLS, SEC, RP/UHPLC(UV)-MS/MS and ELISA. These have allowed the study of the higher order structures of the protein, particle formation and aggregation, the study of isoforms and the determination of post-translational modifications. In this work, forced degradation studies were also carried out on samples of the medicine, which was subjected to various stressful conditions, such as high temperatures, freeze/thaw cycles, exposure to light,

Sharp & Dohme B.V., Países Bajos). En él se ha realizado un análisis comprensivo del medicamento mencionado mediante su caracterización fisicoquímica y funcional a través del empleo de distintas técnicas analíticas complementarias. Entre las técnicas utilizadas encontramos CD, IT-FS, DLS, SEC, RP/UHPLC(UV)-MS/MS y ELISA. Estas han permitido el estudio de las estructuras de orden superior de la proteína, la formación de particulado y agregación, el estudio de las isoformas y la determinación de las modificaciones postraduccionales. En este trabajo también se llevaron a cabo estudios de degradación forzada de muestras del medicamento, el cual fue sometido a diversas condiciones estresantes, tales como altas temperaturas, ciclos de congelación/descongelación, exposición a la luz, exposición a agitación fuerte y suave y exposición a una alta concentración salina. Todas las muestras sometidas a estos estreses fueron analizadas mediante la metodología desarrollada *ad hoc* y validada empleando las técnicas analíticas mencionadas; los resultados fueron siempre comparados con los resultados de la muestra control del medicamento, es decir, una muestra no sometida a ningún tipo de estrés. De esta forma, los trabajos recogidos en los capítulos 4 y 5 evalúan el impacto de la manipulación hospitalaria sobre la estabilidad de los medicamentos Opdivo® y Keytruda®, y ofrecen recomendaciones

exposure to strong and gentle agitation, and exposure to high salt concentration. All samples subjected to these stresses were analysed using the methodology developed ad hoc and validated using the above-mentioned analytical techniques; the results were always compared with the results of the control sample of the medicine, i.e., a sample not subjected to any stress. Thus, the works in chapters 4 and 5 assess the impact of hospital handling on the stability of Opdivo® and Keytruda® medicines, and provide recommendations on the correct handling of these medicines during their manipulation.

Finally, the third section presents the last chapter of this Thesis, chapter 6, which includes a work carried out on a total of ten different commercial therapeutic mAbs. This work consisted of the optimisation of the ReFOLD assay, an isothermal method that allows predicting the long-term stability of mAb-based drugs by means of a chemical denaturation process with urea. For this purpose, selected mAbs (at three different concentrations each) were subjected to two different high concentrations of urea (6 M and 6.5 M). The results obtained were compared with the results of previous tests carried out with a urea concentration of 10 M, with the aim of improving the difficulties encountered with such a high urea concentration, since the 10 M concentration showed undesired effects on several of the tested

sobre el correcto manejo de los mismos durante su manipulación.

Por último, la tercera sección está formada por el último capítulo de esta Tesis, capítulo 6, el cual recoge un trabajo realizado sobre un total de diez mAbs terapéuticos comerciales diferentes. Este trabajo consistió en la optimización del ensayo ReFOLD, un método isotérmico que permite predecir la estabilidad a largo plazo de medicamentos basados en mAbs mediante un proceso de desnaturalización química con urea. Para ello, se sometieron los distintos mAbs seleccionados (a tres concentraciones diferentes cada uno) a dos concentraciones altas y distintas de urea (6 M y 6.5 M). Los resultados obtenidos fueron comparados con los resultados de ensayos previos realizados con una concentración de urea de 10 M, con el objetivo de mejorar las dificultades encontradas con tan alta concentración de urea, ya que la concentración de 10 M mostró efectos indeseados en varios de los productos farmacéuticos ensayados, tales como la formación de precipitados. Además, también se estudió la capacidad de mantener una clasificación de la estabilidad de los productos farmacéuticos ensayados con las nuevas concentraciones de urea. Como técnica analítica, en este caso, se empleó SEC para estudiar la capacidad de recuperación del estado nativo de la proteína tras ser sometida a las altas concentraciones de urea.

pharmaceuticals, such as the formation of precipitates. In addition, the ability to maintain a stability ranking of the tested pharmaceuticals with the new urea concentrations was also studied. As an analytical technique, in this case, SEC was used to study the recovery capacity of the native state of the protein after being subjected to the high urea concentrations.

INTRODUCCIÓN

1. MEDICAMENTOS BIOTECNOLÓGICOS PROTEICOS

Los medicamentos biotecnológicos se enmarcan dentro de los medicamentos biológicos, es decir, son un subgrupo de los mismos. Los medicamentos biológicos, según el Real Decreto 1345/2007 del 11 de octubre [1], se definen como aquellos productos cuyo material de partida es toda sustancia de origen biológico, tales como microorganismos, órganos y tejidos de origen vegetal o animal, las células o fluidos (incluyendo sangre y plasma) de origen humano o animal y los diseños celulares biotecnológicos (sustratos celulares, sean o no recombinantes, incluidas las células primarias). Por tanto, los medicamentos biotecnológicos son aquellos medicamentos biológicos obtenidos por técnicas tales como el ADN recombinante, la expresión génica controlada o la tecnología de hibridomas, cuyo principio activo se denomina biofármaco [2].

Generalmente, la mayor parte de los medicamentos biotecnológicos están compuestos por proteínas de distinta naturaleza, como pueden ser los anticuerpos monoclonales, proteínas de fusión, enzimas, hormonas, anticoagulantes, factores de crecimiento o citoquinas. Entre ellos, los más importantes y complejos serían los mAbs y las proteínas de fusión [3].

En España, la regulación y evaluación de los aspectos de calidad de este tipo de medicamentos, así como su registro y vigilancia en el mercado, se lleva a cabo por la Agencia Española de Medicamentos y Productos Sanitarios (AEMPS [4]) bajo la coordinación de la Agencia Europea de Medicamentos (*European Medicines Agency*, EMA [5]). A nivel europeo, es la EMA la que coordina y regula las autorizaciones de los medicamentos provenientes de la tecnología del ADN recombinante, siguiendo lo que se conoce como un procedimiento centralizado en el que todos los países miembros de la Unión Europea toman una decisión unánime para llevar a cabo las autorizaciones pertinentes.

2. ANTICUERPOS MONOCLONALES TERAPÉUTICOS

2.1. Definición

Cuando se produce una respuesta inmunológica especifica en el cuerpo humano, por la exposición del mismo a un agente extraño o antígeno, se origina una respuesta policlonal, es decir, la producción de anticuerpos contra un rango amplio de estructuras presentes en el antígeno. En cambio, la respuesta monoclonal se da cuando los anticuerpos solo son capaces de reconocer una única estructura o región presente en el agente extraño.

Por tanto, los anticuerpos monoclonales (mAbs, del inglés *monoclonal antibodies*) se tratan de anticuerpos homogéneos que tienen la capacidad de reconocer una parte del

antígeno de forma específica y que proceden de un único clon de linfocitos B. Dicho clon tiene su origen en una célula hibrida creada por la fusión de una célula madre del sistema inmune y otra plasmática de tipo tumoral. Debido a que los mAbs proceden de un único linfocito B, presentan un alto grado de especificidad frente al antígeno para el que son diseñados [3].

Gracias a su gran especificidad, los mAbs son ampliamente utilizados hoy en día en la prevención, diagnóstico y tratamiento de enfermedades de gran prevalencia, como el cáncer o las enfermedades autoinmunes (artritis reumatoide, enfermedad de Crohn, etc.). Además, son considerados el grupo terapéutico más innovador y de mayor expansión en la industria farmacéutica global [6,7].

2.2. Estructura y tipos de mAbs terapéuticos

Los mAbs son inmunoglobulinas humanas fundamentalmente del tipo G (IgG) que pueden pertenecer a cuatro isotipos distintos: IgG1, IgG2, IgG3 e IgG4. Hasta el momento, los mAbs más empleados en terapia pertenecen al isotipo IgG1, aunque, en los últimos años, se ha ido incrementando el empleo de mAbs IgG2 e IgG4, dejando en última posición a los del isotipo 3. La razón por la que las IgG1 siempre han sido las más empleadas es debido, entre otras razones, a su mayor vida media en el organismo, mientras que las IgG3 presentan una vida media muy corta. En cambio, las IgG2 e IgG4 han experimentado un notable progreso en el desarrollo de formatos más estables de las mismas por parte de empresas farmacéuticas y biotecnológicas, lo que ha permitido el incremento de productos terapéuticos basados en estos isotipos [8,9].

Estructuralmente, todos los isotipos de IgGs son glicoproteínas de alto peso molecular (en torno a 150 kDa) que están constituidos por cuatro cadenas polipeptídicas: dos cadenas pesadas, de aproximadamente 50 kDa cada una y formadas por 450 – 550 aminoácidos, y dos ligeras, de unos 25 kDa y 220 aminoácidos aproximadamente. Gracias a la presencia de puentes disulfuro e interacciones no covalentes, estas inmunoglobulinas adquieren una conformación tridimensional en forma de “Y”. La diferencia estructural entre los distintos isotipos de IgGs radica en el número de puentes disulfuro que presentan: las IgG1 e IgG4 presentan 16 puentes disulfuro, las IgG2 18 y las IgG3 25. Además, los puentes disulfuro de la región bisagra (región que une las 4 cadenas) también varía entre los distintos isotipos: dos para las IgG1 e IgG4, cuatro para las IgG2 y once para las IgG3. Los puentes disulfuro restantes, es decir, los que no pertenecen a la región bisagra, se tratan de puentes intermoleculares que delimitan 6 dominios diferentes: 2 en las cadenas ligeras (uno variable (VL) y otro constante (CL)), y 4 en las cadenas pesadas (uno variable (VH) y tres constantes (CH_1, CH_2 y CH_3)).

Funcionalmente, las IgGs cuentan con una región de reconocimiento y unión a antígenos, conocida como región Fab (*Fragment-antibody binding*), que se localiza en las regiones amino terminales de las cadenas ligeras y pesadas. También poseen una región con función efectora y fácilmente cristalizable, conocida como región Fc (*Fragment-crystallizable*), que se localiza en los extremos carboxilo terminales de las cadenas pesadas. Como podemos observar en la Figura 1 el fragmento Fc formaría la base de la "Y", mientras que los dos fragmentos Fab formarían los dos brazos. En el fragmento Fab, además, encontramos una región denominada CDR (*Complementary Determining Region*), de aproximadamente 30 aminoácidos, formada por 6 polipéptidos situados en las cadenas ligeras y pesadas, y es la encargada del reconocimiento específico del antígeno.

Como se ha comentado anteriormente, los mAbs presentan una región bisagra que une sus cuatro cadenas y se ubica concretamente entre los dominios CH_1 y CH_2. La longitud de esta región puede variar entre 10 y 60 aminoácidos, en función del tipo de IgG, y su aminoácido predominante es la prolina. Esta proporciona flexibilidad a la molécula, lo cual le permite su orientación espacial para poder unirse eficazmente a su antígeno.

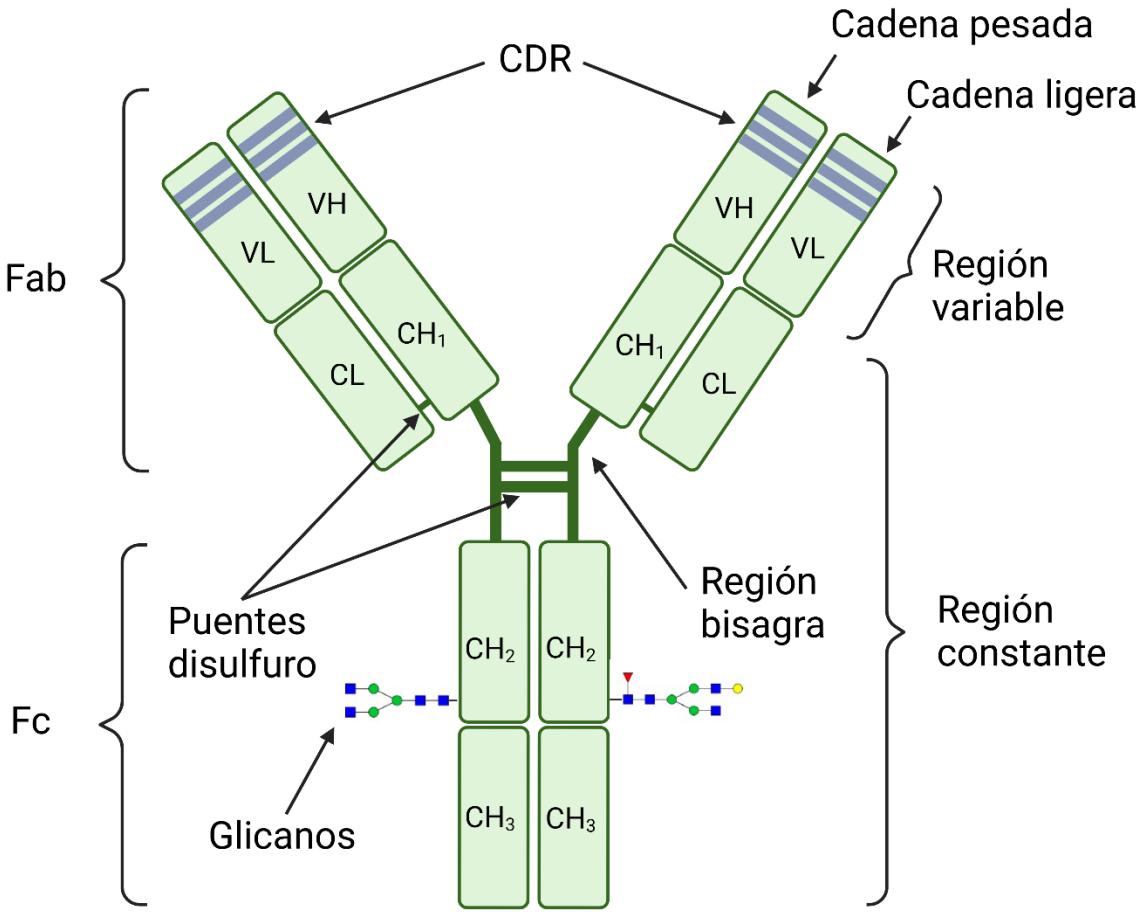

Figura 1. Diagrama de la estructura de un mAb. Elaboración propia.

En función de su origen, los mAbs terapéuticos pueden clasificarse en cuatro tipos distintos (Figura 2) [6]:

- **mAbs murinos:** la total estructura del anticuerpo procede del ratón. Sin embargo, este hecho ha supuesto que el sistema inmune humano reconozca a estos mAbs como extraños y se genere una respuesta inmune frente a ellos, limitando e incluso inactivando su actividad. Por ello, sus aplicaciones son muy limitadas. Se identifican mediante el sufijo "-omab".
- **mAbs quiméricos:** las regiones variables del anticuerpo proceden del ratón, mientras que las regiones constantes son humanas. Estos mAbs se crearon con la finalidad de reducir la respuesta inmune que generaban los murinos y son construidos mediante técnicas de ingeniería genética. Se identifican mediante el sufijo "-ximab".
- **mAbs humanizados:** se trata de anticuerpos de origen totalmente humano, a excepción de las CDR de las partes variables, las cuales proceden del ratón. La tendencia es a producir este tipo de mAbs, ya que disminuyen en gran medida la respuesta inmunogénica de los pacientes. Se identifican mediante el sufijo "-zumab".
- **mAbs humanos:** la total estructura del anticuerpo es de origen humano. De esta forma, la respuesta inmune se ve muy reducida. Sin embargo, estos son los que presentan un mayor impacto económico, dada la gran complejidad de su desarrollo y producción. Se identifican mediante el sufijo "-umab".

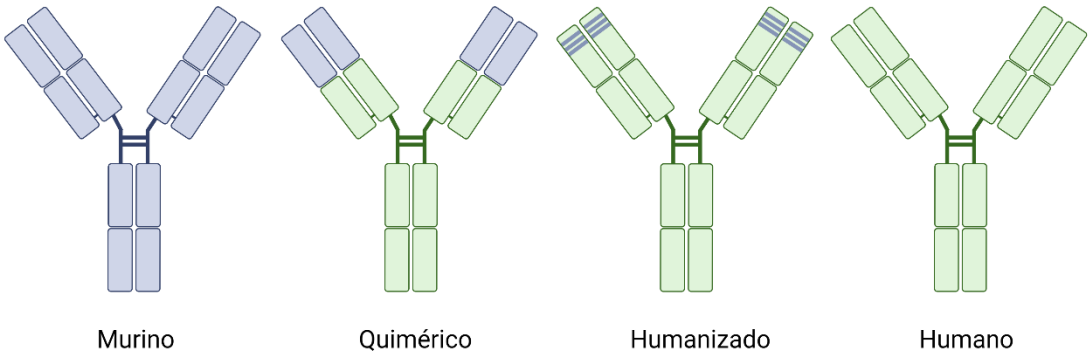

Figura 2. Tipos de mAbs terapéuticos en función de su origen. Elaboración propia.

2.3. Modificaciones postraduccionales

Las modificaciones postraduccionales (PTMs, del inglés *post-translational modifications*) son procesos covalentes que cambian las propiedades de una proteína por

escisión proteolítica y adición de un grupo modificador, como acetilo, fosforilo, glicosilo y metilo, a uno o más aminoácidos. Estas desempeñan un papel clave en numerosos procesos biológicos al afectar significativamente a la estructura y dinámica de las proteínas. Generalmente, una PTM puede ser reversible o irreversible. Las reversibles contienen modificaciones covalentes, y las irreversibles, que proceden en una sola dirección, incluyen modificaciones proteolíticas. Las PTMs ocurren en un solo tipo de aminoácido o en múltiples aminoácidos y conducen a cambios en las propiedades químicas de los sitios modificados. Estas modificaciones afectan a una amplia gama de comportamientos y características de las proteínas, como la función y el ensamblaje de enzimas, la vida útil de las proteínas, las interacciones proteína-proteína, las interacciones célula-célula y célula-matriz, el tráfico molecular, la activación de receptores, y la solubilidad, plegamiento y la localización de las proteínas. Por lo tanto, estas modificaciones están implicadas en diversos procesos biológicos, como la transducción de señales, la regulación de la expresión génica, la activación de genes, la reparación del ADN y el control del ciclo celular. Las PTMs ocurren en varios orgánulos celulares, incluyendo el núcleo, el citoplasma, el retículo endoplásmico y el aparato de Golgi [10].

Más concretamente, las PTMs de las proteínas terapéuticas, como los mAbs, pueden clasificarse en dos grandes clases: modificaciones enzimáticas y químicas. Las enzimáticas se definen como el procesamiento catalizado por enzimas de las proteínas después de la traducción por diferentes quinasas, fosfatasas, proteasas, transferasas, ligasas, etc. Las PTMs más comunes en esta clase incluyen la glicosilación, la formación de enlaces disulfuro y la escisión proteolítica de la cadena principal de la proteína. Las modificaciones químicas se generan a menudo durante el procesamiento, la formulación y el almacenamiento, siendo las más comunes la oxidación, la desamidación, la glicación y la formación de piroglutamato [11].

La gran mayoría de las proteínas terapéuticas, contienen al menos una o más PTMs. Estas proteínas normalmente se sintetizan en los ribosomas unidos al retículo endoplasmático y posteriormente son transportadas al espacio extracelular. Algunas de estas modificaciones ocurren durante este proceso biológico, y se producen modificaciones adicionales durante las manipulaciones in vitro, tales como la purificación, la formulación, el almacenamiento y la inyección a los sujetos de ensayo. Por tanto, las distintas PTMs que una proteína puede sufrir dependen de la localización donde se originan (retículo endoplasmático, aparato de Golgi o espacio extracelular). La Tabla 1 recoge estas distintas PTMs, con la localización en la que ocurren y los aminoácidos en los que tienen lugar. La N-glicosilación es la única PTM que puede ocurrir en dos localizaciones diferentes: el retículo endoplasmático y el aparato de Golgi [12]. Además, resulta interesante comentar que no todos los aminoácidos son susceptibles de

sufrir PTMs, en concreto, los aminoácidos que no se suelen modificar son glicina, alanina (aminoácidos pequeños), leucina, isoleucina, valina o triptófano (aminoácidos hidrófobos) [3].

Tabla 1. Localización y aminoácidos donde ocurren las principales PTMs en mAbs [12].

Localización	**Modificación**	**Aminoácido**
Retículo endoplasmático	Formación de puentes disulfuro	Cisteína
	ɣ-carboxilación	Glutamato
	β-hidroxilación	Asparagina
		Aspartato
	N-glicosilación	Asparagina
Aparato de Golgi	Sulfonación	Tirosina
	O-glicosilación	Serina
		Treonina
		Fenilalanina
	Fosforilación	Serina
		Treonina
		Tirosina
	N-glicosilación	Asparagina
Espacio extracelular	Deamidación	Asparagina
		Glutamina
	Glicación	Lisina
	Formación de piroglutamato (N-terminal)	Glutamina
	Oxidación	Cisteína
		Histidina
		Metionina
		Triptófano
		Tirosina
	Ruptura de la lisina C-terminal	Lisina

La diversidad de PTM puede afectar a la actividad biológica, la semivida y la inmunogenicidad de los mAbs, y la heterogeneidad de los productos puede dar lugar a problemas de seguridad. Por ello, es necesario caracterizar, controlar y supervisar exhaustivamente estas PTMs durante el proceso de desarrollo de los mAbs terapéuticos. Para su caracterización, se emplean una serie de técnicas analíticas, como puede ser la espectrometría de masas (MS, del inglés *mass* spectrometry) de alta resolución, aspecto que se tratará con mayor profundidad en el apartado *4.2.3. Espectrometría de masas (MS)* de esta Introducción.

A continuación, se describen más detalladamente las PTMs más importantes que se dan en proteínas terapéuticas [3,12]:

- **Formación de puentes disulfuro:** tiene lugar entre dos residuos de cisteínas y su finalidad es ayudar a estabilizar la estructura terciaria de la proteína, además de mantener su integridad conformacional. Se trata de una de las PTMs más comunes en proteínas extracelulares, como los mAbs, los cuales contienen 16 puentes disulfuro que ayudan a mantener unidas las cadenas pesadas y ligeras entre sí.
- **ɣ-Carboxilación:** esta modificación ocurre en los residuos de glutamato (Glu), convirtiendo dicho aminoácido en ɣ-carboxiglutamato (Gla). Este proceso se lleva a cabo gracias a la enzima GGCX en presencia de CO_2, O_2 y vitamina K.
- **β-hidroxilación:** en este caso, por acción de una enzima hidoxilasa, se convierten los residuos de aspartato (Asp) en β-hidroxiaspartato o los residuos de asparagina (Asn) en β-hidroxiasparagina. Esta reacción está catalizada por una proteína de membrana β-hidroxilasa, la cual introduce un grupo hidroxilo (OH) reemplazando a su vez un átomo de hidrógeno (H).
- **N-glicosilación:** es una modificación que puede ocurrir tanto en el retículo endoplasmático como en el aparato de Golgi. Se trata de la PTM más común en células eucariotas. Consiste en la unión de un azúcar ramificado, de diferentes monómeros, al residuo de la asparagina (Asn) perteneciente a la secuencia Asn-X-Ser o Asn-X-Thr, donde X puede ser cualquier aminoácido excepto prolina (Pro). En el apartado *2.4. N-glicosilación* de esta Introducción se amplía la información acerca de esta importante PTM.
- **Sulfonación:** es una reacción catalizada por la enzima TPST en la que se introduce un grupo sulfato a un residuo de tirosina (Tyr).
- **O-glicosilación:** a diferencia de la N-glicosilación, esta ocurre únicamente en el aparato de Golgi. En este caso, se produce la unión de un azúcar, la N-acetilgalactosamina (GalNAc), a un residuo de serina (Ser) o de treonina (Thr), y la elongación de dicho azúcar puede dar lugar a 8 diferentes estructuras de O-glicanos.
- **Fosforilación:** se lleva a cabo por las enzimas proteínquinasas, las cuales transfieren el grupo fosfato del ATP.
- **Deamidación:** se trata de una reacción no enzimática muy común, que se produce por una reacción hidrolítica con el agua para formar aspartato (Asp) y glutamato (Glu) a partir de los residuos de asparagina (Asn) y glutamina (Gln), respectivamente, mediante intermediarios de succinimida. Esta modificación

suele asociarse con procesos de degradación de la proteína. Cuando tiene lugar, esta contribuye a la heterogeneidad de carga de la proteína terapéutica ya que introduce especies más ácidas de forma que la proteína adquiere una carga más negativa.

- **Glicación:** a diferencia de la glicosilación (reacción enzimática), esta se trata de una reacción de condensación entre el grupo carbonilo de un azúcar reductor y una amina de una lisina lateral. Esta reacción permite añadir a la estructura proteica residuos de glucosa o fructosa, generando heterogeneidad y pudiendo afectar a la estabilidad del producto.
- **Formación de piroglutamato:** se produce la formación de un grupo piroglutamato cíclico gracias al proceso de ciclación del extremo N-terminal de una glutamina con su propio grupo amino terminal. Es muy común encontrarlo en las cadenas pesadas y ligeras de los mAbs. Si esta reacción ocurre, la masa molecular de la proteína disminuye en 17 Da.
- **Oxidación:** se trata de una reacción no enzimática y muy abundante en los mAbs. Aunque es una reacción que ocurre más comúnmente en residuos de metionina (Met), la cual se oxida para dar metionina sulfóxido, también la podemos encontrar en residuos de cisteína, histidina, triptófano y tirosina. Esta modificación incrementa la masa de la proteína en 16 Da y hace que aumente la polaridad de la cadena. Si esta reacción ocurre, se considera un proceso de degradación proteica.
- **Ruptura de la lisina C-terminal:** esta modificación es muy común en la cadena pesada de los mAbs, pero que no afecta a la eficacia y estabilidad del producto final. Cuando tiene lugar, la masa molecular de la proteína se ve disminuida en 128 Da y le confiere una unidad de carga positiva a la molécula.

2.4. N-glicosilación

La N-glicosilación es la PTM más común en proteínas terapéuticas. Como se ha comentado en el apartado anterior, este proceso ocurre en el retículo endoplasmático y en el aparato de Golgi. Esta modificación es de gran interés ya que afecta a la estabilidad, función e integridad estructural de los productos biofarmacéuticos. El sitio de N-glicosilación en los mAbs terapéuticos es un residuo conservado en el dominio CH_2 de la cadena pesada, localizado aproximadamente en Asn297 [13].

Los N-glicanos se clasifican en tres grupos principales: glicanos de oligomanosa, glicanos complejos y glicanos híbridos. Todos ellos comparten una estructura de núcleo común, la cual está constituida por dos residuos de N-acetilglucosamina y tres residuos de

manosa. Los N-glicanos de oligomanosa contienen, además del núcleo común, únicamente unidades de monosacáridos de manosa, por lo que también se les conoce como “altos en manosa”. Los N-glicanos complejos suelen contener un residuo de fucosa en el núcleo y residuos de galactosa y ácido N-acetilneurámico. El tercer y último grupo, los N-glicanos híbridos, contienen elementos de ambos grupos anteriores. La Figura 3 muestra de forma esquemática los tres grupos principales de N-glicanos.

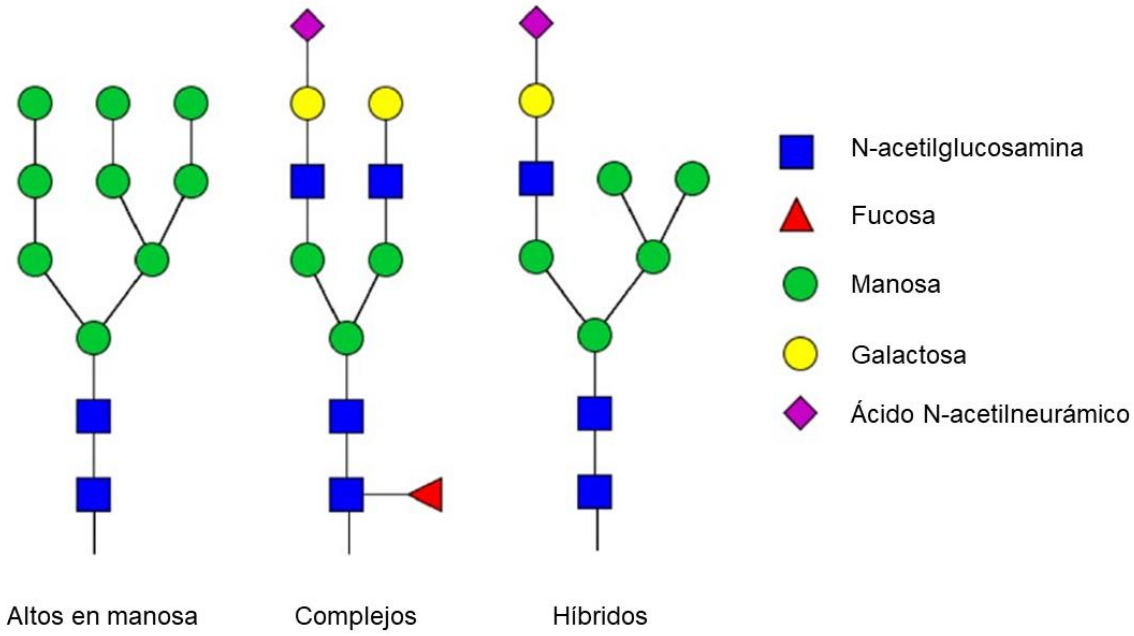

Figura 3. Tipos principales de N-glicanos [3].

Con el objetivo de hacer más fácil la descripción de los glicanos, sin necesidad de dibujar su estructura completa, se han establecido distintas nomenclaturas que permiten una denominación más fácil de los mismos. De todas las existentes actualmente, la ‘Consortium for Functional Glycomics (CFG) notation’ es la más habitual. La Tabla 2 recopila estas nomenclaturas para los N-glicanos más abundantes en los mAbs [14].

Tabla 2. N-glicanos más comunes en mAbs [3].

Estructura	Nomenclatura	Estructura	Nomenclatura
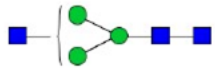	A1G0	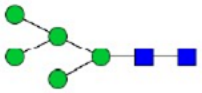	M5
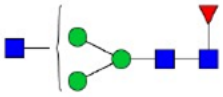	A1G0F	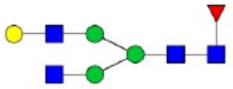	A2G1F
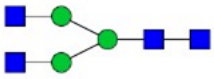	A2G0	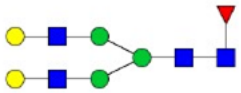	A2G2F
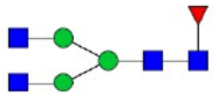	A2G0F	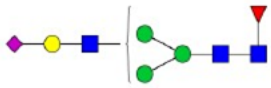	A1G1S1F
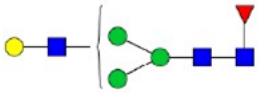	A1G1F	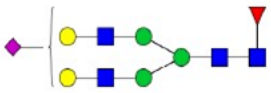	A2G2S1F

La tecnología recombinante actual para la producción de glicoproteínas terapéuticas se basa principalmente en líneas celulares de mamíferos, sobre todo células de ovario de hámster chino (células CHO). Las líneas celulares de mamíferos son las más utilizadas para la expresión de proteínas terapéuticas debido a su capacidad para realizar PTMs similares a las humanas (incluida la glicosilación). Las líneas celulares CHO predominan como línea celular huésped de producción comercial debido a un historial normativo establecido, su facilidad de uso, su capacidad para crecer en cultivo en suspensión en condiciones de medios químicamente definidos y su historial de seguridad ejemplar hasta la fecha. Sin embargo, una desventaja de la línea celular CHO es que la glicosilación proteica no es consistente debido a la actividad diferencial de cientos de enzimas implicadas en el proceso de glicosilación que varían en respuesta a las diferencias en el entorno celular durante el cultivo. Esto da lugar a diferentes patrones de glicosilación y a una menor repetibilidad entre lotes [15]. Y lo que es más importante, estas variaciones moleculares podrían alterar el efecto terapéutico de la proteína expresada [14]. Por tanto, la glicosilación tiene un impacto sustancial en las propiedades fisicoquímicas, farmacológicas y farmacocinéticas de las proteínas terapéuticas, y una glicosilación adecuada es necesaria para una eficacia y seguridad óptimas del producto biofarmacéutico [16]. De este modo, los cambios en los patrones de glicosilación de las proteínas terapéuticas desempeñan un papel crucial en términos de estructura, estabilidad, solubilidad, aclaramiento, actividad e incluso inmunogenicidad [14].

Por todas las implicaciones comentadas que tiene la N-glicosilación, se requiere de una producción eficiente y controlada del producto biofarmacéutico con el objetivo de obtener un patrón de glicosilación constante. Esto puede conseguirse minimizando las variaciones en las diferentes etapas del proceso de producción, y realizando una caracterización efectiva de dicho patrón. Para llevar a cabo esta caracterización en los mAbs terapéuticos se siguen las especificaciones de la guía de la Conferencia Internacional para la Harmonización de los requerimientos de comercialización de medicamentos de uso humano, la ICH Q6B [17].

2.5. Nomenclatura

La nomenclatura de los mAbs se basa en un sistema estandarizado que incluye diferentes componentes para describir las características y propiedades de cada anticuerpo de manera precisa y consistente. A lo largo de los años, diferentes organizaciones internacionales y nacionales, como la Organización Mundial de la Salud (OMS), han establecido directrices para implantar un sistema de nomenclatura coherente para los mAbs que ha dado lugar al esquema de la Denominación Común Internacional (DCI), o más internacionalmente conocido como la "*International Nonproprietary Name*" (INN [18]).

El objetivo del programa INN era proporcionar un "nombre único, reconocido mundialmente y de propiedad pública". Dichos INN se asignan a los mAbs previa solicitud a la OMS y superando positivamente un procedimiento de selección por parte de un grupo de expertos [19].

Los elementos clave de la nomenclatura de los mAbs son los siguientes:

- Prefijo: es la parte aleatoria, es decir, la elige el fabricante y no debe seguir ninguna regla establecida salvo contribuir a que el nombre final del producto sea eufónico y distintivo.
- Primer afijo: esta parte hace referencia al objetivo o la diana terapéutica a la que va dirigida el mAb. Por ejemplo, el afijo -b(a)- indica que ese mAb tiene objetivo bacteriano, el afijo -c(i)- es para el sistema circulatorio, -l(i)- para el sistema inmune o -t(u)- para el tratamiento tumoral, entre muchos otros.
- Segundo afijo: este hace referencia al origen del mAb. El afijo -o- es para indicar origen murino, -xi- para quimérico, -zu- para humanizado y -u- para humano.
- Sufijo: este indica el tipo de anticuerpo. En el caso de los mAbs terapéuticos, este siempre será -mab.

A modo de ejemplo, uno de los mAbs objeto de estudio de esta Tesis Doctoral es nivolumab, cuyo nombre se puede dividir en: nivo- l- u- mab. Concretamente, "nivo" es el nombre especifico y distintivo de este mAb, "l" hace referencia a que va dirigido al sistema

inmune, “u” es el indicativo de que su origen es humano y “mab” indica que es un anticuerpo del tipo monoclonal.

Sin embargo, es interesante comentar que esta nomenclatura se utilizó hasta 2017, pero a partir de dicho año el programa OMS/INN suprimió completamente el segundo afijo, que aporta la información del origen. Un primer ejemplo de este tipo es el anticuerpo anti-PD1 denominado cemiplimab, que se sometió a revisión reglamentaria a finales de 2017 para el tratamiento del carcinoma cutáneo de células escamosas [19].

3. ANTICUERPOS MONOCLONALES ESTUDIADOS

En esta Tesis Doctoral se han estudiado tres mAbs en total, para lo cual se han empleado los medicamentos comerciales que los contienen como compuesto activo. Los primeros estudios desarrollados corresponden al mAb tocilizumab, cuyo medicamento recibe el nombre de RoActemra®. A continuación, se llevaron a cabo los estudios con nivolumab, cuyo medicamento es Opdivo® y, por último, se realizaron los estudios de pembrolizumab utilizando el medicamento Keytruda®. Además, en la investigación correspondiente al último capítulo de esta Tesis Doctoral, se realizó un estudio sobre un total de diez mAbs para los que también se utilizaron sus medicamentos comerciales. En este caso, la identidad de los mAbs utilizados y, por tanto, la de sus productos comerciales, es información confidencial de uso exclusivo por la empresa Coriolis Pharma Research GmbH (Múnich, Alemania), lugar donde se realizó dicha investigación.

Considerando los tres mAbs objeto principal de estudio en esta Tesis Doctoral, podemos hacer una clasificación separada de los mismos en función de su mecanismo de acción. Tocilizumab corresponde al grupo de fármacos inmunosupresores, en concreto, a los “inhibidores de la interleucina-6”, mientras que nivolumab y pembrolizumab son mAbs denominados “inhibidores de puntos de control inmunitario”.

A continuación, se hace una descripción más detallada de dichos grupos farmacológicos y los citados mAbs.

3.1. MAbs inmunosupresores inhibidores de la interleucina-6

Los mAbs inmunosupresores son aquellos que tienen la capacidad de inhibir o disminuir la intensidad de la respuesta inmunitaria del organismo. Las interleucinas (IL) son un tipo de citoquinas expresadas por distintas células corporales. Desempeñan un papel esencial en la activación y diferenciación de las células inmunitarias, así como en la proliferación, maduración, migración y adhesión. También tienen propiedades proinflamatorias

y antiinflamatorias. Su función principal es, por tanto, modular el crecimiento, la diferenciación y la activación durante las respuestas inflamatorias e inmunitarias. Las IL son un gran grupo de proteínas que pueden provocar muchas reacciones en células y tejidos uniéndose a receptores de alta afinidad en las superficies celulares [20].

En concreto, la interleucina-6 (IL-6) es producida por linfocitos T y B, fibroblastos y macrófagos en respuesta a diferentes estímulos (IL-1, IL-17 y TNF-α) durante la inflamación sistémica. Se trata de un potente mediador proinflamatorio importante en la defensa inmunitaria y en las enfermedades inmunomediadas. Es, por tanto, una citocina multifuncional proinflamatoria que media funciones pleiotrópicas en las respuestas inmunológicas durante la infección del huésped, las enfermedades inflamatorias, la hematopoyesis y la oncogénesis. También puede tener efectos antiinflamatorios. Se ha implicado a la IL-6 en la patogenia de enfermedades como enfermedades inflamatorias, osteoporosis y neoplasias.

Hoy en día, existen cuatro mAbs inhibidores farmacológicos de la IL-6 disponibles para uso clínico: tocilizumab, sarilumab y satralizumab, dirigidos contra el receptor de la IL-6 (IL-6R), y siltuximab, específico de la IL-6 [21,22]. De todos ellos, el mAb de interés en esta Tesis Doctoral es tocilizumab y será expuesto en más detalle a continuación.

3.1.1. Tocilizumab

Tocilizumab (TCZ) es un mAb IgG1 recombinante humanizado, producido en células CHO mediante tecnología del ADN recombinante. Actúa como agente inmunosupresor inhibiendo la acción de la IL-6. Este se une específicamente a los receptores de IL-6 tanto solubles como unidos a membranas (IL-6Rs e IL-6Rm) y es capaz de inhibir la señalización mediada por los mismos.

TCZ es el principio activo del medicamento RoActemra® (Roche Registration GmbH, Grenzach-Wyhlen, Alemania). Este medicamento lo podemos encontrar tanto para administración intravenosa (IV), cuya forma farmacéutica es un concentrado para solución para perfusión, como subcutánea (SC), en forma de solución inyectable en jeringa precargada. En ambos casos, RoActemra® es una solución transparente, de incolora a amarillo pálido [23].

La forma IV se comercializa a una concentración de 20 mg/mL y contine los siguientes excipientes: sacarosa, polisorbato 80, fosfato disódico dodecahidrato, fosfato dihidrógeno sódico dihidrato y agua para preparaciones inyectables.

Por otro lado, la forma SC está disponible a una concentración de 162 mg de TCZ en 0,9 mL y sus excipientes son: L-histidina, monohidrocloruro de L-histidina monohidrato, L-

arginina/hidrocloruro de L-arginina, L-metionina, polisorbato 80 y agua para preparaciones inyectables.

RoActemra®, tanto IV como SC, presenta las siguientes indicaciones farmacéuticas [23]:

1- El tratamiento de la artritis reumatoide (AR) grave, activa y progresiva en adultos no tratados previamente con metotrexato.
2- El tratamiento de la AR de moderada a grave en pacientes adultos con respuesta inadecuada o intolerancia a un tratamiento previo con uno o más fármacos antirreumáticos modificadores de la enfermedad (FAMEs) o con antagonistas del factor de necrosis tumoral (TNF).
3- El tratamiento de la artritis idiopática juvenil sistémica (AIJs) activa en pacientes desde 1 año de edad y mayores, que no han respondido adecuadamente a tratamientos anteriores con AINEs y corticoides sistémicos.
4- El tratamiento de artritis idiopática juvenil poliarticular (AIJp; factor reumatoide positivo o negativo y oligoartritis extendida) en pacientes de 2 años de edad y mayores.

En la mayoría de los casos, está indicado su uso en terapia combinada junto con metotrexato, pero también puede usarse en monoterapia cuando existe una intolerancia al metotrexato o cuando el tratamiento continuado con el mismo es inadecuado.

Además de estas indicaciones, la forma IV también está indicada para (1) el tratamiento de la enfermedad por coronavirus 2019 (COVID-19) en adultos que reciben corticosteroides sistémicos y requieren suplemento de oxígeno o ventilación mecánica, y (2) para el tratamiento del síndrome de liberación de citoquinas grave o potencialmente mortal inducido por receptor de antígeno quimérico de células T, en adultos y en población pediátrica de 2 años de edad y mayores.

Por otro lado, la forma SC también se puede utilizar para el tratamiento de Arteritis de Células Gigantes (ACG) en pacientes adultos.

En esta Tesis Doctoral nos centraremos en el empleo de este mAb para el tratamiento de la COVID-19, por su capacidad para inhibir la tormenta inflamatoria o tormenta de citoquinas que se produce en algunos pacientes infectados por el SARS-CoV-2. La Figura 4 muestra el mecanismo de acción por el cual tocilizumab inhibe la tormenta inflamatoria.

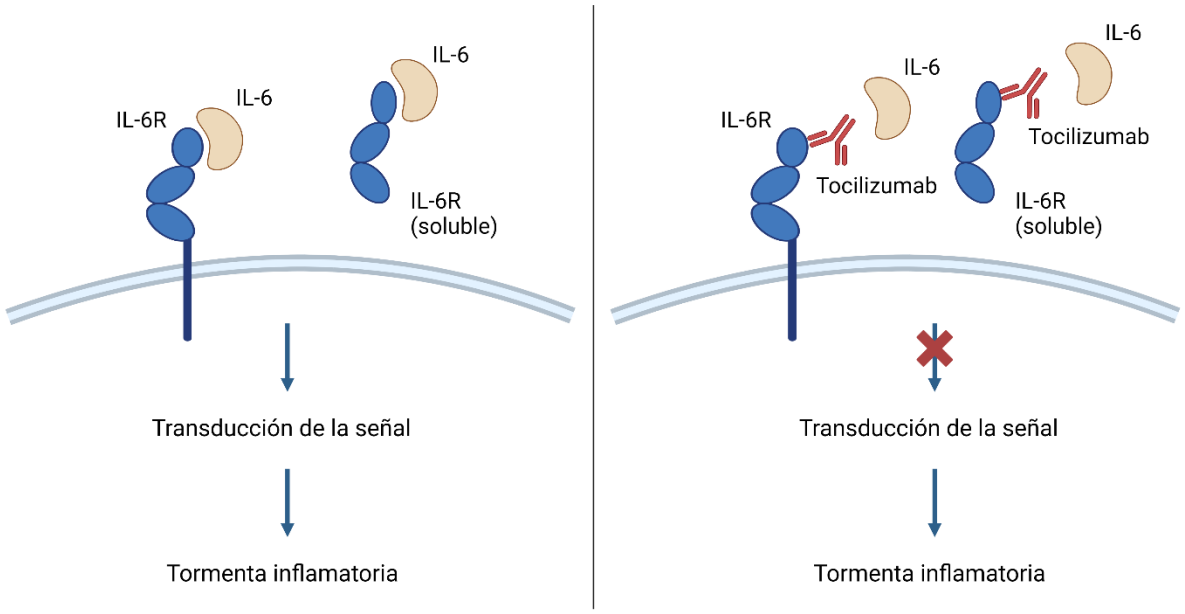

Figura 4. Mecanismo de acción de tocilizumab. Elaboración propia usando BioRender [24].

3.2. MAbs inhibidores de puntos de control inmunitario

Los inhibidores de puntos de control inmunitario (ICI) son inmunoterapias que potencian las respuestas inmunitarias contra el cáncer dirigiéndose a receptores inmunológicos de la superficie de los linfocitos T. Por lo tanto, los ICI se consideraron una opción de tratamiento novedosa en 2011 con la aprobación de ipilimumab, revolucionando el tratamiento del cáncer. Estos medicamentos permitieron obtener resultados duraderos con un perfil de toxicidad menor en algunas circunstancias. A diferencia de las estrategias terapéuticas tradicionales, los ICI actúan revigorizando el sistema inmunitario del huésped para que luche contra las células tumorales [25]. Estos puntos de control inmunitario son un grupo de vías inhibitorias y estimuladoras que influyen en la actividad de las células inmunitarias. Los anticuerpos dirigidos contra receptores inmunitarios inhibidores, como CTLA-4 (*Cytotoxic T-Lymphocyte Antigen 4* - antígeno 4 de linfocitos T citotóxicos), PD-1 (*Programmed cell death protein-1* - receptor 1 de muerte programada) y PD-L1 (*Programmed death ligand-1* - ligando 1 de muerte programada), han sido los agentes inmunoterapéuticos más utilizados en la última década. Actualmente, podemos encontrar varios mAbs aprobados por la EMA y la FDA (Administración de Alimentos y Medicamentos de Estados Unidos, del inglés *Food and Drug Administration*) para el tratamiento de diversos tipos de cáncer, los cuales se pueden dividir en los siguientes tres grupos (Figura 5):

- Inhibidores de PD-1: nivolumab, pembrolizumab y cemiplimab
- Inhibidores de PD-L1: atezolimumab, durvalumab y avelumab

- Inhibidores de CTLA-4: ipilimumab

Además, varios anticuerpos y pequeños compuestos dirigidos a diversas proteínas de punto de control inmunitario se encuentran en fase de desarrollo clínico, como B7H3, CD39, CD73, el receptor de adenosina A2A y CD47 [26,27].

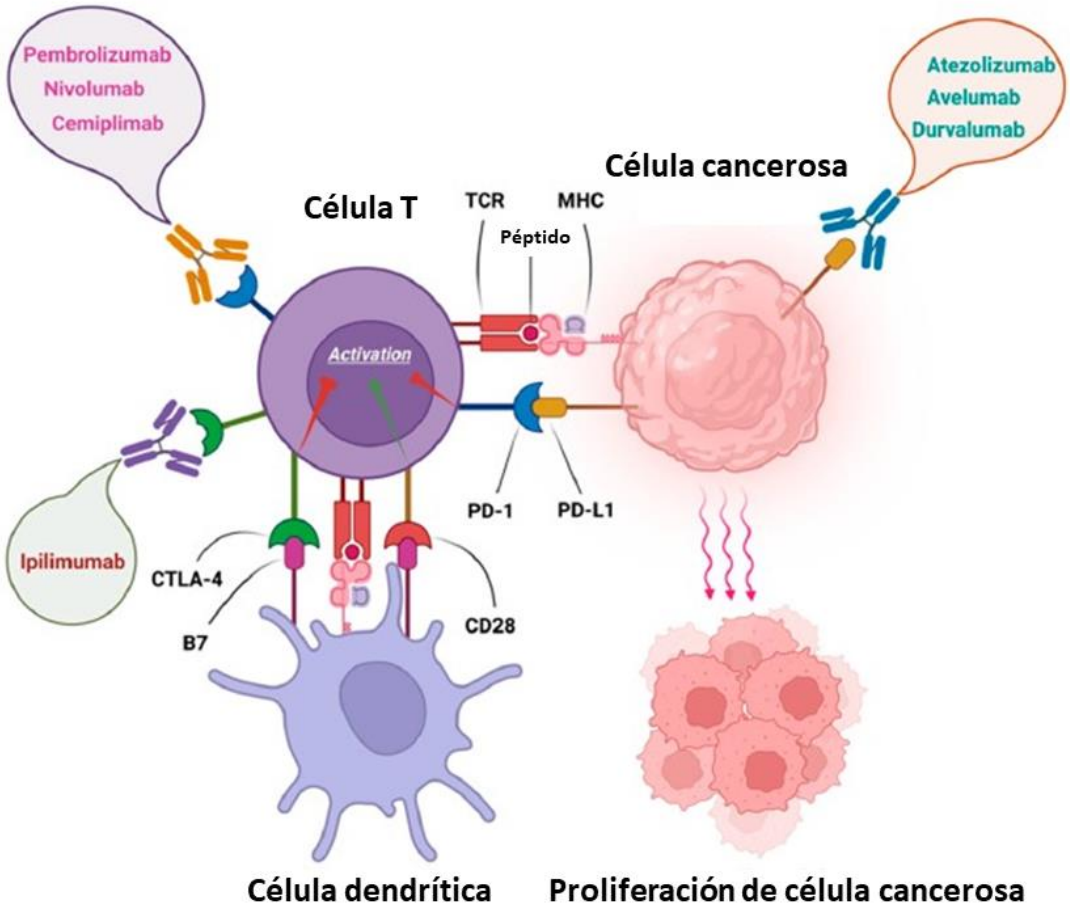

Figura 5. Mecanismo de acción de mAbs inhibidores de puntos de control inmunitario [26].

A continuación, dado que dos de los mAbs estudiados en esta Tesis Doctoral son nivolumab y pembrolizumab, nos centraremos en describir las características del grupo de los inhibidores de PD-1 para, posteriormente, describir los mAbs mencionados.

3.2.1. Inhibidores de PD-1

La proteína-1 de muerte celular programada (PD-1), un receptor inhibidor de la fase de respuesta inmunitaria, desempeña un papel clave en la señalización de la muerte celular programada para regular las respuestas mediadas por células del sistema inmunitario [26]. PD-1 es ampliamente expresada en células inmunitarias (células T, células B, macrófagos y

ciertos tipos de células dendríticas, etc.) y células tumorales por la señalización de receptores de antígenos y citoquinas [28].

Existen dos ligandos inmunorreguladores principales de PD-1, el ligando de muerte celular programada 1 y 2 (PD-L1/PD-L2) [29]. PD-L1 se expresa ampliamente tanto en el tejido linfoide como en el no linfoide, así como en las células presentadoras de antígenos (macrófagos, células dendríticas, etc.) y en todo tipo de células tumorales [30–32]. Tanto PD-1 como PD-L1 pertenecen a la familia de proteínas del punto de control inmunitario y actúan regulando las respuestas mediadas por células T.

En circunstancias normales, el sistema inmunitario produce una respuesta inmunitaria anticancerosa mediante la ejecución del ciclo de inmunidad contra el cáncer que elimina las células cancerosas. Sin embargo, la vía PD-1/PD-L1 es un mecanismo de resistencia inmunitaria adaptativa de las células tumorales a la actividad antitumoral inmunitaria endógena [33,34]. La interacción PD-1/PD-L1 regula a la baja la respuesta inmunitaria durante la regresión de la infección o el tumor o el desarrollo de la autotolerancia. PD-L1 suele sobreexpresarse en las células tumorales o en las células no transformadas del microambiente tumoral. De esta forma, inhibe las células T citotóxicas al unirse al receptor PD-1 de las células T activadas, lo que provoca un escape inmunitario.

Los inhibidores de PD-1 actúan inhibiendo la interacción entre PD-L1 y el receptor PD-1, impidiendo así que las células cancerosas eludan el sistema inmunitario y así reactivan el proceso de muerte de las células tumorales mediado por células T [28].

Se ha demostrado que las inmunoterapias dirigidas a la vía PD-1 han revolucionado el panorama del tratamiento de diferentes tipos de cáncer, como el carcinoma de células de Merkel, el melanoma, el carcinoma de células escamosas de cabeza y cuello y el cáncer de pulmón no microcítico [26].

3.2.2. Nivolumab

Nivolumab es un mAb humano de tipo IgG4, producido en células CHO mediante tecnología del ADN recombinante. Actúa uniéndose al receptor PD-1 de las células T y bloquea su interacción con PD-L1 y PD-L2. De esta forma, como se ha comentado anteriormente, se potencia la respuesta antitumoral de las células T [35].

Opdivo® (Bristol-Myers Squibb Pharma EEIG, Dublín, Irlanda) es el nombre comercial que recibe el medicamento que contiene nivolumab. Este medicamento se comercializa en estado líquido a una concentración de 10 mg/mL como un concentrado para solución para perfusión. Su apariencia es incolora/amillo pálido, transparente y tiene un pH de

aproximadamente 6,0. El listado de excipientes que contiene este medicamento sería el siguiente: citrato sódico dihidratado, cloruro sódico, manitol (E421), ácido pantético, polisorbato 80 (E433), hidróxido sódico, ácido clorhídrico y agua para preparaciones inyectables.

Las indicaciones terapéuticas de Opdivo® son las siguientes [35]:

1- Melanoma avanzado en adultos
2- Tratamiento adyuvante del melanoma en adultos con afectación de los ganglios linfáticos o enfermedad metastásica que hayan sido sometidos a resección completa
3- Cáncer de pulmón no microcítico
4- Mesotelioma pleural maligno
5- Carcinoma de células renales
6- Linfoma de Hodgkin clásico
7- Cáncer de células escamosas de cabeza y cuello
8- Carcinoma urotelial
9- Tratamiento adyuvante del carcinoma urotelial
10- Cáncer colorrectal
11- Carcinoma de células escamosas de esófago
12- Tratamiento adyuvante del cáncer de esófago o de la unión gastroesofágica
13- Adenocarcinoma gástrico, de la unión gastroesofágica o de esófago

Muchos de estos tratamientos se realizan en combinación con ipilimumab, un ICI inhibidor de CTLA-4, cuya terapia combinada ha demostrado dar una actividad antitumoral sinérgica. Nivolumab también puede combinarse, según las necesidades, con la quimioterapia tradicional (por ejemplo, basada en platino).

3.2.3. Pembrolizumab

Pembrolizumab se trata de un mAb humanizado de tipo IgG4, producido en células CHO mediante tecnología del ADN recombinante. Al igual que nivolumab, este actúa uniéndose al receptor PD-1 de las células T y bloquea su interacción con PD-L1 y PD-L2. Como resultado, se potencia las respuestas de las células T, incluyendo las respuestas antitumorales, mediante el bloqueo de PD-1, unido a PD-L1 y PD-L2, que se expresan en las células presentadoras de antígenos y que se pueden expresar por tumores u otras células en el microambiente tumoral [36].

El nombre comercial del medicamento que contiene pembrolizumab es Keytruda® (Merck Sharp & Dohme B.V., Haarlem, Países Bajos), el cual se comercializa a una concentración de 25 mg/mL como concentrado para solución para perfusión. Se trata de una

solución transparente incolora o ligeramente amarilla, con un pH entre 5,2 y 5,8. Los excipientes que contiene este medicamento son: L-histidina, hidrocloruro de L-histidina monohidrato, sacarosa, polisorbato 80 (E433) y agua para preparaciones inyectables.

Keytruda® presenta las siguientes indicaciones terapéuticas [36]:

1- Melanoma avanzado en adultos y adolescentes a partir de 12 años
2- Cáncer de pulmón no microcítico
3- Linfoma de Hodgkin clásico
4- Carcinoma urotelial
5- Carcinoma de células escamosas de cabeza y cuello
6- Carcinoma de células renales
7- Cáncer colorrectal
8- Cáncer gástrico, de intestino delgado o biliar
9- Carcinoma de esófago
10- Cáncer de mama triple negativo
11- Cáncer de endometrio
12- Cáncer de cuello de uterino

Pembrolizumab puede utilizarse en monoterapia o en combinación con otros fármacos, dependiendo de la enfermedad, como pueden ser pemetrexed, paclitaxel, axitinib, lenvatinib o bevacizumab. Además, también puede combinarse con quimioterapia basada en platino y 5-fluorouracilo en algunos casos.

4. ANÁLISIS COMPRENSIVOS DE ANTICUERPOS MONOCLONALES: ATRIBUTOS CRÍTICOS DE LA CALIDAD

Para realizar el análisis comprensivo de un mAb debe llevarse a cabo una caracterización exhaustiva de acuerdo con las directrices reguladoras, como las de la EMA y documentadas en la "Guía sobre el desarrollo, producción, caracterización y especificación de anticuerpos monoclonales y productos relacionados" [37]. La caracterización detallada implica la elucidación de las propiedades estructurales, fisicoquímicas, inmunológicas y biológicas, por un lado, y la evaluación de las impurezas y la cuantificación del anticuerpo, por otro, en línea con las especificaciones de la guía ICH Q6B [17]. Esta caracterización se lleva a cabo mediante el empleo de una serie de técnicas analíticas adecuadas [38].

Los atributos críticos de la calidad (CQAs, del inglés *Critical Quality Attributes*) son definidos en la guía ICH Q8(R2) [39] como una propiedad o característica física, química, biológica o microbiológica que debe encontrarse dentro de un límite, intervalo o distribución

adecuados para garantizar la calidad deseada del producto biofarmacéutico. Esta definición se refiere únicamente a los posibles impactos en los pacientes.

Los CQAs se utilizan para determinar las especificaciones (es decir, la identificación, la potencia y la pureza) que mantiene el perfil analítico de los lotes clínicos. Esto se consigue mediante una evaluación exhaustiva y sistemática de las variantes del producto, las impurezas relacionadas con el proceso, la composición y la resistencia del producto, el aspecto y los atributos microbiológicos, así como los excipientes y las materias primas para determinar su criticidad.

Los atributos de calidad pueden clasificarse en diferentes categorías. La lista de CQAs comprende generalmente variantes del producto e impurezas relacionadas con el proceso de producción que pueden afectar potencialmente a los mecanismos de acción/toxicidad de la molécula, o a las propiedades generales de seguridad o farmacocinéticas. Aunque no se puede estudiar directamente la relación de cada CQA con los resultados clínicos, se puede inferir el impacto potencial en el paciente a partir de la caracterización analítica y biológica, incluidos los estudios de estructura-función.

La identificación de los CQAs comienza en las primeras fases del desarrollo y evoluciona a medida que se adquiere un mayor conocimiento del producto [40]. La identificación temprana de los CQA ayuda a centrar los esfuerzos de desarrollo en aquellos atributos que pueden requerir un mayor conocimiento o control. Los CQAs finales suelen confirmarse en las fases posteriores del desarrollo del proceso comercial, anticipándose a la finalización de la estrategia de control comercial.

El enfoque para la identificación de CQAs para un mAb depende de la categoría del atributo de calidad que se esté evaluando. Los atributos se dividen en las siguientes categorías de evaluación [41]:

- **Variantes del producto e impurezas relacionadas con el proceso de producción:** Estas se evalúan para determinar su criticidad en función del producto para tener en cuenta las modificaciones únicas, la indicación de los mecanismos de acción y la vía de administración. Las variantes del producto formadas en los residuos de aminoácidos en/cerca de los sitios de unión a antígenos o receptores, las estructuras de glicanos y las variantes en las terminaciones polipeptídicas pueden considerarse para la evaluación de la bioactividad y la farmacocinética. Las variantes formadas en todos los sitios de anticuerpos deben considerarse para la evaluación de la inmunogenicidad y el impacto en la seguridad. Los atributos de calidad pueden incluir variantes relacionadas con el tamaño, la carga, la oxidación, glicosilación, variantes estructurales e impurezas relacionadas con el proceso de producción.

- **CQAs obligatorios:** Debido a su gran importancia para la eficacia y la seguridad del producto o para los requisitos reglamentarios, algunos atributos de calidad se clasifican por defecto como CQAs obligatorios. Dentro de los mismo encontramos los relativos a la composición y la potencia (contenido proteico, osmolaridad, pH, buffer utilizado, etc.), al aspecto del medicamento (color, claridad, opalescencia), a los específicos del producto (presencia de partículas visibles o subvisibles, esterilidad) y a la ausencia de agentes adventicios (virus, bacterias, endotoxinas).
- **Materias primas:** La toxicidad de las materias primas utilizadas en el proceso de fabricación de sustancias farmacológicas se evalúa teniendo en cuenta una ingesta diaria estimada teórica, comparada con un umbral de preocupación toxicológica, proporcionado por un toxicólogo. Los excipientes no se evalúan utilizando este enfoque, ya que la información de seguridad puede estar disponible a través de la experiencia con productos biofarmacéuticos comercializados o adquirida a través de los ensayos clínicos con un nuevo producto.
- **Compuestos lixiviables:** El enfoque para la identificación de lixiviables como CQA depende de si un compuesto específico puede detectarse en el producto final. Si se demuestra que un lixiviable específico supera los niveles aceptables y seguros, por ejemplo, según lo determinado sobre la base de ICH M7 [42], ese compuesto se designa como CQA.

En concreto, en esta Tesis Doctoral se han seleccionado una serie de técnicas analíticas y estrategias para analizar CQAs de medicamentos biotecnológicos basados en mAbs. Los atributos estudiados incluyen: estructuras secundarias, estructuras terciarias, perfil de oligómeros, perfil de particulado, perfil de variantes de carga, perfil de glicanos, perfil de PTMs, concentración y funcionalidad. Mediante el análisis conjunto de los resultados derivados de estos CQAs, se puede llevar a cabo el análisis comprensivo que permita evaluar de forma rigurosa la estabilidad de las preparaciones farmacéuticas de mAbs frente al impacto de su manipulación rutinaria en hospitales. Esto se demuestra y expone en los capítulos experimentales de esta Tesis Doctoral.

4.1. Caracterización fisicoquímica y funcional de mAbs terapéuticos

La caracterización fisicoquímica de los productos biofarmacéuticos, tal y como establece la guía ICH Q6B [17], debe abarcar el análisis de la secuencia de aminoácidos, la secuenciación N-terminal y C-terminal, la cartografía peptídica, la identificación de puentes disulfuro, la N-glicosilación, la estructura de los glicanos y las PTMs, como la oxidación, la

desamidación, etc. Las estructuras secundarias, terciarias y cuaternarias se conocen colectivamente como estructuras de orden superior y son responsables de la forma tridimensional y del correcto plegamiento del biofármaco [43]. Una forma tridimensional incorrecta afecta a la funcionalidad de la proteína y puede provocar la inhibición de la unión al antígeno, la exposición de epítopos inmunogénicos y la agregación de la proteína [38].

Por lo general, los mAbs presentan diversos recursos de heterogeneidad, como el procesamiento de la lisina C-terminal, la oxidación, la desamidación, la fragmentación, la isomerización, el desajuste del enlace disulfuro, la N-glicosilación, que dan lugar a un complejo perfil de pureza/impureza que comprende varias entidades o variantes moleculares [44]. Estos incluyen la determinación de propiedades fisicoquímicas, por ejemplo, peso o tamaño molecular, patrón de isoformas, datos cromatográficos (basados en tamaño, carga, hidrofobicidad/hidrofilicidad) y perfiles espectroscópicos (análisis de estructura, como secundaria y terciaria) [38].

Por otro lado, la caracterización funcional de mAbs terapéuticos se puede llevar a cabo estudiando su actividad biológica. Esta actividad puede evaluarse mediante ensayos adecuados in vitro (métodos enzimáticos/radioisótopos/florescencia) e in vivo [38].

En el siguiente apartado se recogen y describen las principales técnicas analíticas utilizadas en esta Tesis Doctoral para la caracterización fisicoquímica y funcional de mAbs terapéuticos.

4.2. Técnicas analíticas para el análisis de mAbs terapéuticos

Para la caracterización de mAbs terapéuticos se han desarrollado, puesto a punto y validado estrategias de análisis nuevas y en constante evolución que incluyen métodos cromatográficos, espectroscópicos y de espectrometría de masas, entre otros. Estos procesos analíticos proporcionan una caracterización exhaustiva de los mAbs, ilustrando la organización de la proteína. La Tabla 3 recoge una recopilación de las técnicas analíticas empleadas en los estudios llevados a cabo en esta Tesis Doctoral, las cuales son descritas en los siguientes subapartados.

Tabla 3. Técnicas analíticas empleadas en esta Tesis Doctoral para la caracterización de mAbs terapéuticos.

Clasificación	Técnica analítica	Atributo en estudio
Técnicas cromatográficas	Cromatografía de exclusión molecular (SEC)	Perfil de agregación
	Cromatografía de intercambio iónico (ICX)	Perfil de variantes de carga
	Cromatografía de fase inversa (RPC)	Cuantificación del contenido proteico
Técnicas espectroscópicas	Dicroísmo circular (CD)	Estructura secundaria
	Fluorescencia intrínseca de triptófanos (IT-FS)	Estructura terciaria
	Dispersión de luz dinámica (DLS)	Particulado en solución
Técnica espectrométrica	Espectrometría de masas (MS)	Isoformas, PTMs
Inmunoensayos	ELISA	Actividad biológica

4.2.1. Cromatografía de líquidos

La cromatografía de líquidos de altas/ultra altas prestaciones (HPLC/UHPLC) es una de las técnicas clave para la caracterización de productos biofarmacéuticos, ya que permite separar los componentes de una mezcla entre las dos fases -móvil y estacionaria- en función de sus propiedades fisicoquímicas.

La cromatografía de líquidos que se usa para la caracterización de mAbs terapéuticos puede utilizarse en dos modos distintos, conocidos como: no desnaturalizantes y desnaturalizantes. Por un lado, los modos no desnaturalizantes o nativos se caracterizan por emplear fases móviles que no desnaturalizan la proteína y le permite mantener su conformación original. A esta clasificación pertenecen la cromatografía de exclusión molecular (SEC, del inglés *size exclusion chromatography*) y la cromatografía de intercambio iónico (IXC, del inglés *ionic exchange chromatography*). Por otro lado, los modos cromatográficos desnaturalizantes utilizan fases móviles agresivas para la estructura de la proteína (pH elevados, fuerzas iónicas elevadas, etc.) que hacen que esta se desnaturalice durante el proceso cromatográfico. Dentro de esta clasificación podemos encontrar la cromatografía de fase inversa (RPC, del inglés *reverse phase chromatography*).

4.2.1.1. Cromatografía de exclusión molecular (SEC)

La SEC es una técnica tradicional ampliamente empleada para la caracterización detallada de proteínas terapéuticas. Se considera una técnica de referencia para la evaluación cualitativa y cuantitativa de agregados, dímeros, trímeros y fragmentos de las mismas [45]. Esta separa las biomoléculas de diferente tamaño en función de su volumen. La fase estacionaria consiste en partículas porosas esféricas con un tamaño de poro cuidadosamente controlado, a través de las cuales las biomoléculas se difunden en función de su diferencia de volumen molecular utilizando un tampón acuoso como fase móvil en modo isocrático [46]. En concreto, las partículas más pequeñas se quedan más tiempo retenidas porque penetran más profundamente en las partículas porosas, mientras que las de mayor tamaño serán menos retenidas por impedimento estérico, lo que hace que las moléculas más grandes eluyan primero de la columna [47].

La principal ventaja de este enfoque son las condiciones suaves de la fase móvil que permiten la caracterización de proteínas con un impacto mínimo en la estructura conformacional y el entorno local [45].

Las columnas SEC clásicas son de polímero o de sílice; sin embargo, actualmente se utiliza en las columnas una capa hidrófila de diol modificada covalentemente que reduce la unión imprecisa de las proteínas a la sílice [38]. Además, en los últimos años se han producido una serie de avances en SEC que mejoran la cantidad de información que puede obtenerse de una sola inyección. Entre ellos, el uso de columnas más cortas (por ejemplo, 15 cm) y estrechas (4,6 mm de diámetro interno) con partículas de menor tamaño (inferior a 3 µm) mejoran el rendimiento y la resolución, pero hay que tener cuidado para evitar el riesgo de degradación por la alta presión (>400 bar) [46].

Esta técnica también se utiliza para la estimación de la masa molecular de los analitos en estudio realizando una "calibración de la columna". Esta calibración consiste en el análisis de un patrón comercial que contiene una mezcla de diversas proteínas de las que se conoce exactamente su masa molecular. De esta forma, se puede establecer una relación funcional (no lineal) entre los tiempos de retención que se obtienen al analizar con una determinada columna esta mezcla de proteínas, y las correspondientes masas moleculares. Mediante la ecuación de la función establecida se puede estimar la masa molecular de una proteína desconocida [47].

Los detectores analíticos empleados en la técnica SEC son usualmente de absorción Ultravioleta/Visible (UV/Vis). Además, en los últimos años es común también encontrar esta técnica acoplada a un espectrómetro de masas, lo que ha sido posible gracias al empleo de fases móviles compuestas por sales volátiles –en lugar de no volátiles- que permiten una

adecuada ionización de la muestra para la detección mediante MS [48–50], aunque no siempre se consiguen óptimos resultados.

En la presente Tesis Doctoral se han utilizado métodos SEC de ultra altas prestaciones con detección UV (SE/(U)HPLC-DAD), usando sales no volátiles, para evaluar la formación de oligómeros de tocilizumab (*Capítulo 2*), nivolumab (*Capítulo 4*), pembrolizumab (*Capítulo 5*) y diferentes mAbs (*Capítulo 6*). Además, también se ha utilizado la SEC acoplada a MS (SE/UHPLC-UV-MS(Orbitrap)), usando sales volátiles, para caracterizar el perfil de isoformas de nivolumab (*Capítulo 4*).

4.2.1.2. Cromatografía de intercambio iónico (IXC)

La IXC se utiliza para la caracterización de la heterogeneidad de carga de las proteínas resultante de modificaciones enzimáticas o químicas. La IXC permite la separación de las moléculas en función de la carga iónica neta mediante el uso de polímeros de intercambio iónico, los cuales retienen los solutos gracias a fuerzas electrostáticas. La fase estacionaria lleva en su superficie cargas eléctricas fijas que retienen contraiones móviles, los cuales se intercambian por iones de la fase móvil. De esta forma, la separación de proteínas se lleva a cabo por competencia entre entidades con distinta carga superficial y los grupos con carga opuesta sobre una matriz de intercambio iónico (fase estacionaria).

Dentro de la IXC, encontramos dos variedades cromatográficas: la cromatografía de intercambio aniónico (AXC, del inglés *anionic exchange chromatography*) y cromatografía de intercambio catiónico (CXC, del inglés *cationic exchange chromatography*). Sin embargo, para el análisis de mAbs, la más usada es la CXC, ya que estas proteínas presentan más cargas positivas (aminoácidos con cadenas laterales básicas) en su superficie que negativas, es decir, son proteínas con punto isoeléctrico básico [3,45].

Para realizar un análisis por CXC, se pueden utilizar dos modos de elución diferentes. Por un lado, tenemos la elución por gradiente de sales, el enfoque clásico, que implica un aumento de la concentración de sal durante el gradiente, lo que debilita las interacciones iónicas y provoca la elución de la proteína [51]. Por otro lado, el segundo modo aplica un gradiente de pH, de forma que cambia la carga de la proteína y, por lo tanto, su interacción con la fase estacionaria [52]. También resulta interesante comentar que se pueden utilizar ambos modos de elución de forma combinada. La separación de las proteínas, por tanto, se basa en su punto isoeléctrico [38]. Al igual que en la SEC, en la IXC se suele utilizar la detección mediante un detector UV/Vis, ya que suelen emplearse sales no volátiles, incompatibles con la detección mediante espectrometría de masas.

En cuanto a las fases estacionarias, los intercambiadores de iones pueden clasificarse como intercambiadores débiles o fuertes. Los intercambiadores de cationes débiles están compuestos por un ácido débil que pierde gradualmente su carga a medida que disminuye el pH (por ejemplo, grupos carboximetilo), mientras que los intercambiadores de cationes fuertes están compuestos por un ácido fuerte que es capaz de mantener su carga en un amplio rango de pH (por ejemplo, grupos sulfopropilo).

Se ha demostrado que la IXC resuelve con éxito las heterogeneidades que podrían surgir de las PTMs, ya que estas modificaciones pueden producir un cambio en la carga neta de la proteína. De esta forma, existen PTMs que inducen cargas negativas en la superficie de la proteína, dando lugar a modificaciones ácidas, mientras que otras inducen cargas positivas en su superficie, originando modificaciones básicas. Esto lleva a que se puedan distinguir en el cromatograma tres tipos de zonas: la zona de variantes de carga ácidas, la zona correspondiente al pico de la especie neutra (mayoritaria) y la zona de variantes de carga básicas. En CXC las variantes ácidas eluirán antes que el pico de la variante neutra, y por último las variantes básicas. Por el contratio, en el modo de AXC, el orden de elución es al contrario [53].

Dentro de las PTMs, la deamidación, la glicación y la presencia de ácido siálico en los glicanos contribuyen a la formación de variantes ácidas del mAb. En cambio, la lisina C-terminal, la amidación de la prolina C-terminal y la glutamina N-terminal no ciclada contribuyen a la formación de las variantes básicas [54,55].

En la presente Tesis Doctoral se ha empleado un método de cromatografía líquida de ultra altas prestaciones de intercambio catiónico fuerte con detección UV (SCX/UHPLC-UV), en el que se ha llevado a cabo una separación de las variantes de carga del mAb tocilizumab por gradiente de sales (*Capítulo 2*).

4.2.1.3. Cromatografía de fase inversa (RPC)

En la RPC, la retención de solutos se produce principalmente a través de las interacciones hidrófobas entre los residuos de aminoácidos no polares de las proteínas y los ligandos n-alquílicos enlazados de la fase estacionaria. De este modo, las proteínas eluyen en función de su hidrofobicidad. Por esta razón, las condiciones isocráticas son poco prácticas y se recomienda el modo de elución en gradiente [45]. Debido al carácter anfifílico de las proteínas, estas interaccionan con la fase estacionaria solo por pequeñas partes apolares. Al inicio del gradiente, la fase móvil suele ser de naturaleza acuosa y a medida que el gradiente avanza, la molécula quedará totalmente desorbida de la fase estacionaria, provocando su elución [56].

Usualmente se usan fases estacionarias apolares como son las particuladas de C18 y C8. Como fases móviles se suele usar acetonitrilo o metanol y ácido trifluoroacético (TFA, del inglés *trifluoroacetic acid*) o ácido fórmico (FA, del inglés *formic acid*) al 0,1%. El TFA y el FA se usan como modificadores que mejoran el perfil de los picos cromatográficos y la ionización de las moléculas en el caso de acoplamiento con MS. Esta técnica requiere además el empleo de altas temperaturas (70-90 °C), para incrementar la difusión de las proteínas en la fase móvil, y la detección se realiza mediante espectrofotometría de absorción UV/Vis [3,45].

La eficacia de la RPC es superior a la de otros modos cromatográficos y su robustez la hace muy adecuada para su uso en un entorno de análisis rutinario. Sus principales ventajas sobre cualquier otro modo cromatográfico son su alto poder de resolución y su compatibilidad inherente con la MS, lo que le permite evaluar las variaciones de las proteínas derivadas de diferentes reacciones químicas o PTMs. El amplio uso y la popularidad de la RPC pueden atribuirse a su flexibilidad y adaptabilidad, con una versatilidad para separar prácticamente cualquier tipo de analito y su compatibilidad para ser acopada a la espectrometría de masas.

Dentro de su versatilidad, la RPC se ha utilizado para el análisis de proteínas intactas o de grandes fragmentos proteicos generados tras una digestión enzimática. La técnica se aplica a menudo en la industria biofarmacéutica para evaluar la identidad, la pureza, la estabilidad, la vida útil y también como prueba de liberación. En general, se pueden separar y cuantificar las formas oxidadas, reducidas y deamidadas, entre muchas otras, que poseen una hidrofobicidad diferente en comparación con la proteína nativa [55].

Actualmente, la RPC es muy utilizada para una caracterización exhaustiva de los mAbs, como la deducción de la secuencia de aminoácidos y la identificación de las modificaciones y degradaciones postraduccionales. Para ello, el mapeo peptídico es el enfoque preferido, que requiere una separación completa de los péptidos y una cobertura absoluta de la secuencia [38,57].

En esta Tesis Doctoral se ha empleado un método de cromatografía líquida de ultra altas prestaciones de fase inversa con detección UV y acoplada a MS ((RP)UHPLC/UV-(HESI/Orbitrap™)MS) para el desarrollo de un método validado indicador de la estabilidad para la cuantificación proteica de nivolumab y la identificación de isoformas (*Capítulo 3*). Esta técnica, en su modalidad de masas/masas ((RP)UHPLC/UV-(HESI/Orbitrap™)MS/MS) también se ha empleado para el análisis de isoformas y el estudio de PTMs (mapeo peptídico) de pembrolizumab (*Capítulo 5*).

4.2.2. Técnicas espectroscópicas

Para dilucidar las estructuras específicas de orden superior de los mAbs (estructura terciaria y secundaria) se pueden emplear diferentes métodos espectroscópicos. Aunque varios métodos analíticos, como la cromatografía líquida o el mapeo peptídico, aportan información sobre la estructura covalente de las proteínas (secuencias de aminoácidos y PTMs), ninguno aporta información sobre las estructuras de orden superior de los mAbs. En los últimos años, la aplicación de numerosas estrategias espectroscópicas avanzadas, como el dicroísmo circular (CD, del inglés *circular dichroism*) o la espectroscopía de fluorescencia, en concreto la fluorescencia intrínseca de triptófanos (IT-FS, del inglés *intrinsic tryptophan fluorescence spectroscopy*), *se* han utilizado para determinar estas estructuras de los mAbs [38]. Además, la técnica de dispersión de luz dinámica (DLS, del inglés *dynamic light scattering*) es otra de las técnicas espectroscópicas ampliamente utilizadas para la caracterización de mAbs en disolución, fundamentalmente para el estudio del particulado.

A continuación, se describen las técnicas mencionadas, especificando sus aplicaciones en el estudio de proteínas terapéuticas.

4.2.2.1. Espectropolarimetría de dicroísmo circular (CD) en el UV lejano

La espectropolarimetría de CD es una técnica espectroscópica de absorción basada en la medida de CD en un intervalo de longitud de onda concreto. El CD hace referencia a la absorción diferencial entre la luz circularmente polarizada a la derecha y la luz circularmente polarizada a la izquierda [58]. Las señales de CD solo aparecen allí donde se produce la absorción de la radiación, por lo que las bandas espectrales se asignan fácilmente a distintas características estructurales de una molécula.

El CD es una técnica consolidada que determina fácilmente la estructura de orden superior de las proteínas y de los mAbs en particular [59]. La estructura secundaria de una proteína se determina por CD utilizando el intervalo de longitudes de onda del UV lejano (190-250 nm), donde el cromóforo de enlace peptídico es activo. En cambio, la región de longitud de onda UV cercana (250-340 nm) puede detectar cambios en la orientación quiral relativa de residuos aromáticos internos como triptófanos (266, 295-305 nm), tirosinas (265-290 nm) y fenilalaninas (265 nm), y puede proporcionar información sobre cambios en la estructura terciaria global de una proteína [60]. De esta forma, el CD aporta información estructural complementaria de varias regiones espectrales.

Los diferentes tipos de estructura secundaria que se encuentran en las proteínas dan lugar a espectros de CD característicos en el UV lejano. Existen varios algoritmos que utilizan los datos de los espectros CD de UV lejano para proporcionar una estimación de la

composición de la estructura secundaria de las proteínas. La mayoría de los procedimientos emplean conjuntos de datos básicos que comprenden los espectros de CD de proteínas de varios tipos de pliegues cuyas estructuras se han resuelto mediante cristalografía de rayos X. Se ha desarrollado un servidor en línea, DICHROWEB [61,62], alojado en el *Birkbeck College* de la Universidad de Londres (Reino Unido), que permite introducir datos en varios formatos y analizarlos mediante los distintos algoritmos con una selección de bases de datos de proteínas de referencia. Entre los algoritmos más utilizados se encuentran SELCON3 [63], VARSLC [64], CDSSTR [65], K2d [66] y CONTIN [67]. Finalmente, con el objetivo de evaluar la comparación de los resultados experimentales con los teóricos calculados, DICHROWEB permite calcular un parámetro de la bondad del ajuste denominado 'raíz de la desviación cuadrática media normalizada' (NRMSD, del inglés *normalised root mean squared deviation*). Valores inferiores a 0,1 indican que los cálculos realizados son confiables [68].

Cabe destacar que, para un análisis fiable de la estructura secundaria, es necesario asegurarse de que se conoce con precisión la concentración de la solución de proteína. Además, también es importante tener en cuenta que los iones de cloruro absorben fuertemente por debajo de 195 nm y, por lo tanto, no se recomiendan altas concentraciones de sales de cloruro como componente de una disolución tampón para el trabajo con CD [69].

Las principales ventajas del CD se derivan de la rapidez y comodidad de la técnica. En comparación con la cristalografía de rayos X y la resonancia magnética nuclear, las mediciones de CD pueden llevarse a cabo rápidamente; así, en poco tiempo pueden obtenerse espectros de buena calidad en el UV lejano y cercano. Los estudios de CD en el UV lejano, en particular, sólo requieren pequeñas cantidades de material y, puesto que la técnica no es destructiva, suele ser posible recuperar la mayor parte o la totalidad de la disolución y, por tanto, realizar múltiples experimentos con la misma muestra. La posibilidad de utilizar cubetas con trayectorias que difieren en varios órdenes de magnitud significa que es relativamente fácil estudiar un intervalo muy amplio de concentraciones de proteínas.

La principal limitación del CD es que solo proporciona información estructural de resolución relativamente baja. Así, aunque el CD en el UV lejano puede dar estimaciones razonablemente fiables del contenido de estructura secundaria de una proteína (en términos de proporciones de α-hélice, láminas β, giros β y estructuras desordenadas), hay que tener en cuenta que se trata de cifras globales y no indican qué regiones de la proteína son de qué tipo estructural. Sin embargo, el CD puede seguir desempeñando un papel muy útil en el trabajo estructural, especialmente cuando se emplea de forma complementaria con otras técnicas estructurales. Aparte de los estudios de desdoblamiento y plegamiento de proteínas, el CD se ha aplicado ampliamente en el campo de la ingeniería de proteínas [70].

En esta Tesis Doctoral se ha utilizado la técnica de CD en el UV lejano para caracterizar las estructuras secundarias de nivolumab (*Capítulo 4*) y pembrolizumab (*Capítulo 5*). Posteriormente, se ha utilizado DICHROWEB para la deconvolución de los espectros obtenidos por CD y el cálculo del contenido porcentual de estructuras secundarias.

4.2.2.2. Espectroscopía de fluorescencia intrínseca de triptófanos (IT-FS)

La espectroscopía de fluorescencia es una técnica ampliamente utilizada en estudios sobre el plegamiento y la dinámica conformacional de proteínas. En general, la razón de su gran aplicabilidad en estudios de proteínas se debe a tres propiedades fundamentales. En primer lugar, las señales de fluorescencia son muy sensibles al entorno inmediato del fluoróforo en estudio, por lo que, si se produce un cambio conformacional que afecte a la posición del mismo, la señal de fluorescencia cambiará drásticamente. En segundo lugar, la técnica proporciona una relación señal-ruido muy elevada utilizando cantidades relativamente pequeñas de proteína, convirtiéndola en una técnica muy sensible. En tercer lugar, además de la alta sensibilidad de detección de la fluorescencia, la escala temporal de emisión está en el rango de los nanosegundos. Esto, unido a la elevada relación señal-ruido, permite que los tiempos de adquisición de datos sean bastante rápidos en relación con las escalas de tiempo de las transiciones de plegamiento y conformación. Además, debido a su alta sensibilidad, se requiere una cantidad pequeña de material proteico [71,72].

Sin embargo, también hay que reconocer una serie de limitaciones. En general, la fluorescencia es una señal local, que aporta información acerca del entorno que rodea directamente al fluoróforo. Esto limita y complica la interpretación de los cambios en la señal de fluorescencia en términos de su origen y localización estructural. Normalmente, la información que se puede obtener directamente de la interpretación de los parámetros de fluorescencia se limita al grado de exposición del fluoróforo al disolvente y al alcance de su movilidad local.

La mayoría de las proteínas contienen residuos de aminoácidos que son intrínsecamente fluorescentes: triptófano, tirosina y fenilalanina. De estos tres aminoácidos aromáticos, el triptófano es, con diferencia, el más útil. Aunque los grandes cambios en la conformación de la proteína modifican claramente la intensidad de la fluorescencia de la tirosina y la fenilalanina, sus bajos coeficientes de extinción y rendimientos cuánticos, junto con la relativa falta de sensibilidad ambiental de su energía de emisión, los hacen significativamente menos útiles que el triptófano. En realidad, esto puede ser una ventaja porque las proteínas tienden a contener menos residuos de triptófano que de tirosina y fenilalanina y, por lo tanto, se puede obtener información local más específica excitando

selectivamente los residuos de triptófano utilizando longitudes de onda de excitación de 295 nm o superiores [72].

Por tanto, si excitamos a 280 nm, la fluorescencia intrínseca de la proteína se deberá principalmente al triptófano y, en menor medida, a la tirosina y la fenilalanina, siendo el triptófano el que absorberá a mayor longitud de onda de los tres aminoácidos y el que presentará el mayor coeficiente de extinción. Si por el contrario excitamos a longitudes de onda entre 295 y 305 nm, los residuos de triptófano emitirán fluorescencia de forma selectiva, por lo que la mayoría de los estudios sobre la estabilidad de los mAbs se refieren a la emisión de triptófano cuando investigan la fluorescencia intrínseca de la proteína [71].

El triptófano, debido a su carácter aromático, se encuentra a menudo (aunque no siempre) total o parcialmente enterrado en el núcleo hidrofóbico del interior de las proteínas. Al alterarse la estructura terciaria o cuaternaria de la proteína, estas cadenas laterales quedan más expuestas al disolvente. Dado que el momento dipolar de estado excitado del triptófano es bastante grande, la energía de emisión es muy sensible a la polaridad (y dinámica) del entorno. Aquellos residuos que están total o parcialmente enterrados en el interior relativamente hidrofóbico de las proteínas mostrarán una emisión desplazada hacia el azul. Los espectros del triptófano en proteínas plegadas son claramente identificables en relación con el espectro del triptófano cuando se expone al agua, con un máximo a 355 nm [72].

Aunque la energía de emisión de un residuo de triptófano, incluso parcialmente enterrado, en una proteína plegada se desplazará invariablemente hacia el rojo al desplegarse, no es posible predecir cuál será el efecto de la exposición al disolvente sobre el rendimiento cuántico (intensidad total) de la emisión. Esto se debe al hecho de que el rendimiento cuántico del triptófano en las proteínas es difícil de predecir [72], ya que la emisión del triptófano es altamente sensible a las condiciones del disolvente, proximidad de aminoácidos ácidos, número y localización de triptófanos [73].

En la presente Tesis Doctoral se ha empleado la espectroscopía de fluorescencia para evaluar la estructura terciaria, empleando los espectros de emisión intrínseca del triptófano (excitación a 298 nm), de tocilizumab (*Capítulo 2*), nivolumab (*Capítulo 4*) y pembrolizumab (*Capítulo 5*). Los datos obtenidos por esta técnica se han empleado para el cálculo del centro de masas del espectro, con la finalidad de detectar desplazamientos del máximo de emisión del triptófano.

4.2.2.3. Dispersión de luz dinámica (DLS)

DLS es una técnica fisicoquímica empleada para la determinación de la distribución de tamaños de partículas en suspensión o macromoléculas en disolución, tales como proteínas.

Cuando la luz láser alcanza estas partículas/macromoléculas, se dispersa en todas las direcciones posibles y se obtendrá una dispersión determinada [74]. Esta dispersión está relacionada con el movimiento browniano de las partículas/macromoléculas, el cual se produce debido a los choques no compensados de estas con las moléculas del disolvente. El movimiento de las macromoléculas depende de su tamaño, temperatura y viscosidad del disolvente [75]. Por tanto, el conocimiento de la temperatura exacta es esencial para las mediciones en DLS, ya que la viscosidad del disolvente depende de la temperatura [76]. Cuando se monitoriza el movimiento de las partículas a lo largo de un intervalo de tiempo, puede obtenerse información sobre el tamaño de las macromoléculas, ya que las partículas grandes difunden lentamente, lo que da lugar a posiciones similares en diferentes puntos temporales, en comparación con las partículas pequeñas, que se mueven más rápidamente y, por tanto, no adoptan una posición específica [77]. El térmico 'dinámica' no se refiere al movimiento de la muestra como un conjunto, sino a la 'vibración' de las partículas que la componen [74].

DLS es una técnica muy útil para controlar la integridad estructural de las preparaciones de mAbs y puede utilizarse para distinguir entre una muestra homogénea monodispersa y una agregada. Las ventajas de esta técnica son su rapidez para caracterizar el tamaño de las biomoléculas, el bajo volumen de muestra requerida, su facilidad de uso y su naturaleza no invasiva. Además, los análisis se pueden llevar a cabo utilizando el entorno o tampón nativo en el que se encuentras las moléculas a analizar, lo que significa que su comportamiento no se ve comprometido por influencias externas. Todas estas características convierten esta técnica en una herramienta ideal para la caracterización rutinaria de biomoléculas en el laboratorio. Además, esta técnica funciona sin un conocimiento exacto de la concentración de la muestra, el único requisito es que se disperse suficiente luz para lograr una precisión estadística suficiente del tamaño determinado para las muestras analizadas [78].

Sin embargo, en DLS también encontramos algunas debilidades, tales como su baja resolución (no permite discriminar entre distintos oligómeros -dímeros o trímeros-), su gran sensibilidad a cambios de la temperatura y viscosidad, el hecho de solo poder estudiar muestras trasparentes y que la intensidad dispersada depende del diámetro, por lo que ínfimas contaminaciones (como motas de polvo) pueden dominar la distribución, de forma que se recomienda filtrar las muestras antes de su análisis [58].

Durante mucho tiempo se ha utilizado esta técnica para monitorizar fenómenos de agregación en soluciones de proteínas. Algunos ejemplos son el estudio de la influencia de diversos factores en su estado de agregación, la detección y monitorización de agregados indeseables en proteínas terapéuticas que provocan reacciones inmunogénicas o tienen

efectos adversos durante su administración en pacientes, y la investigación de enfermedades de agregación de proteínas [79]. DLS también puede ser empleado para métodos fiables para caracterizar la estabilidad de biomoléculas [80].

En esta Tesis Doctoral, se ha utilizado la técnica DLS para caracterizar el particulado en disolución de las proteínas terapéuticas estudiadas (*Capítulo 2, Capítulo 4* y *Capítulo 5*). En todos los casos, se han discutido distintos parámetros, como la polidispersidad y la distribución de tamaños por volumen.

4.2.3. Espectrometría de masas (MS)

Entre todas las técnicas analíticas utilizadas para la caracterización de los mAbs, la MS desempeña un papel fundamental ya que proporcionan información sobre secuencias primarias (incluida la caracterización detallada de las PTMs), estructuras de orden superior y conformaciones, convirtiéndose en una de las técnicas analíticas más utilizadas en la investigación y desarrollo farmacéuticos.

La caracterización estructural de un mAb por MS puede llevarse a cabo por su análisis a nivel de la proteína o a nivel peptídico. A nivel proteico, podemos encontrar diferentes enfoques: se puede analizar la proteína intacta o bien fragmentos grandes de la misma.

El análisis de la proteína intacta permite obtener un espectro de perfil de todo el anticuerpo que da acceso a la confirmación de la composición elemental, la identificación de las principales PTMs y la caracterización de las principales isoformas (glicoformas).

Por otro lado, se puede realizar el análisis de un anticuerpo tras su escisión en grandes fragmentos, conocido por su término en inglés como *middle-up*. Esto podría lograrse mediante la reducción de los enlaces disulfuro que generan las cadenas pesada y ligera. También podría implicar una escisión proteolítica limitada, en condiciones no desnaturalizantes, en la región bisagra de la cadena pesada, dando lugar a fragmentos Fab o (Fab′)2 y fragmentos Fc. Se han utilizado diferentes proteasas en los enfoques *middle-up*; las más comunes son la papaína, la pepsina, y la proteasa LysC [48].

Aunque los estudios de proteínas intactas y *middle-up* descritos anteriormente son muy valiosos, en los últimos años se han complementado con la fragmentación para obtener información adicional sobre la estructura, la secuencia, las modificaciones y los lugares de modificación. Este procedimiento suele denominarse *top-down* o *middle-down*, dependiendo de si se fragmentan proteínas intactas o grandes fragmentos [55]. Estos enfoques permiten acceder a la confirmación de la secuencia de las regiones terminales, así como a los dominios variables, a la identificación y localización de las principales modificaciones y a la

caracterización de las principales glicoformas. El análisis *top/middle-down* tiene la ventaja de implicar una manipulación limitada de la muestra, lo que puede dar lugar a un mínimo de artefactos debidos al procesamiento de la muestra [48].

Sin embargo, la enorme cantidad de información que puede obtenerse mediante los enfoques basados en MS descritos anteriormente no resuelve el análisis químico estructural completamente. Los análisis de proteínas intactas *top-down* y de fragmentos *middle-up* dan una idea de la identidad y las modificaciones (PTMs), pero no proporcionan la secuencia de aminoácidos ni permiten la localización concreta de esas modificaciones. Esto hace que estas dos estrategias de MS -muy útiles- tengan que ser complementadas con el enfoque *bottom-up* en términos de cobertura de la secuencia y determinación de las modificaciones, así como de los lugares específicos de modificación [55].

El enfoque *bottom*-up comprende la caracterización estructural de mAbs a nivel peptídico, el cual se refiere al análisis MS y MS/MS de péptidos generados a partir de la proteína tras una digestión enzimática utilizando proteasas de alta calidad como tripsina, quimotripsina, AspN, GluC y LysC, siendo la tripsina la más empleada. Este análisis suele comprender un paso previo de separación de péptidos, normalmente por RPC, aunque estas técnicas de separación no suelen resolver todos los péptidos en los digeridos de proteínas. Por ello, la separación adicional basada en m/z en sistemas MS de alta resolución, como Orbitrap, aumenta significativamente la cobertura de la secuencia y permite resaltar niveles bajos de PTMs [81]. En la mayoría de las aplicaciones, la MS/MS se utiliza para secuenciar los péptidos, aumentando así la confianza de las identificaciones y para localizar con precisión más modificaciones, como los sitios de glicosilación, los puentes disulfuro, las deamidaciones o las oxidaciones, entre otras [55,82]. La Figura 7 recoge las principales características de las técnicas basadas en MS para la caracterización de mAbs terapéuticos.

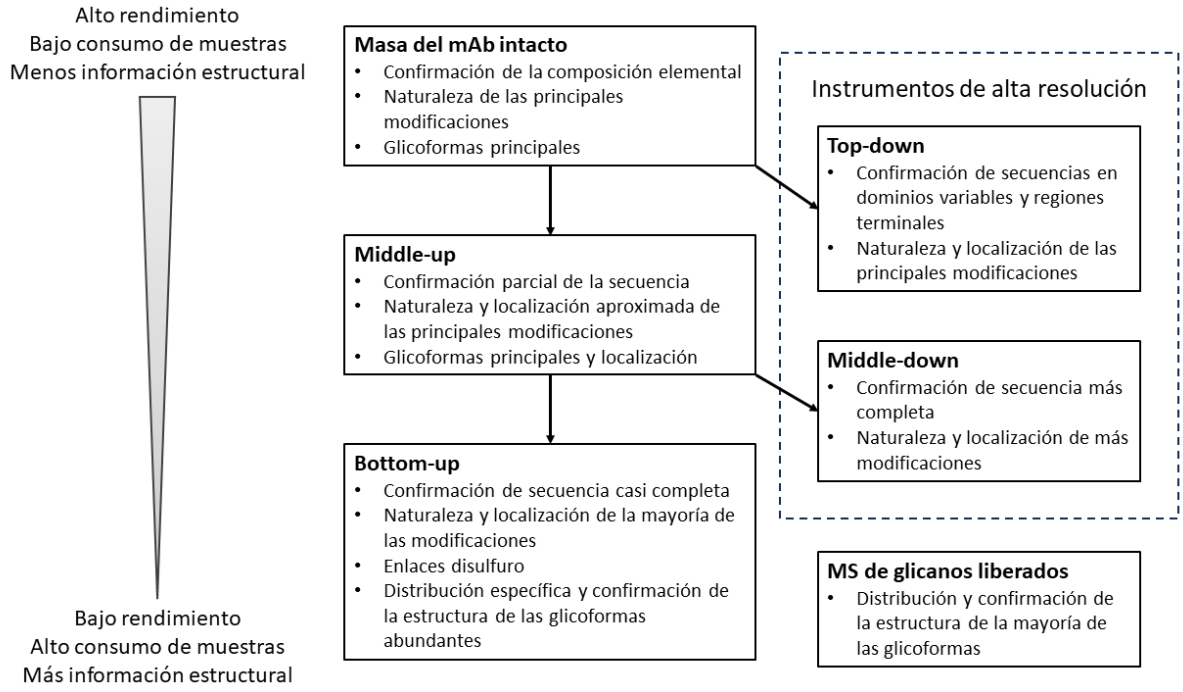

Figura 7. Resumen de diferentes técnicas basadas en MS para la caracterización química estructural de mAbs. Imagen adaptada de [82].

En la actualidad, se utilizan potentes softwares de apoyo biofarmacéutico para analizar todos los datos obtenidos por MS, incluidos los datos obtenidos tras la digestión enzimática y el análisis por MS/MS, que normalmente son desarrollados por los mismos proveedores de los instrumentos de MS [48].

En esta Tesis Doctoral se han realizado varios estudios utilizando la técnica MS. En concreto, el espectrómetro de masas utilizado es de alta resolución y masa exacta, el cual produce una ionización de la muestra por electroespray (fuente de ionización de tipo HESI, del inglés *heat electrospray ionization*) y cuenta con dos analizadores de masas, un cuadrupolo y un Orbitrap. Por un lado, en el *Capítulo 3* se han llevado a cabo estudios centrados en el análisis de nivolumab intacto para realizar estudios de cuantificación (contenido proteico), así como para la determinación de sus glicoformas principales, mediante el empleo de la técnica RP/UHPLC(UV)-(HESI/Orbitrap)MS. Por otro lado, en el *Capítulo 4* se han realizado estudios de determinación de las glicoformas principales de nivolumab mediante SE/UHPLC(UV)-(HESI/Orbitrap)MS, para lo cual se utilizaron sales volátiles. Por último, el *Capítulo 5* incluye el estudio de las glicoformas principales de pembrolizumab, mediante RP/UHPLC(UV)-(HESI/Orbitrap)MS. Además, también recoge el enfoque *bottom-up*, donde se ha utilizado la tripsina como enzima para realizar la digestión proteica de pembrolizumab y se ha realizado el análisis mediante RP/UHPLC(UV)-(HESI/Orbitrap)MS/MS, lo cual ha permitido la determinación exhaustiva de las PTMs principales de este mAb.

4.2.4. Inmunoensayos

Los inmunoensayos son métodos bioanalíticos en los que la cuantificación del analito depende de la reacción de un antígeno y un anticuerpo. Principalmente, estos métodos se basan en una reacción de unión competitiva entre un analito marcado y su sitio de unión altamente específico. El análisis se realiza midiendo la actividad de la etiqueta (por ejemplo, radiación, fluorescencia o enzima) en la fracción unida o libre y se construye una curva estándar que representa la señal medida en función de la concentración del analito.

Los métodos de inmunoensayo se han utilizado ampliamente en muchas áreas importantes del análisis farmacéutico, como el diagnóstico de enfermedades, la monitorización de fármacos terapéuticos, la farmacocinética clínica y los estudios de bioequivalencia en el descubrimiento de fármacos y las industrias farmacéuticas [83]. El análisis en estas áreas suele implicar la medición de concentraciones muy bajas de fármacos de bajo peso molecular, biomoléculas macromoleculares de interés farmacéutico, metabolitos y/o biomarcadores que indican el diagnóstico de enfermedades o el pronóstico. La importancia y la amplia difusión de los métodos de inmunoensayo en el análisis farmacéutico se atribuyen a su especificidad inherente, alto rendimiento y alta sensibilidad para el análisis de una amplia gama de analitos en muestras biológicas [84]. La detección precisa de analitos en fases tempranas es un requisito esencial en todos los entornos bioanalíticos para controlar y gestionar eficazmente la calidad de los medicamentos biofarmacéuticos, los alimentos y el medio ambiente.

Debido a la altísima sensibilidad, especificidad, precisión y rendimiento del ensayo inmunoenzimático (ELISA, del inglés *enzyme linked immunosorbent assay*), este formato ha sido el de uso preferente por muchos investigadores para llevar a cabo análisis por inmunoensayos [85]. Por ello, en esta Tesis Doctoral se ha empleado el ELISA para realizar el análisis funcional de los mAbs en estudio. En concreto, se ha empleado el formato de ELISA indirecto, el cual se describe a continuación.

4.2.4.1. ELISA indirecto

El ELISA es un ensayo inmunológico que se utiliza ampliamente en ámbito biomédico para detectar y cuantificar diferentes clases de moléculas biológicas, como proteínas, péptidos, anticuerpos y hormonas. Los ensayos ELISA suelen realizarse en placas de poliestireno de 96 pocillos, lo que permite medir varias muestras en una sola serie [86]. De forma general, los ELISA implican la adición gradual y la reacción de reactivos a una sustancia ligada en fase sólida, a través de la incubación y la separación de los reactivos ligados y libres

mediante pasos de lavado. A continuación, se utiliza una reacción enzimática para dar color y cuantificar la reacción, mediante el uso de un reactivo marcado con enzimas [87].

En concreto, el ELISA indirecto requiere dos anticuerpos: un anticuerpo primario no conjugado y un anticuerpo secundario unido a la enzima que genera la señal de lectura [86]. Para llevar a cabo este tipo de ELISA, en primer lugar y de forma resumida (se explicará en más detalle dentro de los *Capítulos 4* y *5* de esta Tesis Doctoral, en los cuales se utiliza dicha técnica), se realiza la siembra del antígeno en la base de los pocillos de las placas ELISA. Estos son principalmente de naturaleza proteica y se adherirán pasivamente al plástico durante un periodo de incubación. Después de la incubación, cualquier exceso de antígeno se elimina mediante un simple paso de lavado. A continuación, se procede a la adición de anticuerpos detectores no marcados, se incuba y se lava el exceso de anticuerpos (no unidos) para conseguir una unión específica. Posteriormente, se añade el conjugado (marcado con enzimas), seguido de incubación y lavado para lograr la unión del conjugado. Por último, se añade el sustrato/cromóforo al conjugado unido y se desarrolla el color, para finalmente realizar la lectura de absorbancia en un espectrofotómetro [87].

Actualmente, ELISA es el inmunoensayo más empleado para evaluar la actividad biológica de mAbs terapéuticos. Para ello, se deben seguir las recomendaciones de la guía ICH Q6B [17], la cual indica que los ensayos biológicos son los adecuados para determinar la actividad biológica de este tipo de proteínas terapéuticas. Además, esta guía también establece que los resultados de los ensayos biológicos se deben expresar en unidades de actividad biológica previamente calibrados frente a estándares de referencia (esto siempre que sea posible, sino se aceptan los estándares de referencia 'in house'). Esta consideración pone de manifiesto que los ELISA son ideales para evaluar la funcionalidad de proteínas terapéuticas en relación a los ensayos que emplean líneas celulares, puesto que en estos últimos la calibración es más difícil y la variabilidad es mucho mayor [58].

Si bien es cierto que el ELISA indirecto presenta algunas desventajas, como su extenso protocolo si se compara con el ELISA directo y la posible reactividad cruzada del anticuerpo secundario, este presenta numerosas ventajas: señal amplificada (varios anticuerpos secundarios se unirán al anticuerpo primario), gran flexibilidad (el mismo anticuerpo secundario puede usarse para varios anticuerpos primarios) y alta sensibilidad y especificidad [88].

En la presente Tesis Doctoral, se han optimizado y validado métodos ELISA indirectos para llevar a cabo la caracterización funcional y, por tanto, la determinación de la actividad biológica de dos mAbs: nivolumab (*Capítulo 4*) y pembrolizumab (*Capítulo 5*). Estos métodos se han optimizado para los mAbs citados a partir de aquellos desarrollados y validados

previamente en nuestro grupo de investigación [89]. La Figura 6 muestra el esquema general del formato ELISA indirecto seguido para los mAbs estudiados.

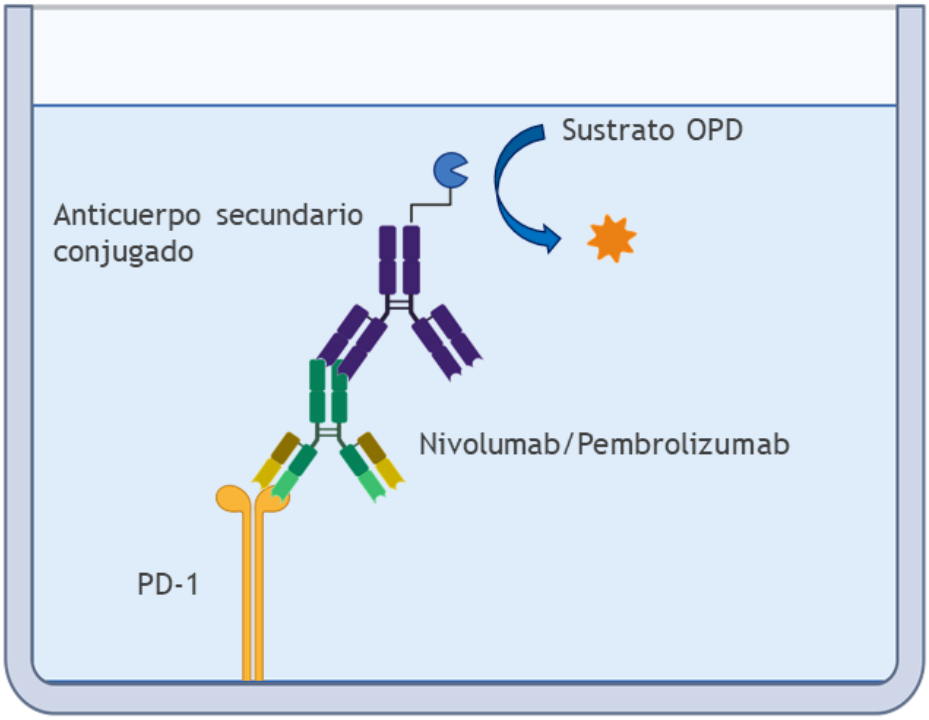

Figura 6. Representación esquemática del formato ELISA indirecto seguido para evaluar la funcionalidad de nivolumab y pembrolizumab. Elaboración propia usando BioRender [24].

5. DESARROLLO Y VALIDACIÓN DE METODOLOGÍA ANALÍTICA: GUÍAS ICH

La Conferencia Internacional para la Armonización (ICH, del inglés *International Conference on Harmonization*) de los requisitos técnicos de los productos farmacéuticos de uso humano reúne a las autoridades reguladoras de medicamentos de Europa, Estados Unidos y Japón y a la industria farmacéutica para tratar los aspectos científicos y técnicos de los productos farmacéuticos. La misión de la ICH es lograr una mayor armonización en todo el mundo para garantizar que se desarrollen, registren y mantengan medicamentos seguros, eficaces y de alta calidad de la manera más eficiente posible en cuanto a recursos, al tiempo que se cumplen normas estrictas. Para ello, sus actividades consisten en la elaboración de guías, pautas o recomendaciones unificadas e implementadas por los laboratorios farmacéuticos para asegurar la calidad de los medicamentos que producen. Organismos internacionales como la EMA y la FDA también establecen recomendaciones para la evaluación de medicamentos biotecnológicos, todas ellas basadas en las guías que elabora este organismo, conocidas comúnmente como guías ICH [90].

La ICH hace una clasificación de sus guías en cuatro categorías, las cuales reflejan los principales criterios para la aprobación y autorización de nuevos medicamentos: calidad (Q), seguridad (S), eficacia (E) y multidisciplinar (M), siendo esta última para tratar temas de diversa naturaleza. Para la realización del trabajo de investigación llevado a cabo en esta Tesis Doctoral se han empleado parte de las guías ICH relacionadas con la calidad. Dentro de las mismas existe un grupo dirigido exclusivamente a los productos biotecnológicos, las guías ICH Q5, las cuales se crearon a partir del gran crecimiento que comenzaron a adquirir los productos biotecnológicos y con la finalidad de dar respuesta a las necesidades de la industria farmacéutica. Sin embargo, en los demás grupos de las guías de calidad también podemos encontrar algunas dirigidas a los productos biotecnológicos (Tabla 4).

Tabla 4. Guías ICH de calidad de productos biotecnológicos.

Subgrupo	Código	Título
Estabilidad (Q1A)	Q1A(R2) [91]	Pruebas de estabilidad de nuevos fármacos y productos farmacéuticos
	Q1B [92]	Pruebas de estabilidad: prueba de fotoestabilidad de nuevas sustancias y productos farmacéuticos
Validación analítica (Q2)	Q2(R1) [93]	Validación de procedimientos analíticos: texto y metodología
Calidad de productos biotecnológicos (Q5)	Q5A(R1&R2) [94,95]	Evaluación de seguridad viral de productos biotecnológicos derivados de líneas celulares de origen humano o animal
	Q5B [96]	Análisis de la expresión creada en líneas celulares usadas para la expresión de r-ADN derivado de productos proteicos
	Q5C [97]	Análisis de la estabilidad de productos biotecnológicos/biológicos
	Q5D [98]	Derivación y caracterización de sustratos celulares utilizados para la producción de productos biotecnológicos/biológicos
	Q5E [99]	Comparabilidad de productos biotecnológicos/biológicos sujetos a cambios en su proceso de fabricación
Especificaciones (Q6)	Q6B [17]	Procedimientos de ensayo y criterios de aceptación para productos biotecnológicos/biológicos
Desarrollo farmacéutico (Q8)	Q8(R2) [39]	Desarrollo farmacéutico

De todas las guías ICH recogidas en la Tabla 4, el trabajo experimental de la presente Tesis Doctoral ha sido diseñado siguiendo las pautas indicadas en las guías que se detallan a continuación.

5.1. Guía Q6B. Procedimientos de ensayo y criterios de aceptación para productos biotecnológicos/biológicos

La guía ICH Q6B se trata de una guía de especificaciones. Normalmente, una especificación enumera un conjunto de atributos del producto, una prueba para cada atributo, una referencia a un procedimiento analítico para la prueba y los criterios de aceptación apropiados para el procedimiento analítico. La especificación establece los criterios mediante los cuales se evalúa la aceptabilidad de un producto farmacéutico, una sustancia farmacéutica, una materia prima, un producto intermedio u otros materiales asociados a la fabricación farmacéutica para los usos previstos [100]. Esta guía ofrece orientación para establecer especificaciones aplicables a los productos biotecnológicos/biológicos comerciales, de forma que ofrece las pautas sobre qué tipo de caracterización y métodos analíticos deben aplicarse y qué límites de aceptación deben establecerse para garantizar la identidad, el contenido, la calidad y la pureza del fármaco biotecnológico [101]. Entre sus recomendaciones, se pueden destacar las dirigidas a la caracterización de medicamentos y productos biotecnológicos mediante la determinación de sus propiedades fisicoquímicas, actividad biológica, propiedades inmunoquímicas, pureza e impurezas. Por ejemplo, para la determinación de las propiedades fisicoquímicas, se establecen las distintas técnicas analíticas que pueden emplearse, i.e., SEC para la determinación del peso o tamaño molecular o CD para la determinación de estructuras de orden superior. Esta guía también ofrece recomendaciones acerca de la evaluación del contenido proteico de los productos biotecnológicos. En cuanto a las consideraciones analíticas, la guía ofrece recomendaciones sobre los materiales y estándares de referencia que deben emplearse [17].

En resumen, la guía ICH Q6B establece estándares y recomendaciones para el desarrollo y evaluación de productos biotecnológicos, asegurando la calidad, la seguridad y la eficacia de estos productos a lo largo de su ciclo de vida.

Las recomendaciones recogidas en esta guía se han aplicado a lo largo de toda la parte experimental de la presente Tesis Doctoral (*Capítulos 2 – 6*), para llevar a cabo la caracterización de los mAbs estudiados en la misma.

5.2. Guía ICH Q8(R2). Desarrollo farmacéutico

La guía ICH Q8(R2) ofrece orientación sobre el desarrollo farmacéutico en las presentaciones reglamentarias, es decir, las solicitudes de nuevos medicamentos o las solicitudes de autorización de comercialización. De este modo, esta guía propone un nuevo enfoque tanto en el desarrollo farmacéutico como, posteriormente, en el control de calidad dentro del ámbito de la fabricación comercial, ya que el proceso de desarrollo está ahora específicamente diseñado para apoyarlo [100].

En concreto, la guía ICH Q8(R2) proporciona orientación sobre los principios y enfoques para el desarrollo de productos farmacéuticos. Su objetivo principal es promover un enfoque científico y basado en riesgos para el desarrollo farmacéutico, con el fin de garantizar la calidad, seguridad y eficacia de los medicamentos. Esta guía promueve el concepto de 'diseño de calidad farmacéutica' (QbD, del inglés *quality by design*). Esto implica definir y comprender claramente los atributos críticos del producto y del proceso, y utilizar este conocimiento para diseñar un proceso de fabricación controlado que cumpla con los requisitos de calidad. Además, se alienta a los fabricantes a adoptar un enfoque basado en riesgos para la identificación y control de los parámetros críticos del proceso y del producto. Esto implica evaluar y priorizar los riesgos potenciales para la calidad del producto y enfocar los recursos en los aspectos más críticos.

Esta guía, además, enfatiza la importancia de considerar el ciclo de vida completo del producto, desde el desarrollo hasta la retirada del mercado. Esto implica realizar evaluaciones periódicas de la calidad y llevar a cabo mejoras continuas a lo largo del tiempo. También destaca la importancia de una comunicación efectiva entre los fabricantes y las autoridades regulatorias, ya que promueve que se establezca un diálogo temprano y continuo para abordar cualquier problema o incertidumbre que pueda surgir durante el desarrollo del producto.

El aspecto más importante que recoge esta guía, como se ha comentado, son los CQAs propios del producto biotecnológico que se deben definir en el proceso del desarrollo del método analítico para la evaluación de su impacto en la calidad del mismo. En ella, los CQAs se definen como "una propiedad o característica física, química, biológica o microbiológica que debe encontrarse dentro de un límite, rango o distribución adecuados para garantizar la calidad deseada del producto". Estos se asocian generalmente con el principio activo, los excipientes, los productos intermedios (materiales en proceso) y el producto farmacéutico [39]. En el apartado *4. Análisis comprensivos de anticuerpos monoclonales: atributos críticos de la calidad* de esta Introducción se ha descrito ya más información específica relativa a los CQAs de los productos biotecnológicos, específicamente los referidos a los mAbs terapéuticos -moléculas objeto de estudio de la presente Tesis Doctoral-.

Esta guía ha sido aplicada en toda la parte experimental recogida en esta Tesis Doctoral (*Capítulos 2 – 6*), ya que a lo largo de la misma se han evaluado distintos CQAs para cada uno de los mAbs estudiados.

5.3. Guía ICH Q2(R1). Validación de procedimientos analíticos: texto y metodología

La guía ICH Q2(R1) proporciona una descripción general de los criterios que se necesitan para validar un procedimiento analítico. El objetivo de la validación de un método analítico es 'demostrar que es adecuado para el propósito previsto', siendo esto un requisito fundamental de las agencias reguladoras. De esta forma, dicha guía proporciona directrices para la validación de métodos analíticos utilizados en la industria farmacéutica. Su objetivo principal es garantizar la fiabilidad y la precisión de los resultados de los métodos analíticos utilizados para evaluar la calidad y seguridad de los productos farmacéuticos [100].

Esta guía establece que la validación de un método analítico debe incluir una serie de parámetros clave, como la especificidad, la precisión, la exactitud, la linealidad, el intervalo de concentraciones de aplicación, el límite de detección y el límite de cuantificación. Estos parámetros evalúan la capacidad del método para medir de manera precisa y confiable las propiedades analíticas del producto. Además, esta guía también proporciona una metodología para llevar a cabo dicha validación, la cual incluye la selección de características críticas del método, la realización de experimentos para evaluar los parámetros de validación y el análisis estadístico de los datos obtenidos. Se enfatiza la importancia de realizar la validación en diferentes etapas del ciclo de vida del método, desde su desarrollo inicial hasta su uso rutinario.

Por otro lado, es interesante comentar que la guía ICH Q2(R1) aborda la realización de estudios específicos de degradación forzada como requisito para la validación de métodos analíticos aplicados también a la caracterización de productos biotecnológicos, es decir, los estudios de degradación forzada son parte integral del desarrollo y la validación de métodos analíticos para productos farmacéuticos. Estos estudios implican someter el producto a condiciones extremas, como calor, luz, humedad, pH ácido y básico, para simular las posibles condiciones de degradación a las que podría estar expuesto durante su vida útil. Por tanto, esta guía enfatiza la importancia de realizar estudios de degradación forzada para evaluar la estabilidad del producto y la capacidad del método analítico para detectar y cuantificar los productos de degradación. Estos estudios permiten identificar los posibles productos de degradación y evaluar su impacto en la calidad y la seguridad del producto [93].

En términos de validación de métodos analíticos, la guía ICH Q2(R1) sugiere que los estudios de degradación forzada pueden utilizarse para evaluar la especificidad y la

selectividad del método. Estos estudios proporcionan información sobre la capacidad del método para detectar y cuantificar el analito de interés en presencia de productos de degradación y otros componentes, y dan lugar a los denominados “métodos indicadores de la estabilidad” de fármacos y/o medicamentos concretos.

Además, también menciona que los estudios de degradación forzada pueden ayudar en la determinación de los parámetros de validación, como la linealidad y el intervalo de aplicación del método analítico. Estos estudios permiten evaluar la respuesta analítica del método en diferentes concentraciones de analito y productos de degradación.

Actualmente, la guía ICH Q2(R1) se encuentra bajo un proceso de revisión. Su finalidad es incluir nuevos enfoques para la validación de métodos analíticos basados en técnicas novedosas, como las técnicas cromatográficas acopladas a MS y las técnicas espectroscópicas, tales como la espectroscopia de infrarrojo cercano o la espectroscopia de Raman, que utilizan técnicas quimiométricas para el tratamiento de los datos analíticos y que se suelen utilizar en procesos de control de calidad de productos biotecnológicos [101].

En concreto, en el *Capítulo 3* de esta Tesis Doctoral se ha llevado a cabo la validación de un método analítico para la cuantificación de nivolumab por (RP)UHPLC/UV-(HESI/Orbitrap™)MS, por lo que las directrices aportadas por esta guía han sido de gran relevancia en su desarrollo. Además, en los *Capítulos 4* y *5* se ha llevado a cabo la validación de un método ELISA para la evaluación de la funcionalidad de nivolumab y pembrolizumab, respectivamente, aplicando de nuevo directrices aportadas por la guía ICH Q2(R1).

5.4. Guía ICH Q5C. Análisis de estabilidad de productos biotecnológicos/biológicos

La guía ICH Q5C se refiere al análisis de estabilidad de productos biotecnológicos y proporciona pautas para evaluar la estabilidad de medicamentos biotecnológicos, como proteínas y péptidos recombinantes, vacunas y terapias génicas. Su objetivo es establecer principios generales para el diseño de estudios de estabilidad y la interpretación de los datos resultantes para productos biotecnológicos.

Esta guía aporta información sobre el diseño de estos estudios de estabilidad, donde se describen los principios y las pautas generales para llevarlos a cabo, incluyendo el tamaño de muestra, los protocolos de almacenamiento y las condiciones de prueba.

Por un lado, la guía ICH Q5C proporciona información importante sobre los estudios de estabilidad a largo plazo para productos biotecnológicos, y recomienda su realización con la finalidad de evaluar la estabilidad del producto durante un periodo de tiempo prolongado.

Para ello, aporta información valiosa para su realización, desde la duración y las condiciones de almacenamiento adecuadas hasta el muestreo, análisis y evaluación de los resultados.

Por otro lado, esta guía también proporciona información relevante sobre los estudios de estabilidad acelerada para productos biotecnológicos, sugiriendo su realización con el fin de evaluar la estabilidad del producto en un periodo de tiempo más corto. Estos últimos estudios se llevan a cabo bajo condiciones de almacenamiento más severas para acelerar los posibles procesos de degradación. En este tipo de estudios, se deben evaluar diferentes parámetros de estabilidad, como la identidad, la pureza, la actividad biológica, la impureza y la degradación del producto, así como las características físicas y químicas. Al igual que para los estudios de estabilidad en el tiempo, esta guía ofrece información acerca de las condiciones de almacenamiento, duración del estudio, muestreo, análisis y evaluación de los resultados. Estos estudios ayudan a evaluar rápidamente la estabilidad del producto y brindan información importante para su desarrollo y formulación.

Además de evaluar la estabilidad del producto en sí, esta guía también sugiere que se deben realizar estudios para evaluar la estabilidad del contenedor y el cierre utilizado para almacenar el producto. También se proporcionan directrices para la evaluación de los datos de estabilidad y la extrapolación de los resultados a condiciones de almacenamiento futuras.

En resumen, la guía ICH Q5C establece las pautas para el diseño y la realización de estudios de estabilidad de productos biotecnológicos, con el objetivo de garantizar la calidad y la estabilidad de estos medicamentos a lo largo de su vida útil [97].

En concreto, en esta Tesis Doctoral se han llevado a cabo estudios de degradación acelerada en condiciones de uso hospitalario basados en las directrices aportadas por esta guía, los cuales están recogidos en los *Capítulos 2, 4* y *5*, realizados a los mAbs tocilizumab, nivolumab y pembrolizumab, respectivamente.

5.5. Guía ICH Q1B. Pruebas de estabilidad: prueba de fotoestabilidad de nuevas sustancias y productos farmacéuticos

La guía ICH Q1B se trata de una guía de estabilidad que proporciona las directrices detalladas para llevar a cabo los estudios de estabilidad fototérmica de los productos farmacéuticos. Esta guía permite evaluar cómo la exposición a la luz y al calor puede afectar a la estabilidad de los medicamentos a lo largo del tiempo y, por tanto, a su calidad, seguridad y eficacia [92].

La exposición a la luz y al calor puede desencadenar reacciones químicas que pueden afectar a la composición y la potencia de un medicamento, lo que puede ser perjudicial para

los pacientes. Por lo tanto, esta guía es fundamental para la industria farmacéutica para cumplir con los requisitos regulatorios y asegurar la calidad de sus productos.

En esta guía se recogen las pautas sobre la selección de condiciones de exposición adecuadas, la duración de los estudios, la medición y evaluación de los resultados, y la presentación de datos a las autoridades regulatorias. En concreto, la guía distingue entre dos tipos de estudios de estabilidad fototérmica: estudios de fotodegradación, los cuales evalúan cómo la exposición a la luz puede causar la degradación del medicamento, y estudios de calor-luz, que evalúan cómo la exposición simultánea a la luz y al calor puede afectar la estabilidad del medicamento. Los resultados de estos estudios ayudan a determinar las condiciones óptimas de almacenamiento y empaque para los productos farmacéuticos, así como a establecer fechas de caducidad y proporcionar orientación sobre cómo proteger los medicamentos de la degradación relacionada con la luz y el calor [92].

En resumen, la guía ICH Q1B es una herramienta esencial para la industria farmacéutica y los reguladores para garantizar que los medicamentos sean estables y seguros, incluso cuando se exponen a condiciones de luz y calor. Ayuda a establecer estándares de calidad y a garantizar que los medicamentos cumplan con los requisitos regulatorios. Esto es importante para garantizar que los medicamentos mantengan su eficacia y calidad durante su vida útil y que los pacientes reciban productos farmacéuticos seguros y eficaces [100].

En concreto, esta Tesis Doctoral recoge estudios de fotodegradación en cuatro de sus capítulos (*Capítulos 2, 3, 4 y 5*), donde se han expuesto los mAbs tocilizumab, nivolumab y pembrolizumab a una irradiación por luz en cámara de envejecimiento durante 24 horas aplicando recomendaciones (condiciones) recogidas en esta guía.

6. ESTRUCTURA DE LA TESIS DOCTORAL Y COHERENCIA ENTRE LOS CAPÍTULOS

La presente Tesis Doctoral sigue una estructura clásica y está compuesta por los apartados *hipótesis y objetivos, resumen, introducción, capítulos, conclusiones, perspectivas futuras y bibliografía*. El apartado de *resultados y discusión* ha sido sustituido por *capítulos*, los cuales recogen los distintos trabajos de investigación que han sido desarrollados a lo largo de la Tesis Doctoral. Todos los *capítulos* muestran resultados que han sido publicados -o se encuentran en vías de publicación (*Capítulo 5)*- en revistas científicas de alto impacto e indexadas en el *Journal Citation Reports* (JCR), a excepción del *Capítulo 6,* el cual no se contempla para una futura publicación. La mayor parte del trabajo de investigación llevado a cabo satisface los objetivos que quedan recogidos en los siguientes proyectos de

investigación: “Estudios de estabilidad en el tiempo de sobrantes de medicamentos biotecnológicos –anticuerpos monoclonales y proteínas de fusión–. Estudios conformacionales comprensivos” (FEDER/Ministerio de Ciencia e Innovación-Instituto de Salud Carlos III, Fondos de Investigación en Salud, Proyecto **FIS PI17-00547**) y “Estabilidad de anticuerpos monoclonales terapéuticos antineoplásicos en condiciones de uso clínico: evaluación de parámetros fisicoquímicos y funcionalidad biológica en el tiempo y durante su manipulación y administración. Potenciales fuentes de inestabilidad” (FEDER/Junta de Andalucía-Consejería de Transformación Económica, Industria, Conocimiento y Universidades, Proyecto **P20-01029** y FEDER/Junta de Andalucía-Consejería de Transformación Económica, Industria, Conocimiento y Universidades, Proyecto **B-FQM-308-UGR20**).

El inicio de esta Tesis Doctoral -octubre de 2019- coincide con el comienzo de la pandemia de la COVID-19. Es por ello que, los primeros dos capítulos de esta Memoria son trabajos relacionados con la enfermedad causada por el coronavirus SARS-CoV-2. Concretamente, y dado que esta Tesis Doctoral se centra en el estudio de mAbs, el *Capítulo 1* se trata de un trabajo de revisión sobre los distintos mAbs empleados para el tratamiento de dicha enfermedad. En esta revisión se hace una diferenciación entre dos grupos de dianas terapéuticas: los mAbs no específicos del SARS-CoV-2, dirigidos a las respuestas del sistema inmunitario (centrándose especialmente en los anti-IL-6/IL-6R) y los mAbs específicos del SARS-CoV-2, diseñados para neutralizar la estructura proteica del virus. Este trabajo, titulado “The Relevance of Monoclonal Antibodies in the Treatment of COVID-19”, fue publicado en la revista *Vaccines (año 2021, volumen 9, páginas 557)* de la editorial MDPI*,* con un factor de impacto de 7,8 y situada en el primer cuartil (Q1) (JCR, 2022). Este trabajo fue llevado a cabo por invitación de la revista.

Por otro lado, el *Capítulo 2* recoge un trabajo de investigación acerca de tocilizumab (RoActemra®), un mAb anti-IL-6 empleado para el tratamiento de la COVID-19 por ser capaz de neutralizar los factores inflamatorios clave en el síndrome de liberación de citoquinas (tormenta inflamatoria), el cual desempeña un papel importante en los casos graves de COVID-19. Este trabajo fue realizado como respuesta a los requerimientos necesarios de la situación actual de aquel momento en los hospitales, donde se estaba administrando dicho medicamento de forma intravenosa a los pacientes graves infectados por COVID-19 que mostrasen signos del síndrome de liberación de citoquinas. Esta situación dio lugar a un desabastecimiento de la forma de administración intravenosa debido a la alta demanda que había de la misma. Por ello, con el trabajo recogido en este capítulo, se quiso estudiar la posibilidad de poder utilizar la forma farmacéutica subcutánea de dicho medicamento para preparar las disoluciones de uso intravenoso. Para ello, se llevó a cabo un estudio analítico

comparativo en el que se estudiaron los atributos críticos de calidad fisicoquímicos de las formas farmacéuticas intravenosa y subcutánea. El artículo científico derivado de tal estudio, el cual recibe por título “Use of subcutaneous tocilizumab to prepare intravenous solutions for COVID-19 emergency shortage: Comparative analytical study of physicochemical quality attributes”, fue publicado en la revista *Journal of Pharmaceutical Analysis* (año 2020, volumen 10, páginas 532 – 545) de la editorial Elsevier*,* con un factor de impacto de 8,8 y situada en el primer cuartil (Q1) y primer decil (D1) (JCR, 2022). Este trabajo fue realizado en tiempo récord -marzo de 2020- a petición de los hospitales de Granada (España) ante el desabastecimiento de la forma IV. Tras su publicación, durante la segunda mitad del año 2020 estuvo entre los 10 artículos más descargados de la revista.

Los siguientes capítulos recogen los trabajos de investigación relacionados con mAbs terapéuticos que no van dirigidos al tratamiento de la COVID-19, sino que se tratan de mAbs inhibidores de puntos de control inmunitario. En primer lugar, el *Capítulo 3* recoge un trabajo sobre la validación de un método analítico indicador de la estabilidad para la cuantificación de nivolumab (Opdivo®) intacto, y la determinación de su perfil de isoformas, siguiendo las directrices de la guía ICH Q2(R1). En este trabajo, se presenta una estrategia basada en el uso combinado de los datos obtenidos para desarrollar y validar un método (RP)UHPLC/UV-(HESI/Orbitrap™)MS para la determinación del contenido proteico (atributo crítico de la calidad) de nivolumab en su forma medicamentosa. Además, también recoge un estudio comparativo de los resultados obtenidos por UV y MS. El artículo científico derivado de esta investigación recibe el título de “Combined use of UV and MS data for ICH Stability-Indication Method: Quantification and isoforms identification of intact nivolumab” y fue publicado en la revista *Microchemical Journal* (año 2022, volumen 182, páginas 107896) de la editorial Elsevier, con un factor de impacto de 4,8 y situada en el primer cuartil (Q1) (JCR, 2022).

El *Capítulo 4* continúa con la investigación acerca del mAb nivolumab. En este trabajo, se ha llevado a cabo un análisis comprensivo de las características fisicoquímicas y funcionales de dicha proteína. Para ello, se han empleado diversas técnicas analíticas, desarrollado metodología de análisis *ad hoc* y se ha sometido el medicamento (Opdivo®) a estudios de degradación forzada que han permitido obtener datos sobre la estabilidad del mismo frente a la manipulación hospitalaria, además de validar las metodologías de análisis. Este trabajo de investigación fue titulado como “Comprehensive Analysis of Nivolumab, A Therapeutic Anti-Pd-1 Monoclonal Antibody: Impact of Handling and Stress” y publicado en la revista *Pharmaceutics* (año 2022, volumen 14, páginas 692) de la editorial MDPI, con un factor de impacto de 5,4 y situada en el primer cuartil (Q1) (JCR, 2022).

En el *Capítulo 5* se recoge un estudio similar al realizado en el capítulo anterior, pero se emplea pembrolizumab (Keytruda®) como mAb en estudio. De forma similar, se realiza la

caracterización fisicoquímica y funcional de dicha proteína mediante el empleo de distintas y complementarias técnicas analíticas, desarrollando y validando la metodología de análisis *ad hoc* para este mAb. Además, también se ha sometido el medicamento a estudios de degradación forzada en los que se ha expuesto a diversas condiciones estresantes, las cuales nos han permitido obtener información acerca de las modificaciones fisicoquímicas y/o funcionales que pueden ocurrir en la proteína tras ser manipulada en la práctica clínica rutinaria de los hospitales. Este trabajo ha sido titulado como "Physicochemical and functional comprehensive analysis of pembrolizumab based on controlled degraded studies: impact on antigen-antibody binding" y ha sido enviado a revista JCR de primer cuartil (JCR, 2022). Este trabajo presenta una estructura similar al recogido en el *Capítulo 4*, aunque hay algunas diferencias en cuanto a las técnicas/metodologías empleadas. Por ejemplo, el *Capítulo 5* contempla el estudio de las PTMs de pembrolizumab tras la realización de una digestión enzimática y un mapeo peptídico, mientras que el capítulo anterior no recoge este tipo de estudio ya que, aunque realizado, formará parte de una futura publicación independiente. Otro ejemplo es el tipo de técnica empleada para la determinación del perfil de isoformas, puesto que en el *Capítulo 4* se emplea la técnica SEC acoplada a MS utilizando sales volátiles para su determinación en nivolumab. En cambio, en el *Capítulo 5* se emplea la técnica RPC acoplada a MS para la determinación de las isoformas de pembrolizumab. Estos trabajos ponen de manifiesto la gran variedad de técnicas y metodologías analíticas que se pueden utilizar, incluso con diferentes combinaciones, para obtener el perfil indicador de la estabilidad de mAbs terapéuticos.

Por último, el *Capítulo 6* de la presente Tesis Doctoral contempla el trabajo de investigación llevado a cabo en la empresa *Coriolis Pharma Research GmbH* (Múnich, Alemania) y que justifica la mención internacional de esta Tesis Doctoral. La investigación realizada en esta estancia internacional, de 3 meses de duración y financiada mediante una *EMBO Scientific Exchange Grant* (Ref. 9629), recoge un estudio novedoso llevado a cabo con mAbs terapéuticos empleando técnicas analíticas cromatográficas, por lo que está en total concordancia con la línea de investigación que se sigue en esta Tesis Doctoral. Concretamente, este capítulo, titulado "Optimization of the ReFOLD Assay for Protein Stability Prediction", contempla la optimización del ensayo ReFOLD, un método isotérmico basado en la desnaturalización química. Este ensayo es un método potencial para la predicción de la estabilidad de las proteínas durante el almacenamiento a largo plazo, y se planteó su optimización mediante la reducción de la concentración del agente desnaturalizante (urea) necesario para llevar a cabo dicho ensayo, ya que una concentración elevada (10 M) demostró no ser la idónea en estudios anteriores. Para evaluar los resultados obtenidos se utilizó la técnica SEC y se realizaron estudios comparativos entre las distintas concentraciones de urea estudiadas. Su objetivo es obtener la concentración de urea más adecuada que permita

reducir los efectos indeseados obtenidos en estudios previos con urea 10 M (tales como formación de gel o cristalización) y que permita mantener un intervalo de estabilidad adecuado para los mAbs ensayados.

En conclusión, esta Tesis Doctoral comienza con un trabajo de revisión y otro científico sobre mAbs empleados en el tratamiento de la COVID-19, para continuar con los estudios sobre mAbs inhibidores de puntos de control inmunitario y finalizar con la optimización de un ensayo novedoso utilizando una gama variada de mAbs. El punto común de toda la investigación llevada a cabo a lo largo de esta Tesis Doctoral es que todos los mAbs estudiados son mAbs terapéuticos de uso hospitalario y se ha centrado en estudios de estabilidad, para lo cual se ha requerido el uso de un conjunto amplio de técnicas analíticas, mediante las cuales se ha desarrollado y puesto a punto metodología de análisis *ad hoc* para evaluar distintos CQAs de los mismos.

REFERENCIAS

[1] BOE-A-2007-19249 Real Decreto 1345/2007, de 11 de octubre, por el que se regula el procedimiento de autorización, registro y condiciones de dispensación de los medicamentos de uso humano fabricados industrialmente., (n.d.). https://www.boe.es/buscar/act.php?id=BOE-A-2007-19249 (accessed June 26, 2023).

[2] BOE.es - DOUE-L-2004-80948 Reglamento (CE) nº 726/2004 del Parlamento Europeo y del Consejo de 31 de marzo de 2004 por el que se establecen procedimientos comunitarios para la autorización y el control de los medicamentos de uso humano y veterinario y por, (n.d.). https://www.boe.es/buscar/doc.php?id=DOUE-L-2004-80948 (accessed June 26, 2023).

[3] R. Pérez Robles, Analytical strategies for the structural characterization of monoclonal antibodies and fusion proteins using mass spectrometry, 2020. http://hdl.handle.net/10481/59769.

[4] División de Productos Biológicos, Terapias Avanzadas y Biotecnología | Agencia Española de Medicamentos y Productos Sanitarios, (n.d.). https://www.aemps.gob.es/laaemps_estructura_humanos_biologicos/ (accessed June 26, 2023).

[5] European Medicines Agency |, (n.d.). https://www.ema.europa.eu/en (accessed June 26, 2023).

[6] R.M. Lu, Y.C. Hwang, I.J. Liu, C.C. Lee, H.Z. Tsai, H.J. Li, H.C. Wu, Development of therapeutic antibodies for the treatment of diseases, J. Biomed. Sci. 27 (2020) 1–30. https://doi.org/10.1186/s12929-019-0592-z.

[7] H. Kaplon, S. Crescioli, A. Chenoweth, J. Visweswaraiah, J.M. Reichert, Antibodies to watch in 2023, MAbs. 15 (2023). https://doi.org/10.1080/19420862.2022.2153410.

[8] O. Hernandez-Alba, E. Wagner-Rousset, A. Beck, S. Cianférani, Native Mass Spectrometry, Ion Mobility, and Collision-Induced Unfolding for Conformational Characterization of IgG4 Monoclonal Antibodies, Anal. Chem. 90 (2018) 8865–8872. https://doi.org/10.1021/acs.analchem.8b00912.

[9] S. Saito, H. Namisaki, K. Hiraishi, N. Takahashi, S. Iida, A stable engineered human IgG3 antibody with decreased aggregation during antibody expression and low pH stress, Protein Sci. 28 (2019) 900–909. https://doi.org/10.1002/pro.3598.

[10] S. Ramazi, J. Zahiri, Post-translational modifications in proteins: Resources, tools and prediction methods, Database. 2021 (2021) 1–20. https://doi.org/10.1093/database/baab012.

[11] Post-Translational Modifications (PTMs) Analysis - Creative Biolabs, (n.d.). https://www.creative-biolabs.com/drug-discovery/therapeutics/post-translational-modifications-ptms-analysis.htm (accessed June 26, 2023).

[12] X. Zhong, J.F. Wright, Biological insights into therapeutic protein modifications throughout trafficking and their biopharmaceutical applications, Int. J. Cell Biol. 2013 (2013). https://doi.org/10.1155/2013/273086.

[13] F. Higel, A. Seidl, F. Sörgel, W. Friess, N-glycosylation heterogeneity and the influence on structure, function and pharmacokinetics of monoclonal antibodies and Fc fusion proteins, Eur. J. Pharm. Biopharm. 100 (2016) 94–100. https://doi.org/10.1016/j.ejpb.2016.01.005.

[14] A. Planinc, J. Bones, B. Dejaegher, P. Van Antwerpen, C. Delporte, Glycan characterization of biopharmaceuticals: Updates and perspectives, Anal. Chim. Acta. 921 (2016) 13–27. https://doi.org/10.1016/j.aca.2016.03.049.

[15] N. Sethuraman, T.A. Stadheim, Challenges in therapeutic glycoprotein production, Curr. Opin. Biotechnol. 17 (2006) 341–346. https://doi.org/10.1016/J.COPBIO.2006.06.010.

[16] X. Yang, M.G. Bartlett, Glycan analysis for protein therapeutics, J. Chromatogr. B Anal. Technol. Biomed. Life Sci. 1120 (2019) 29–40. https://doi.org/10.1016/j.jchromb.2019.04.031.

[17] ICH Q6B: Test procedures and acceptance criteria for biotechnological/biological products, International Conference on Harmonization of Technical Requirements for Registration of Pharmaceuticals for Human Use, Geneva (Switzerland), 1999.

[18] World Health Organization (WHO), International nonproprietary names (INN) for biological and biotechnological substances (a review), World Heal. Organ. (2016) 1–80. http://www.who.int/medicines/services/inn/BioRev2014.pdf.

[19] P. Mayrhofer, R. Kunert, Nomenclature of humanized mAbs: Early concepts, current challenges and future perspectives, Hum. Antibodies. 27 (2018) 37–51. https://doi.org/10.3233/HAB-180347.

[20] A.A.J. Vaillant, A. Qurie, Interleukin, StatPearls. (2022). https://www.ncbi.nlm.nih.gov/books/NBK499840/ (accessed June 26, 2023).

[21] M. Akdis, S. Burgler, R. Crameri, T. Eiwegger, H. Fujita, E. Gomez, S. Klunker, N. Meyer, L. O'Mahony, O. Palomares, C. Rhyner, N. Quaked, A. Schaffartzik, W. Van De Veen, S. Zeller, M. Zimmermann, C.A. Akdis, Interleukins, from 1 to 37, and interferon-γ: Receptors, functions, and roles in diseases, J. Allergy Clin. Immunol. 127 (2011) 701-721.e70. https://doi.org/10.1016/j.jaci.2010.11.050.

[22] Interleukin 6 inhibitors: Biology, principles of use, and adverse effects - UpToDate, (n.d.). https://www.uptodate.com/contents/interleukin-6-inhibitors-biology-principles-of-use-and-adverse-effects (accessed June 26, 2023).

[23] ROACTEMRA. ANNEX I SUMMARY OF PRODUCT CHARACTERISTICS. EUROPEAN MEDICINE AGENCY., n.d.

[24] Scientific Image and Illustration Software | BioRender, (n.d.). https://www.biorender.com/ (accessed July 4, 2023).

[25] X. Cai, H. Zhan, Y. Ye, J. Yang, M. Zhang, J. Li, Y. Zhuang, Current Progress and Future Perspectives of Immune Checkpoint in Cancer and Infectious Diseases, Front. Genet. 12 (2021) 785153. https://doi.org/10.3389/FGENE.2021.785153/BIBTEX.

[26] Y. Shiravand, F. Khodadadi, S.M.A. Kashani, S.R. Hosseini-Fard, S. Hosseini, H. Sadeghirad, R. Ladwa, K. O'byrne, A. Kulasinghe, Immune Checkpoint Inhibitors in Cancer Therapy, Curr. Oncol. 29 (2022) 3044–3060. https://doi.org/10.3390/CURRONCOL29050247.

[27] S. Chrétien, I. Zerdes, J. Bergh, A. Matikas, T. Foukakis, Beyond PD-1/PD-L1 Inhibition: What the Future Holds for Breast Cancer Immunotherapy, Cancers (Basel). 11 (2019) 628. https://doi.org/10.3390/CANCERS11050628.

[28] L. Ai, J. Chen, H. Yan, Q. He, P. Luo, Z. Xu, X. Yang, Research status and outlook of pd-1/pd-l1 inhibitors for cancer therapy, Drug Des. Devel. Ther. 14 (2020) 3625–3649. https://doi.org/10.2147/DDDT.S267433.

[29] J. Inokuchi, M. Eto, Profile of pembrolizumab in the treatment of patients with unresectable or metastatic urothelial carcinoma, Cancer Manag. Res. 11 (2019) 4519–4528. https://doi.org/10.2147/CMAR.S167708.

[30] P. Du Rusquec, O. De Calbiac, M. Robert, M. Campone, J.S. Frenel, Clinical utility of pembrolizumab in the management of advanced solid tumors: An evidence-based review on the emerging new data, Cancer Manag. Res. 11 (2019) 4297–4312. https://doi.org/10.2147/CMAR.S151023.

[31] L.M. Francisco, P.T. Sage, A.H. Sharpe, The PD-1 pathway in tolerance and autoimmunity, Immunol. Rev. 236 (2010) 219–242. https://doi.org/10.1111/j.1600-065X.2010.00923.x.

[32] Y. Iwai, J. Hamanishi, K. Chamoto, T. Honjo, Cancer immunotherapies targeting the PD-1 signaling pathway, J. Biomed. Sci. 24 (2017) 1–11. https://doi.org/10.1186/s12929-017-0329-9.

[33] H. Dong, S.E. Strome, D.R. Salomao, H. Tamura, F. Hirano, D.B. Flies, P.C. Roche, J. Lu, G. Zhu, K. Tamada, V.A. Lennon, E. Cells, L. Chen, Tumor-associated B7-H1 promotes T-cell apoptosis: A potential mechanism of immune evasion, Nat. Med. 8 (2002) 793–800. https://doi.org/10.1038/nm730.

[34] Y. Iwai, M. Ishida, Y. Tanaka, T. Okazaki, T. Honjo, N. Minato, Involvement of PD-L1 on tumor cells in the escape from host immune system and tumor immunotherapy by PD-L1 blockade, Proc. Natl. Acad. Sci. U. S. A. 99 (2002) 12293–12297. https://doi.org/10.1073/pnas.192461099.

[35] OPDIVO. ANNEX I SUMMARY OF PRODUCT CHARACTERISTICS. EUROPEAN MEDICINE AGENCY., n.d.

[36] KEYTRUDA. ANNEX I SUMMARY OF PRODUCT CHARACTERISTICS. EUROPEAN MEDICINE AGENCY., n.d.

[37] Guideline on development, production, characterisation and specification for monoclonal antibodies and related products. European Medicines Agency, 2008. www.ema.europa.eu/contact (accessed June 26, 2023).

[38] H.A. Alhazmi, M. Albratty, Analytical Techniques for the Characterization and Quantification of Monoclonal Antibodies, Pharmaceuticals. 16 (2023). https://doi.org/10.3390/ph16020291.

[39] ICH Q8(R2): Pharmaceutical development, International Conference on Harmonization of Technical Requirements for Registration of Pharmaceuticals for Human Use, Geneva (Switzerland), 2009.

[40] C. Finkler, L. Krummen, Introduction to the application of QbD principles for the development of monoclonal antibodies, Biologicals. 44 (2016) 282–290. https://doi.org/10.1016/j.biologicals.2016.07.004.

[41] N. Alt, T.Y. Zhang, P. Motchnik, R. Taticek, V. Quarmby, T. Schlothauer, H. Beck, T. Emrich, R.J. Harris, Determination of critical quality attributes for monoclonal antibodies using quality by design principles, Biologicals. 44 (2016) 291–305. https://doi.org/10.1016/j.biologicals.2016.06.005.

[42] ICH M7(R2): Assessment and control of DNA reactive (mutagenic) impurities in pharmaceuticals to limit potential carcinogenic risk, International Conference on Harmonization of Technical Requirements for Registration of Pharmaceuticals for Human Use, 2023.

[43] J. Qiu, T. Qiu, Y. Huang, Z. Cao, Identifying the epitope regions of therapeutic antibodies based on structure descriptors, Int. J. Mol. Sci. 18 (2017) 2457. https://doi.org/10.3390/ijms18122457.

[44] C. Jakes, S. Millán-Martín, S. Carillo, K. Scheffler, I. Zaborowska, J. Bones, Tracking the Behavior of Monoclonal Antibody Product Quality Attributes Using a Multi-Attribute Method Workflow, J. Am. Soc. Mass Spectrom. 32 (2021) 1998–2012. https://doi.org/10.1021/jasms.0c00432.

[45] S. Fekete, D. Guillarme, Ultra-high-performance liquid chromatography for the characterization of therapeutic proteins, TrAC - Trends Anal. Chem. 63 (2014) 76–84. https://doi.org/10.1016/j.trac.2014.05.012.

[46] Chromatographic Characterization of Biopharmaceuticals: Recent Trends and New Tools | American Pharmaceutical Review - The Review of American Pharmaceutical Business & Technology, (n.d.). https://www.americanpharmaceuticalreview.com/Featured-Articles/177646-Chromatographic-Characterization-of-Biopharmaceuticals-Recent-Trends-and-New-Tools/ (accessed June 26, 2023).

[47] A. Chakrabarti, Separation of Monoclonal Antibodies by Analytical Size Exclusion Chromatography, in: Antib. Eng., 2018. https://doi.org/10.5772/intechopen.73321.

[48] A. Beck, E. Wagner-Rousset, D. Ayoub, A. Van Dorsselaer, S. Sanglier-Cianférani, Characterization of therapeutic antibodies and related products, Anal. Chem. 85 (2013) 715–736. https://doi.org/10.1021/ac3032355.

[49] M. Haberger, M. Leiss, A.K. Heidenreich, O. Pester, G. Hafenmair, M. Hook, L. Bonnington, H. Wegele, M. Haindl, D. Reusch, P. Bulau, Rapid characterization of biotherapeutic proteins by size-exclusion chromatography coupled to native mass spectrometry, MAbs. 8 (2016) 331–339. https://doi.org/10.1080/19420862.2015.1122150.

[50] M. Tassi, J. De Vos, S. Chatterjee, F. Sobott, J. Bones, S. Eeltink, Advances in native high-

performance liquid chromatography and intact mass spectrometry for the characterization of biopharmaceutical products, J. Sep. Sci. 41 (2018) 125–144. https://doi.org/10.1002/jssc.201700988.

[51] L. Zhang, S. Luo, B. Zhang, Glycan analysis of therapeutic glycoproteins, MAbs. 8 (2016) 205–215. https://doi.org/10.1080/19420862.2015.1117719.

[52] S. Maslen, P. Sadowski, A. Adam, K. Lilley, E. Stephens, Differentiation of isomeric N-glycan structures by normal-phase liquid chromatography - MALDI-TOF/TOF tandem mass spectrometry, Anal. Chem. 78 (2006) 8491–8498. https://doi.org/10.1021/ac0614137.

[53] E. Wagner-Rousset, S. Fekete, L. Morel-Chevillet, O. Colas, N. Corvaïa, S. Cianférani, D. Guillarme, A. Beck, Development of a fast workflow to screen the charge variants of therapeutic antibodies, J. Chromatogr. A. 1498 (2017) 147–154. https://doi.org/10.1016/j.chroma.2017.02.065.

[54] O.O. Dada, N. Jaya, J. Valliere-Douglass, O. Salas-Solano, Characterization of acidic and basic variants of IgG1 therapeutic monoclonal antibodies based on non-denaturing IEF fractionation, Electrophoresis. 36 (2015) 2695–2702. https://doi.org/10.1002/ELPS.201500219.

[55] S. Fekete, D. Guillarme, P. Sandra, K. Sandra, Chromatographic, Electrophoretic, and Mass Spectrometric Methods for the Analytical Characterization of Protein Biopharmaceuticals, Anal. Chem. 88 (2016) 480–507. https://doi.org/10.1021/acs.analchem.5b04561.

[56] J. Moebius, R. Swart, A. Sickmann, Chromatography-Based Separation of Proteins, Peptides, and Amino Acids, in: Handb. Pharm. Biotechnol., 2006: pp. 585–610. https://doi.org/10.1002/9780470117118.ch05d.

[57] C.D. Whitmore, L.A. Gennaro, Capillary electrophoresis-mass spectrometry methods for tryptic peptide mapping of therapeutic antibodies, Electrophoresis. 33 (2012) 1550–1556. https://doi.org/10.1002/elps.201200066.

[58] J. Hermosilla Fernández, Análisis estructurales comprensivos de anticuerpos monoclonales y proteínas de fusión terapéuticos. Aplicaciones en estudios de estabilidad en condiciones reales de uso hospitalario, 2021.

[59] W.C. Johnson, Protein secondary structure and circular dichroism: A practical guide, Proteins Struct. Funct. Bioinforma. 7 (1990) 205–214. https://doi.org/10.1002/prot.340070302.

[60] J.C. Lin, Z.K. Glover, A. Sreedhara, Assessing the Utility of Circular Dichroism and FTIR Spectroscopy in Monoclonal-Antibody Comparability Studies, J. Pharm. Sci. 104 (2015) 4459–4466. https://doi.org/10.1002/jps.24683.

[61] A. Lobley, L. Whitmore, B.A. Wallace, DICHROWEB: An interactive website for the analysis of protein secondary structure from circular dichroism spectra, Bioinformatics. 18 (2002) 211–212. https://doi.org/10.1093/bioinformatics/18.1.211.

[62] L. Whitmore, B.A. Wallace, DICHROWEB, an online server for protein secondary structure

analyses from circular dichroism spectroscopic data, Nucleic Acids Res. 32 (2004). https://doi.org/10.1093/nar/gkh371.

[63] N. Sreerama, R.W. Woody, A Self-Consistent Method for the Analysis of Protein Secondary Structure from Circular Dichroism, Anal. Biochem. 209 (1993) 32–44. https://doi.org/10.1006/abio.1993.1079.

[64] P. Manavalan, W.C. Johnson, Variable selection method improves the prediction of protein secondary structure from circular dichroism spectra, Anal. Biochem. 167 (1987) 76–85. https://doi.org/10.1016/0003-2697(87)90135-7.

[65] W.C. Johnson, Analyzing protein circular dichroism spectra for accurate secondary structures, Proteins Struct. Funct. Genet. 35 (1999) 307–312. https://doi.org/10.1002/(SICI)1097-0134(19990515)35:3<307::AID-PROT4>3.0.CO;2-3.

[66] M.A. Andrade, P. Chacón, J.J. Merelo, F. Morán, Evaluation of secondary structure of proteins from uv circular dichroism spectra using an unsupervised learning neural network, Protein Eng. Des. Sel. 6 (1993) 383–390. https://doi.org/10.1093/protein/6.4.383.

[67] S.W. Provencher, J. Glöckner, Estimation of Globular Protein Secondary Structure from Circular Dichroism, Biochemistry. 20 (1981) 33–37. https://doi.org/10.1021/bi00504a006.

[68] A.J. Miles, S.G. Ramalli, B.A. Wallace, DichroWeb, a website for calculating protein secondary structure from circular dichroism spectroscopic data, Protein Sci. 31 (2022) 37–46. https://doi.org/10.1002/pro.4153.

[69] S.M. Kelly, T.J. Jess, N.C. Price, How to study proteins by circular dichroism, Biochim. Biophys. Acta - Proteins Proteomics. 1751 (2005) 119–139. https://doi.org/10.1016/j.bbapap.2005.06.005.

[70] S. Kelly, N. Price, The Use of Circular Dichroism in the Investigation of Protein Structure and Function, Curr. Protein Pept. Sci. 1 (2005) 349–384. https://doi.org/10.2174/1389203003381315.

[71] P. Garidel, M. Hegyi, S. Bassarab, M. Weichel, A rapid, sensitive and economical assessment of monoclonal antibody conformational stability by intrinsic tryptophan fluorescence spectroscopy, Biotechnol. J. 3 (2008) 1201–1211. https://doi.org/10.1002/biot.200800091.

[72] C.A. Royer, Probing Protein Folding and Conformational Transitions with Fluorescence, Chem. Rev. 106 (2006) 1769–1784. https://doi.org/10.1021/cr0404390.

[73] G. Thiagarajan, A. Semple, J.K. James, J.K. Cheung, M. Shameem, A comparison of biophysical characterization techniques in predicting monoclonal antibody stability, MAbs. 8 (2016) 1088–1097. https://doi.org/10.1080/19420862.2016.1189048.

[74] A. Cuadros-Moreno, R. Casañas Pimentel, E. San Martín-Martínez, J. Yañes Fernandez, Dispersión de luz dinámica en la determinación de tamaño de nanopartículas poliméricas, Am. J. Phys. Educ. 8 (2014) 1–5. http://www.lajpe.org.

[75] S.E. Harding, K. Jumel, Light Scattering, Curr. Protoc. Protein Sci. 11 (1998) 7.8.1-7.8.14. https://doi.org/10.1002/0471140864.PS0708S11.

[76] Stephen Ernest Harding, Protein hydrodynamics, Protein A Compr. Treatise. 2 (1999) 271–305.

[77] J. Stetefeld, S.A. McKenna, T.R. Patel, Dynamic light scattering: a practical guide and applications in biomedical sciences, Biophys. Rev. 8 (2016) 409–427. https://doi.org/10.1007/s12551-016-0218-6.

[78] U. Nobbmann, M. Connah, B. Fish, P. Varley, C. Gee, S. Mulot, J. Chen, L. Zhou, Y. Lu, F. Sheng, J. Yi, S.E. Harding, Dynamic light scattering as a relative tool for assessing the molecular integrity and stability of monoclonal antibodies, Biotechnol. Genet. Eng. Rev. 24 (2007) 117–128. https://doi.org/10.1080/02648725.2007.10648095.

[79] B. Lorber, F. Fischer, M. Bailly, H. Roy, D. Kern, Protein analysis by dynamic light scattering: Methods and techniques for students, Biochem. Mol. Biol. Educ. 40 (2012) 372–382. https://doi.org/10.1002/bmb.20644.

[80] F. Mirasol, Stability Testing of Protein Therapeutics Using DLS, BioPharm Int. 34 (2021) 41–43, 46–41–43, 46. https://www.biopharminternational.com/view/stability-testing-of-protein-therapeutics-using-dls (accessed June 12, 2023).

[81] P. Bults, B. Spanov, O. Olaleye, N.C. van de Merbel, R. Bischoff, Intact protein bioanalysis by liquid chromatography – High-resolution mass spectrometry, J. Chromatogr. B Anal. Technol. Biomed. Life Sci. 1110–1111 (2019) 155–167. https://doi.org/10.1016/j.jchromb.2019.01.032.

[82] Z. Zhang, H. Pan, X. Chen, Mass spectrometry for structural characterization of therapeutic antibodies, Mass Spectrom. Rev. 28 (2009) 147–176. https://doi.org/10.1002/MAS.20190.

[83] J.W.A. Findlay, W.C. Smith, J.W. Lee, G.D. Nordblom, I. Das, B.S. DeSilva, M.N. Khan, R.R. Bowsher, Validation of immunoassays for bioanalysis: a pharmaceutical industry perspective, J. Pharm. Biomed. Anal. 21 (2000) 1249–1273. https://doi.org/10.1016/S0731-7085(99)00244-7.

[84] I.A. Darwish, Immunoassay Methods and their Applications in Pharmaceutical Analysis: Basic Methodology and Recent Advances., Int. J. Biomed. Sci. 2 (2006) 217–35. http://www.ncbi.nlm.nih.gov/pubmed/23674985%0Ahttp://www.pubmedcentral.nih.gov/articlerender.fcgi?artid=PMC3614608.

[85] S.K. Vashist, J.H.T. Luong, Immunoassays: An overview, Handb. Immunoass. Technol. Approaches, Performances, Appl. (2018) 1–18. https://doi.org/10.1016/B978-0-12-811762-0.00001-3.

[86] H. Kaur, S.R. Bhagwat, T.K. Sharma, A. Kumar, Analytical techniques for characterization of biological molecules - Proteins and aptamers/oligonucleotides, Bioanalysis. 11 (2019) 103–117. https://doi.org/10.4155/bio-2018-0225.

[87] J. Crowther, The ELISA Guidebook, Second Edi, 2009. http://link.springer.com/10.1007/978-1-60327-254-4.

[88] Basic principles and types of ELISA - Abcam, (n.d.). https://www.abcam.com/kits/elisa-principle (accessed June 27, 2023).

[89] I. Suárez, A. Salmerón-García, J. Cabeza, L.F. Capitán-Vallvey, N. Navas, Development and use of specific ELISA methods for quantifying the biological activity of bevacizumab, cetuximab and trastuzumab in stability studies, J. Chromatogr. B. 1032 (2016) 155–164. https://doi.org/10.1016/j.jchromb.2016.05.045.

[90] ICH Official web site, (n.d.). https://ich.org/ (accessed June 27, 2023).

[91] ICH Q1A(R2): Stability testing of new drug substances and products, International Conference on Harmonization of Technical Requirements for Registration of Pharmaceuticals for Human Use, Geneva (Switzerland), 2003.

[92] ICH Q1B: Stability testing: photostability testing of new drug substances and products, International Conference on Harmonization of Technical Requirements for Registration of Pharmaceuticals for Human Use, Geneva (Switzerland), 1996.

[93] ICH Q2(R1): Validation of analytical procedures: text and methodology, International Conference on Harmonization of Technical Requirements for Registration of Pharmaceuticals for Human Use, Geneva (Switzerland), 2005.

[94] ICH Q5A(R1): Viral safety evaluation of biotechnology products derived from cell lines of human or animal origin, International Conference on Harmonization of Technical Requirements for Registration of Pharmaceuticals for Human Use, Geneva (Switzerland), 1999.

[95] ICH Q5A(R2): Viral safety evaluation of biotechnology products derived from cell lines of human or animal origin, International Conference on Harmonization of Technical Requirements for Registration of Pharmaceuticals for Human Use, Geneva (Switzerland), 2022.

[96] ICH Q5B: Quality of biotechnological products: analysis of the expression construct in cells used for production of r-DNA protein products, International Conference on Harmonization, Geneva (Switzerland), 1995.

[97] ICH Q5C: Quality of biotechnological products: stability testing of biotechnological/biological products, International Conference on Harmonization, Geneva (Switzerland), 1995.

[98] ICH Q5D: Derivation and characterisation of cell substrates used for production of biotechnological/biological products, International Conference on Harmonization, Geneva (Switzerland), 1997.

[99] ICH Q5E: Comparability of biotechnological/biological products subject to changes in their manufaturing process, International Conference on Harmonization of Technical Requirements for Registration of Pharmaceuticals for Human Use, Geneva (Switzerland), 2004.

[100] A. Teasdale, D. Elder, R.W. Nims, ICH Quality Guidelines : an implementation guide, 2018. https://www.wiley.com/en-ae/ICH+Quality+Guidelines%3A+An+Implementation+Guide-p-9781118971116 (accessed June 28, 2023).

[101] A. Martínez Ortega, Nuevas aplicaciones analíticas para la caracterización de medicamentos basados en anticuerpos monoclonales. Estudios de estabilidad en el tiempo en condiciones hospitalarias, 2022.

SECCIÓN 1

Therapeutic monoclonal antibodies for the treatment of COVID-19

CAPÍTULO 1

The relevance of monoclonal antibodies in the treatment of COVID-19

INTRODUCCIÓN AL CAPÍTULO 1

Este Capítulo 1 se trata de un trabajo de revisión bibliográfica sobre los mAbs empleados en el tratamiento de la enfermedad COVID-19. En general, estos mAbs se dirigen a neutralizar la respuesta del sistema inmune, mientras que otros se dirigen directamente a neutralizar la estructura proteica del virus SARS-CoV-2, el causante de la COVID-19. De este modo, el principal objetivo de este trabajo de revisión es presentar el estado actual de los mAbs más investigados hasta el momento (año del artículo) para el tratamiento de la nueva enfermedad por coronavirus. En él se han dividido estos mAbs en dos grandes grupos: mAbs no específicos del SARS-CoV-2 y mAbs específicos del SARS-CoV-2.

El primer grupo recoge aquellos mAbs cuya diana terapéutica no va dirigida hacia la estructura proteica del virus, sino que su objetivo es bloquear algún punto clave de la respuesta del sistema inmune de los pacientes infectados. En concreto, este trabajo se centra en los mAbs que se han empleado para tratar a pacientes que han mostrado una respuesta inmune exagerada, conocida como “tormenta de citoquinas” y, más específicamente, en los mAbs anti-IL-6/IL-6R, dado que IL-6 es una de las citoquinas clave encontradas en esta respuesta exacerbada. Por tanto, los mAbs recogidos en esta sección son tocilizumab, sarilumab y siltuximab.

Por otro lado, el grupo de los mAbs específicos del SARS-CoV-2 recoge aquellos mAbs que son capaces de neutralizar la estructura proteica del virus. Concretamente, estos mAbs se dirigen a bloquear la unión del virus con su receptor, es decir, impiden la entrada del virus en la célula huésped al unirse a la proteína S del virus (localizada en su superficie) y bloqueando así su unión con el receptor, la enzima convertidora de angiotensina 2 (ACE2), localizado en la célula huésped. Dentro de este grupo se distinguen tres subgrupos de mAbs considerados: el primer subgrupo recoge aquellos mAbs que han sido aislados de pacientes infectados por SARS-CoV-2 (B5, B38, H2, H4 y EY6A), el segundo grupo se centra en los mAbs que son capaces de neutralizar tanto al SARS-CoV como al SARS-CoV-2 (47D11 y CR3022) y, por último, el tercer grupo recoge aquellos mAbs que han recibido una autorización de uso de emergencia (Emergency Use Authorization (EUA)), como serían bamlanivimab, el uso combinado de casirivimab e imdevimab y la terapia combinada de bamlanivimab y etesevimab. Sin embargo, existen controversias en cuanto a la eficacia del tratamiento del COVID-19 con estos mAbs específicos ya que este virus, como cualquier otro, está sujeto a mutaciones, por lo que si esas mutaciones ocurren en la proteína S (diana terapéutica de este tipo de mAbs), este tratamiento dejaría de ser efectivo. La terapia combinada de varios mAbs

es una buena alternativa cuando las nuevas variantes víricas han acumulado una alta tasa de mutaciones. Como conclusión de este trabajo se extrae que los mAbs específicos del SARS-CoV-2 son significativamente más eficaces que los no específicos.

REVIEW

The Relevance of Monoclonal Antibodies in the Treatment of COVID-19

Anabel Torrente-López[1], Jesús Hermosilla[1], Natalia Navas[1,*], Luis Cuadros-Rodríguez[1], José Cabeza[2] and Antonio Salmerón-García[2]

[1] Department of Analytical Chemistry, Science Faculty, Biohealth Research Institute (ibs.GRANADA), University of Granada, E-18071 Granada, Spain; anabeltl@ugr.es (A.T.-L.); herfer@correo.ugr.es (J.H.); lcuadros@ugr.es (L.C.-R.)

[2] Department of Clinical Pharmacy, Biohealth Research Institute (ibs.GRANADA), San Cecilio University Hospital, E-18012 Granada, Spain; jose.cabeza.sspa@juntadeandalucia.es (J.C.); asalgar6@gmail.com (A.S.-G.)

* Correspondence: natalia@ugr.es

Vaccines 9 (2021) 557

Accepted: 22 May 2021

DOI: 10.3390/vaccines9060557

vaccines

MDPI

Review

The Relevance of Monoclonal Antibodies in the Treatment of COVID-19

Anabel Torrente-López [1], Jesús Hermosilla [1], Natalia Navas [1,*], Luis Cuadros-Rodríguez [1], José Cabeza [2] and Antonio Salmerón-García [2]

[1] Department of Analytical Chemistry, Science Faculty, Biohealth Research Institute (ibs.GRANADA), University of Granada, E-18071 Granada, Spain; anabeltl@ugr.es (A.T.-L.); herfer@correo.ugr.es (J.H.); lcuadros@ugr.es (L.C.-R.)
[2] Department of Clinical Pharmacy, Biohealth Research Institute (ibs.GRANADA), San Cecilio University Hospital, E-18012 Granada, Spain; jose.cabeza.sspa@juntadeandalucia.es (J.C.); asalgar6@gmail.com (A.S.-G.)
* Correspondence: natalia@ugr.es

Abstract

Major efforts have been made in the search for effective treatments since the outbreak of the COVID-19 infection in December 2019. Extensive research has been conducted on drugs that are already available and new treatments are also under development. Within this context, therapeutic monoclonal antibodies (mAbs) have been the subject of widespread investigation focusing on two target-based groups, i.e., non-SARS-CoV-2 specific mAbs, that target immune system responses, and SARS-CoV-2 specific mAbs, designed to neutralize the virus protein structure. Here we review the latest literature about the use of mAbs in order to describe the state of the art of the clinical trials and the benefits of using these biotherapeutics in the treatment of COVID-19. The clinical trials considered in the present review include both observational and randomized studies. We begin by presenting the studies conducted using non-SARS-CoV-2 specific mAbs for treating different immune disorders that were already on the market. Within this group of mAbs, we focus particularly on anti-IL-6/IL-6R. This is followed by a discussion of the studies on SARS-CoV-2 specific mAbs. Our findings indicate that SARS-CoV-2 specific mAbs are significantly more effective than non-specific ones.

Keywords

COVID-19 treatment

Clinical trials

Monoclonal antibodies

Non-SARS-CoV-2 specific

SARS-CoV-2 specific

1. Introduction

Coronavirus disease 2019 (COVID-19), caused by severe acute respiratory syndrome coronavirus 2 (SARS-CoV-2), has emerged as a new infectious disease which has reached pandemic proportions. This coronavirus belongs to the Betacoronavirus genus in the Coronaviridae family, together with other previously identified coronaviruses, such as SARS-CoV and MERS-CoV. These viruses have a positive-sense RNA genome which encodes structural and non-structural proteins [1]. SARS-CoV-2 transmission is mainly mediated by respiratory droplets and aerosols and most infected patients are asymptomatic or present mild symptoms, such as fever, cough, dyspnoea, diarrhoea, muscle pain, sore throat, headache, and loss of smell and/or taste. However, about 20% of patients undergo a serious illness with dyspnoea, pneumonia, and supplemental oxygen requirements. The most seriously ill patients can suffer respiratory failure and cardiopulmonary collapse or shock that can lead to death [2]. In response to this global emergency, a wide range of therapeutic agents such as chloroquine, hydroxychloroquine, antivirals, antibodies, corticosteroids, or convalescent plasma among others have been or are currently being evaluated for the treatment of COVID-19 [3], in addition to the development of vaccines. Unfortunately, not all these agents have proved successful and some, such as chloroquine, hydroxychloroquine and several antivirals, have already been discarded as possible treatments [4–6].

One of the strategies considered for defeating COVID-19 is passive immunotherapy (Figure 1). There are two ways to guarantee passive immunization: (i) via natural antibodies using convalescent plasma therapy (CPT) in which plasma is extracted from a hyperimmune patient and transfused into a COVID-19 patient; or (ii) via antibodies that are biotechnologically designed, i.e., therapeutic monoclonal antibodies (mAbs) or a cocktail of polyclonal antibodies (pAbs) [7]. Of these two passive immunization strategies, the use of mAbs offer the most innovative approach to the prevention and treatment of infectious diseases, such as COVID-19, where current research aims at developing treatments based on specific mAbs to block and/or neutralize SARS-CoV-2 in infected patients [8]. In addition, already available mAbs have been used off-label based on the knowledge acquired during the pandemic regarding the pathogenesis of the disease. Therefore, the characteristic of mAbs made them perfectly suitable for the treatment of COVID-19 [9].

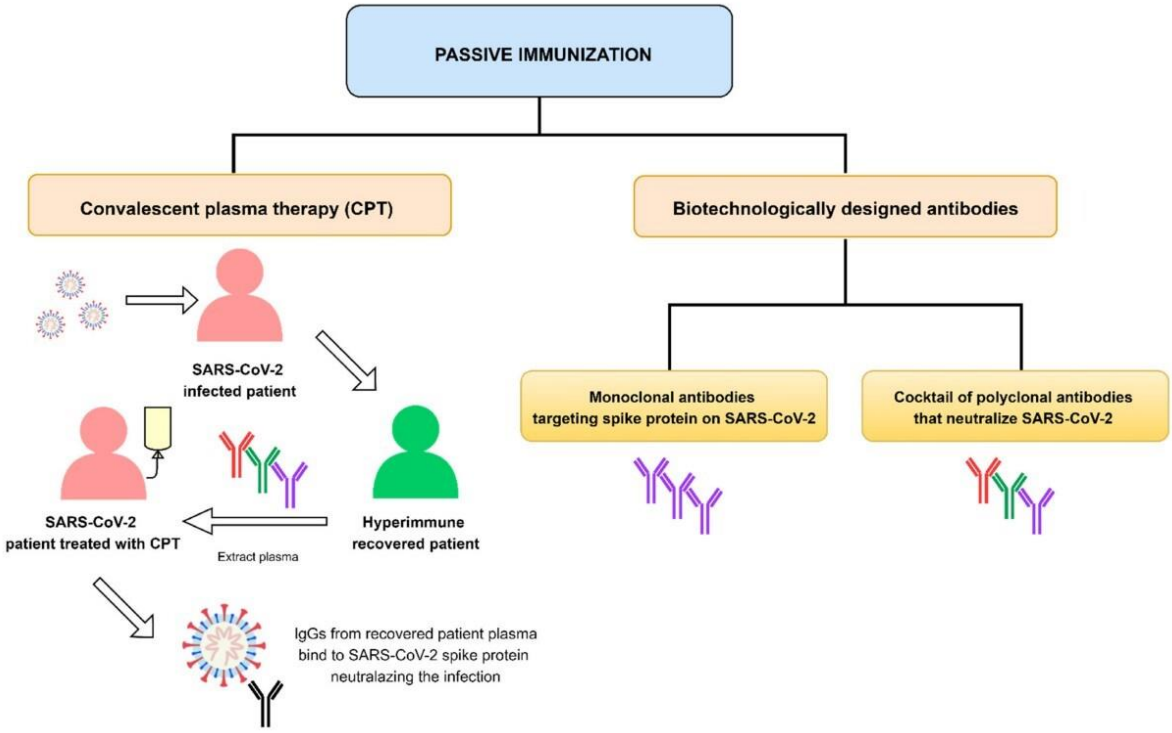

Figure 1. Different strategies to guarantee passive immunization using antibodies.

The off-label use of drugs can be defined as their use for a non-officially approved condition. It also refers to the use of drugs with an unapproved dosage, route of administration, or in an unlicensed combination regimen [10]. Off-label administration of drugs to treat COVID-19 is an extensive practice. However, this is not the first time that mAbs have been prescribed off-label. Several mAbs have proven safe and effective for treatments not indicated in their respective Summary of Product Characteristics (SPC). One example is bevacizumab: an anti-cancer biotherapeutic which is currently widely administered intravitreally to treat age-related macular degeneration (AMD) instead of the approved drug, ranibizumab [11]. Although both biotherapeutics have similar efficacy and safety, bevacizumab is now preferred due to its better cost–benefit ratio.

Several clinical trials are currently being conducted to test the efficacy and safety of different mAbs for the treatment of COVID-19, some of which are already being administered in hospitals while others are under evaluation [12]. Many of them target immune system responses (non-SARS-CoV-2 specific mAbs) while others are designed to neutralize the SARS-CoV-2 protein structure (SARS-CoV-2 specific mAbs) (Figure 2) [7]. This paper aims to present the state of the art on the most investigated mAbs currently under consideration for the treatment of the novel coronavirus disease.

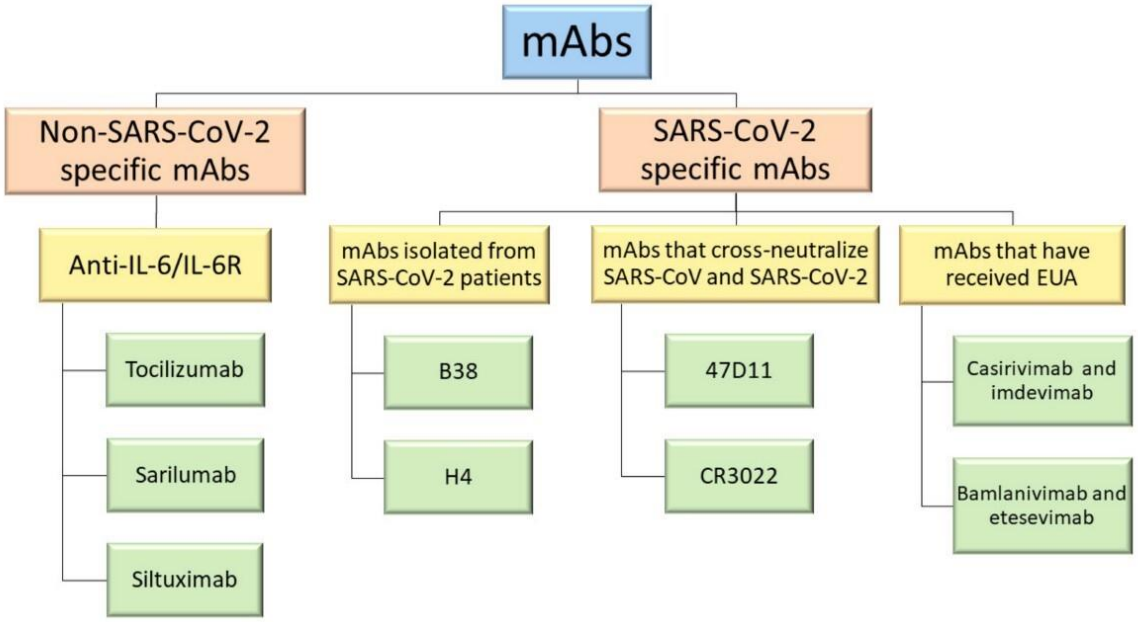

Figure 2. Relevant mAbs used to treat COVID-19 deeper discussed in this review.

2. Non-SARS-CoV-2 Specific Monoclonal Antibodies

The mAbs that are currently being used in hospitals to treat COVID-19 focus on the immune responses provoked by the virus, which can affect the severity of COVID-19 disease [7]. One of these immune responses involves the sudden release of large numbers of certain cytokines into circulation, in what is known as a 'cytokine storm', a life-threatening systemic inflammatory syndrome [13]. IL-6 is one of the key pro-inflammatory cytokines found in COVID-19 patients, which is why anti-IL-6/IL-6R biological drugs have been used for the treatment of this disease from the beginning. The mAbs selected to treat COVID-19 patients with high IL-6 levels include tocilizumab, sarilumab, and siltuximab. Several clinical trials are currently underway to test their efficacy, which has yet to be fully proven [2].

Clinical trials are also ongoing with other non-SARS-CoV-2 specific mAbs whose therapeutic targets are not IL-6/IL-6R, such as bevacizumab, clazakizumab, eculizumab, emapalumab, gimsilumab, itolizumab, mavrilimumab, meplazumab, nivolumab, pembrolizumab, etc. [2,12,14]. The therapeutic, anti-IL-1R protein, anakinra, has also been used [15]. No conclusive results have been obtained with any of them as yet. Due to their widespread use, in this paper we will be focusing specifically on the anti-IL-6/IL-6R mAbs and their use in the treatment of the COVID-19-associated cytokine storm.

2.1. Tocilizumab (TCZ)

TCZ is a humanized IgG1 mAb that targets both soluble and membrane-bound IL-6 receptors and inhibits the signal mediated by them. It is frequently used in the treatment of

different autoimmune diseases such as rheumatoid arthritis and systemic juvenile idiopathic arthritis [16].

Soon after the pandemic outbreak, off-label use of mAbs became a standard part of care in patients with COVID-19 in different parts of the world. Of the arsenal of therapeutics proposed as anti-COVID-19 candidates, the anti-IL-6 mAbs seemed to be useful in severe patients. Of these, TCZ has been the most frequently administered in hospitals due to its greater supply, its longer history on the market and its availability in intravenous (IV) pharmaceutical format [17]. Its efficacy and safety in the treatment of COVID-19 are beginning to be assessed in a large number of observational studies, and also in various randomized clinical trials. To date, a total of 78 clinical trials have been registered [18].

Systematic reviews and meta-analyses have already been published which bring together the results from the clinical studies found in the literature. Boregowda et al. [19] published a systematic review and meta-analysis of studies that evaluated the benefits of TCZ in reducing mortality in severe COVID-19 patients as compared to similar patients who only received the standard treatment. This review included a total of 16 articles, most of them retrospective. The authors found statistical differences between the mortality rate of the TCZ group (22.4%) and that of the control group (26.21%), leading them to conclude that TCZ administration might reduce the mortality in severe COVID-19 patients, while stressing the need to conduct larger randomized clinical trials (RCT). However, the results of this meta-analysis have not been certified by peer-review. Berardicurti et al. [20] published a systematic review and meta-analysis evaluating the effect of TCZ administration on mortality. They included 22 studies, most of them retrospective. They reported a reduction in the odds of mortality in TCZ-treated patients when compared to the control group. Cortegiani et al. [21] also published a systematic review of 31 clinical studies; most of them single-center and retrospective, none of them randomized. Although some of these studies claimed that TCZ might be effective and could be related to better outcomes, they emphasized the observational nature of the studies and concluded, therefore, that they had a degree of inaccuracy due to different bias sources, mainly due to confounding. Of the 31 studies they analyzed, 15 had a comparison control group without TCZ, and 5 of these 15 were classified as presenting a serious risk of bias while the rest were considered of moderate risk. Khan et al. [15] published a systematic review and meta-analysis of studies assessing the effects of four anti-IL-6 agents against COVID-19. They primarily evaluated severity on an Ordinal Scale measured at day 15 from intervention and in terms of the number of days to hospital discharge. They also evaluated overall mortality as a secondary endpoint. TCZ was analyzed in a total of 60 studies (12 prospective with control arm, 8 prospective without control arm, and 40 retrospective). In the

prospective studies TCZ was related to a lower relative risk of mortality. However, its effects were inconclusive for other outcomes.

There have also been various reviews analysing the results of the RCTs conducted to evaluate the efficacy of TCZ in the treatment of COVID-19 (Table 1). A recently published review performed a meta-analysis of randomized clinical trials evaluating the effect of TCZ on all-cause mortality as the first outcome and a combined endpoint of requirement of mechanical ventilation as the second outcome [22]. In this research the authors included six clinical trials that were assessed for their risk of bias and were classified as of low and moderate risk. These RCTs included a total of 1177 patients who were randomly selected and administered TCZ and 880 patients who were randomized to the control group and did not receive TCZ. This meta-analysis demonstrated that the administration of TCZ reduced the likelihood of progression to mechanical ventilation and/or all-cause mortality among hospitalized patients with COVID-19. However, no clear benefits on mortality as an endpoint were reported with the administration of TCZ to hospitalized patients with COVID-19.

Table 1. Published randomized clinical trials evaluating the efficacy of anti-IL-6 mAbs.

Drug	Authors	Design	Patients Enrolled	Regimen	Primary Outcomes	Main Findings
TCZ	Stone et al.	Prospective, multicenter, randomized, double blind, placebo-controlled trial	243 (162 TCZ group; 81 placebo group)	Standard care plus a single dose of either TCZ (8 mg/kg, IV, max 800 mg) or placebo	Intubation or death, assessed in a time-to-event analysis	TCZ was not effective in preventing intubation or death in moderately ill hospitalized patients with COVID-19
	Rosas et al.	Randomized, double-blind, placebo-controlled, multicenter study	452 (294 TCZ group; 144 placebo group)	A single IV infusion of TCZ (8 mg/kg, max 800 mg) or placebo plus standard care. A second infusion of TCZ or placebo could be administered 8 to 24 h after the first dose	Clinical status at day 28 on an ordinal scale ranging from 1 (discharged or ready for discharge) to 7 (death)	Administration of TCZ did not result in significantly better clinical status or lower mortality than placebo at day 28
	Salvarani et al.	Open-label randomized multicenter study	126 (60 TCZ group; 66 control group)	IV TCZ (8 mg/kg infusion, Max 800 mg) within 8 h from randomization, followed by a second dose after 12 h	Admission to the intensive care unit with invasive mechanical ventilation, death from all causes, or clinical aggravation documented by the finding of a PaO2/FIO2 ratio of less than 150 mmHg	No benefits in terms of disease progression were observed compared with standard care
	Hermine et al.	Cohort-embedded, investigator-initiated, multicenter, open-label, bayesian randomized clinical trial	131 (64 TCZ group; 67 usual care group)	IV TCZ (8 mg/kg infusion, max 800 mg) on day 1, with additional fixed dose of 400 mg as intravenous infusion on day 3 if required	Scores higher than 5 on the World Health Organization 10-point Clinical Progression Scale (WHO-CPS) on day 4 and survival without need for ventilation (including non-invasive ventilation) at day 14	TCZ did not reduce WHO-CPS scores to less than 5 at day 4 but might have reduced the risk of NIV, MV, or death by day 14. No difference was found in mortality on day 28
	Salama et al.	Randomized, double-blind, placebo-controlled, multicenter clinical trial	389 (249 TCZ group; 128 placebo group)	IV TCZ (8 mg/kg infusion, max 800 mg), with a second dose 8–24 h later if required)	Mechanical ventilation (invasive mechanical ventilation or extracorporeal membrane oxygenation) or death at day 28	TCZ reduced the likelihood of progression to the composite outcome of mechanical ventilation or death, but it did not improve survival

Table 1. *Cont.*

Drug	Authors	Design	Patients Enrolled	Regimen	Primary Outcomes	Main Findings
	Gordon et al.	Open-label, randomized, multifactorial, adaptive platform trial	747 (350 TCZ group; 397 control group)	TCZ (8 mg/kg, max 800 mg), was administered as an IV infusion over one hour; this dose could be repeated 12–24 h later at the discretion of the treating clinician	The primary outcome was an ordinal scale combining in-hospital mortality (assigned−1) and days free of organ support to day 21	In critically ill patients with COVID-19 receiving organ support in intensive care, treatment with TCZ improved outcome, including survival
	Veiga et al.	Multicenter, randomized, open label, parallel group, superiority trial	129 (65 TCZ group; 64 standard care group)	TCZ was administered as a single IV infusion at a dose of 8 mg/kg (max 800 mg)	The primary outcome, clinical status measured at 15 days using a seven- level ordinal scale, was analyzed as a composite of death or mechanical ventilation because the assumption of odds proportionality was not met	In patients with severe or critical COVID-19, TCZ plus standard care did not achieve better results than standard care alone in clinical outcomes at 15 days, and it might increase mortality
	Soin et al.	Open-label, multicenter, randomized, controlled, phase 3 trial	180 (90 TCZ group; 90 standard care group)	A single IV infusion at 6 mg/kg up to a maximum dose of 480 mg. An additional dose of 6 mg/kg (max 480 mg/kg) could be administered if required	The primary efficacy endpoint was the proportion of patients with progression of COVID-19 from moderate to severe or from severe to death up to day 14	Routine use of TCZ in patients admitted to hospital with moderate to severe COVID-19 is not supported. However, post-hoc evidence from this study suggests TCZ might still be effective in patients with severe COVID-19 and so should be investigated further in future studies
Sarilumab	Gordon et al.	Open-label, randomized, multifactorial, adaptive platform trial	442 (45 sarilumab group; 397 control group)	Sarilumab (400 mg) was administered once only as an IV infusion	The primary outcome was an ordinal scale combining in-hospital mortality (assigned−1) and days free of organ support to day 21	In critically ill patients with COVID-19 receiving organ support in intensive care, treatment with sarilumab, improved outcome, including survival
	Lescure et al.	Multinational, randomized, adaptive, phase 3, double-blind, placebo-controlled trial	416 (159 sarilumab 200 mg; 173 sarilumab 400 mg; 84 placebo)	Sarilumab 200 mg, 400 mg or placebo were administered as an IV infusion. A second dose could be administered within 24–48 h of the first dose if required	The primary endpoint was time to ≥2-point clinical improvement (7-point scale; range: 1 (death) to 7 (not hospitalized))	The efficacy of sarilumab was not demonstrated in patients hospitalized with COVID-19 and receiving supplemental oxygen

The National Institute for Health and Care Excellence (NICE) periodically updates a summary of the existing evidence on clinical trials evaluating the efficacy and safety of TCZ in the treatment of COVID-19 [23]. It also includes a section about the limitations of such studies. The evidence comes from five clinical studies conducted on hospitalized patients with COVID-19 pneumonia [24–27]. These studies were included in the meta-analysis discussed above [22]. They include evidence from another study by Veiga et al. [28], who performed a randomized open-label clinical trial (NCT04403685) in which they evaluated the use of a single dose of IV TCZ (8 mg/kg) plus standard care as compared to standard care alone. They concluded that TCZ plus standard care did not improve clinical outcomes at day 15 compared to standard care alone, and it might increase mortality in patients with severe or critical COVID-19. Gordon et al. [29] conducted a Randomized, Embedded, Multifactorial Adaptive Platform Trial for Community-Acquired Pneumonia (REMAPCAP; NCT02735707) for evaluating the use of anti-IL-6 mAbs, i.e., TCZ and sarilumab in the treatment of critical cases of COVID-19. The main conclusion they reached was that the treatment with the IL-6 receptor antagonists (TCZ and sarilumab) improved outcomes, including survival. As a consequence, the National Health Service (NHS) encouraged doctors to consider prescribing either TCZ or sarilumab in the treatment of Intensive Care Unit (ICU) patients with COVID-19 pneumonia [17]. A short while ago, Horby et al. [30] published their preliminary results from a randomized, controlled, open-label clinical trial (RECOVERY; NCT04381936) performed in the UK. They concluded that TCZ administered intravenously in patients with hypoxia and systemic inflammation, improved survival and other secondary outcomes. Preliminary evidence from these two RCTs highlight a possible benefit in adults who have been hospitalized with severe COVID-19 and have clinical evidence of progressive disease (hypoxia and systemic inflammation) [30]; or with severe COVID-19 who are critically ill and receiving respiratory or cardiovascular organ support in an intensive care setting [29]. The most recent study was conducted in India [31]. The results of this open-label, multicenter, randomized, controlled, phase 3 trial showed that the primary and secondary endpoints were not significantly different between TCZ plus standard care and standard care alone. Consequently, they did not support routine use of TCZ in adults with COVID-19.

2.2. Sarilumab

Sarilumab is a human IgG1 mAb that targets both soluble and membrane-bound IL-6 receptors (IL-6R), and it inhibits IL-6-mediated signalling. It is indicated, in combination with methotrexate, for the treatment of moderate to severe rheumatoid arthritis in adult patients [32].

Although sarilumab is also an anti-IL-6 therapeutic agent, it has not been the subject of as much research as TCZ. To date a total of 17 clinical trials are ongoing [18,33]. Of these,

five have been completed. Limited published studies exploring the benefits of this therapeutic against COVID-19 are available [15]. The first evidence came from observational studies. Khiali et al. [34] reviewed the potential use of sarilumab in the treatment of COVID-19 among other issues. They included four studies conducted in Italy: a clinical series study [35]; an observational clinical cohort study [36]; an open-label observational study [37]; and a retrospective case series [38]. Although the treatment with sarilumab 400 mg seemed to be safe, no clear evidence could be obtained from these studies and the authors therefore concluded that further clinical trials were necessary. The systematic review and meta-analysis done by Khan et al. [15] discussed five prospective studies that included a total of 389 participants who received sarilumab. This research concluded that there is a lack of evidence regarding the efficacy of sarilumab and highlighted the need for further studies.

Very recently, Castelnovo et al. [39] provided new evidence on the use of sarilumab to improve prognosis and reduce hospitalization times and mortality in COVID-19 pneumonia. Although their study was monocentric and retrospective, the authors argue that sarilumab seemed to be effective in the treatment of medium to severe forms of COVID-19 pneumonia, reducing the mortality risk driven by multi-organ failure, acting at the systemic level, and reducing inflammation levels and, therefore, microvascular complications.

RCTs are also being conducted to evaluate the efficacy of sarilumab in the treatment of COVID-19. In September 2020, Sanofi announced its phase III clinical trial results: sarilumab at a dose of 200 mg or 400 mg in severely or critically ill patients hospitalized with COVID-19 did not meet either its primary endpoint or its key secondary endpoint when compared to a placebo combined with standard hospital care [40]. The NICE also includes updated evidence on the benefits of sarilumab in the treatment of COVID-19. This site includes one prepublication [29] which suggests that sarilumab is beneficial in adults with severe COVID-19 [41]. The latest published literature on the use of sarilumab to treat COVID-19 includes a study conducted by Lescure et al. [42], who carried out a multinational, randomized, adaptive, phase 3, double-blind, placebo-controlled trial (NCT04327388), which involved SARS-CoV-2 positive patients with pneumonia who required oxygen supplementation or intensive care. Patients were randomized on a 2:2:1 ratio, receiving IV sarilumab 400 mg, sarilumab 200 mg, or placebo. This trial failed to demonstrate the efficacy of sarilumab in patients hospitalized with COVID-19 and receiving supplemental oxygen (Table 1).

2.3. Siltuximab

Siltuximab is a chimeric human-murine mAb that prevents human IL-6 from binding to both soluble and membrane IL-6 receptors (IL-6R). It is indicated for the treatment of multicentric Castleman's disease (MCD) in adult patients [43].

Currently, there are three ongoing and one completed clinical trial that involve siltuximab [18]. Gritti et al. [44] conducted an observational, control cohort, single-center study (NCT04322188) on a total of 60 COVID-19 patients to assess their mortality rate. A total of 30 patients were allocated to the siltuximab treatment cohort group and the other 30 patients were placed in the control group. The mortality rate was assessed on day 30 of the study and was found to be significantly lower in siltuximab-treated patients than in the control group. This study therefore showed that the administration of siltuximab could be beneficial for COVID-19 patients with rapid progression to respiratory failure requiring ventilatory support, as it reduces the hyperinflammation caused by the cytokine storm, which is associated with severe disease. However, the authors recommended that their findings be validated in a randomized controlled clinical trial.

3. SARS-CoV-2 Specific Monoclonal Antibodies

Phylogenetic analysis has shown that SARS-CoV and SARS-CoV-2 are very similar in genetic and structural terms. This helped scientists understand the pathogenesis of COVID-19 and provided a basis for initial research. Indeed, the glycosylated spike (S) proteins from both coronaviruses have a primary amino acid sequence homology of 77.5% [7,8]. The S proteins are located on the surface of these coronaviruses and are a key component in infection. They mediate viral host cell entry by binding to the host cell receptor angiotensin-converting enzyme 2 (ACE2). The SARS-CoV-2 S protein is composed of 1273 amino acids (aa) and consists of three segments: an extracellular N-terminus, a transmembrane (TM), and a short intracellular C-terminal segment. A signal peptide is located at the N-terminus domain which consists of a few aa (1–13 residues). The rest of the protein is divided into two large regions: S1 and S2 subunits. The S1 subunit (14–685 aa) is responsible for receptor binding and consists of an N-terminal domain (NTD) and a receptor-binding domain (RBD). The S2 subunit (686–1273 aa) comprises the fusion peptide (FP), heptapeptide repeat sequence 1 (HR1), HR2, TM domain, and cytoplasm domain, and is involved in the fusion of the viral and host cell membranes and the consequent release of the viral genome into the host cell (Figure 3a). The RBD region is considered a critical target for neutralizing antibodies (nAbs) since it allows the spike protein to bind to the cell receptor ACE2. A deeper knowledge about the structure and configuration of the SARS-CoV-2 S protein can be found in references [45,46].

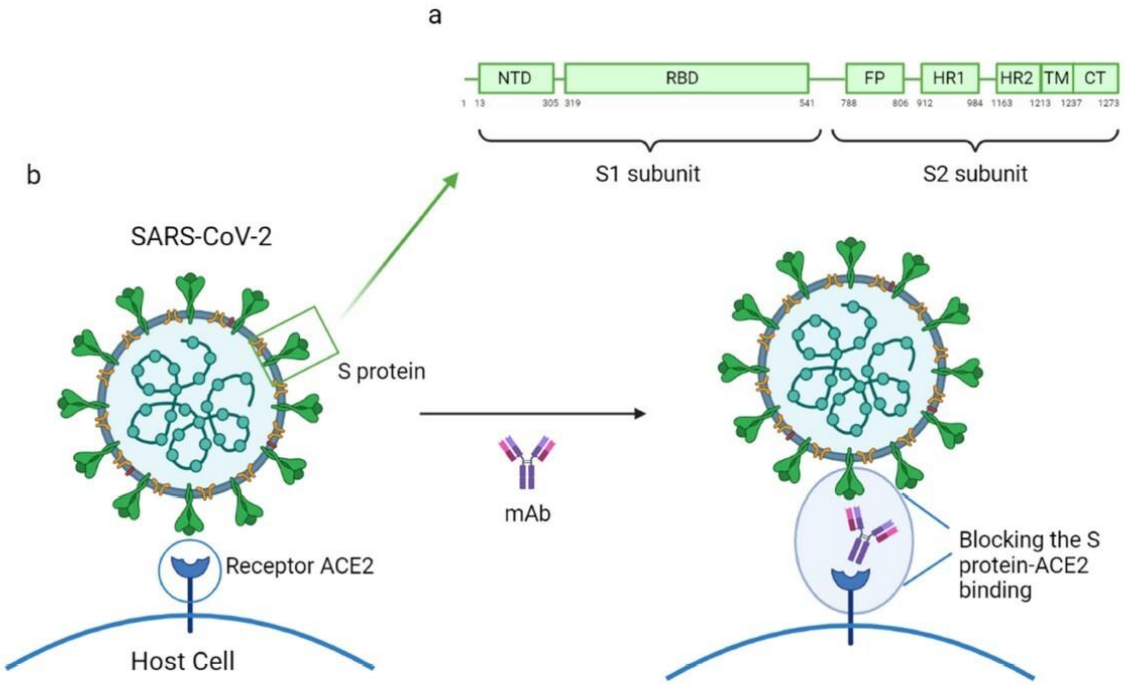

Figure 3. (a) Mechanism of action of a mAb by blocking the SARS-CoV-2 S protein and human ACE2 receptor binding; (b) structure of the SARS-CoV-2 S protein. This figure was composed using BioRender (available at: https://biorender.com/. Accessed on 12 May 2021).

The mAbs specifically designed to combat SARS-CoV-2 can be classified into three groups based on their respective objectives: (1) inhibiting virus attachment and entry by targeting either the virus structure or host receptors; (2) interfering with virus replication and transcription; and (3) hindering various stages of the immune system response [7]. Most of the mAbs currently under development target the S protein, which the virus uses to enter host cells [47]. Some reports highlighting the efficacy of specific mAbs against COVID-19 have already been published. These reports propose B38, H4, 47D11, and CR3022 as potential SARS-CoV-2 specific mAbs as they have demonstrated significant capacity to prevent infection by the virus. All these mAbs act by binding to the receptor-binding domain (RBD), therefore inhibiting the union between the virus and the human-ACE2 receptor (Figure 3b). It was also noted that B38 and H4, which had been isolated from a convalescent patient, bind exclusively to SARS-CoV-2 RBD, while 47D11 and CR3022 were tested against SARS-CoV and have demonstrated their ability to cross-neutralize SARSCoV and SARS-CoV-2 [7,8,48]. In Table 2 are shown the binding site and the mechanism of action of the SARS-CoV-2 specific mAbs discussed in this review.

3.1. mAbs Isolated from SARS-CoV-2 Patients

Plasma from convalescent COVID-19 patients is regarded as an important source of a variety of specific SARS-CoV-2 mAbs that directly target SARS-CoV-2 neutralization.

However, the infusion of convalescent plasma in late stages of the illness has proved unsuccessful at improving patient condition. It was therefore decided to test the potential benefits of plasma administration in an earlier phase of the illness. To this end, a randomized, double-blind, placebo-controlled clinical trial was conducted to evaluate the administration of high-titer convalescent plasma within 72 h after the onset of mild COVID-19 symptoms. In this study, severe respiratory disease was considered the primary end point and a total of 160 patients were enrolled. Despite the fact that this trial had to be suspended, the results showed a reduction in COVID-19 progression in older adults who received early administration of convalescent plasma [49].

Table 2. Binding site and mechanism of action of SARS-CoV-2 specific mAbs discussed in this review.

Groups of specific mAbs	Name	Binding site and mechanism of action
MAbs isolated from SARS-CoV-2 patients	B5	SARS-CoV-2 RBD; partial competition with ACE2
	B38	SARS-CoV-2 RBD; complete competition with ACE2
	H2	SARS-CoV-2 RBD; no competition with ACE2
	H4	SARS-CoV-2 RBD; complete competition with ACE2
	EY6A	SARS-CoV-2 RBD and SARS-CoV RBD with lower affinity; site spatially separate from that of ACE2
MAbs that cross-neutralize SARS-CoV and SARS-CoV-2	47D11	SARS-CoV-2 and SARS-CoV RBD; conserved epitope in the RBD
	CR3022	SARS-CoV RBD and SARS-CoV-2 RBD with lower affinity; conserved epitope in the RBD. Do not neutralize SARS-CoV-2
MAbs that have received Emergency Use Authorization (EUA)	Bamlanivimab (LY-CoV555)	SARS-CoV-2 RBD; EUA revoked
	Casirivimab (REGN10933) and imdevimab (REGN10987) in a combined therapy	Non-overlapping epitopes of the SARS-CoV-2 RBD
	Bamlanivimab (LY-CoV555) and etesevimab (LY-CoV016) in a combined therapy	Different, but overlapping, epitopes of the SARS-CoV-2 RBD

In order to find specific mAbs to combat this coronavirus, various antibodies have been isolated from the blood of convalescent patients. Some of the findings are discussed below.

Wu et al. [48] isolated four human-origin mAbs from a convalescent COVID-19 patient which were given the names B5, B38, H2, and H4. All of these mAbs were able to block the union between the S protein RBD domain and the ACE2 human cell receptor. These authors also found out that the newly discovered mAbs bound to SARS-CoV-2 RBD but not to SARS-CoV RBD, which suggests that the epitopes of both receptors are immunologically distinct. In

order to test the ability of each mAb to perform their neutralizing activity, the authors carried out a competition assay using biolayer interferometry (BLI). Their results showed that B38 and H4 displayed complete competition with ACE2 for RBD binding. B5, however, showed only partial competition and H2 did not compete with ACE2. In order to identify the epitope targeted by B38 and H4, they performed an epitope competition assay. The results suggested that these mAbs recognize different epitopes on RBD. This study concluded that B38 and H4 are promising candidates for use as part of antibody-based prophylactic and therapeutic COVID-19 treatment.

For their part, Zhou et al. [50] isolated another antibody, EY6A, from a convalescent COVID-19 patient. ELISA assays showed that EY6A bound to SARS-CoV-2 S protein and cross-reacted SARS-CoV with lower affinity. Using surface plasmon resonance (SPR), they determined that this mAb bound to SARS-CoV-2 RBD in a site that was spatially separate from that of ACE2. They also conducted three different neutralization assays which demonstrated that SARS-CoV-2 was highly neutralized by EY6A, which means that this antibody is also a possible candidate for use in the treatment of COVID-19.

3.2. mAbs That Cross-Neutralize SARS-CoV and SARS-CoV-2

Other studies have shown that 47D11 and CR3022 can bind to a highly conserved epitope in the RBD of the S protein in both coronaviruses [51,52]. Preclinical studies are being carried out with these mAbs in order to demonstrate their ability to cross-neutralize SARS-CoV and SARS-CoV-2.

Wang et al. [53] developed an ELISA-cross-reactivity assay with the aim of identifying cross-neutralizing SARS-CoV and SARS-CoV-2 mAbs. Only one antibody (47D11) showed cross-neutralizing activity. Furthermore, the ELISA assays demonstrated that 47D11 targeted the RBD of both coronaviruses and their bindings displayed similar affinities. The authors explain this cross-neutralization as a consequence of 47D11 binding to a conserved epitope in the RBD. They concluded that this mAb has good potential in the prevention and treatment of SARS-CoV-2 infected patients in either mono- or combined therapy.

Tian et al. [54] reported for the first time that CR3022, a SARS-CoV-specific mAb which was previously isolated from the blood of a convalescent SARS-CoV patient, could potentially bind to SARS-CoV-2 RBD. This result was determined by ELISA and BLI assays which confirmed that CR3022 could be considered as a candidate therapeutic for the treatment and prevention of COVID-19. Nevertheless, this study revealed that some potent SARS-CoV-specific neutralizing antibodies are unable to bind to the SARS-CoV-2 S protein, a result that was attributed to the differences between the C-terminus residues of the two coronaviruses. These differences had a significant impact on the cross-neutralizing activity of SARS-CoV-

specific antibodies, which highlights the need to develop novel SARS-CoV-2-specific mAbs. Yuan et al. [55] determined the complex crystal structure of CR3022-SARS-CoV-2 RBD. Their outcomes showed that this mAb targets a highly conserved epitope which is responsible for the cross-reactive binding to SARS-CoV and SARS-CoV-2. However, despite the fact that CR3022 is able to bind to both coronaviruses, it does not neutralize SARS-CoV-2. Wrobel et al. [56] supported these findings by using cryo-electron microscopy to study the mechanism by which CR3022 and SARS-CoV-2 S protein bind together. Their results confirmed that some rearrangements in the S1 domain are needed for such a union to occur, which result in dissociation of the S protein. They also reported that CR3022 did not neutralize SARS-CoV-2. Later, Wu et al. [57] performed a study involving CR3022 which again highlighted the different affinity of this mAb for the two types of coronavirus under consideration. Therefore, the authors studied the molecular basis leading to the difference in the binding affinity and neutralizing potency of CR3022 to SARS-CoV and SARS-CoV-2. They performed mutagenesis and binding experiments and demonstrated that the amino-acid located at residue 384 of the SARS-CoV-2 RBD structure was responsible for the different affinity. Moreover, given that the CR3022 epitopes in SARS-CoV and SARS-CoV-2 differ by four residues, the authors decided to use four SARS-CoV-2 mutants. This study showed that a single mutation (SARS-CoV-2 P384A mutant) improved the neutralization of SARS-CoV-2 with a similar potency to that shown in the neutralization of SARS-CoV. Their findings shed light on the cross-reactivity that some antibodies such as CR3022 can exhibit. In order to boost the therapeutic potential of CR3022, Atyeo et al. [58] dissected various strategies based on the use of selectively engineered Fc variants to enhance its functionality. However, their results showed an increased pathology in the animal models used, while highlighting the need for strategic Fc engineering for the treatment of COVID-19.

Given that each mAb has different binding sites, it has been suggested that a combination therapy of two or more mAbs that recognize neutralizing and non-neutralizing epitopes could well be the most effective way of using mAbs to treat COVID-19, as a single therapy might not be sufficient [51].

3.3. mAbs That Have Received Emergency Use Authorization (EUA)

Recently, the FDA issued an EUA for certain mAbs undergoing clinical trials that have shown significant efficacy in COVID-19 infected patients. An EUA is different from FDA approval and is based on all the available scientific evidence. The potential benefits of the drugs that have received an EUA outweigh the potential risks when used for the treatment of COVID-19 in the authorized population. These mAbs have been authorized for use in non-hospitalized adult and pediatric patients (12 years of age or older weighing at least 40 kg) with mild to moderate COVID-19 but at high risk of disease progression and/or hospitalization. The

authorized mAbs may not be administered to hospitalized COVID-19 patients or to patients who require oxygen therapy due to COVID-19, as no studies have been conducted on hospitalized COVID-19 patients, a fact made clear on the information sheets for these mAbs. Some studies even indicate that hospitalized COVID-19 patients who require high flow oxygen or mechanical ventilation could undergo worse clinical outcomes if treated with these mAbs [59–61].

The first mAb under clinical trial to receive an EUA (November 09, 2020) from the FDA was bamlanivimab (LY-CoV555) [62], which was specifically designed to prevent the SARS-CoV-2 S protein from binding to and entering the host cells. The bamlanivimab EUA is supported by an ongoing, randomized, double-blind, placebo-controlled, single-dose phase 2 clinical trial (NCT04427501) conducted amongst 452 non-hospitalized patients that were diagnosed with mild or moderate COVID-19. These patients were divided into four groups according to the dose of bamlanivimab or placebo they received via intravenous infusion: (1) 101 patients were assigned to 700 mg of LY-CoV555 monotherapy; (2) 107 patients were assigned to 2800 mg of LY-CoV555 monotherapy; (3) 101 patients were assigned to 7000 mg of LY-CoV555 monotherapy; and (4) 143 patients were assigned to the placebo group. The quantitative virologic endpoints and clinical outcomes were evaluated and the results from the interim analysis (at day 11) showed that the second treatment (group 2) was the only one that appeared to accelerate the natural decline in viral load over time. Moreover, the patients who received LY-CoV555 showed slightly less severe symptoms over the period from day 2 to 6 than those in the placebo group. The percentage of COVID-19 patients who were hospitalized or had to visit an emergency department was lower (1.6%) in the LY-CoV555 patients than in the placebo group (6.3%) [63].

Subsequently, on November 21, 2020, the FDA announced an EUA for casirivimab (REGN10933) and imdevimab (REGN10987) used in a combined cocktail called REGNCOV2 [64]. Both mAbs bind to non-overlapping epitopes of the SARS-CoV-2 S protein RBD and potently neutralize the entry of the virus into the host cells. In a previous preclinical study [65], in vivo efficacy of REGN-COV2 was assessed in two animal models, in which rhesus macaques and golden hamsters were used to evaluate mild and severe disease respectively. In this study, reduction in viral load in the upper and lower airways, reduction in virus-induced pathology (in rhesus macaques) and loss of weight (in hamsters) were assessed in order to evaluate the efficacy of combined therapy with casirivimab and imdevimab. The study concluded that REGN-COV2 successfully reduced virus load in the upper and lower airways. Furthermore, this combined therapy decreased virus-induced pathological sequelae when administered in rhesus macaques and limited the weight loss in hamsters. Given the significant efficacy of REGN-COV2 shown in preclinical studies, a clinical trial (NCT04425629) was

carried out in order to evaluate the decrease in viral load in symptomatic non-hospitalized COVID-19 patients and also to assess the safety and efficacy of this therapy. The main reason for employing a cocktail of mAbs was to reduce the risk of treatment-resistant mutant virus emergence. The first 275 patients included in this ongoing, multicenter, randomized, double-blind, phase 1–3 clinical trial were selected to describe the results of an initial analysis. All patients were randomly assigned: (1) 92 patients received 2.4 g of REGN-COV2; (2) 90 patients received 8.0 g of REGN-COV2; and 93 patients received a placebo. Results of the study revealed a reduction in the viral load when using this mAbs cocktail [66], on the basis of which the FDA decided to issue the aforementioned EUA.

The FDA later issued an EUA (February 09, 2021) for the combined administration of bamlanivimab (LY-CoV555) and etesevimab (LY-CoV016) [67]. In a similar way to bamlanivimab, etesevimab is specifically directed against the SARS-CoV-2 S protein and blocks the entry of the virus into the host cells. However, these mAbs bind to different, but overlapping, epitopes within the RBD of the SARS-CoV-2 S protein. This EUA relies on an ongoing, phase 2/3, randomized, double-blind, placebo-controlled clinical trial (NCT04427501) in which 577 non-hospitalized patients with mild to moderate COVID-19 symptoms were randomized to receive a single infusion of bamlanivimab, the combination treatment, or a placebo: (1) 101 patients were assigned to 700 mg of bamlanivimab; (2) 107 patients were assigned to 2800 mg of bamlanivimab; (3) 101 patients were assigned to 7000 mg of bamlanivimab; (4) 112 patients were assigned to 2800 mg of bamlanivimab and 2800 mg of etesevimab; and (5) 156 patients were assigned to placebo. The aim of this clinical trial was to determine the effect of the monotherapy and the combination therapy on viral load in mild to moderate COVID-19. The results drawn from this study conclude that the viral load reduction was statistically significant at day 11 in the combination therapy, compared with the placebo group. Nevertheless, bamlanivimab monotherapy showed no significant improvements in terms of viral load reduction [68].

On April 16, 2021, the FDA revoked the EUA for bamlanivimab monotherapy due to the fact that there had been an increase across the U.S. in the number of SARS-CoV-2 variants which are resistant to this treatment. The FDA therefore concluded that the known and potential benefits of bamlanivimab as a monotherapy no longer outweighed its known and potential risks. Importantly, alternative monoclonal antibody therapies remain available under EUA, including REGEN-COV, and bamlanivimab and etesevimab, administered together, for the same uses as had been previously authorized for bamlanivimab alone. Both therapies remain appropriate for treating patients with COVID-19 when used in accordance with the authorized labelling [69].

As regards the use of mAbs authorized by the FDA for emergency use in COVID-19 treatment and the recently initiated vaccination process, the Advisory Committee on Immunization Practices (ACIP) has recommended a precautionary measure as to date there are no data on the effectiveness and safety of either the Pfizer-BioNTech or Moderna COVID-19 vaccines (both mRNA vaccines) in SARS-CoV-2 infected patients who had previously received one of the aforementioned mAbs therapies. The ACIP suggests postponing the vaccination for 90 days after using mAbs for COVID-19 treatment. This recommendation is based on available data considered by the agency which suggests that there is a low risk of SARS-CoV-2 reinfection in the 90 days after initial infection and considering the estimated half-life of mAbs. The purpose of this measure is to avoid interferences between the mAbs used in the COVID-19 treatment and the vaccine-induced immune response [70–72].

3.4. How SARS-CoV-2 Mutations Could Affect the Efficacy of the Treatment with mAbs

Although specific mAbs are more promising in the treatment of COVID-19 than nonspecific ones, some concerns are arising given the advent of new SARS-CoV-2 variants, such as B.1.351 and B.1.1.7. Recent publications [73,74] have discussed how new SARS-CoV-2 variants could affect the efficacy of the treatments with antibodies. It might seem logical that the efficacy of CPT treatment would be less impaired by the new variants due to the presence of antibodies with specificity for different S protein epitopes. However, it has been demonstrated in preclinical studies that S protein mutations escape from polyclonal serum [75] and CPT has reduced neutralizing activity against some viral variants [74]. Nevertheless, a preprint article dated last February has suggested that the variants identified in the United Kingdom and South Africa are more resistant to CPT [76].

With regard to mAbs, a combination of them could be necessary if the new variants are the results of high mutation rate in the virus. In the case of low mutation rates or highly conserved epitopes, a combined mAbs therapy could be not required. On the other hand, RNA viruses display high mutation rates due to the errors introduced by the RNA-dependent RNA polymerases (RdRp). However, coronaviruses encode a 3’ to 5’ exoribonuclease that helps to correct errors made by the RdRp during replication. This leads to a lower probability of escaping from antibody neutralization in comparison with other RNA viruses that do not encode this enzyme [75]. Focusing on mAbs directed to SARSCoV-2, it has been very recently reported —April 2021— drug resistance in new variants, for example, to bamlanivimab as indicated above [69]. To date, a proper knowledge of the effect of new variants on the neutralizing capacity of mAbs is unknown [73].

4. Expert Opinion

In recent years, mAbs and Fc-fusion proteins have made it possible to take qualitative and quantitative steps forward in terms of therapeutic options for diseases with a clearly defined biological target, such as infectious diseases and, in this specific case, COVID-19. MAbs open up a new world in the field of passive immunization, which enables us to administer specific neutralizing antibodies against certain highly conserved epitopes of SARS-CoV-2 and also to obtain new drugs in record time, so that in just one year there are now more than 10 monoclonal antibodies in different stages of clinical development for use against COVID. Some of them are very promising and are almost ready for commercial launch.

5. Conclusions

Although mAb production is time-consuming and expensive, especially for use against new pathogens, they have been regarded as a good option for the treatment of COVID-19 since the beginning of the pandemic and many clinical trials on both non- and SARS-CoV-2 specific mAbs are currently ongoing. However, the outcomes of clinical trials for non-SARSCoV-2 specific mAbs are proving controversial, as their efficacy has yet to be definitively demonstrated, whilst SARS-CoV-2 specific mAbs have demonstrated significant levels of efficacy. So far, two specific mAb-based COVID-19 treatments have received an EUA from the FDA. The first involves combined administration of casirivimab and imdevimab, and the second, combined administration of bamlanivimab and etesevimab. These clinical trials have therefore shown the importance of developing mAbs that are specifically targeted at SARS-CoV-2 rather than those aimed at the COVID-19-associated cytokine storm.

Author Contributions: Conceptualization, A.T.-L. and J.H. Funding acquisition, N.N., J.C., and A.S.-G. Project administration, N.N. and A.S.-G. Supervision, N.N., L.C.-R., and A.S.-G. Writing—original draft preparation, A.T.-L. and J.H. Writing—review and editing, N.N., L.C.-R., and A.S.-G. Visualization, A.T.-L. and J.H. All authors have read and agreed to the published version of the manuscript.

Funding: This study was partially funded by Project FIS: PI-17/00547 (Institute of Health ‘Carlos III’, Ministry of Economy and Competitiveness, Spain), which means that it was also partially supported by European Regional Development Funds (ERDF).

Institutional Review Board Statement: Not applicable.

Informed Consent Statement: Not applicable.

Data Availability Statement: Not applicable.

Acknowledgments: Anabel Torrente-López is currently benefiting from a FPU predoctoral grant (ref.: FPU18/03131) from the Ministry of Universities, Spain. Jesús Hermosilla is currently benefiting from a research contract (E-18-2019-0231782) from the Fundación Investigación Biosanitaria Andalucia Oriental (FIBAO), Granada (Spain).

Conflicts of Interest: The authors declare no conflict of interest.

Abbreviations

ACE2: Angiotensin-Converting Enzyme 2; CPT: Convalescent Plasma Therapy; EUA: Emergency Use Authorization; FDA: Food and Drug Administration; ICU: Intensive Care Unit; IL-1R: Interleukin-1 Receptor; IL-6: Interleukin-6; IL-6R: Interleukin-6 Receptor; IV: intravenous; mAb: monoclonal antibody; pAb: polyclonal antibody; RBD: Receptor-Binding Domain; RCT: Randomized Clinical Trial; SARS-CoV: Severe Acute Respiratory Syndrome-Coronavirus; TCZ: tocilizumab.

References

1. World Health Organization, Coronavirus disease (COVID-19) outbreak. https://www.who.int/1. Renn, A.; Fu, Y.; Hu, X.; Hall, M.D.; Simeonov, A. Fruitful Neutralizing Antibody Pipeline Brings Hope To Defeat SARS-Cov-2. Trends Pharmacol. Sci. 2020, 41, 815–829. [CrossRef] [PubMed]

2. Cantini, F.; Goletti, D.; Petrone, L.; Najafi Fard, S.; Niccoli, L.; Foti, R. Immune Therapy, or Antiviral Therapy, or Both for COVID-19: A Systematic Review. Drugs 2020, 80, 1929–1946. [CrossRef] [PubMed]

3. Gavriatopoulou, M.; Ntanasis-Stathopoulos, I.; Korompoki, E.; Fotiou, D.; Migkou, M.; Tzanninis, I.-G.; Psaltopoulou, T.; Kastritis, E.; Terpos, E.; Dimopoulos, M.A. Emerging treatment strategies for COVID-19 infection. Clin. Exp. Med. 2021, 21, 167–179. [CrossRef] [PubMed]

4. RECOVERY Collaborative Group. Effect of Hydroxychloroquine in Hospitalized Patients with Covid-19. N. Engl. J. Med. 2020, 383, 2030–2040. [CrossRef] [PubMed]

5. WHO Solidarity Trial Consortium. Repurposed Antiviral Drugs for Covid-19—Interim WHO Solidarity Trial Results. N. Engl. J. Med. 2021, 384, 497–511. [CrossRef]

6. Horby, P.W.; Mafham, M.; Bell, J.L.; Linsell, L.; Staplin, N.; Emberson, J.; Palfreeman, A.; Raw, J.; Elmahi, E.; Prudon, B.; et al. Lopinavir–ritonavir in patients admitted to hospital with COVID-19 (RECOVERY): A randomised, controlled, open-label, platform trial. Lancet 2020, 396, 1345–1352. [CrossRef]

7. Owji, H.; Negahdaripour, M.; Hajighahramani, N. Immunotherapeutic approaches to curtail COVID-19. Int. Immunopharmacol. 2020, 88, 106924. [CrossRef]

8. Jahanshahlu, L.; Rezaei, N. Monoclonal antibody as a potential anti-COVID-19. Biomed. Pharmacother. 2020, 129, 110337. [CrossRef]

9. An, Z. Therapeutic Monoclonal Antibodies; JohnWiley & Sons, Inc.: Hoboken, NJ, USA, 2009; ISBN 9780470485408.

10. Zarkali, A.; Karageorgopoulos, D.E.; Rafailidis, P.I.; Falagas, M.E. Frequency of the off-label use of monoclonal antibodies in clinical practice: A systematic review of the literature. Curr. Med. Res. Opin. 2014, 30, 471–480. [CrossRef]

11. Brechner, R.J.; Rosenfeld, P.J.; Babish, J.D.; Caplan, S. Pharmacotherapy for Neovascular Age-Related Macular Degeneration: An Analysis of the 100% 2008 Medicare Fee-For-Service Part B Claims File. Am. J. Ophthalmol. 2011, 151, 887–895. [CrossRef]

12. DeFrancesco, L. COVID-19 antibodies on trial. Nat. Biotechnol. 2020, 38, 1242–1252. [CrossRef]

13. Fajgenbaum, D.C.; June, C.H. Cytokine Storm. N. Engl. J. Med. 2020, 383, 2255–2273. [CrossRef]

14. European Medicines Agency. Treatments and Vaccines for COVID-19—European Medicines Agency. Available online: https://www.ema.europa.eu/en/human-regulatory/overview/public-health-threats/coronavirus-disease-covid-19/treatments-vaccines-covid-19#research-and-development-section (accessed on 16 March 2021).

15. Khan, F.A.; Stewart, I.; Fabbri, L.; Moss, S.; Robinson, K.; Smyth, A.R.; Jenkins, G. Systematic review and meta-analysis of anakinra, sarilumab, siltuximab and tocilizumab for COVID-19. Thorax 2021, 1–13. [CrossRef]

16. European Medicines Agency. Tocilizumab: Summary of Product Characteristics. Available online: https://www.ema.europa.eu/en/documents/product-information/roactemra-epar-product-information_en.pdf (accessed on 17 March 2021).

17. Fazakerley, I. COVID-19 Therapeutic Alert: Interleukin-6 Inhibitors (Tocilizumab or Sarilumab) for Patients Admitted to ICU with COVID-19 Pnuemonia (Adults). Available online:

https://www.sehd.scot.nhs.uk/publications/DC20210108interleukin-6_inhibitors.pdf (accessed on 16 March 2021).

18. ClinicalTrials.gov Home Page. Available online: https://clinicaltrials.gov/ (accessed on 16 March 2021).

19. Boregowda, U.; Perisetti, A.; Nanjappa, A.; Gajendran, M.; Kutti Sridharan, G.; Goyal, H. Addition of Tocilizumab to the Standard of Care Reduces Mortality in Severe COVID-19: A Systematic Review and Meta-Analysis. Front. Med. 2020, 7, 586221. [CrossRef]

20. Berardicurti, O.; Ruscitti, P.; Ursini, F.; D'Andrea, S.; Ciaffi, J.; Meliconi, R.; Iagnocco, A.; Cipriani, P.; Giacomelli, R. Mortality in tocilizumab-treated patients with COVID-19: A systematic review and meta-analysis. Clin. Exp. Rheumatol. 2020, 38, 1247–1254.

21. Cortegiani, A.; Ippolito, M.; Greco, M.; Granone, V.; Protti, A.; Gregoretti, C.; Giarratano, A.; Einav, S.; Cecconi, M. Rationale and evidence on the use of tocilizumab in COVID-19: A systematic review. Pulmonology 2021, 27, 52–66. [CrossRef] [PubMed]

22. Kow, C.S.; Hasan, S.S. The effect of tocilizumab on mortality in hospitalized patients with COVID-19: A meta-analysis of randomized controlled trials. Eur. J. Clin. Pharmacol. 2021, 1–6. [CrossRef]

23. COVID-19 Rapid Evidence Summary: Tocilizumab for COVID-19. Available online: https://www.nice.org.uk/advice/es33/chapter/Factors-for-decision-making (accessed on 16 March 2021).

24. Salama, C.; Han, J.; Yau, L.; Reiss, W.G.; Kramer, B.; Neidhart, J.D.; Criner, G.J.; Kaplan-Lewis, E.; Baden, R.; Pandit, L.; et al. Tocilizumab in Patients Hospitalized with Covid-19 Pneumonia. N. Engl. J. Med. 2021, 384, 20–30. [CrossRef] [PubMed]

25. Hermine, O.; Mariette, X.; Tharaux, P.-L.; Resche-Rigon, M.; Porcher, R.; Ravaud, P.; Bureau, S.; Dougados, M.; Tibi, A.; Azoulay, E.; et al. Effect of Tocilizumab vs Usual Care in Adults HospitalizedWith COVID-19 and Moderate or Severe Pneumonia. JAMA Intern. Med. 2021, 181, 32. [CrossRef]

26. Stone, J.H.; Frigault, M.J.; Serling-Boyd, N.J.; Fernandes, A.D.; Harvey, L.; Foulkes, A.S.; Horick, N.K.; Healy, B.C.; Shah, R.; Bensaci, A.M.; et al. Efficacy of Tocilizumab in Patients Hospitalized with Covid-19. N. Engl. J. Med. 2020, 383, 2333–2344. [CrossRef]

27. Salvarani, C.; Dolci, G.; Massari, M.; Merlo, D.F.; Cavuto, S.; Savoldi, L.; Bruzzi, P.; Boni, F.; Braglia, L.; Turrà, C.; et al. Effect of Tocilizumab vs Standard Care on ClinicalWorsening in Patients Hospitalized With COVID-19 Pneumonia. JAMA Intern. Med. 2021, 181, 24. [CrossRef]

28. Veiga, V.C.; Prats, J.A.G.G.; Farias, D.L.C.; Rosa, R.G.; Dourado, L.K.; Zampieri, F.G.; Machado, F.R.; Lopes, R.D.; Berwanger, O.; Azevedo, L.C.P.; et al. Effect of tocilizumab on clinical outcomes at 15 days in patients with severe or critical coronavirus disease 2019: Randomised controlled trial. BMJ 2021, 372, n84. [CrossRef]

29. Gordon, A.C.; Mouncey, P.R.; Al-Beidh, F.; Rowan, K.M.; Nichol, A.D.; Arabi, Y.M.; Annane, D.; Beane, A.; Van Bentum-Puijk, W.; Berry, L.R.; et al. Interleukin-6 Receptor Antagonists in Critically Ill Patients with Covid-19. N. Engl. J. Med. 2021, 384, 1491–1502. [CrossRef] [PubMed]

30. Horby, P.W.; Campbell, M.; Staplin, N.; Spata, E.; Emberson, J.; Pessoa-Amorim, G.; Peto, L. Tocilizumab in patients admitted to hospital with COVID-19 (RECOVERY): Preliminary results of a randomised, controlled, open-label, platform trial. medRxiv 2021, 397, 1637–1645. [CrossRef]

31. Soin, A.S.; Kumar, K.; Choudhary, N.S.; Sharma, P.; Mehta, Y.; Kataria, S.; Govil, D.; Deswal, V.; Chaudhry, D.; Singh, P.K.; et al. Tocilizumab plus standard care versus standard care in patients in India with moderate to severe COVID-19-associated cytokine release syndrome (COVINTOC): An open-label, multicenter, randomised, controlled, phase 3 trial. Lancet Respir. Med. 2021, 9, 511–521. [CrossRef]

32. European Medicines Agency. Sarilumab: Summary of Product Characteristics. Available online: https://www.ema.europa.eu/en/documents/product-information/kevzara-epar-product-information_en.pdf (accessed on 17 March 2021).

33. Ucciferri, C.; Vecchiet, J.; Falasca, K. Role of monoclonal antibody drugs in the treatment of COVID-19. World J. Clin. Cases 2020, 8, 4280–4285. [CrossRef] [PubMed]

34. Khiali, S.; Rezagholizadeh, A.; Entezari-Maleki, T. A comprehensive review on sarilumab in COVID-19. Expert Opin. Biol. Ther. 2020, 21, 615–626. [CrossRef] [PubMed]

35. Benucci, M.; Giannasi, G.; Cecchini, P.; Gobbi, F.L.; Damiani, A.; Grossi, V.; Infantino, M.; Manfredi, M. COVID-19 pneumonia treated with Sarilumab: A clinical series of eight patients. J. Med. Virol. 2020, 92, 2368–2370. [CrossRef] [PubMed]

36. Gremese, E.; Cingolani, A.; Bosello, S.L.; Alivernini, S.; Tolusso, B.; Perniola, S.; Landi, F.; Pompili, M.; Murri, R.; Santoliquido, A.; et al. Sarilumab use in severe SARS-CoV-2 pneumonia. medRxiv 2020, 27, 1–8. [CrossRef]

37. Della-Torre, E.; Campochiaro, C.; Cavalli, G.; De Luca, G.; Napolitano, A.; La Marca, S.; Boffini, N.; Da Prat, V.; Di Terlizzi, G.; Lanzillotta, M.; et al. Interleukin-6 blockade with sarilumab in severe COVID-19 pneumonia with systemic hyperinflammation: An open-label cohort study. Ann. Rheum. Dis. 2020, 79, 1277–1285. [CrossRef]

38. Montesarchio, V.; Parella, R.; Iommelli, C.; Bianco, A.; Manzillo, E.; Fraganza, F.; Palumbo, C.; Rea, G.; Murino, P.; De Rosa, R.; et al. Outcomes and biomarker analyses among patients with COVID-19 treated with interleukin 6 (IL-6) receptor antagonist sarilumab at a single institution in Italy. J. Immunother. Cancer 2020, 8, e001089. [CrossRef]

39. Castelnovo, L.; Tamburello, A.; Lurati, A.; Zaccara, E.; Marrazza, M.G.; Olivetti, M.; Mumoli, N.; Mastroiacovo, D.; Colombo, D.; Ricchiuti, E.; et al. Anti-IL6 treatment of serious COVID-19 disease. Medicine 2021, 100, e23582. [CrossRef]

40. Kevzara Fails in PhIII COVID-19 Trial—PharmaTimes. Available online: http://www.pharmatimes.com/news/kevzara_fails_in_phiii_covid-19_trial_1347570 (accessed on 17 March 2021).

41. COVID-19 Rapid Evidence Summary: Sarilumab for COVID-19. Available online: https://www.nice.org.uk/advice/es34/chapter/Factors-for-decision-making (accessed on 17 March 2021).

42. Lescure, F.-X.; Honda, H.; Fowler, R.A.; Lazar, J.S.; Shi, G.; Wung, P.; Patel, N.; Hagino, O.; Bazzalo, I.J.; Casas, M.M.; et al. Sarilumab in patients admitted to hospital with severe or critical COVID-19: A randomised, double-blind, placebo-controlled, phase 3 trial. Lancet Respir. Med. 2021, 9, 522–532. [CrossRef]

43. European Medicines Agency. Siltuximab: Summary of Product Characteristics. Available online: https://www.ema.europa.eu/en/documents/product-information/sylvant-epar-product-information_en.pdf (accessed on 17 March 2021).

44. Gritti, G.; Raimondi, F.; Ripamonti, D.; Riva, I.; Landi, F.; Alborghetti, L.; Frigeni, M.; Damiani, M.; Micò, C.; Fagiuoli, S.; et al. IL-6 signalling pathway inactivation with siltuximab in patients with COVID-19 respiratory failure: An observational cohort study. medRxiv 2020. [CrossRef]

45. Huang, Y.; Yang, C.; Xu, X.; Xu, W.; Liu, S. Structural and functional properties of SARS-CoV-2 spike protein: Potential antivirus drug development for COVID-19. Acta Pharmacol. Sin. 2020, 41, 1141–1149. [CrossRef]

46. Valdez-Cruz, N.A.; García-Hernández, E.; Espitia, C.; Cobos-Marín, L.; Altamirano, C.; Bando-Campos, C.G.; Cofas-Vargas, L.F.; Coronado-Aceves, E.W.; González-Hernández, R.A.; Hernández-Peralta, P.; et al. Integrative overview of antibodies against SARS-CoV-2 and their possible applications in COVID-19 prophylaxis and treatment. Microb. Cell Fact. 2021, 20, 88. [CrossRef]

47. Marovich, M.; Mascola, J.R.; Cohen, M.S. Monoclonal Antibodies for Prevention and Treatment of COVID-19. JAMA 2020, 324, 131. [CrossRef]

48. Wu, Y.;Wang, F.; Shen, C.; Peng,W.; Li, D.; Zhao, C.; Li, Z.; Li, S.; Bi, Y.; Yang, Y.; et al. A noncompeting pair of human neutralizing antibodies block COVID-19 virus binding to its receptor ACE2. Science 2020, 368, 1274–1278. [CrossRef]

49. Libster, R.; Pérez Marc, G.; Wappner, D.; Coviello, S.; Bianchi, A.; Braem, V.; Esteban, I.; Caballero, M.T.; Wood, C.; Berrueta, M.; et al. Early High-Titer Plasma Therapy to Prevent Severe Covid-19 in Older Adults. N. Engl. J. Med. 2021, 384, 610–618. [CrossRef] [PubMed]

50. Zhou, D.; Duyvesteyn, H.M.E.; Chen, C.-P.; Huang, C.-G.; Chen, T.-H.; Shih, S.-R.; Lin, Y.-C.; Cheng, C.-Y.; Cheng, S.-H.; Huang, Y.-C.; et al. Structural basis for the neutralization of SARS-CoV-2 by an antibody from a convalescent patient. Nat. Struct. Mol. Biol. 2020, 27, 950–958. [CrossRef] [PubMed]

51. Ho, M. Perspectives on the development of neutralizing antibodies against SARS-CoV-2. Antib. Ther. 2020, 3, 109–114. [CrossRef]

52. Ku, Z.; Ye, X.; Salazar, G.T.; Zhang, N.; An, Z. Antibody therapies for the treatment of COVID-19. Antib. Ther. 2020, 3, 101–108. [CrossRef]

53. Wang, C.; Li, W.; Drabek, D.; Okba, N.M.A.; van Haperen, R.; Osterhaus, A.D.M.E.; van Kuppeveld, F.J.M.; Haagmans, B.L.; Grosveld, F.; Bosch, B.-J. A human monoclonal antibody blocking SARS-CoV-2 infection. Nat. Commun. 2020, 11, 2251. [CrossRef] [PubMed]

54. Tian, X.; Li, C.; Huang, A.; Xia, S.; Lu, S.; Shi, Z.; Lu, L.; Jiang, S.; Yang, Z.; Wu, Y.; et al. Potent binding of 2019 novel coronavirus spike protein by a SARS coronavirus-specific human monoclonal antibody. Emerg. Microbes Infect. 2020, 9, 382–385. [CrossRef] [PubMed]

55. Yuan, M.; Wu, N.C.; Zhu, X.; Lee, C.-C.D.; So, R.T.Y.; Lv, H.; Mok, C.K.P.; Wilson, I.A. A highly conserved cryptic epitope in the receptor binding domains of SARS-CoV-2 and SARS-CoV. Science 2020, 368, 630–633. [CrossRef] [PubMed]

56. Wrobel, A.G.; Benton, D.J.; Hussain, S.; Harvey, R.; Martin, S.R.; Roustan, C.; Rosenthal, P.B.; Skehel, J.J.; Gamblin, S.J. Antibodymediated disruption of the SARS-CoV-2 spike glycoprotein. Nat. Commun. 2020, 11, 5337. [CrossRef] [PubMed]

57. Wu, N.C.; Yuan, M.; Bangaru, S.; Huang, D.; Zhu, X.; Lee, C.-C.D.; Turner, H.L.; Peng, L.; Yang, L.; Burton, D.R.; et al. A natural mutation between SARS-CoV-2 and SARS-CoV determines neutralization by a cross-reactive antibody. PLoS Pathog. 2020, 16, e1009089. [CrossRef] [PubMed]

58. Atyeo, C.; Slein, M.D.; Fischinger, S.; Burke, J.; Schäfer, A.; Leist, S.R.; Kuzmina, N.A.; Mire, C.; Honko, A.; Johnson, R.; et al. Dissecting strategies to tune the therapeutic potential of SARS-CoV-2–specific monoclonal antibody CR3022. JCI Insight 2021, 6, e143129. [CrossRef]

59. FDA. Coronavirus (COVID-19) Update: FDA Authorizes Monoclonal Antibody for Treatment of COVID-19. 2020. Available online: https://www.fda.gov/news-events/press-announcements/coronavirus-covid-19-update-fda-authorizes-monoclonalantibody-treatment-covid-19 (accessed on 17 March 2021).

60. FDA. Coronavirus (COVID-19) Update: FDA Authorizes Monoclonal Antibodies for Treatment of COVID-19. 2020. Available online: https://www.fda.gov/news-events/press-announcements/coronavirus-covid-19-update-fda-authorizes-monoclonalantibodies-treatment-covid-19 (accessed on 17 March 2021).

61. FDA. Coronavirus (COVID-19) Update: FDA Authorizes Monoclonal Antibodies for Treatment of COVID-19. 2021. Available online: https://www.fda.gov/news-events/press-announcements/coronavirus-covid-19-update-fda-authorizes-monoclonalantibodies-treatment-covid-19-0 (accessed on 17 March 2021).

62. Fact Sheet for Health Care Providers Emergency Use Authorization (EUA) of Bamlanivimab Authorized Use. Available online: https://www.fda.gov/media/143603/download (accessed on 17 March 2021).

63. Chen, P.; Nirula, A.; Heller, B.; Gottlieb, R.L.; Boscia, J.; Morris, J.; Huhn, G.; Cardona, J.; Mocherla, B.; Stosor, V.; et al. SARS-CoV-2 Neutralizing Antibody LY-CoV555 in Outpatients with Covid-19. N. Engl. J. Med. 2021, 384, 229–237. [CrossRef]

64. Fact Sheet for Health Care Providers Emergency Use Authorization (EUA) of Casirivimab and Imdevimab Authorized Use. Available online: https://www.fda.gov/media/143892/download (accessed on 17 March 2021).

65. Baum, A.; Ajithdoss, D.; Copin, R.; Zhou, A.; Lanza, K.; Negron, N.; Ni, M.;Wei, Y.; Mohammadi, K.; Musser, B.; et al. REGNCOV2 antibodies prevent and treat SARS-CoV-2 infection in rhesus macaques and hamsters. Science 2020, 370, 1110–1115. [CrossRef]

66. Weinreich, D.M.; Sivapalasingam, S.; Norton, T.; Ali, S.; Gao, H.; Bhore, R.; Musser, B.J.; Soo, Y.; Rofail, D.; Im, J.; et al. REGN-COV2, a Neutralizing Antibody Cocktail, in Outpatients with Covid-19. N. Engl. J. Med. 2021, 384, 238–251. [CrossRef]

67. Fact Sheet for Health Care Providers Emergency Use Authorization (EUA) of Bamlanivimab and Etesevimab Authorized Use. Available online: https://www.fda.gov/media/145802/download (accessed on 17 March 2021).

68. Gottlieb, R.L.; Nirula, A.; Chen, P.; Boscia, J.; Heller, B.; Morris, J.; Huhn, G.; Cardona, J.; Mocherla, B.; Stosor, V.; et al. Effect of Bamlanivimab as Monotherapy or in Combination With Etesevimab on Viral Load in Patients With Mild to Moderate COVID-19. JAMA 2021, 325, 632–644. [CrossRef]

69. Bamlanivimab Revocation Letter. Available online: https://www.fda.gov/media/147629/download (accessed on 19 April 2021).

70. Frequently Asked Questions on the Emergency Use Authorization for Bamlanivimab. Available online: https://www.fda.gov/media/143605/download (accessed on 17 March 2021).

71. Frequently Asked Questions on the Emergency Use Authorization of Casirivimab and Imdevimab. Available online: https://www.fda.gov/media/143894/download (accessed on 17 March 2021).

72. Frequently Asked Questions on the Emergency Use Authorization for Bamlanivimab and Etesevimab. Available online: https://www.fda.gov/media/145808/download (accessed on 17 March 2021).

73. Taylor, P.C.; Adams, A.C.; Hufford, M.M.; de la Torre, I.; Winthrop, K.; Gottlieb, R.L. Neutralizing monoclonal antibodies for treatment of COVID-19. Nat. Rev. Immunol. 2021. [CrossRef]

74. Wang, P.; Nair, M.S.; Liu, L.; Iketani, S.; Luo, Y.; Guo, Y.;Wang, M.; Yu, J.; Zhang, B.; Kwong, P.D.; et al. Antibody resistance of SARS-CoV-2 variants B.1.351 and B.1.1.7. Nature 2021, 593, 130–135. [CrossRef] [PubMed]

75. Liu, Z.; VanBlargan, L.A.; Bloyet, L.-M.; Rothlauf, P.W.; Chen, R.E.; Stumpf, S.; Zhao, H.; Errico, J.M.; Theel, E.S.; Liebeskind, M.J.; et al. Identification of SARS-CoV-2 spike mutations that attenuate monoclonal and serum antibody neutralization. Cell Host Microbe 2021, 29, 477–488. [CrossRef] [PubMed]

76. Wang, P.; Liu, L.; Iketani, S.; Luo, Y.; Guo, Y.; Wang, M.; Yu, J.; Zhang, B.; Kwong, P.D.; Graham, B.S.; et al. Increased Resistance of SARS-CoV-2 Variants B.1.351 and B.1.1.7 to Antibody Neutralization. bioRxiv 2021. [CrossRef]

CAPÍTULO 2

Use of subcutaneous tocilizumab to prepare intravenous solutions for COVID-19 emergency shortage: Comparative analytical study of physicochemical quality attributes

INTRODUCCIÓN AL CAPÍTULO 2

Este capítulo recoge un estudio analítico comparativo de los atributos fisicoquímicos de la calidad de tocilizumab (TCZ), un mAb empleado para el tratamiento de la COVID-19. TCZ (RoActemra®), de administración intravenosa, se ha empleado en hospitales en pacientes infectados por SARS-CoV-2 que han mostrado una respuesta exagerada de su sistema inmune frente a esta infección, conocida como síndrome de liberación de citoquinas (cytokine release syndrom (CRS)), dado que este mAb actúa bloqueando a una de las principales citoquinas responsables de esta respuesta exacerbada, la IL-6. El estudio que aquí se presenta se planteó tras la problemática que surgió en los hospitales debido a la escasez de la forma farmacéutica de administración intravenosa (IV) de este medicamento debido a su alta demanda. Por esta razón, se quiso estudiar si la forma farmacéutica subcutánea (SC) podría ser empleada de forma IV con la finalidad de solventar el problema. Para ello, se llevó a cabo un estudio de comparabilidad evaluando los principales atributos fisicoquímicos críticos de la calidad de las disoluciones de TCZ utilizadas para infusión, a 6 mg/mL y 4 mg/mL, preparadas a partir de RoActemra® 20 mg/mL (forma IV) y de RoActemra® 162 mg (jeringa precargada de 0,9 mL de solución, forma SC). De forma general, para este estudio se consideraron dos lotes diferentes para el análisis. Se utilizó un lote de cada medicamento, IV y SC, para preparar las muestras de disolución clínica a 6 mg/mL y 4 mg/mL de TCZ. Se utilizó un lote diferente de los medicamentos para corroborar los resultados obtenidos previamente, con el fin de evaluar las diferencias entre lotes. A lo largo del estudio se emplearon distintas técnicas analíticas para el desarrollo de metodología que permitieron el estudio comprensivo de las distintas características fisicoquímicas de TCZ, entre las que se incluyen la dispersión de luz dinámica (DLS) para estudiar el particulado de las disoluciones, la cromatografía de exclusión molecular ((SE)HPLC-DAD) para estudiar el perfil de agregación, la cromatografía de intercambio catiónico ((CEX)UHPLCDAD) para estudiar el perfil de variantes de carga, y la fluorescencia intrínseca de triptófanos (IT-F) para evaluar la estructura conformacional tridimensional de TCZ. Además, también se llevaron a cabo estudios de degradación controlada con la finalidad de validar todos los métodos desarrollados y para evaluar la comparabilidad entre las soluciones clínicas IV y SC de TCZ, asumiendo que entidades moleculares similares tenían comportamientos y vías de degradación similares. También fueron útiles para comparar la estabilidad de TCZ frente a la degradación. Estas condiciones estresantes a las que fue sometido TCZ fueron las siguientes: (i) exposición a 40 °C durante 24 horas; (ii) exposición a irradiación por luz en una cámara de envejecimiento durante 24

horas; (iii) exposición a un medio ácido al 1% para ser analizado inmediatamente después de su preparación y tras 24 horas de almacenaje; y (iv) exposición a un medio básico al 1% para ser analizado inmediatamente después de su preparación y tras 24 horas de almacenaje.

Este trabajo reveló una gran similitud entre los atributos críticos de calidad fisicoquímica de las disoluciones clínicas de TCZ a 6 mg/mL y 4 mg/mL preparadas para infusión usando el medicamento SC (RoActemra® 162 mg) y los de las disoluciones clínicas de TCZ a 6 mg/mL y 4 mg/mL preparadas para infusión usando el medicamento IV (RoActemra® 20 mg/mL). Las disoluciones clínicas SC también demostraron una alta comparabilidad con las disoluciones clínicas IV en términos de estabilidad durante 24 h y patrones de degradación cuando se sometieron a estudios de degradación controlada. Además, TCZ en su forma SC (RoActemra® 162 mg) no sufre ninguna degradación y/o modificación como consecuencia de su dilución en NaCl al 0,9% para preparar las soluciones clínicas diluidas a 6 y 4 mg/mL para perfusión, por lo que este estudio no se encontró ninguna evidencia que desaconseje la recomendación de utilizar TCZ en su forma SC (RoActemra® 162 mg) para preparar soluciones diluidas en NaCl al 0,9% a 6 y 4 mg/mL para ser utilizadas para administración IV.

SCIENTIFIC ARTICLE

Use of subcutaneous tocilizumab to prepare intravenous solutions for COVID-19 emergency shortage: Comparative analytical study of physicochemical quality attributes

Natalia Navas[a, *], Jesús Hermosilla[a, 1], Anabel Torrente-López[a, 1], José Hernández-Jiménez[a, 1], Jose Cabeza[b], Raquel Pérez-Robles[a], Antonio Salmerón-García[b]

[a] Department of Analytical Chemistry, Science Faculty / Biomedical Research Institute ibs.Granada, University of Granada, Granada, E-18071, Spain

[b] UGC Farmacia Hospitalaria, Biomedical Research Institute ibs.Granada. Hospital Universitario San Cecilio de Granada, Granada, E-18012, Spain

Journal of Pharmaceutical Analysis 10 (2020) 532–545

Accepted: 24 June 2020

DOI: 10.1016/j.jpha.2020.06.003

Journal of Pharmaceutical Analysis 10 (2020) 532–545

Contents lists available at ScienceDirect

Journal of Pharmaceutical Analysis

journal homepage: www.elsevier.com/locate/jpa

Original article

Use of subcutaneous tocilizumab to prepare intravenous solutions for COVID-19 emergency shortage: Comparative analytical study of physicochemical quality attributes

Natalia Navas [a, *], Jesús Hermosilla [a, 1], Anabel Torrente-López [a, 1], José Hernández-Jiménez [a, 1], Jose Cabeza [b], Raquel Pérez-Robles [a], Antonio Salmerón-García [b]

[a] Department of Analytical Chemistry, Science Faculty / Biomedical Research Institute ibs.Granada, University of Granada, Granada, E-18071, Spain
[b] UGC Farmacia Hospitalaria, Biomedical Research Institute ibs.Granada. Hospital Universitario San Cecilio de Granada, Granada, E-18012, Spain

Abstract

COVID-19, a disease caused by the novel coronavirus SARS-CoV-2, has produced a serious emergency for global public health, placing enormous stress on national health systems in many countries. Several studies suggest that cytokine storms (interleukins) may play an important role in severe cases of COVID-19. Neutralizing key inflammatory factors in cytokine release syndrome (CRS) could therefore be of great value in reducing the mortality rate. Tocilizumab (TCZ) in its intravenous (IV) form of administration -RoActemra® 20 mg/mL (Roche)- is indicated for treatment of severe CRS patients. Preliminary investigations have concluded that inhibition of IL-6 with TCZ appears to be efficacious and safe, with several ongoing clinical trials. This has led to a huge increase in demand for IV TCZ for treating severe COVID-19 patients in hospitals, which has resulted in drug shortages. Here, we present a comparability study assessing the main critical physicochemical attributes of TCZ solutions used for infusion, at 6 mg/mL and 4 mg/mL, prepared from RoActemra® 20 mg/mL (IV form) and from RoActemra® 162 mg (0.9 mL solution pre-filled syringe, subcutaneous(SC) form), to evaluate the use of the latter for preparing clinical solutions required for IV administration, so that in a situation of shortage of the IV medicine, the SC form could be used to prepare the solutions for IV delivery of TCZ. It is important to remember that during the current pandemic all the medicines are used off-label, since none of them has yet been approved for the treatment of COVID-19.

Keywords

COVID-19

Tocilizumab

Critical quality attributes

IV and SC medicines

1. Introduction

In humans, infection by the new severe acute respiratory syndrome coronavirus 2 (SARS-CoV-2) causes coronavirus disease 2019 (COVID-19), as named by the World Health Organization (WHO) [1]. COVID-19 has spread worldwide, becoming a pandemic and causing a global public health crisis. As of April 22, 2020, the disease had caused more than 2.5 million infections worldwide, with a fatality rate of 6.9% (more than 180,000) and a recovery rate of 27% (704,647 cases), although the data are constantly changing [2].

The SARS-CoV-2 virus affects different people in different ways. COVID-19 is a respiratory disease and most infected people have only mild symptoms which are not life-threatening, but the number of deaths is still high due to the large population base. People who have underlying medical conditions and those over 60 years old have a higher risk of developing severe symptoms and of dying. COVID-19 has different symptoms including in most cases fever, tiredness and a dry cough. Other symptoms such as shortness of breath, pains, sore throat, diarrhoea, nausea and a runny nose may also appear [3].

Several studies suggest that cytokine storms (interleukins) may play an important role in severe cases of COVID-19, which means that neutralizing key inflammatory factors in the cytokine release syndrome (CRS) could be of great value in reducing the mortality rate in severe cases [4,5]. The virus binds to alveolar epithelial cells, thus activating the innate immune system and adaptive immune system, resulting in the release of a large number of cytokines, including interleukin-6 (IL-6) [6]. IL-6 can be produced by almost all stromal cells and immune system cells, such as B lymphocytes, T lymphocytes, macrophages, monocytes, dendritic cells, mast cells and other non-lymphocytes such as fibroblasts, endothelial cells, keratinocytes, glomerular mesangial cells and tumour cells [7]. The classic IL-6 signal is limited to the cells (macrophages, neutrophils, T cells, etc.) that express IL-6R, and plays a leading role in the low level of IL-6. The combination of IL-6 and IL-6R leads to the gp130 co-receptor (CD130) initiating the inflammatory process [8].

Experimental research findings indicate that an excessive immune response and a strong CRS, which may include high levels of granulocyte-macrophage colony stimulating factor and IL-6, are activated in severe COVID-19 [9]. The monoclonal antibody (mAb) tocilizumab (TCZ) has been found to be effective in the treatment of severe CRS patients [10]. TCZ is the active ingredient of the medicinal product for intravenous (IV) administration RoActemra® 20 mg/mL (Roche Registration GmbH, Germany), which is indicated for the treatment of chimeric antigen receptor (CAR) T cell-induced severe or life-threatening CRS in adults and paediatric patients of 2 years of age and older [11]. On this basis, this medicine has been used to treat severe COVID-19 patients and several recent studies have already proposed the efficacy of TCZ in the treatment of COVID-19 [4-6,12-14]. Exploratory studies

detected high IL-6 levels in complicated cases of COVID-19 and suggested that the anti-IL-6 TCZ could have beneficial effects in complicated cases. Based on this last one, a systematic review and meta-analysis to assess this evidence was performed [15]. This work concluded that inhibition of IL-6 with TCZ appears to be efficacious and safe in preliminary investigation, although the results of several ongoing clinical trials should be awaited to better define the role of TCZ in COVID-19. Due to the sudden, unexpected health emergency produced by the COVID-19, there has recently been a huge increase in demand for the IV form of TCZ based on its indication for treating CRS. This high demand has produced shortages of the IV TCZ medicine for treating severe COVID-19 patients in some hospitals, for example in Spain, one of the countries most affected by this new coronavirus.

TCZ is a humanized anti-interleukin-6 receptor (IL-6R) mAb (IgG1). It binds to both soluble and membrane-bound IL-6 receptors and inhibits signalling mediated by the IL-6/IL-6R complex formation [16]. It is frequently used in the treatment of different autoimmune diseases [17] i.e., for the treatment of rheumatoid arthritis [18] and systemic juvenile idiopathic arthritis [19]. It has also been found to play a role in Castleman disease [20] and Crohn's disease [21]. A biosimilar called HS628 has also been proposed, and its physicochemical and biological similarity to that of the TCZ originator has been demonstrated [22].

TCZ is currently marketed in two different formulations based on the route of administration: IV (medicinal product named RoActemra® 20 mg/mL concentrate for solution for infusion) or subcutaneous (SC) (medicinal product named RoActemra® 162 mg solution for injection in pre-filled syringe) [11]. RoActemra® IV medicine was licensed in Europe for the management of patients with rheumatoid arthritis in 2009 and the SC formulation was approved in 2014 [23]. Although these two different routes of TCZ administration do not have identical clinical indications, several studies have already demonstrated that TCZ in SC form has similar levels of effectiveness to the IV form in terms of its clinical aspects [24,25]. SC TCZ is therefore an alternative for the treatment of several indications in which the clinical equivalence of the two formulations has been demonstrated.

SC formulations of mAbs medicine are generally perceived as more economical than IV ones mainly because of the limited drug preparation time, but also because only minimal skills are required for administration and it is less invasive, thus enabling patients to self-administer in a home setting [26-28]. These reasons may lead to the administration of SC medicines. Nevertheless, regardless of the route of administration, the mAb active ingredient in both formulations must have previously been proved comparable in terms of the functionality and quality of their critical physicochemical attributes, taking into account that these drugs have a degree of inherent variability due to their biotechnological nature. This means that the TCZ drug product in the two forms of administration must be similar; in other words, the

manufacturing process for SC TCZ must not affect quality attributes such as potency, aggregates order size or charge variant or the levels of process related impurities [29]. This means that if the excipients present in the SC form are compatible for IV delivery, the SC form could be used for IV administration, once the stability of the TCZ after dilution (to prepare the solution for infusion) has been proved. In this case, it could be used to treat severe COVID-19 patients, even though the SC medicinal product, i.e., RoActemra® 162 mg, is not specifically indicated for the treatment of the CRS produced by treatment with CAR-T immunotherapy.

To this end, in this paper we have conducted a comparability study assessing the main critical physicochemical attributes of the TCZ clinical solutions used for infusion, i.e., 6 mg/mL and 4 mg/mL, prepared from RoActemra® 20 mg/mL (IV form) and from RoActemra® 162 mg (SC form), in order to evaluate the use of the latter for preparing the 6 mg/mL and 4 mg/mL clinical solutions required for IV administration. If this is viable, in a hospital shortage situation of the medicine for IV administration (20 mg/mL), the SC form (162 mg in 0.9 mL solution pre-filled syringe) could be used to prepare the IV delivery of TCZ. It is important to bear in mind that during the current pandemic all the medicines are being used off-label, as none of them has yet been approved for the treatment of COVID-19.

2. Material and methods

2.1. Materials

2.1.1. Chemicals

The 100 mL sodium chloride (0.9%) infusion bags were from Fresenius Kiabi Espa~na S.A.U. (Marina 16e18, 08005 Barcelona, Spain; Bach 13NLS041, Ex.10/2021). Omnifix® Luer Lock Solo 3 mL syringes (Bach 19M18C8, Ex.11/2024) were obtained from B. Braun Melsungen AG (34209 Melsungen, Germany). Sodium chloride, sodium hydroxide, hydrochloric acid, disodium phosphate monohydrate and potassium phosphate monobasic were supplied by Panreac (Barcelona, Spain). A reconstituted solution of infliximab (IFX) (Remicade® 100 mg vial, Janssen Biotech, Horsham, U.S.A.) was used as quality control to assess the estimated molecular weight in size exclusion chromatography (SEC). Reverse-osmosis quality water purified (≥18 M/cm) with a Milli-RO plus Milli-Q station from Millipore Corp. (Madrid, Spain) was used throughout the study.

2.1.2. Tocilizumab medicines

Two vials each from different batches (B2084H09, Ex.04/2022 and B2084H09, Ex.10/2021; named throughout IV-Batch 1 and IV-Batch 2 respectively) of the medicine RoActemra® 20 mg/mL concentrate for solution for infusion, containing 200 mg/10 mL of TCZ

and two pre-filled syringes each from different batches (B1120, Ex.05/2021 and B1126, Ex.09/2021; named throughout SC-Batch 1 and SC-Batch 2 respectively) of the medicine RoActemra® 162 mg solution for injection with a content of 162 mg of TCZ in 0.9 mL (Roche Registration GmbH, Emil-Barrell-Strasse 1, 79639 Grenzach-Wyhlen, Germany) were used in this study. They were supplied by our Pharmacy Service at the University Hospital San Cecilio (Granada, Spain).

RoActemra® 20 mg/mL is supplied in a vial (type I glass) with a stopper (butyl rubber); the excipients are sucrose, polysorbate 80, disodium phosphate dodecahydrate, sodium dihydrogen phosphate dehydrate, and water for injections; each 200 mg vial contains 0.20 mmol (4.43 mg) sodium [11]. RoActemra® 162 mg is supplied in 0.9 mL solution in a pre-filled syringe (type I glass) with a staked-in needle containing 162 mg TCZ assembled into a prefilled pen; the syringe is closed by a rigid needle shield (elastomer seal with a polypropylene shell) and a plunger stopper (butyl rubber with a fluororesin coating). The excipients in RoActemra® 162 mg are L-histidine, L-histidine monohydrochloride monohydrate, L-arginine, L-arginine hydrochloride, L-methionine, polysorbate 80 and water for injections [11].

2.1.3. Tocilizumab solutions of 6 mg/mL and 4 mg/mL in 0.9% NaCl prepared from IV and SC medicines

Solutions of 6 mg/mL and 4 mg/mL of TCZ for infusion were prepared from RoActemra® 20 mg/mL in polyolefin infusion bags of 100 mL (Baxter, BN:18A23E4Z) by appropriate dilution in isotonic 0.9% NaCl under sterile conditions in a laminar flow cabinet as indicated in the summary of the product characteristics [11]. 2 mL of these IV TCZ solutions were taken directly from the bags and placed in lab amber glass vials for immediate analysis. Throughout this work, these samples were referred to as “IV” clinical solution samples.

Similarly, 2 mL of TCZ solutions at the same concentration as the IV clinical solutions, i.e., 6 mg/mL and 4 mg/mL, were prepared using the medicine for SC administration, i.e., RoActemra® 162 mg instead of RoActemra® 20 mg/mL, by appropriate dilutions in an isotonic aqueous medium 0.9% NaCl under sterile conditions in a laminar flow cabinet. These diluted solutions were placed in lab amber glass vials for immediate analysis. Throughout this work, these samples were referred to as “SC” clinical solution samples, so as to indicate that they were prepared from the medicine for SC administration even though they were not intended for SC use.

2.2. Methods

2.2.1. Visual inspection

A quick visual inspection was carried out daily prior to experimentation in order to check for evidence of large aggregate formation, turbidity, suspended particles, colour changes and gas formation. To this end, samples were visually inspected with the naked eye.

2.2.2. Dynamic light scattering (DLS)

Soluble particulates were assessed by DLS using a Zetasizer Nano-ZS90 Malvern (UK). Particle size distribution was determined on 0.5 mL of sample volume using 10 mm spectrophotometry disposable cuvettes. Each sample record was the cumulative result of 100 reads, acquired at a thermostatically controlled temperature of 20 °C and with a time acquisition of 10 s per read. The average hydrodynamic diameter (HD), polydispersity index (PDI), volume size distribution and intensity size distribution of all the samples analysed were compared and discussed.

2.2.3. Size exclusion high performance liquid chromatographic method with diode array detection ((SE)HPLC-DAD)

Aggregates were analyzed using an Agilent 110 HPLC system equipped with a quaternary pump, a degasser, an autosampler, a column oven and a photodiode array detector (Agilent Technologies, Madrid, Spain). The instrument was connected to a personal computer fitted with an HPLC ChemStation workstation for LC 3D systems (rev. A.0903, Agilent Technologies). The chromatographic analyses were carried out in a 300 mm × 4.6 mm i.d., 5 µm particle size, wide pore 300 Å size exclusion analytical column (300Bio SEC-5, Agilent Technologies, USA). All samples were eluted at an isocratic flow rate of 0.38 mL/min for 15 min with a mobile phase composition of buffer phosphate (150 mM, pH 7.00) prepared with anhydrous Na_2HPO_4 and adjusted with 0.1 M HCl. The temperature of the column was maintained at 25 °C, and the injection volume was 1 mL. UV-visible spectra were recorded between 190 nm and 500 nm, with a data point every 0.5 nm. Chromatograms were registered at $\lambda = 214 \pm 5$ nm and at $\lambda = 280 \pm 5$ nm, using $\lambda = 360 \pm 20$ nm signal as a reference. Samples were not filtered before being injected into the chromatograph to avoid aggregate loss in the filter. Similarity tests available in the HPLC ChemStation were used to evaluate the spectral peak purities to assess the monomers and aggregates [30].

2.2.4. Strong cation exchange ultra-high performance liquid chromatographic method with diode array detection ((CEX)UHPLCDAD)

Charge variant profiles were obtained using a strong cation exchange column (MAbPac™ SCX-10 RS, 2.1 mm × 50 mm, 5 mm, Thermo Scientific, P/N 082675) connected to a Dionex Ultimate 3000 UHPLC system. Mobile phase A consisted of 10 mM sodium phosphate (pH 7.5), and mobile phase B consisted of 10mMsodium phosphate and 100 mM sodium chloride (pH 7.5). The separation gradient was set as follows: 0-3 min, holding at 15%

B; 3-6 min, 15%-30% B; 6-20 min, 30%-55% B; and 20-22 min, 55%-100% B. The column was then washed with 100% B for 5 min, followed by equilibration using 15% B for 15 min. The mobile phase flow rate was 0.4 mL/min and the injection volume was 2 mL. The column temperature was set at 30 °C and chromatograms were registered at different wavelengths, i.e., λ = 214 nm, λ = 220 nm and λ = 280 nm, using λ = 350 ± 10 nm as the reference wavelength in all cases. At least duplicated analysis of the samples was made.

2.2.5. Intrinsic tryptophan fluorescence (IT-F)

Conformational tridimensional structure was assessed by IT-F and measurements were carried out on a Cary Eclipse spectrofluorometer (Agilent, Santa Clara, CA, USA). Emission spectra were recorded from 305 to 400 nm with the excitation wavelength set to 298 nm. The temperature of the samples was kept at room temperature. A total of 10 spectral accumulations were performed for all measurements. For all the samples, the excitation and emission slits were set to 5 nm. Raw spectra for each sample were visually checked, looking initially for either shifts in the maximum peaks or a decrease in fluorescence intensity. The spectral centre of mass (C.M.) was considered as a mathematical representation of each spectrum and was determined as such for each sample tested, using the following equation:

$$C.M. = \frac{\sum_i^n (\lambda i * fi)}{\sum_i^n fi}$$

in which λi is the wavelength and fi the fluorescence intensity.

2.3. Controlled degradation studies

Different ways of degradation were assessed by subjecting samples of TCZ solutions of 6 mg/mL prepared from both medicines, for IV and SC administration, to several stress conditions. These included (i) exposure to heat stress by keeping solutions at 40 °C for 24 h; (ii) exposure to light irradiation (250 W/m^2) in an ageing chamber (Solarbox 3000e RH, Cofomegra, Milan, Italy) for 24 h following the guidelines laid down by the International Conference for Harmonization (ICH Q1B) for photostability testing [31], (iii) exposure to 1% acidic medium with analysis immediately after preparation and after 24 h of storage, and (iv) exposure to 1% basic medium with analysis immediately after preparation and after storage for 24 h.

2.4. Methodology applied to compare the IV and SC TCZ samples

Table 1 shows the methodology applied to compare the IV and SC TCZ samples studied in this research. An assessment was made of the critical quality attributes of the medicines for SC and IV TCZ administration and of the diluted clinical solutions at 6 mg/mL and 4 mg/mL of TCZ prepared with both SC and IV medicines. Two different batches were

considered for the analysis. One batch of each medicine, SC and IV, was used to prepare the 4 mg/mL and 6 mg/mL TCZ clinical solution samples in order to assess similarity by comparing the results of the analysis of the critical quality attributes. A different batch of the medicines was used to corroborate the previously obtained results, in order to evaluate batch-to-batch differences.

The stability-indicating nature of all the methods used in this study was corroborated by accelerated degradation studies. These experiments were also useful for evaluating comparability between the IV and SC TCZ clinical solutions, assuming that similar molecular entities had similar degradation behaviour and pathways. They were also useful for comparing the stability of TCZ against degradation. Table 1 also indicates the analytical technique used to evaluate each of the critical quality attributes of the biotechnological drug TCZ in all these solutions, IV and SC medicinal products and IV and SC clinical solutions.

Analyses of the clinical solutions of 6 mg/mL and 4 mg/mL prepared by appropriate dilutions of the SC and IV medicine, as indicated above, were performed immediately after preparation (D0). The solutions were stored refrigerated at 4 °C and the analyses were repeated 24 h after preparation (D1). Results were then compared as discussed next.

Table 1. Methodology for comparing IV and SC TCZ samples: medicines and 6 mg/mL and 4 mg/mL.

Methodology	Technique	Samples
1. Critical quality control attributes		
Visual characteristics	Naked eye	Medicine (IV and SC)
Soluble particulate: Hydrodynamic diameter and polydispersity	DLS	6 mg/mL (IV and SC)
Aggregates profile	(SE)HPLC-DAD	4 mg/mL (IV and SC)
Charge variant profile	(CEX)UHPLC-UV	
Tertiary structure	IT-F	
2. Forced degradation (stress)		
Exposure 24 h to light	All the techniques:	6 mg/mL (IV and SC)
Exposure 24 h at 40 °C	DLS, (SE)HPLC-DAD,	
Exposure to 1% acidic medium (10 min and 24 h)	(CEX)UHPLC-UV, and	
Exposure to 1% basic medium (10 min and 24 h)	IT-F	

IT-F: Intrinsic tryptophan fluorescence, DLS: Dynamic light scattering, (SE) HPLC-UV: Size exclusion ultra-high performance liquid chromatography with diode array detector, (CEX)UHPLC-UV: Cation exchange ultra-high performance liquid chromatography with ultraviolet detector.

3. Results

3.1. Visual particulates

Visual inspection by the human eye can detect particulates of ~100 µm or larger [32]. The IV and SC TCZ clinical solution samples of 6 mg/mL and 4 mg/mL remained clear for the 24 h duration of the study with no precipitates or particulate matter detected with the naked eye. No changes in colour or turbidity were observed over the test period.

3.2. DLS: soluble particulates

Soluble particulates up to 10 µm were assessed by DLS. The results are presented in Fig. 1 and Tables 2 and 3, and are discussed next.

3.2.1. Comparability study of 6 mg/mL and 4 mg/mL IV and SC TCZ clinical solutions

Particulate size distributions by volume in the IV and SC TCZ clinical solutions at D0 and D1 are shown in Figs. 1A and B. This distribution was very similar in all the solutions, regardless of the concentration (4 mg/mL or 6 mg/mL) or the storage time (analysis conducted immediately after preparation (D0) or after storage for 24 h (D1). The results also indicated the detection of a single population of particulates with similar hydrodynamic volume measured as HD (Table 2), in all the solutions analysed and attributed to the monomers of TCZ. The graphs showing the particulate size distributions by intensity are shown in Fig. S1, and also indicate that this single population is almost exclusively responsible for the dispersion of light (99.9%).

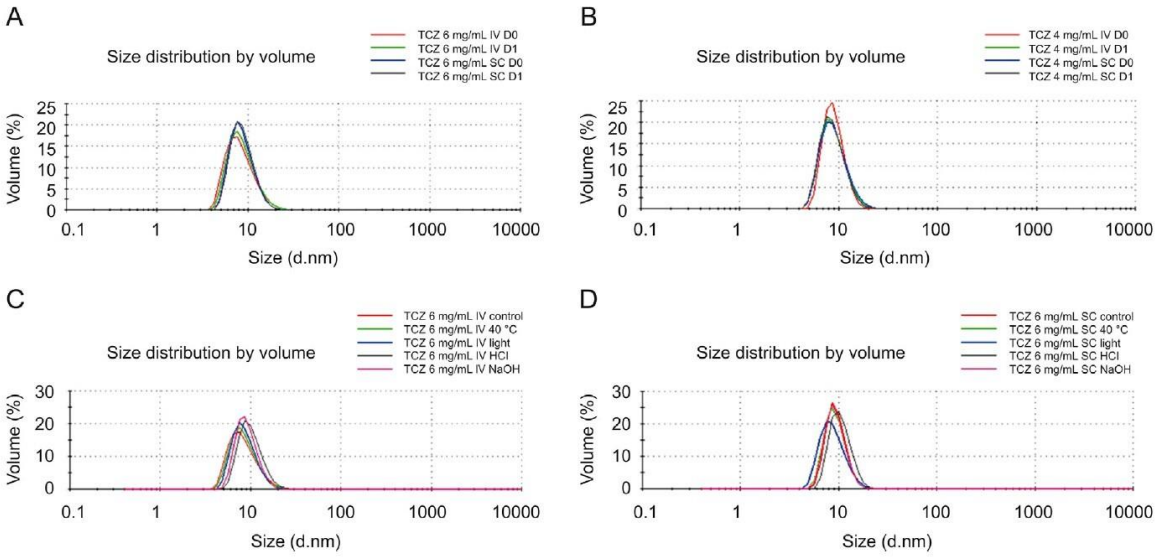

Fig. 1. Size distribution volume (DLS) comparability study of (A) 6 mg/mL IV and SC TCZ clinical solutions, and (B) 4 mg/mL IV and SC TCZ clinical solutions; all samples were prepared from IV-batch-1 and SC-batch-1. Stress study of (C) 6 mg/mL IV TCZ clinical solutions (IV-batch-1), and (D) 6 mg/mL SC TCZ clinical solutions (SC-batch-2).

Table 2. Hydrodynamic diameter (HD) and polydispersity index (PDI) comparability study of IV and SC clinical solutions: 6 mg/mL and 4 mg/mL TCZ.

Sample	HD (nm)		PDI	
	D0	D1	D0	D1
6 mg/mL IV	8.5 ± 3.3	8.7 ± 3.1	0.19	0.20
6 mg/mL SC	8.7 ± 2.6	8.8 ± 2.6	0.11	0.18
4 mg/mL IV	9.0 ± 2.1	8.9 ± 2.6	0.12	0.23
4 mg/mL SC	9.1 ± 2.8	8.8 ± 2.5	0.20	0.25

When the 6 mg/mL IV and SC TCZ solutions were compared, they displayed practically identical values for the HD at D0, i.e., 8.5 ± 3.3 nm and 8.7 ± 2.6 nm, respectively, and there were no significant differences between the values at D0 and the values at D1. Similar results were found for the 4 mg/mL TCZ solutions, with HD values practically identical at D0, i.e., 9.0 ± 2.1 nm and 9.1 ± 2.8 nm for the IV and SC, respectively, and no significant differences at D1. When the solutions at different concentrations were compared, no significant differences were detected between them either in the HD values or in the particulate size volume distributions. Our previous studies on other therapeutic IgG1 such as infliximab, rituximab and bevacizumab in 0.9% NaCl solutions at 1 mg/mL displayed HD values of around 12.7 nm, 9.7 nm and 8.4 nm, which means that TCZ has similar HD values to those of rituximab and bevacizumab [33-35].

In addition, in order to corroborate the single particulate population in all the TCZ solutions (assigned to the TCZ monomers), the PDI was obtained. This parameter is dimensionless ranging from 0 to 1 and scaled such that values of less than 0.05 are rarely seen other than with highly monodisperse standards. Values greater than 0.7 indicate that the sample has a very broad size distribution and that it is probably not suitable for study using the DLS technique. The PDI for all the samples was around 0.2, which confirmed that the solutions were mainly monodisperse (Table 2). Furthermore, the values were similar for both preparations, IV and SC, and were unchanged after storage for 24 h. In addition to all these, the polydispersity (%, Pd) of the single population corresponding to the TCZ was calculated as follows:

$$Pd = \frac{(St.Dev)^2}{(Size)^2}$$

in which St. Dev is the standard deviation (SD) of the population in nm and Size is the mean size of the population, also in nm. The Pd (%) measures the width of the assumed distribution. In terms of protein analysis, a Pd of 20% or less indicates that the sample is monodisperse. In

the 6 mg/mL solution, this value was 16% and 5% for the IV and SC solutions at D0 and 14% and 8.3% for IV and SC, respectively at D1. For the 4 mg/mL solutions, the Pd (%) was 4.7% (IV) and 9.6% (SC) at D0 and 8.4% (IV) and 7.5% (SC) at D1. The PDI therefore corroborated again that all the solutions are characterized by a single particulate population, which on the basis of its size is assigned to the monomers of TCZ.

All these results confirm high levels of similarity between the soluble particulate in 6 mg/mL and 4 mg/mL IV and SC solutions.

3.2.2. Comparability study of the stress tests on the 6 mg/mL IV and SC TCZ clinical solutions

TCZ degraded similarly in IV and SC solutions at 6 mg/mL when submitted to several controlled degradation or stress conditions, as can be deduced from the results set out in Figs. 1C and D and Table 3.

Table 3. Hydrodynamic diameter (HD) and polydispersity index (PDI) comparability stress study of IV and SC clinical solutions: 6 mg/mL TCZ.

Stress condition	Sample	HD (nm)		PDI	
		Control	Stress	Control	Stress
Light irradiation	IV	8.5 ± 3.3	8.7 ± 2.7	0.19	0.20
	SC	9.5 ± 2.1	8.9 ± 2.6	-	-
Temp. 40 °C	IV	8.5 ± 3.3	8.7 ± 3.0	0.19	0.16
	SC	9.5 ± 2.2	9.3 ± 2.2	-	-
Acidic medium	IV	8.5 ± 3.3	10.1 ± 3.0	0.19	0.35
	SC	9.5 ± 2.2	10.5 ± 2.6	-	-
Basic medium	IV	8.5 ± 3.3	9.1 ± 2.5	0.19	0.35
	SC	9.5 ± 2.2	9.3 ± 2.1	-	-

The graph displaying the particulate size distributions by volume (Figs. 1C and D) shows no new populations of particulate with higher or smaller volume, and no significant changes regarding the original particulate population in the TCZ control solution sample. Although the intensity distribution graph indicated the detection of a new particulate population of larger size (Figs. S1C and D), the contribution made by these larger size populations to the total volume in the solutions was close to 0.1% in all cases; it was therefore not clear whether these particle populations could be attributed to possible degradation of TCZ by aggregation or to particles of dust. These populations were only detected in IV samples subjected to acidic

and basic media, scattering at 500 nm and 300 nm respectively. In the case of the SC solutions samples, these populations were also detected scattering at 500 nm but only when subjected to light stress and at 300 nm in all the stressed samples and in the control, contributing 50%-70% of the total intensity registered, but representing only 0.1% of the total volume. This particle population was not detected in any of the solutions analysed in the comparability study; therefore, given its small contribution to the total volume (0.1%), it was probably due to the inclusion of dust when preparing the 6 mg/mL TCZ solution for the stress study.

In the IV and SC TCZ solution samples, the HD values for the stressed solution samples were similar to those of their respective control samples and similar to those of each other (Table 3). The PDI was close to 0.2 for all the IV stressed solution samples except for those subjected to acidic and basic media, in which this value increased to 0.35 due to the detection of the particle population at 300 and 500 nm. For the SC samples, PDI was not calculated because of the distortion in intensity caused by the particles thought to be dust.

3.3. (SE)HPLC-DAD method: chromatographic aggregates profile

The TCZ solution samples (both clinical solutions at 6 and 4 mg/mL) and the IV and SC medicinal products were analysed by SEC in order to obtain their chromatographic aggregate profile.

3.3.1. Comparability study of 6 mg/mL and 4 mg/mL IV and SC TCZ clinical solutions

The chromatographic aggregates profiles were invariant in all the samples and no modifications were observed either in shape or in the areas under the peaks, as can be seen in Fig. 2 for the two control days (D0 and D1). When the IV and SC samples were compared, the profile was also very similar. The only difference between them was the peak detected at the highest retention time at around 10.4 min in the IV samples and at 12.1 min in the SC, which is discussed next. In all the samples, the peak of the TCZ monomers was detected at 7.1 e 7.8 min IFX solutions of 10 mg were used as a control to test the retention time of the TCZ monomers, as both therapeutic mAbs belong to the IgG1 class and share a similar molecular weight at around 150 kDa (Fig. S2). The spectral peak purity factor calculated for the peaks for the TCZ monomers was greater than 98.7% in all the analyzed samples. The TCZ spectra for the monomers were the same regardless of their provenance, i.e., IV or SC medicines or dilutions (Figs. 3A2 and C2).

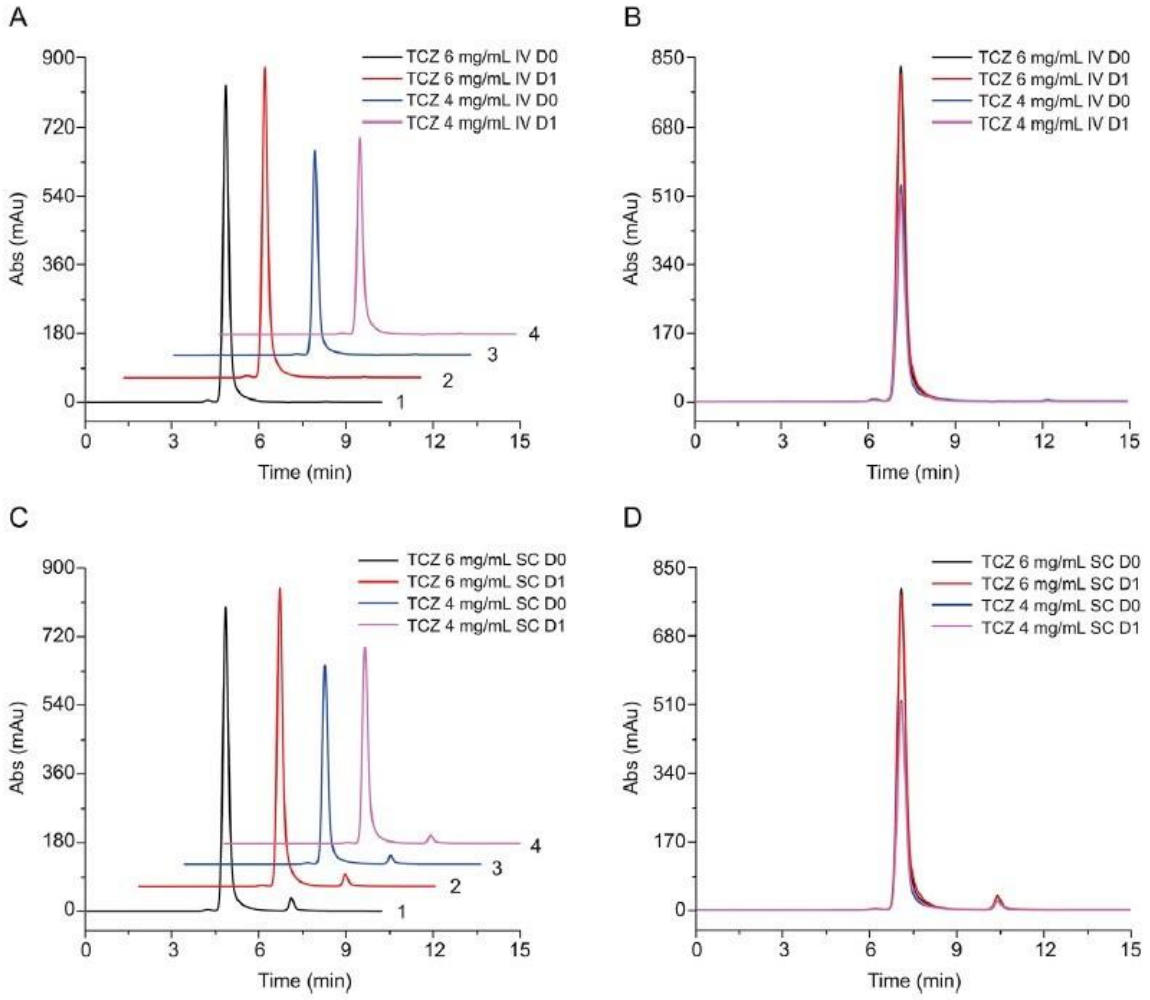

Fig. 2. TCZ SEC comparability study of 6 mg/mL and 4 mg/mL IV and SC clinical solutions. (A) SEC profile of the IV samples: (1) 6 mg/mL D0, (2) 6 mg/mL D1, (3) 4 mg/mL D0 and (4) 4 mg/mL D1; (B) overlaid profile of all the previous IV samples; (C) SEC profile of the SC samples: (1) 6 mg/mL D0, (2) 6 mg/mL D1, (3) 4 mg/mL D0 and (4) 4 mg/mL D1; (D) overlaid profile of all the previous SC samples. All samples were prepared from IV-batch-1 and SC-batch-1.

As regards to the peak at the shortest retention time at around 6.1 min, this was assigned to TCZ dimers (natural aggregates). This was also done by comparison with IFX, which we had studied in great depth in previous work on IgG1 SEC studies [36,37]. The percentage of these natural aggregates of TCZ with respect to the monomers was around 0.6%, and this value was maintained in all the samples, i.e., no differences were detected between IV and SC clinical solution samples either at 6 mg/mL or at 4 mg/mL and between IV or SC samples over the 24 h, i.e., D0 and D1 results. As regards to the UV spectra, these show similar patterns to those of the TCZ monomers, and are the same for IV and SC TCZ samples (Figs. 3A1 and C1).

As regards to the differences between IV and SC clinical solution samples detected in the peak at the largest retention time, these were noted in terms of both elution time and area

under the peak. In the case of IV, the peak was detected at around 12.1 min with an almost negligible percentage of the total area (around 0.1%). In all the SC SEC profiles, the peak was detected at 10.4 min, representing 3.4% of the total area, and this proportion was maintained independently of the dilution applied to the SC medicine to achieve the appropriate clinical concentration for intravenous administration. We then looked at the composition of the excipients used in the SC medicine RoActemra® 162 mg (see 2.1 Materials), but none of them could justify this peak, which had an estimated molecular weight of around 15e17 kDa (based on data from a previous calibration of our SEC column). Therefore, the source of this unknown compound was further investigated to find out whether it was already in the SC medicine RoActemra® 162 mg, or whether it had resulted from the dilution to prepare the concentration at 6 mg/mL and 4 mg/mL required for intravenous administration, or whether it was batch dependent. Fig. 3 shows the results of the analysis of a different batch of the IV (RoActemra® 20 mg/mL) and SC (RoActemra® 162 mg) medicines. The SC medicine had to be diluted to 27 mg/mL in order to avoid instrument saturation in both the chromatographic column and the UV detector. As can be seen in Fig. 3, the peak of this unknown compound was already detected maintaining the same percentage of total area. It could therefore be inferred that this unknown compound was already in the medicine (in both batches studied) and did not result from the dilution of the medicine to prepare the concentration required for intravenous administration in 0.9% NaCl. Also, the fact that this peak was not detected in the chromatogram recorded at 280 nm suggests that this unknown compound is not a protein. Fig. 3C3 also shows the UV spectrum for this compound, which is different from the identical spectra for the TCZ monomers and natural aggregates. Fig. 3A also shows that this unknown compound was not detected in either of the two IV samples, or in the clinical solutions (6 mg/mL and 4 mg/mL from Batch 1) or in the medicine (20 mg/mL, Batch 2). We also carried out a test to make sure that this peak did not correspond to HCl, as suggested in a previous publication on TCZ analysis by 2D chromatography [38]. The high spectral peak purity factor (over 98%) also suggested that only one compound had been detected in this chromatographic peak.

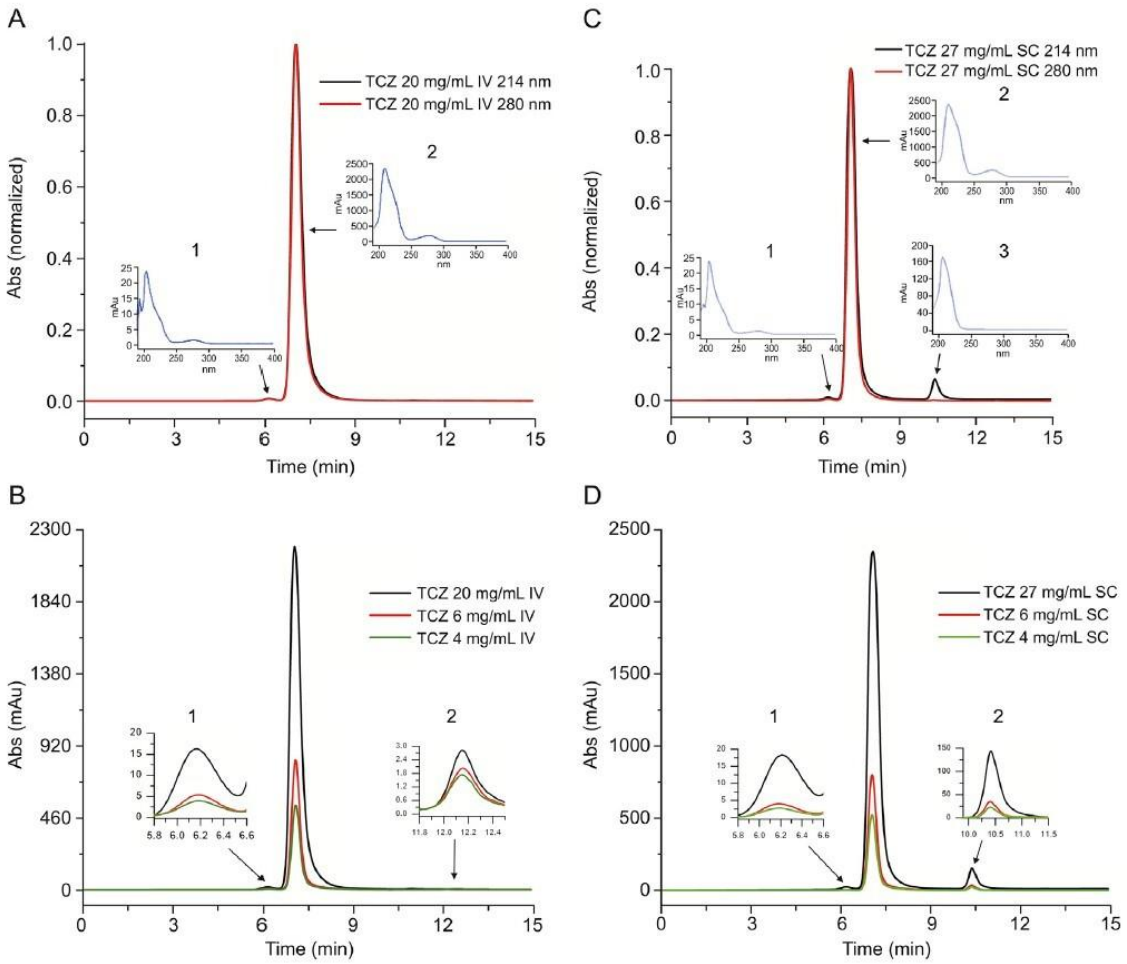

Fig. 3. TCZ SEC profiles comparability study including IV and SC medicinal products. (A) RoActemra® 20 mg/mL (IV-batch-2) at 214 nm and 280 nm: (1) UV dimers spectrum and (2) UV monomers spectrum; (B) RoActemra® 20 mg/mL (IV-batch-2) and the IV clinical solutions 6 mg/mL and 4 mg/mL at 214 nm (IV-batch-1): (1) zoom of dimers and (2) zoom of peak at around 12 min; (C) RoActemra® 162 mg (SC-batch-2) diluted to 27 mg/mL at 214 nm and 280 nm (SC-batch-1): (1) UV dimers spectrum, (2) UV monomers spectrum and (3) unknown compound spectrum; (D) RoActemra® 162 mg (SC-batch-2) diluted to 27 mg/mL and the SC clinical solutions 6 mg/mL and 4 mg/mL (SC-batch-1) at 214 nm: (1) zoom of dimers, (2) zoom of monomers and (3) zoom of unknown compound.

3.3.2. Comparability study of the stress tests on the 6 mg/mL IV and SC TCZ clinical solutions

The IV and SC TCZ clinical solutions degraded in similar ways as can be seen in the results set out in Fig. 4. SEC profiles were very similar except in the peak assigned to the unknown compound of non-protein nature detected in the SC solution samples, which remained un-degraded and was not affected by the stress to which the TCZ samples were subjected. Table 4 shows the percentage of higher order aggregates and the associated percentage of monomers, according to the type of stress to which the samples were subjected. The main degradation pattern was the increase of the peak at 6.1 min and no other chromatographic peaks were detected. As happened with other therapeutic proteins that we had studied in previous research [35,36,39] exposure to light induced TCZ aggregation. This

was slightly higher in the case of IV samples (1.54% compared to 0.98%). When the samples were kept in an acidic medium (pH = 1.7) for 48 h, aggregation increased to 11% (IV) and 14% (SC). This was the stress factor that caused most decay, with the corresponding important decrease in the percentage of monomers. By contrast, the TCZ samples seem to be robust against heat degradation when placed at 40 °C for 24 h with no exposure to light, as practically no changes were observed in the percentage of aggregates/monomers. It is also important to highlight that the degradation caused by exposure to a basic medium (pH = 11.0) decreased the percentage of aggregation.

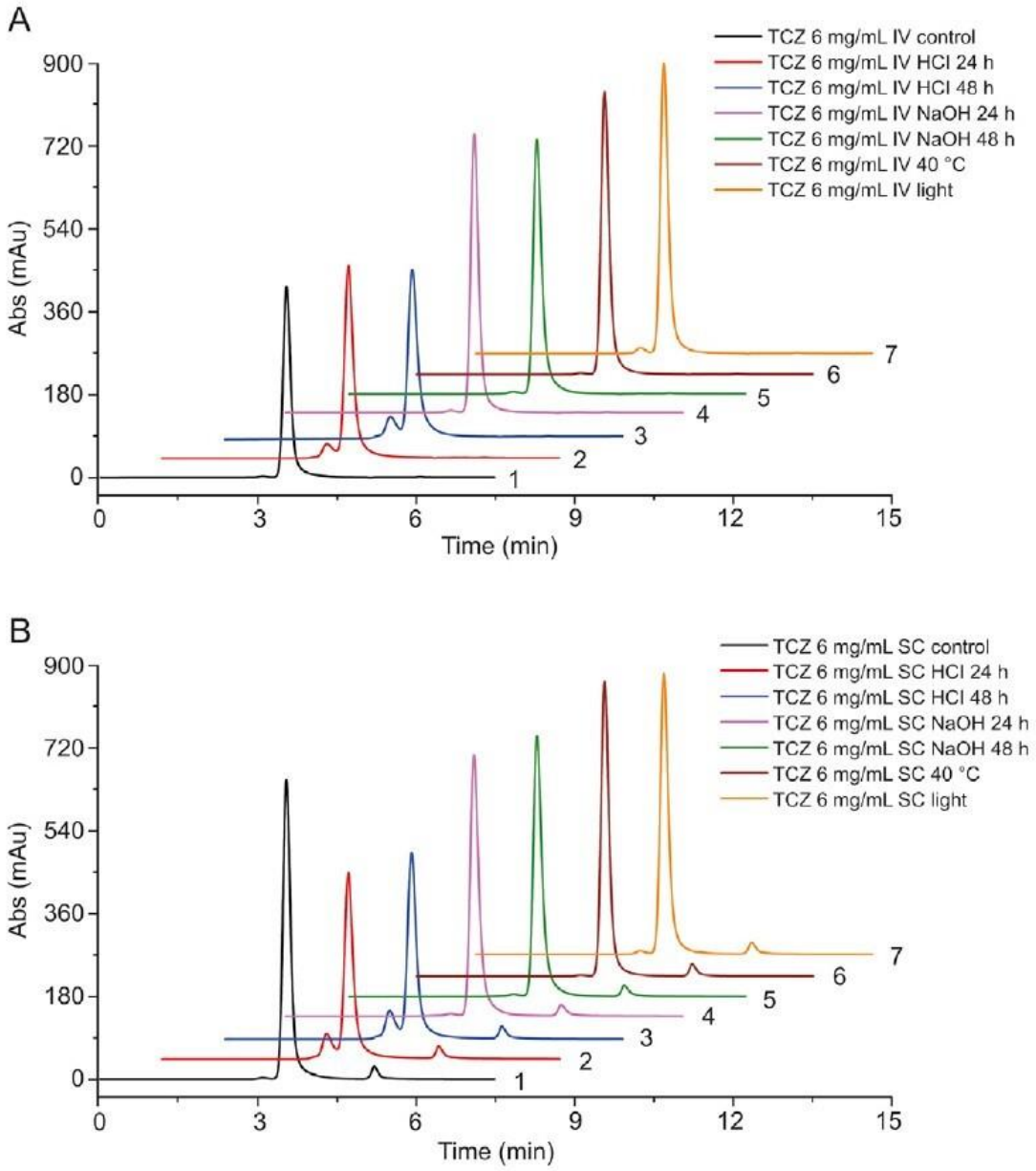

Fig. 4. TCZ stress study by SEC. (A) SEC profiles of samples of 6 mg/mL IV clinical solutions: (1) non-stressed sample, (2) acidic medium, 24 h, (3) acidic medium, 48 h, (4) basic medium, 24 h, (5) basic medium, 48 h, (6) temperature 40 °C and (7) light stress; (B) SEC profiles of samples of 6 mg/mL SC clinical solutions: (1) non-stressed sample, (2) acidic medium, 24 h, (3) acidic

medium, 48 h, (4) basic medium, 24 h, (5) basic medium, 48 h, (6) temperature 40 °C and (7) light stress. Samples shown are from IV-batch-1 and SC-batch-1 and SC-batch-2.

Table 4. Percentages of aggregation according to type of stress.

Stress condition	% of aggregation		% of monomer	
	Intravenous TCZ	Subcutaneous TCZ	Intravenous TCZ	Subcutaneous TCZ
Acid, 24 h	7.99	13.27	92.01	86.73
Acid, 48 h	11.17	14.13	88.83	85.87
Base, 24 h	0.73	0.54	99.27	99.46
Base, 48 h	0.74	0.62	99.26	99.38
Temp. 40 °C	0.49	0.38	99.51	99.62
Light	1.54	0.98	98.46	99.02

3.4. (CEX)UHPLC-UV method: chromatographic charge variant profile

Chemical and enzymatic modifications can lead to charge variants in mAbs [40]. Charge heterogeneity can affect the stability, biological activity and pharmacokinetics of antibodies [41]. Therefore, cation exchange chromatography (CEXC) was used to evaluate the TCZ charge variants profile in IV and SC clinical solutions.

The (CEX)UHPLC-UV method used here was adapted from Ref. [24], which presented a detailed physicochemical and biological characterization of the TCZ innovator. Here, the CEX method was optimized by using a strong cation exchange column instead of a weak one. In addition, the chromatograph used was an ultra-high performance model instead of a high-performance one. All of these enabled us to modify the gradient, shortening the analysis time while obtaining a very similar TCZ charge variant profile as in Ref. [22], as will be discussed next.

3.4.1. Comparability study of 6 mg/mL and 4 mg/mL IV and SC TCZ clinical solutions

As in the SEC method, chromatograms were recorded at different characteristic λ values for proteins (214 nm, 220 nm and the very specific to proteins, 280 nm), although the results shown here were mainly obtained at λ = 214 nm, the most sensitive point.

Comparability results for the IV and SC TCZ clinical solutions are shown in Fig. 5 and Table 5. Although the chromatographic charge variant profiles for the IV and SC solutions were very similar, there were some small differences. The most important difference was the increase in the basic variant detected at 12.35 min in the SC clinical solution (Fig. 5).

Consequently, when the abundance of the acidic, neutral and basic variants was analysed, a slightly different composition could be observed in the basic variants (Table 5), in that the percentage of total basic variant in the SC solutions was four percentage points higher than in the IV solutions. There is no clear relationship between this increase and a corresponding decrease in the acidic or neutral variant, as this increase is not particularly important in terms of net quantity. In addition, when the charge variant profiles of the same solution were compared for the different storage times, i.e., comparing D0 with D1 for the same IV or SC solution, no changes were detected in any of the chromatograms (Fig. 6) either in shape or in chromatographic areas.

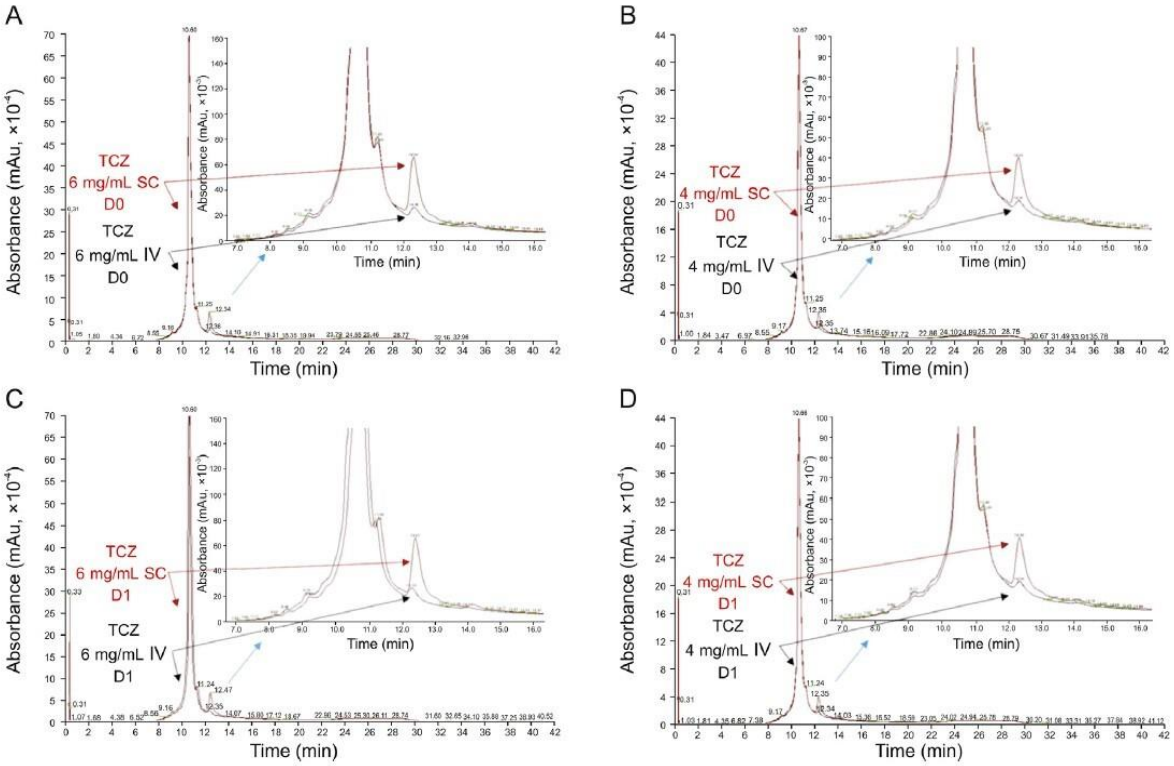

Fig. 5. CEX comparability study of 6 mg/mL and 4 mg/mL TCZ IV and SC clinical solutions. Charge variant profile: (A) 6 mg/mL D0, (B) 4 mg/mL D0, (C) 6 mg/mL D1 and (D) 4 mg/mL D1 of IV and SC samples shown as overlapping chromatograms and their corresponding expansion. Samples were from IV-batch-1 and SC-batch-1.

Table 5. Average abundances of the main peak, acidic variants and basic variants for different TCZ samples on two different days.

Sample	Mean peak (%)		Acidic variants (%)		Basic variants (%)	
	D0	D1	D0	D1	D0	D1
Medicines						
20 mg/mL IV	60.3	-	20.4	-	19.2	-
180 mg/mL SC	54.6	-	18.0	-	27.1	-
Clinical solutions						
6 mg/mL IV	61.1	59.5	16.1	17.3	22.8	23.1
6 mg/mL SC	57.2	55.3	15.4	17.5	27.4	27.1
4 mg/mL IV	55.5	55.3	17.1	18.4	27.4	26.2
4 mg/mL SC	53.7	52.8	14.8	16.2	31.5	31.0

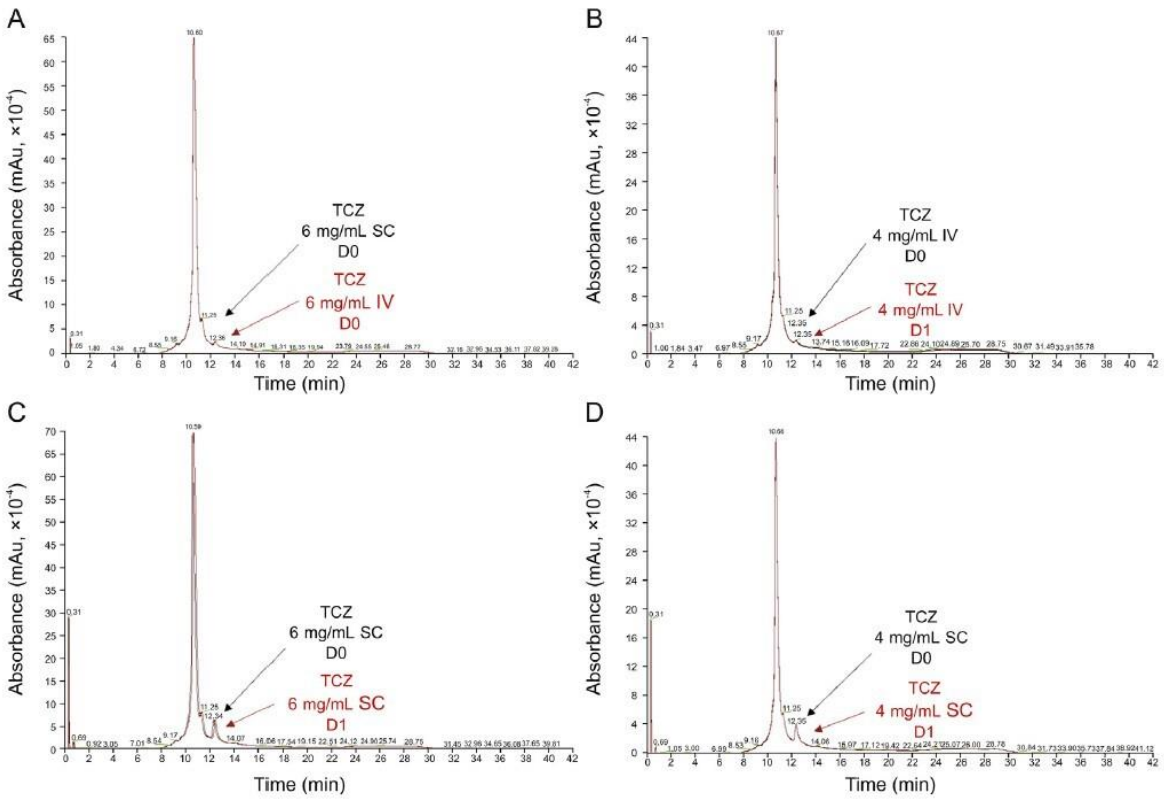

Fig. 6. TCZ charge variant profiles: (A) 6 mg/mL IV, (B) 4 mg/mL IV, (C) 6 mg/mL SC and (D) 4 mg/mL SC on the D0 and D1 shown as overlapping chromatograms to test comparability stability between IV and SC clinical solutions. Samples were from IV-batch-1 and SC-batch-1.

In order to investigate the reason for these differences between the chromatographic variant profiles of TCZ from IV and SC, medicines from different batches were analysed (IV solution 20 mg/mL and SC solution 180 mg/mL). The injection volumes were adjusted to make results comparable as the concentrations of the medicines (0.4 mL for the IV medicine and 0.1 mL for the SC medicine) were higher than in the diluted solutions. Thus, the amount (in mg) of TCZ injected was in the same order of magnitude as in the diluted samples at 6 mg/mL and 4 mg/mL. Fig. 7 shows the results of these experiments, which also appear in Table 5. Fig. 7A presents the profiles for the IV TCZ clinical solutions at 6 mg/mL and 4 mg/mL and the profile for the medicine (IV TCZ 20 mg/mL). The solutions were prepared from a different batch (Batch 1) to the medicine (Batch 2). The similarity between all the profiles for IV TCZ solutions is evident. For its part, Fig. 7B highlights the similarity between all the profiles for the SC TCZ solutions, regardless of the dilution applied to the medicine or the particular batch. The charge variant profile was also found to be unaffected by the batch of the SC medicine (Batch 1 or 2) used to prepare the clinical solutions (Fig. S3). The average abundance of the acidic, neutral and basic variants of TCZ in the IV medicines was practically the same as that in the IV TCZ clinical solutions. The same pattern was also observed in SC medicines and SC clinical solutions (Table 5).

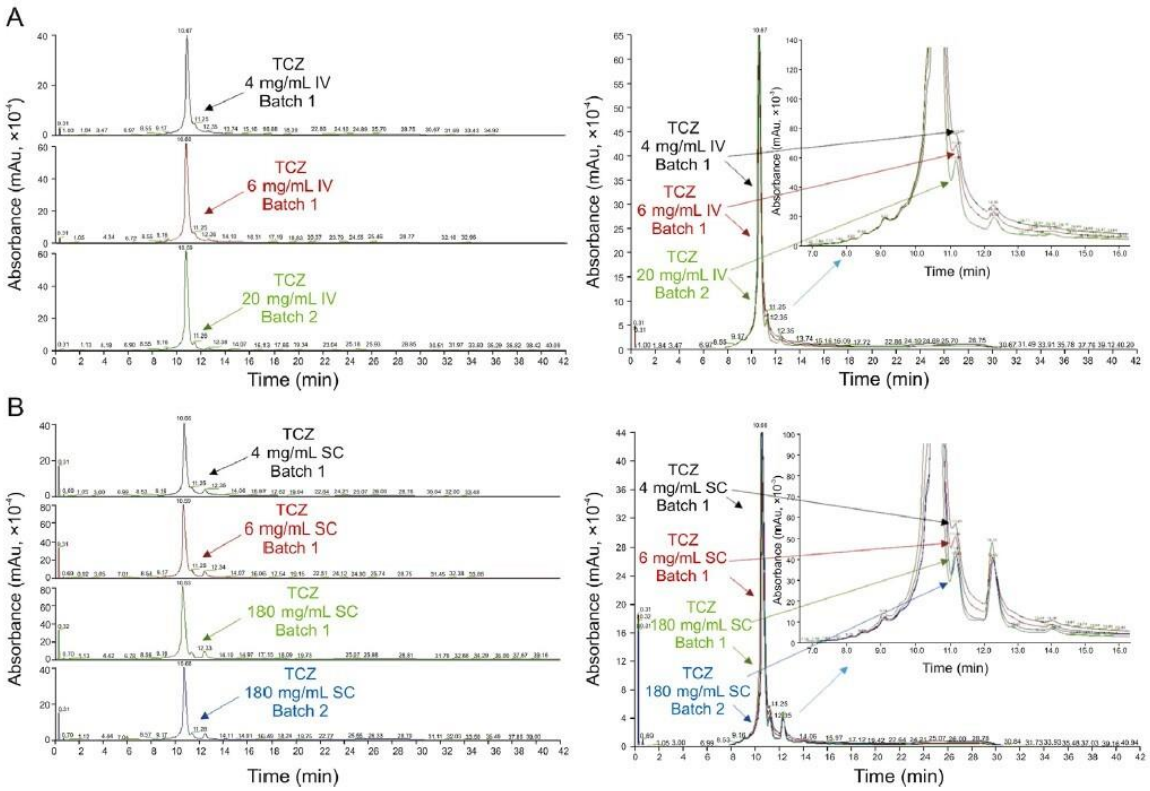

Fig. 7. TCZ charge variant profile comparability study. IV and SC medicinal products and 6 mg/mL and 4 mg/mL clinical solutions: (A) IV and (B) SC shown as separate chromatograms (left) and overlapping chromatograms with their corresponding expansion (right). Samples shown are from IV-batch-1 and SC-batch-1 and SC-batch-2.

Therefore, taking all these results together, it is clear that the small differences detected between the charge variant profiles for the IV and SC solutions are not due to differences between batches of the same medicine (IV or SC) or to instability promoted by the dilution of the SC medicine to prepare the clinical solutions at 6 mg/mL and 4 mg/mL for intravenous administration. According to the literature [22], these differences, detected above all in the basic variants, are probably due to the use of different clones of the Chinese Hamster Ovary (CHO) cell lines used to produce IV or SC TCZ. Miao et al. [22] recorded very similar chromatographic profiles of TCZ to those recorded in our research, which demonstrates that the differences were due to the fact that the different formulations of TCZ were manufactured using different CHO clones.

The CEX chromatograms for all the SC TCZ solutions produced another interesting result. A high peak was detected in the front at 0.31 min for the medicines from the two different batches and the clinical solutions at 6 mg/mL and 4 mg/mL. This must therefore correspond to a non-retained compound. It was confirmed that this peak was in proportion to the TCZ charge variant (by measuring the areas under the unknown peak and the TCZ variants peak, Table S1) in all the samples analysed, including the two medicines from the two different batches. This means that this unknown compound is already present in the SC medicines and dilutes in the same proportion as the sample does. It was not detected in any of the IV TCZ samples. It was also confirmed that this compound is not of a protein nature since it was not detected in the chromatogram registered at 280 nm, the typical and specific UV absorbance maximum for protein (Fig. S4).

3.4.2. Comparability study of the stress tests on the 6 mg/mL IV and SC TCZ clinical solutions

The degradation of TCZ was very similar in both 6 mg/mL clinical solutions prepared from IV or SC medicines with small variations with respect to the control (unstressed) samples, except for the solution subjected to acidic stress in which the stress caused a large change in the chromatographic profile, increasing the basic variants as shown in Fig. 8. Nevertheless, this could also be due to an experimental or similar error since the degraded basic variant had the same charge variant profile, but with different intensities, in both chromatograms for the solutions prepared from the IV or SC medicines. It is also important to highlight that the basic variant at 12.31 min, characteristic of the samples prepared from the SC medicines, was practically unaffected by the various types of stress applied (except for the acidic stress).

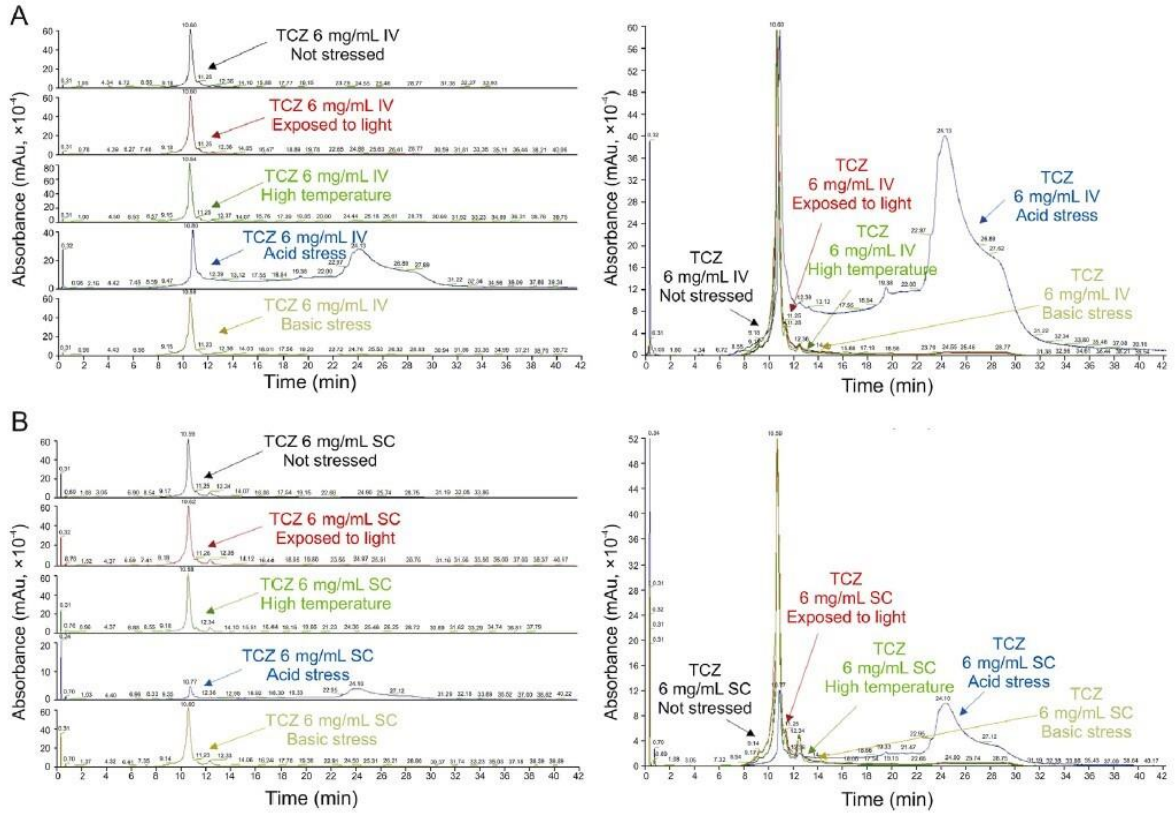

Fig. 8. TCZ stress study by CEX. Chromatograms: (A) 6 mg/mL IV and (B) SC stressed samples including the non-stressed sample, shown as separate chromatograms (left) and overlapping chromatograms (right). Samples shown are from IV-batch-1 and SC-batch-1 and SC-batch-2.

3.5. IT-F: tertiary structure or conformational structure

3.5.1. Comparative study of 6 mg/mL and 4 mg/mL IV and SC TCZ clinical solutions

Figs. 9A and B show the fluorescence spectra for the TCZ solutions. No differences can be observed in these spectra. Nevertheless, in order to conduct a more in-depth analysis, the spectral C.M. was calculated for each recorded spectrum (see Table 6). This parameter is a mathematical representation of each spectrum, in which the spectrum is condensed into a scale. Slight modifications in these spectral C.M. values therefore indicate conformational changes occurring on the protein. The spectral C.M. increases are related to the structural modification on the protein in which tryptophan amino acids are more exposed to the solvent (a modification caused by the denaturation of the protein). The decrease in spectral C.M. is associated with a conformational modification in which tryptophan amino acids are buried inside the protein, in a more hydrophobic environment.

Both fluorescence spectra and calculated spectral C.M. were practically identical in all the TCZ solution samples, therefore indicating that TCZ has the same conformation in all the solutions regardless of the medicine used to prepare them, i.e., IV or SC. Nor is it affected by

the concentration, i.e., 6 mg/mL or 4 mg/mL, the only difference being in the intensity, due to the different concentrations.

Table 6. Spectra center of mass (C.M.) of samples from the stability and stress studies.

Study	Sample	C.M.	
		D0	D1
Stability	6 mg/mL IV	343.5	343.5
	6 mg/mL SC	343.4	343.5
	4 mg/mL IV	343.4	343.4
	4 mg/mL SC	343.4	343.4
Stress			
Temp. 40 °C	6 mg/mL IV	-	343.5
	6 mg/mL SC	-	343.4
Light	6 mg/mL IV	-	343.6
	6 mg/mL SC	-	343.5
Acidic medium (HCl)	6 mg/mL IV	-	346.6
	6 mg/mL SC	-	346.8
Basic medium (NaOH)	6 mg/mL IV	-	347.1
	6 mg/mL SC	-	347.0

3.5.2. Comparability study of the stress tests on the 6 mg/mL IV and SC TCZ clinical solutions

The changes in the conformation of TCZ in the IV and SC solution samples subjected to stress and assessed by IT-F, clearly indicated identical behaviour in response to stress (Figs. 9C and D, and Table 6). The least affected samples were those subjected to light and to temperature of 40 °C; both fluorescence intensity and C.M. remained unaltered in these solutions and similar to those of the control solution. By contrast, significant C.M. increases were observed in the solution samples subjected to an acidic or basic medium. These indicate conformational changes, in both cases, inducing a red shift on the TCZ fluorescence spectra, which indicates that tryptophan amino acids were exposed to the solvent probably due to partial denaturation of the protein. It is important to highlight that when the acidic medium (HCl) was added, the quantum yield increased, but the opposite occurred when the basic medium

(NaOH) was added, in that the quantum yield decreased notably. This might be due to quenching events related to the ions that were added.

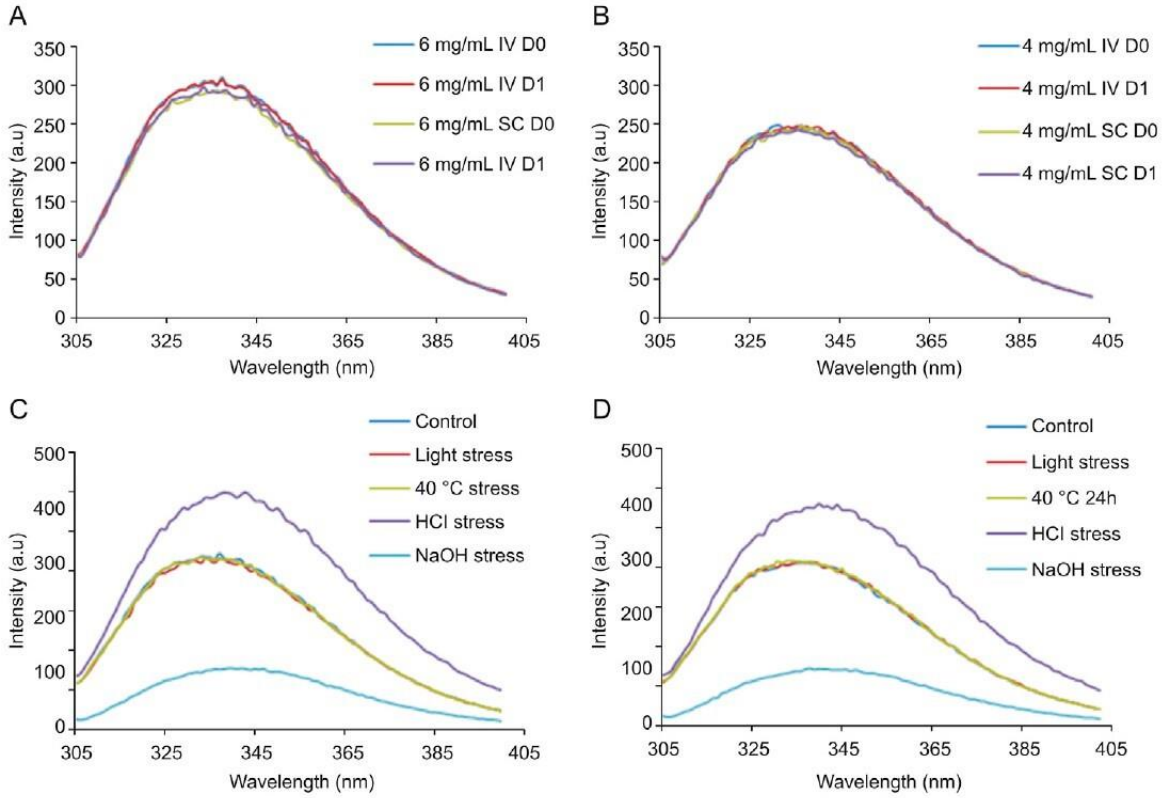

Fig. 9. Conformational study by IT-F. Comparative study of the IV and SC clinical solutions (IV-batch-1 and SC-batch-1) fluorescence spectra: (A) 6 mg/mL samples at D0 and D1 and (B) 4 mg/mL samples at D0 and D1. Stress study. Fluorescence spectra: (C) 6 mg/mL IV stressed samples and (D) SC stressed samples. Samples shown are from IV-batch-1 and SC-batch-1 and SC-batch-2.

4. Discussion

The active ingredient of the medicinal product RoActemra® in both routes of administration, IV and SC, is TCZ. The TCZ solution for SC administration is supplied as a sterile, colourless to yellowish, preservative-free, liquid solution with a pH of around 6.0 (between 5.5 and 6.5). This solution is supplied in a 1 mL ready-to-use, single- use, prefilled syringe with a needle safety device. Each device delivers 0.9 mL of TCZ solution (162 mg), in a histidine buffered solution composed of TCZ (180 mg/mL), polysorbate 80, L-histidine and L-histidine monohydrochloride monohydrate, L-arginine and L-arginine hydrochloride, L-methionine and water for injections [11]. On the basis of the available information in the FDA reviews on the original biologics license applications, the subcutaneous TCZ drug product is manufactured with a process change [27] that does not affect quality attributes such as potency, aggregates order size or charge variants, or the levels of process-related impurities [42] compared to the IV TCZ drug product. The TCZ solution for IV administration [11] has a

lower concentration (20 mg/mL) and different excipients (sucrose, polysorbate 80, disodium phosphate dodecahydrate, sodium dihydrogen phosphate dehydrate and water for injections), with a pH of between 6.2 and 6.8. Therefore, in order to assess the possible use of the SC medicine (180 mg/mL) for preparing clinical solutions of TCZ at 6 mg/mL and 4 mg/mL for IV administration, we focused our study on the impact of the dilution required in 0.9% NaCl on critical physicochemical attributes such as aggregates order size (by measuring visual and soluble particulates, and obtaining SEC profiles), charge variants (by obtaining chromatographic cation exchange variant profiles) and structural conformation (by specific fluorescence measures) by comparing results on the solution for infusion prepared from IV and SC medicines. Also, two different batches of the IV and SC medicinal products (RoActemra®) were used to prepare the clinical solutions for infusion, so as to test the inherent variability of TCZ as a biotechnological drug. Our study also examined the stability of the SC clinical solutions stored refrigerated at 4 °C and protected from daylight for 24 h, so as to compare their stability with that of IV clinical solutions, which is accepted as 24 h [11]. In order to gather more information about the similarity between these IV and SC clinical solutions, a stress study was performed on the 6 mg/mL solution. This study has also proved suitable for testing the stability of TCZ samples as it detected all the changes that took place.

As regards to aggregates order size, over the 24 h period the solution for infusion prepared using the SC RoActemra® proved to be very similar in terms of product quality and stability to the solution prepared with IV RoActemra®. No visible particulates were detected in any of the solutions for infusion, nor did we observe aggregates (assessed by DLS and SEC) that were larger than the natural soluble aggregates. In addition, these natural soluble aggregates were detected (by SEC) in the same proportion (natural aggregates/monomers) in the clinical solutions as in their respective medicinal products, IV and SC. The particle population was mainly TCZ monomers with comparable hydrodynamic volume. No differences were detected in the solution prepared for infusion when samples at the same concentration were compared. The only difference was the detection of an unknown compound of nonprotein nature in all the SC solutions (not detected at 280 nm in either SEC or CEXC), with an estimated molecular weight of around 15 kDa (by SEC) and a non-basic nature (not retained in CEXC). This unknown compound was also detected in the two batches analysed of SC RoActemra®, always in proportion with the TCZ concentration, and this proportion was maintained after dilutions. The latter was corroborated by SEC and CEXC results. The unknown compound was not detected in any of the IV solutions.

No major differences were detected in the chromatographic charge variant profile of the solution prepared for infusion using the SC RoActemra® compared to that for the solutions prepared with the IV medicinal product. An increase in one of the minor basic variants was

observed in all the SC samples analysed, always in the same proportion; this difference in the charge variants is probably due to the use of different CHO clones in the manufacture of TCZ, as indicated in Ref. [38] where a very similar charge variant profile to that found in our solutions of SC TCZ is shown. In previous research [22] it was proposed that the deamidations detected for the TCZ originator occur at various asparagine positions, in both heavy and light chains, and the levels of this process were observed to be comparable in the TCZ originator and the HS628 biosimilar. In this case, both TCZ and HS628 showed similar charge variant profiles to those obtained here for all the IV solutions. Regardless of this difference in the charge variants, all solutions demonstrated great stability over the 24 h period.

The fluorescence technique was used to compare the tertiary structure of TCZ in the solution prepared for infusion from IV and SC medicines, providing a reliable assessment of higher order structure integrity, which was shown to be comparable in both solutions, also proving their stability. It was therefore not necessary to analyse the medicinal products themselves, since all the solutions provided high levels of comparability both in terms of the fluorescence spectra obtained and in terms of stability, with no differences detected that require further investigation in the medicinal products or batch to batch.

As regards to the stress study conducted on the 6 mg/mL clinical solution prepared from IV and SC TCZ medicines, the results indicated high levels of comparability between the two solutions in terms of degradation patterns. All the solutions were resistant to degradation when submitted to 40 °C for 24 h. Light induced aggregation was detected by SEC, but not by DLS. As expected, acidic (pH = 1.87) or basic (pH = 11.04) media promoted the highest degradation on TCZ; both media increased the aggregates detected by SEC, but the acidic medium degraded TCZ more, in that an important decrease in the monomers was detected by SEC, and a great disruption in the charge variant profile was obtained by CEXC. The tertiary structure was also disrupted at these pH values. The TCZ charge variant profile in the basic medium promoted some degradation, although not as much as expected and less extensive than observed in the acidic medium. The samples prepared with IV medicinal products experienced similar degradation to those prepared with SC in all the stress tests to which the TCZ samples were subjected. An interesting additional finding was the resistance to degradation of the unknown compound detected in the SC samples, which was detected by both SEC and CEXC in unaltered condition.

5. Conclusion

The research presented here revealed high levels of similarity between the critical physicochemical quality attributes of the clinical solutions of TCZ at 6 mg/mL and 4 mg/mL

prepared for infusion using the SC medicinal product (RoActemra® 162 mg) and those of the clinical solutions of TCZ at 6 mg/mL and 4 mg/mL prepared for infusion using the IV medical product (RoActemra® 20 mg/mL). The SC clinical solutions also demonstrated high comparability with the IV clinical solutions in terms of stability over 24 h and degradation patterns when subjected to controlled degradation studies.

The minor differences detected between the IV and SC TCZ clinical solutions were already present in the medicinal products used to prepare these solutions, and were not related to the dilutions; they are not batch-to-batch related and instead are directly related to the medicinal product, i.e., IV or SC used. TCZ in its SC form (RoActemra® 162 mg) does not therefore suffer any degradation as a consequence of its dilution in 0.9% NaCl to prepare the clinical solutions diluted at 6 and 4 mg/mL for infusion. The dilutions of the excipients did not affect the stability of the diluted solutions over 24 h, when stored refrigerated at 4 °C protected from daylight.

In view of all the above, we can conclude that in our study we found no evidence that would advise against the recommendation of using TCZ in its SC form RoActemra® 162 mg to prepare diluted solutions in 0.9% NaCl at 6 and 4 mg/mL to be used for intravenous administration. This means that in the event of a shortage of IV RoActemra® 20 mg/mL, as happened during the COVID-19 emergency, the solution contained (0.9 mL) in the prefilled syringes of SC RoActemra® 162mg can be used to prepare the solutions diluted in 0.9% NaCl required for intravenous infusion.

Declaration of competing interest

The authors declare that there are no conflicts of interest.

Acknowledgements

This study was partially funded by Project FIS: PI-17/00547 (Instituto Carlos III, Ministerio de Economía y Competitividad, Spain), which means that it was also partially supported by European Regional Development Funds (ERDF). Anabel Torrente-López is currently granted a FPU predoctoral grant of reference FPU18/03131 from the Ministry of Universities, Spain. The authors would like to thank the University of Granada (Spain) for the support and for enabling us to use the laboratories at the Department of Analytical Chemistry in the Science Faculty during the hard days of lockdown in Spain.

Supplementary material

1. DLS. Size distribution by intensity of TCZ samples (Fig. S1)

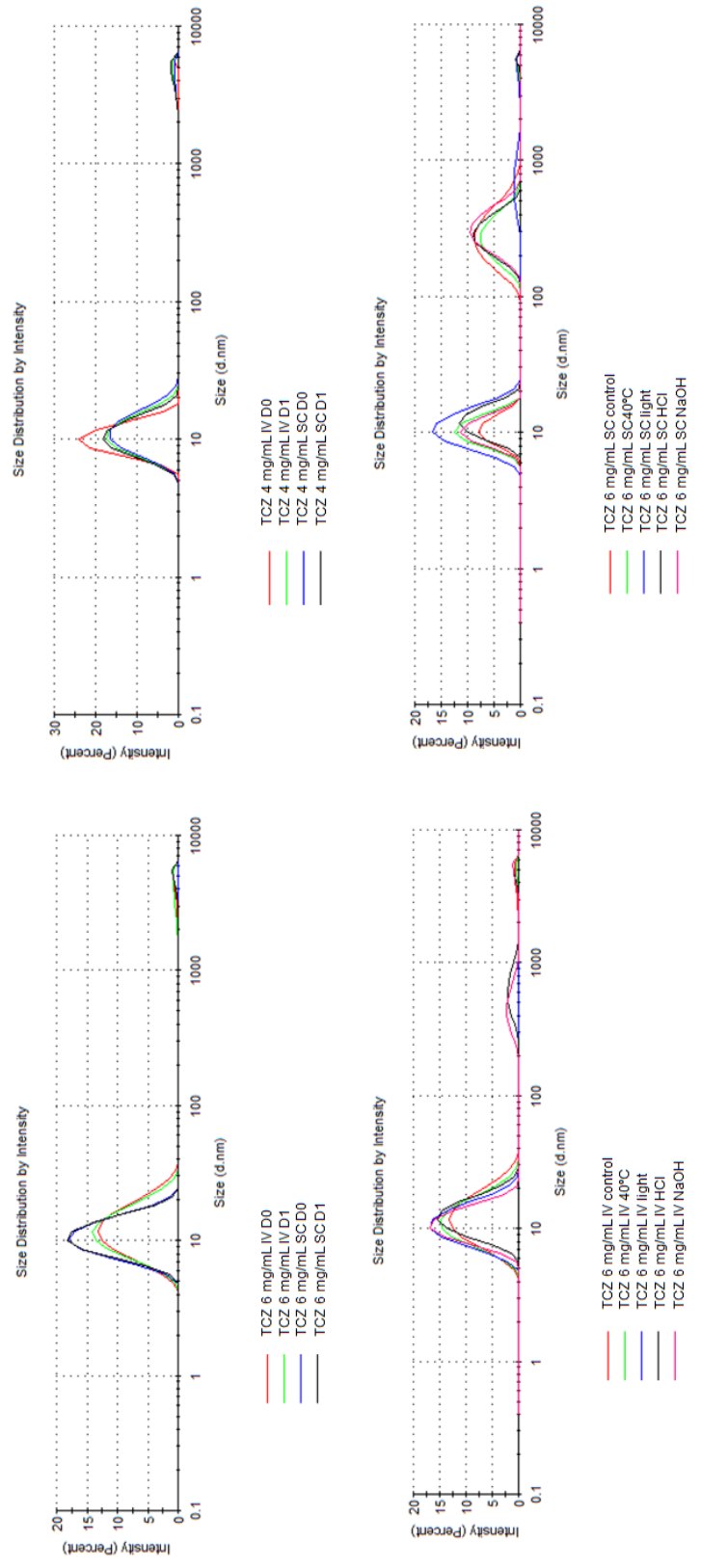

Fig. S1. Particulate size distributions by intensity of tocilizumab intravenous (IV) and subcutaneous (SC) samples: A) stability study of 6 mg/ml IV and SC samples; B) stability study of 4 mg/ml IV ad SC samples; C) stress study of 6 mg/ml IV samples and D) stress study of 6 mg/ml SC samples.

2. (SE)HPLC-DAD. Monomers of infliximab used as control to compare with monomers of TCZ from solutions from IV and SC forms (Fig. S2)

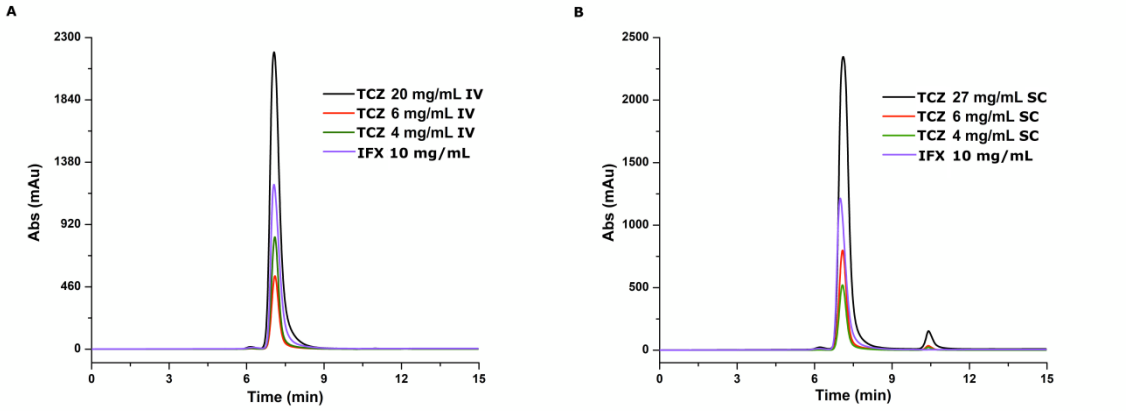

Fig. S2. Monomers of INZ compared with monomers of TCZ from solutions from (A) SC and (B) IV forms

3. (CX)UHPLC-DAD. Charge variant profile was not affected by the batch of the SC medicine (1 or 2) used to prepare the clinical solutions (Fig. S3)

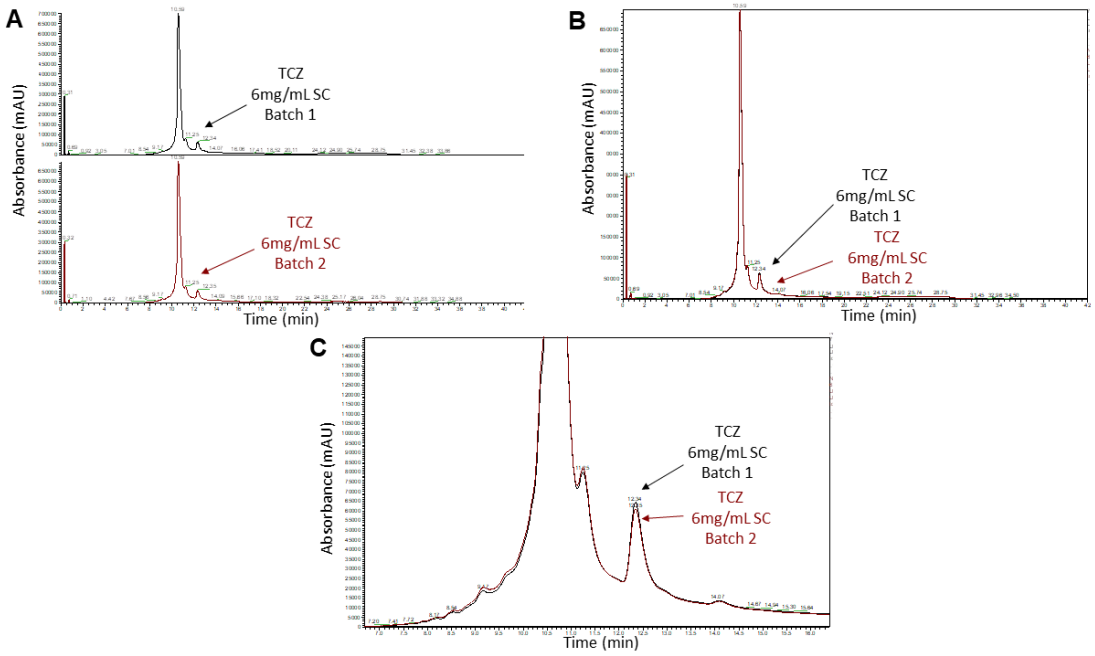

Fig. S3. Chromatograms of TCZ 6 mg/mL SC of two different batches: (A) separated chromatograms, B) overlapping chromatograms and (C) extended overlapping chromatograms.

4. (CX)UHPLC-DAD. Unknown compound in the front of the CEX chromatogram remain invariant and no degraded, it was detected in all the SC samples, included the SC medicinal product (Table S1)

Table S1. Percentage of the area ratio corresponding to the front peak (unknown compound) in (CE)HPLC-DAD to analyses charge variant profile in IV and SC samples of TCZ

Samples	Concentration (mg/mL)	Area ratio corresponding to the front peak (%)	
		IV	SC
Day 0	20 (batch 2)	0.13	
	180 (batch 1)		3.38
	180 (batch 2)		3.44
	6 (batches 1)	0.87	3.42
	4 (batches 1)	1.06	3.46
Day 1	6 (batches 1)	0.66	3.58
	4 (batches 1)	0.73	3.36
Exposure to light	6 (batches 1)	0.54	3.25
High temperature	6 (batches 1)	0.48	3.24
Acid stress	6 (batches 1)	1.41	4.10
Basic stress after 24h	6 (batches 1)	0.37	3.41

5. (CX)UHPLC-DAD. It was also confirmed that the unknown compound is not of a protein nature since it was no detected in the chromatogram registered at 280 nm, the typical and specific UV absorbance maximum of protein (Fig. S4)

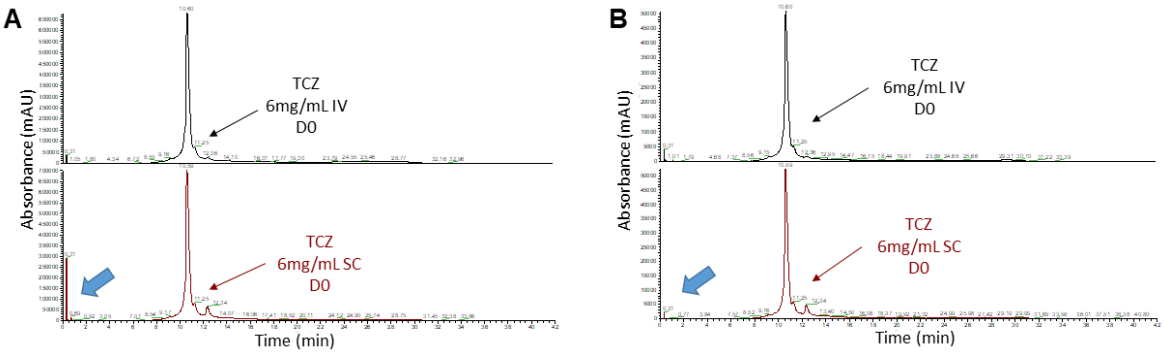

Fig. S4. Chromatograms of TCZ 6 mg/mL IV and SC on the D0 recorded at (A) 214 nm and (B) 280 nm.

References

[1] World Health Organization, Coronavirus disease (COVID-19) outbreak. https://www.who.int/emergencies/diseases/novel-coronavirus-2019/events-as-theyhappen (accessed 22 March 2020).

[2] COVID-19 coronavirus pandemic. https://www.worldometers.info/coronavirus/?utm_campaign¼homeAdUOA?Si (accessed 22 March 2020).

[3] WHO, Coronavirus disease (COVID-19) symptoms, World health organization. https://www.who.int/health-topics/coronavirus#tab¼tab_3 (accessed 22 March 2020).

[4] C. Zhang, Z. Wu, J.W. Li, et al., The cytokine release syndrome (CRS) of severe COVID-19 and Interleukin-6 receptor (IL-6R) antagonist Tocilizumab may be the key to reduce the mortality, Int. J. Antimicrob. Agents (2020) 105954.

[5] M. Zhao, Cytokine storm and immunomodulatory therapy in COVID-19: role of chloroquine and anti-IL-6 monoclonal antibodies, Int. J. Antimicrob. Agents 55 (2020) 105982.

[6] B. Liu, M. Li, Z. Zhou, et al., Can we use interleukin-6 (IL-6) blockade for coronavirus disease 2019 (COVID-19)-induced cytokine release syndrome (CRS)? J. Autoimmun. 6 (2020) 102452.

[7] S.A. Jones, B.J. Jenkins, Recent insights into targeting the IL-6 cytokine family in inflammatory diseases and cancer, Nat. Rev. Immunol. 18 (2018) 773-789.

[8] C. Diaz-Torne, M.A. Ortiz, P. Moya, et al., The combination of IL-6 and its soluble receptor is associated with the response of rheumatoid arthritis patients to tocilizumab, Semin. Arthritis Rheum. 47 (2018) 757-764.

[9] Y. Zhou, B. Fu, X. Zheng, et al., Pathogenic T cells and inflammatory monocytes incite inflammatory storm in severe COVID-19 patients, Natl. Sci. Rev. 7 (2020) 998-1002.

[10] S.A. Grupp, M. Kalos, D. Barrett, et al., Chimeric antigen receptor-modified T cells for acute lymphoid leukemia, N. Engl. J. Med. 368 (2013) 1509-1518.

[11] European public assessment report (EPAR) summary for RoActemra, Annex I: Summary of product characteristics, EMEA/H/C/000955, European Medicines Agency, London, 2018.

[12] M. Cellina, M. Orsi, F. Bombaci, et al., Favorable changes of CT findings in a patient with COVID-19 pneumonia after treatment with tocilizumab, Diagn. Interv. Imaging 101 (2020) 323-324.

[13] F. Bennardo, C. Buffone, A. Giudice, New therapeutic opportunities for COVID-19 patients with tocilizumab: possible correlation of interleukin-6 receptor inhibitors with osteonecrosis of the jaws, Oral Oncol. 106 (2020) 104659.

[14] X. Zhang, K. Song, F. Tong, et al., First case of COVID-19 in a patient with multiple myeloma successfully treated with tocilizumab, Blood Adv 4 (2020) 1307-1310.

[15] E.A. Coomes, M.D.H. Haghbayan, Interleukin-6 in COVID-19: a Systematic Review and Meta-Analysis, medRXiv, 2020.

[16] A. Venkiteshwaran, Tocilizumab, MAbs 862 (2009) 432-438.

[17] T. Tanaka, M. Narazaki, T. Kishimoto, Anti-interleukin-6 receptor antibody, tocilizumab, for the treatment of autoimmune diseases, FEBS Lett. 585 (2011) 3699-3709.

[18] T. Kasama, T. Isozaki, R. Takahashi, et al., Clinical effects of tocilizumab on cytokines and immunological factors in patients with rheumatoid arthritis, Int. Immunopharm. 35 (2016) 301-306.

[19] A.V. Ramanan, A.D. Dick, C. Guly, et al., Tocilizumab in patients with anti-TNF refractory juvenile idiopathic arthritis-associated uveitis: a multicentre, single-arm, phase 2 trial, Lancet Rheumatol 2 (2020) e135-e141.

[20] Y. Katsumata, J. Ikari, N. Tanaka, et al., Tocilizumab-effective multicentric Castleman's disease with infiltration of eosinophil and IgG4-positive plasma cells: a case report, Respir. Med. Case Reports 25 (2018) 25-29.

[21] H. Ito, M. Takazoe, Y. Fukuda, et al., A pilot randomized trial of a human antiinterleukin-6 receptor monoclonal antibody in active Crohn's Disease, Gastroenterology 126 (2004) 989-996.

[22] S. Miao, L. Fan, L. Zhao, et al., Physicochemical and biological characterization of the proposed biosimilar tocilizumab, BioMed Res. Int. 2017 (2017) 1-13.

[23] EMA, European Medicines Agency, RoActemra. https://www.ema.europa.eu/en/medicines/human/EPAR/roactemra (accessed 22 March 2020).

[24] K. Lauper, D. Mongin, F. Iannone, et al., Comparative effectiveness of subcutaneous tocilizumab versus intravenous tocilizumab in a pan-European collaboration of registries, RMD Open 4 (2018) 1-10.

[25] M. Calderón-Goercke, J. Loricera, V. Aldasoro, et al., Tocilizumab in giant cell arteritis. route of administration: intravenous or subcutaneous, Semin. Arthritis Rheum. 49 (2019) 126-135.

[26] A. D'Arpino, M. Savoia, L. Cirillo, et al., Pcn72 comparative cost analysis of subcutaneous trastuzumab originator (Herceptin®) vs intravenous trastuzumab biosimilar (Kanjinti) from a hospital perspective in Italy, Value Health 22 (2019) S449.

[27] Z. Li, R. Easton, Practical considerations in clinical strategy to support the development of injectable drug-device combination products for biologics, mAbs 10 (2018) 18-33.

[28] S. Morar-Mitrica, M. Puri, A.B. Sassi, et al., Development of a stable low-dose aglycosylated antibody formulation to minimize protein loss during intravenous administration, mAbs 7 (2015) 792-803.

[29] ICH Q5E Biotechnological/biological products subject to changes in their manufacturing process: comparability of biotechnological/biological products, CPMP/ICH/5721/03, European Medicines Agency, London, 2005.

[30] M. Stahl, Peak Purity Analysis in HPLC and CE Using Diode-Array Technology, Agilent Technologies, 2003, pp. 588-864.

[31] Ich, Ich Q1B, Stability testing: photostability testing of new drug substances and products, in: International Conference on Harmonisation of Technical Requirements for Registration of Pharmaceuticals for Human Use, Geneva, 1996.

[32] T.K. Das, Protein particulate detection issues in biotherapeutics development current status, AAPS PharmSciTech 13 (2012) 732-746.

[33] S. Akbas, A. Sahin, S. Calis, et al., Characterization of bevacizumab by dynamic light scattering while maintaining its native structure, Pharmazie 73 (2018) 369-374.

[34] A. Hawe, W.L. Hulse, W. Jiskoot, et al., Taylor dispersion analysis compared to dynamic light scattering for the size analysis of therapeutic peptides and proteins and their aggregates, Pharm. Res. (N. Y.) 28 (2011) 2302-2310.

[35] J. Hermosilla, R. Sánchez-Martín, R. Pérez-Robles, et al., Comparative stability studies of different infliximab and biosimilar CT-P13 clinical solutions by combined use of physicochemical analytical techniques and enzyme-linked immunosorbent assay (ELISA), BioDrugs 33 (2019) 193-205.

[36] J. Hernández-Jiménez, A. Salmerón-García, J. Cabeza, et al., The effects of light accelerated degradation on the aggregation of marketed therapeutic monoclonal antibodies evaluated by size-exclusion chromatography with diode array detection, J. Pharmacol. Sci. 105 (2016) 1405-1418.

[37] J. Hernández-Jiménez, A. Martínez-Ortega, A. Salmeron-García, et al., Study of aggregation in therapeutic monoclonal antibodies subjected to stress and long-term stability tests by analyzing size exclusion liquid chromatographic profiles, Int. J. Biol. Macromol. 118 (2018) 511-524.

[38] K. Sandra, M. Steenbeke, I. Vandenheede, et al., The versatility of heart-cutting and comprehensive two-dimensional liquid chromatography in monoclonal antibody clone selection, J. Chromatogr. A 1523 (2017) 283-292.

[39] J. Hermosilla, R. Pérez-Robles, A. Salmerón-García, et al., Comprehensive biophysical and functional study of ziv-aflibercept: characterization and forced degradation, Sci. Rep. 10 (2020) 1-13.

[40] L.A. Khawli, S. Goswami, R. Hutchinson, et al., Charge variants in IgG1: isolation, characterization, in vitro binding properties and pharmacokinetics in rats, mAbs 2 (2010) 613-624.

[41] Y. Du, A. Walsh, R. Ehrick, et al., Chromatographic analysis of the acidic and basic species of recombinant monoclonal antibodies, mAbs 4 (2012) 578-585.

[42] FDA, Center for drug evaluation and research, Application number 125472Origs000, FDA Summary Review, U.S Food and Drug Admin. (2013) 1-12.

SECCIÓN 2

Therapeutic monoclonal antibodies immune checkpoint inhibitors

CAPÍTULO 3

Combined use of UV and MS data for ICH Stability-Indication Method: Quantification and isoforms identification of intact nivolumab

INTRODUCCIÓN AL CAPÍTULO 3

El capítulo 3 recoge el desarrollo y validación de un método (RP)UHPLC/UV-(HESI/Orbitrap™)MS como indicador de la estabilidad para la cuantificación de nivolumab, anticuerpo monoclonal terapéutico IgG4 de punto de control inmunitario, en su forma de medicamento final Opdivo®. Como método indicador de la estabilidad, este debe ser capaz de analizar el fármaco en presencia de sus productos degradados, tal y como indican las directrices de calidad de la Conferencia Internacional de Armonización (ICH) en su guía ICH Q2(R1), o bien capaz de detectar que se ha producido degradación. En concreto, y para conseguir este objetivo, en este trabajo se presenta una estrategia basada en el uso combinado de los datos UV y MS para llevar a cabo dicha cuantificación, y se realiza una comparativa de todas las figuras de mérito obtenidas utilizando datos de ambos detectores. En concreto, se llevó a cabo el estudio de la linealidad, los límites de detección y cuantificación, la precisión, la exactitud, la especificidad, la robustez, el test de la adecuación al sistema (*system suitability test*) y la identificación del perfil de isoformas. Los resultados mostraron que la linealidad fue similar para los dos detectores, mientras que la sensibilidad del método fue mayor cuando se utilizó la señal MS. Sin embargo, la señal UV proporcionó mejor exactitud y precisión que la señal MS, que no cumplió los criterios de robustez del método y adecuación del sistema. A pesar de ello, la señal MS permite obtener el perfil de peso molecular de las isoformas de nivolumab, permitiendo así proponer el perfil de glicanos y detectar modificaciones estructurales debidas a la degradación. En cuanto a la especificidad del método, esta fue evaluada realizando ensayos de degradación forzada en muestras de nivolumab (Opdivo®) tal y como indica la ICH Q2(R1), con el objetivo de evaluar la capacidad del método de detectar estas modificaciones y evaluar la posibilidad de cuantificar nivolumab en presencia de productos de degradación. Se aprovecharon estos estudios de degradación controlada también para determinar factores ambientales que promueven la degradación del medicamento, así como posibles vías de dicha degradación. Los estreses a los que se sometieron muestras del medicamento fueron: (i) exposición a altas temperaturas (60 °C, 1 h), (ii) exposición a luz en una cámara de envejecimiento que simula la luz solar (24 h) (según indicaciones de la guía ICH Q1B), y (iii) exposición a una alta concentración de NaCl (1,5 M, 24 h). Las modificaciones estructurales se detectaron analizando el perfil de isoformas por MS, donde nivolumab mostró tener 5 isoformas principales sin ser sometido a ningún estrés, las cuales solo se vieron modificadas tras la exposición al estrés por luz. De este modo, se demostró que el método (RP)UHPLC/UV-(HESI/Orbitrap™)MS era capaz de detectar la

degradación de nivolumab, por lo que el método queda cualificado para ser empleado en estudios de estabilidad de dicho medicamento Opdivo®. Por ello, a continuación, se realizó un estudio de estabilidad del medicamento almacenado a temperatura ambiente (20 °C) y refrigerado a 4 °C, en ambos casos protegido de la luz, durante 15 días, en donde se llevó a cabo un seguimiento del contenido proteico en el excedente diario del medicamento Opdivo® (nivolumab, 10 mg/mL) con resultados satisfactorios.

SCIENTIFIC ARTICLE

Combined use of UV and MS data for ICH Stability-Indication Method: Quantification and isoforms identification of intact nivolumab

Anabel Torrente-López [a], Jesús Hermosilla [a], Raquel Pérez-Robles [a,b], Antonio Salmerón-García [c], José Cabeza [c], Natalia Navas [a,*]

[a] Department of Analytical Chemistry, Sciences Faculty, Biomedical Research Institute ibs.Granada, University of Granada, E-18071 Granada, Spain

[b] Fundación para la Investigación Biosanitaria de Andalucía Oriental – Alejandro Otero (FIBAO), Junta de Andalucía, Spain

[c] UGC Hospital Pharmacy, Biomedical Research Institute ibs.Granada. San Cecilio University Hospital of Granada, E-18012 Granada, Spain

Microchemical Journal 182 (2022) 107896

Accepted: 17 August 2022

DOI: 10.1016/j.microc.2022.107896

Microchemical Journal 182 (2022) 107896

Contents lists available at ScienceDirect

Microchemical Journal

journal homepage: www.elsevier.com/locate/microc

Combined use of UV and MS data for ICH Stability-Indication Method: Quantification and isoforms identification of intact nivolumab

Anabel Torrente-López [a], Jesús Hermosilla [a], Raquel Pérez-Robles [a,b], Antonio Salmerón-García [c], José Cabeza [c], Natalia Navas [a,*]

[a] Department of Analytical Chemistry, Sciences Faculty, Biomedical Research Institute ibs.Granada, University of Granada, E-18071 Granada, Spain
[b] Fundación para la Investigación Biosanitaria de Andalucía Oriental – Alejandro Otero (FIBAO), Junta de Andalucía, Spain
[c] UGC Hospital Pharmacy, Biomedical Research Institute ibs.Granada. San Cecilio University Hospital of Granada, E-18012 Granada, Spain

Abstract

Nivolumab (Opdivo®) is a fully human immunoglobulin G4 isotype approved for the treatment of many cancers. It acts as an immune checkpoint inhibitor by blocking the interaction between PD-1 (Programmed Cell Death Protein 1) – an inhibitory receptor expressed on activated T cells- and its ligands, PD-L1 and PD-L2. The quantification of therapeutic proteins in their medicines and pharmaceutical preparations remains challenging because the protein content, a critical quality attribute, must be rigorously calculated using a validated stability indicating method, such as that indicated by the International Conference on Harmonization (ICH) quality guidelines, and this requires the analysis of the drug in the presence of its degraded products. In this work, we present an strategy based on the combined use of the UV and MS data to fulfil the requirement of the ICH-Q2 (R1) to develop and validated as stability indicated a (RP)UHPLC/UV-(HESI/Orbitrap™)MS method for the quantification of nivolumab in medicinal products. A comparative study of all figures of merit of the method using UV or MS data are shown and discussed. The results show that linearity was similar for the two detectors and was established over a range of 4–45 µg/mL and 1–45 µg/mL for the UV and (HESI/Orbitrap™)MS signals, respectively. The sensitivity of the method was higher when using the (HESI/Orbitrap™)MS signal (0.2 µg/mL) than with the UV (2.0 µg/mL). However, the UV signal provided better accuracy and precision than the (HESI/Orbitrap™)MS signal, which did not meet the criteria for method robustness and system suitability. In spite of this, the MS signal plays a crucial role in this methodology by obtaining the molecular weight profile of the nivolumab isoforms, so enabling us to propose the glycans profile and detect structural modification due to degradation. The specificity of the method was evaluated by conducting forced degradation tests on samples of nivolumab in medicine form. The aim was to find out whether nivolumab suffers structural modifications when subject to stress. Structural modifications were detected by analysing the MS isoform profile, as changes of this kind promote new isoforms that are not chromatographically separated or detected by the UV signal. In this way, we demonstrated that the (RP)UHPLC/UV-(HESI/Orbitrap™)MS method was capable of detecting nivolumab degradation, and was suitable for use in nivolumab stability studies. Thus, the protein content in the daily surplus of the Opdivo® medicine, stored either at room temperature (20 °C) or refrigerated at 4 °C, could be tracked for 15 days.

Keywords

UV/MS data combined use

Quantification

Isoform profile identification

LC-MS

Nivolumab

1. Introduction

Nivolumab (Opdivo®) is a humanized monoclonal antibody (mAb) IgG4 isotype approved for the treatment of a wide range of cancers, including malignant melanomas, non-small cell lung cancer, renal cell cancer, squamous cell cancer of the head and neck, urothelial cancer and classical renal lymphoma [1]. The FDA approved nivolumab for the treatment of melanoma in December 2014 [2], non-small cell lung cancer in March 2015 [3], renal cell carcinoma in November 2015 [4], and Hodgkin lymphoma in May 2016 [5]. Nivolumab is produced by Bristol-Myers Squibb and works by blocking the interaction between PD-1 receptor and its ligands, PD-L1 and PD-L2. Nivolumab binds to the PD-1 molecule and generates steric hindrance that prevents PD-1 from binding to its ligands. It also activates the PD-1 pathway-mediated immune response, including the anti-tumor immune response [6].

Since mAbs are used as therapeutic substances in medicines, they must comply with strict quality requirements to guarantee patient safety. Their efficacy is also carefully controlled. In the hospital context, quality control of mAbs plays a pivotal role in ensuring that they can be safely and effectively administered to patients [7]. Without such control, mAbs could induce immunogenic responses related to antidrug antibodies generated by patients, which could potentially lead to life threatening situations [8]. The recommendations for ensuring the quality of biotechnological products are set out in the ICH Q5E guidelines issued by the International Conference on the Harmonization (ICH) of Technical Requirements for Pharmaceuticals for Human Use [9]. Particular specifications with regard to the test procedures and the acceptance criteria for biotechnological/biological products are set out in the ICH Q6B guidelines [10]. It is therefore important to develop validated analytical methods that can characterize the mAb structure and any modifications it may undergo. All analytical methods used to characterize mAbs should comply, as far as possible, with the requirements of international drug regulatory organizations. These include, for example, those specified in the ICH Q2(R1) guidelines [11], which include validation principles covering analytical use.

Due to the complex nature of therapeutic mAbs, a variety of orthogonal analytical methods must be used to achieve appropriate characterization. Different experimental strategies could be applied in order to carry out structural characterization: (i) a “top-down” approach, based on intact mAb analysis; (ii) a “bottom-up” approach, based on a prior enzymatic digestion of the mAb and a subsequent analysis of the digested peptides; and (iii) a “middle-down” approach, in which the mAb is partially digested. The “top-down” approach, also called intact protein analysis, does not require the samples to be treated in any way, and they can therefore be analysed more quickly. The disadvantage of intact analysis is that it does not offer as much information as the other approaches. In spite of that, it is widely used in the detection of PTMs, including the glycan isoforms in mAbs [12,13].

Ultra-high performance liquid chromatography hyphenated with mass spectra detection (UHPLC-MS) is one of the most commonly used techniques for characterizing mAbs. This technique can be applied in two different modes, i.e. denaturing mode and native mode, depending on the mobile phase solvents used. In denaturing mode the protein is denatured, while in native mode the protein structure is maintained [14,15]. Native mode can be performed in size exclusion chromatography (SEC), ion exchange chromatography (IXC) and hydrophobic interaction chromatography (HIC). Recent advances have allowed this mode of chromatography to be coupled to mass detectors using volatile salts in the mobile phases. SEC is the standard method for analysing mAbs aggregates [16–19], IXC is used to separate the mAb charge variants [20,21] and HIC allows the mAbs to be separated on the basis of their hydrophobicity under native conditions [22,23].

The denaturing mode includes reverse-phase (RP) chromatography, which is generally considered to be more efficient and more sensitive for the analysis of intact biotherapeutic proteins than other modes of liquid chromatography [24–26]. UHPLC in reverse-phase (RP) needs higher pressures in the system (around 1000 bar) than HPLC. This significantly enhances the efficiency of the separation of intact proteins using common organic solvent composition in the mobile phase, such as mixtures of water and acetonitrile and common ion pairing agents, such as trifluoroacetic acid (TFA) or formic acid (FA) [27]. Column temperatures of up to 80 ◦C are also required [28,29], and a gradient must be applied during chromatographic analysis. All these conditions can also be applied in intact protein analysis when coupled to a mass spectrometer [27], allowing for the separation, quantification and identification of the intact mAbs and its fragments [27,30,31].

In our previous research into the quantification of intact mAbs, we focused on the development and validation of (RP)HPLC methods for analysing single therapeutic mAbs using a wide porous particle size packed column [24–26]. We also assessed the development and validation of (RP)UHPLC-UV-(HESI/Orbitrap™)MS methods for the simultaneous separation, quantification, and identification of mAbs mixtures with a monolithic column [27]. In the research presented here, we used the latter strategy to develop and validate a quantification and identification (RP)UHPLC-UV-(HESI/Orbitrap™)MS method for the analysis of intact nivolumab in a top-down analysis strategy. We also present a comparative analysis of the validation results obtained using either the UV signal or the MS signal for quantification purposes.

Several ELISA and (RP)LC-MS methods for the quantification of nivolumab are proposed in the bibliography we consulted. They are all intended for use in plasma samples analysis [32–36]. One of these also included an (RP)LC-MS/HRMS method [37]. However, these methods using human plasma cannot easily be adapted for quality control analyses of

nivolumab and they would also need to be validated for this purpose. In this research, we propose an strategy based on the combined use of the UV and MS data to fulfil the requirement of the ICH-Q2(R1) to develop and validated as stability indicated a (RP)UHPLC/UV-(HESI/Orbitrap™)MS method, which allows for the rigorous quantification of nivolumab for quality control purposes and for the identification of isoforms. Validation was performed using both the UV and MS signals, in both cases according to different well-known international guidelines. This involved the study of different performance parameters such as linearity, accuracy, precision, detection limits, quantification limits, specificity, system suitability and robustness. A comparative discussion of the results obtained for nivolumab quantification using the two analytical signals is presented here in order to weigh up their respective benefits. The method was used to analyse nivolumab (protein content -quantification- and isoforms identification) in opened vials of the medicine Opdivo® (daily surplus). These vials were stored in darkness and kept at 4 °C and 20 °C for two weeks in order to provide new data about the stability of this expensive biotechnological medicine.

2. Materials and methods

2.1. Chemicals and reagents

Reverse-osmosis-quality water (purified with a Milli-RO plus Milli-Q station from Merk Millipore, Darmstadt, Germany) was used throughout the study. The reagents used were LC-MS purity grade. Acetonitrile (ACN) was purchased from VWR International S.A.S. (Fontenay-sous-Bois, France), while formic acid (FA) was supplied by Thermo Fisher Scientific (Geel, Belgium).

2.2. Nivolumab standard and solutions

Opdivo® (Bristol-Myers Squibb Pharma EEIG, Dublin, Ireland) is the tradename of the medicine format of nivolumab. The Pharmacy Unit of the University Hospital “San Cecilio” (Granada, Spain) kindly agreed to supply us with their daily surplus of this drug. Nivolumab is presented as an aqueous solution for injection containing 10 mg/mL. The medicine indicates that each mL of concentrate contains 10 mg of nivolumab. There are 40, 100 and 240 mg of nivolumab in each single-use vial of 4, 10 and 24 mL, respectively. Each vial also contains sodium citrate dihydrate, sodium chloride, mannitol (E421), pentetic acid (diethylenetriaminepentaacetic acid), polysorbate 80, sodium hydroxide, hydrochloric acid and water for injections, so producing the final concentration of 10 mg/ml.

All standard solutions of nivolumab were prepared from the medicine Opdivo®, as a suitable reference material for nivolumab was impossible to obtain. To this end, appropriate dilutions in reverseosmosis-quality water were prepared using the medicine Opdivo®. This was

done within the expiry date indicated in its technical reports [1], so as to avoid any degradation of the nivolumab and ensure full integrity of the medicine. All nivolumab solutions were freshly prepared daily as required for the experiments. The following batches were used during this study: ABK3907, ABL3361 and ABL3906.

2.3. (DAD)UV absorption spectrum of nivolumab

Fresh samples of Opdivo® (10 mg/mL nivolumab) were used to determine the UV absorption spectrum of nivolumab. This was measured using an Agilent 8453 UV–Visible Spectrophotometer G1103A (Agilent Technologies, U.S.) equipped with a photodiode array (DAD) for simultaneous measurement of the complete ultraviolet-to-visible light spectrum. The UV spectrum was recorded from 190 to 300 nm.

2.4. (RP)UHPLC/UV-(HESI/Orbitrap™)MS analysis of intact nivolumab

For the purposes of this analysis, a proper analytical platform was used (Thermo Scientific, Waltham, MA, USA). Chromatographic separation was performed using a Dionex Ultimate 3000 chromatograph equipped with two ternary bombs, a degasser, an auto-sampler, a thermostatted column compartment and a multiple-wavelength detector (MWD-3000 Vis-UV detector). The UHPLC system was coupled in-line to a Q-Exactive hybrid quadrupole-Orbitrap™ mass spectrometer (Thermo Scientific, Waltham, MA, USA). The chromatographic instrument was operated by Chromeleon™ 7 and Xcalibur™ 4.0 software and the mass spectrometer by Tune™ Software. The BioPharma Finder™ software version 3.1 with ReSpect algorithms was used to obtain the isoform profile of nivolumab by mass spectra deconvolution. All these software programmes were provided by Thermo Fisher Scientific.

The chromatographic analysis of nivolumab was conducted using a MAbPac™ RP column, 4 µm, 2.1 mm × 50 mm (Thermo Fisher Scientific, P/N 088648). The mobile phase flow rate was 0.3 mL/min and the column temperature was set at 70 ◦C. Nivolumab samples were analysed in a gradient mode using an injection volume of 10 µL. The eluent system was composed of 0.1 % FA in deionised water (eluent A) and 0.1 % FA in ACN (eluent B). Gradient conditions were as follows: 25 % B increased to 45 % B in 2.5 min, with a further increase to 80 % B in 0.5 min with a 2 min isocratic hold. Initial conditions were then restored in 0.2 min and maintained for a further 5.8 min to achieve column re-equilibration. Total run time for the analysis was 11 min. The wavelength selected to register chromatograms was 214 nm, using $\lambda = 350 \pm 10$ nm as the reference wavelength, and it was used to obtain all the figures of merit of the method and throughout the work. Chromatograms at 220 nm and 280 nm were also used to register chromatogram, using $\lambda = 350 \pm 10$ nm as the reference wavelength, to corroborate (or not) the protein nature of the chromatographic peaks.

The mass spectrometric parameters used here consisted of full positive polarity MS scans at a resolution setting of 17,500 (defined at m/z 200) with the mass range set to 1500–4500 m/z and an AGC target value of 3.0 × 106 with a maximum injection time of 100 ms and 10 microscans. In-source CID was set to 100 eV. Protein mode was selected to perform the analysis. MS instrumental tune parameters were set as follows: spray voltage - 3.8 kV, sheath gas flow rate - 35 AU, auxiliary gas flow rate - 10 AU, capillary temperature - 275 °C, probe heater temperature - 175 °C and S-lens RF voltage - 80 V.

2.5. Validation of the nivolumab quantification method (protein content)

The (RP)UHPLC/UV-(HESI/Orbitrap™)MS method we developed was validated in terms of linearity, sensitivity, precision, accuracy, specificity, robustness and system suitability according to the guidelines established by the International Conference on Harmonization (ICH Q2 (R1)) [11]. The Food and Drug Administration (FDA) recommendations [38] and Hsu and Chien criteria [39] were also used. The method was validated using the analytical signals from the UV and the MS detectors. The UV (registered at 214 nm with $\lambda = 350 \pm 10$ nm as reference wavelength) and MS (registered at total ion) chromatograms were employed to obtain the figures of merit for this method. A comparative discussion of the results was conducted in order to enable us to select the most appropriate strategy (UV or MS) for quantifying nivolumab.

2.5.1. Linearity and detection and quantification limits

Linearity was assessed by means of a calibration curve established using five standard solutions at 5, 15, 25, 35 and 45 µg/mL of nivolumab. Each standard solution was prepared in quadruplicate and injected into the chromatograph. The least-squares regression method was used to fit a linear calibration function, by relating chromatographic peak areas with concentrations. All the characteristic parameters of linear function, such as slope or the coefficient of determination (R^2), were calculated with the Statgraphics centurion 18® program (Statgraphics Technologies Inc., U.S.). A $R^2 > 0.995$ was established as the criterion for the linearity of the method.

The detection limit (DL) and quantification limit (QL) were estimated from the calibration function. DL was calculated as 3(SD(a)/b) whereas QL was calculated as 10(SD(a)/b), where SD(a) is the standard deviation of the intercept and b is the slope of the calibration function.

2.5.2. Precision

Precision was evaluated as the repeatability (intraday precision) and the intermediate precision (interday precision). Both were given as relative standard deviations (RSDs).

The repeatability of our experiment was determined from the results of our analysis of standard solutions of nivolumab prepared at the same concentration on the same day. Nine

samples with low concentration levels (3 samples of 5 µg/mL), medium concentration levels (3 samples of 25 µg/mL) and high concentration levels (3 samples of 45 µg/mL) were used for this purpose. The intermediate precision was determined from the analysis of standard solutions at the same concentration levels as were used to assess repeatability (5, 25 and 45 µg/mL), but over six consecutive days. Three separate samples of each concentration mentioned were freshly prepared and analysed daily.

Given that the ICH Q2(R1) does not establish any precision criteria for acceptance of the method, we decided to follow the Hsu and Chien precision criteria for HPLC methods for pharmaceutical analysis of biologics [39]. According to these criteria, the method can be considered acceptable in terms of precision when the RSD value is < 5 %.

2.5.3. Accuracy

Accuracy over the established linear range was assessed via the average recovery (%) value, which was calculated by analysing three standard solution replicates at low, medium and high concentrations of nivolumab (5, 25 and 45 µg/mL respectively). The FDA [38] accuracy acceptance criteria for HPLC methods for pharmaceutical analysis were used once again due to the lack of such criteria in the ICH Q2(R1). A recovery percentage value of 100 ± 3 % was established as the criterion for acceptance.

2.5.4. Specificity

Specificity was assessed by studying the forced degradation of nivolumab in its medicine form Opdivo® 10 mg/mL. The chromatograms of the sample solutions submitted to degradation were recorded not only to assess the specificity of the method, but also to detect degradation of nivolumab due to mishandling during manufacturing or in a clinical situation. With this in mind, three different stresses were selected for testing. The mild temperature and light exposure stress tests evaluate the behaviour of the medicine when exposed to heat and daylight respectively, while the high ionic strength test assesses how the medicine would behave if it were mistakenly prepared with a higher concentration of NaCl aqueous solution than indicated in its technical report [1].

The effect of high temperature was assessed by placing aliquots (opened vials) of nivolumab original medicine (Opdivo®) in an Eppendorf ThermoMixer® C (Hamburg, Germany) at a temperature of 60 °C for 1 h.

When studying the effect of high ionic strength, strong conditions were applied. We used a solution of 1.5 M of NaCl. The stressing agent concentration was 40 % (v/v) (160 µL of stressing agent was added to 40 µL of nivolumab medicine). The sample was analysed 24 h after preparation.

In order to investigate the effects of light exposure, aliquots of the medicine (Opdivo®) were placed in an accelerated stress test chamber to simulate sunlight (Solarbox 3000e RH, Cofomegra, Milan, Italy). The samples were light irradiated with a xenon lamp using an S208/S408 UV filter made of soda lime glass to simulate indoor exposure conditions with infrared rejection coating to reduce the temperature of the samples. The temperature was maintained at 20 °C, irradiation was set at 250 W/m^2, between 320 and 800 nm and the samples were exposed to the light for 24 h.

Once the chromatograms for the stressed samples had been registered, they were then compared with the chromatogram for the control sample of nivolumab. We also evaluated the isoform profiles for the stressed samples and compared them with those for the control sample. The control sample was not subjected to any stresses.

2.5.5. Robustness test

The robustness of our method was evaluated by making small changes to the flow rate, the temperature of the column and the mobile phase composition. Several aliquots of nivolumab standard solution of 25 µg/mL were prepared and analysed at each modified condition. In this way, we evaluated the impact of these changes on the analysis results. The robustness of our method was then estimated by means of the retention time, the number of theoretical plates (N) and the capacity factor (k') in the corresponding chromatogram.

2.5.6. System suitability test

The system suitability test was carried out using standard samples of 25 µg/mL of nivolumab. ICH Q2(R1) does not indicate acceptance criteria for system suitability. We therefore decided to use the FDA criteria for HPLC methods of pharmaceutical analysis [38]. As a result, N and k' were evaluated in the chromatograms. The Hsu and Chien criteria for biologics were used to assess injection repeatability [39]. The acceptance criteria were N > 2000, k' > 2.0 and injection repeatability RSD (%) of the chromatographic area of the nivolumab chromatographic peak < 5 %.

2.6. Nivolumab isoform profile identification from MS data

The nivolumab sequence was obtained from the DrugBank database [40]. Mass spectra were used to obtain the N-glycan-based mass isoform profiles of nivolumab using freshly prepared standard solution samples and stressed samples (both at 25 µg/mL nivolumab) by deconvolution of the mass spectra using BioPharma Finder™ 3.1 software (Thermo Fisher Scientific). To perform the deconvolution, some post-translational modifications (PTMs) commonly found in mAbs produced in CHO cell line -such as nivolumab- were taken into account. According to the information extracted from the nivolumab sequence,

these PTMs were 2C term lysine clipping and 2 N-term pyroglutamate formation. The fact that nivolumab has 16 disulphide bonds was also taken into account.

2.7. Application of the method in a long-term stability study of the medicine

Within the framework of a long-term (15 days) stability study, the protein content of the medicine Opdivo® in opened vials (daily surplus) was tracked by analysing two independent aliquots (10 mg/mL, batch ABL3906), each stored at two conditions, i.e., in a refrigerator at 4 °C and on the bench-top at 20 °C. In both cases, the aliquots were protected from daylight. The stability of the solution was assessed using the validated stability-indicating method. This involved measuring its concentration over time for 15 days at intervals of 0 (D0), 1 (D1), 3 (D3), 6 (D6), 7 (D7), 10 (D10) and 15 (D15) days. To this end, we analysed 10 µL of the aliquots previously diluted at 25 µg/mL (the target concentration) with NaCl 0.9 %. The recovery of nivolumab (expressed as the percentage of recovery with regard to the day of preparation, D0) was calculated at each time point and plotted against time.

3. Results and discussion

3.1. Chromatographic analytical procedure

Quantification is an important step in the manufacturing and quality control process of any biopharmaceutical drug. It is a critical quality attribute, given the obligation to specify the protein content (the active product ingredient) of any pharmaceutical product or medicine. One of the best ways of quantifying the protein content of mAbs is via chromatographic analysis. As a starting point for this analysis, we decided to use the same experimental conditions applied in a chromatographic analytical procedure previously developed for the analysis of a group of different therapeutic mAbs [31]. We then optimized these conditions for the quantification of nivolumab. In brief, we used a MAbPac™ RP column because of its specificity for mAbs quantification analysis, and because it has demonstrated higher resolution capacity for mAbs analysis, as shown in our previous work with the chromatographic separation of at least four similar mAbs. The mobile phase was highly MS compatible as it consisted of a combination of water, acetonitrile (ACN) and formic acid (FA) as the additive. Another advantage is that it did not require the use of stronger eluotropic solvent systems, which are widely used in mAbs analysis to reduce column interaction due to the high hydrophobicity of mAbs [41].

The first experiments were carried out using the chromatographic conditions optimized in our previous research [31]. However, nivolumab, whose structure corresponds to IgG4, proved to be a more nonpolar protein than the IgG1 analysed in our earlier research. This is because it was more strongly retained in the column. To solve this problem, the isocratic hold

had to be increased to 2 min, to ensure the elution of nivolumab. In addition, the re-equilibration time had to be extended from 3.8 to 5.8 min, as more time was required to restore the column to its initial conditions. The rest of the chromatographic experimental conditions were as described in the previous study [31] and are set out here in the experimental section. With the optimized chromatographic conditions, the elution of intact nivolumab took place at a retention time of 4.25 ± 0.25 min, with a total analysis time of 11 min. This procedure produced rapid results, which is important for routine quality control analysis.

Moving onto the UV spectrum recorded by the DAD detector, three different wavelengths were selected i.e. λ = 214 nm, 220 nm and 280 nm for recording the chromatograms. The reference wavelength was λ = 350 ± 10 nm. The figures of merit for the proposed method were calculated using signals from λ = 214 nm, as this enabled higher sensitivity due to the higher absorbance of nivolumab at this λ. Another advantage was that the analytical signal recorded at this λ was less affected by the inherent heterogeneity of nivolumab. With all these chromatographic and UV conditions, suitable peaks of nivolumab were obtained (Fig. 1a) to enable us to carry out the validation of the quantification procedure. Signals from 220 nm and 280 nm were also used to corroborate the protein nature of the chromatographic peaks, since the absorption at these two wavelengths is characteristic of proteinaceous compounds, improving the specificity of the method.

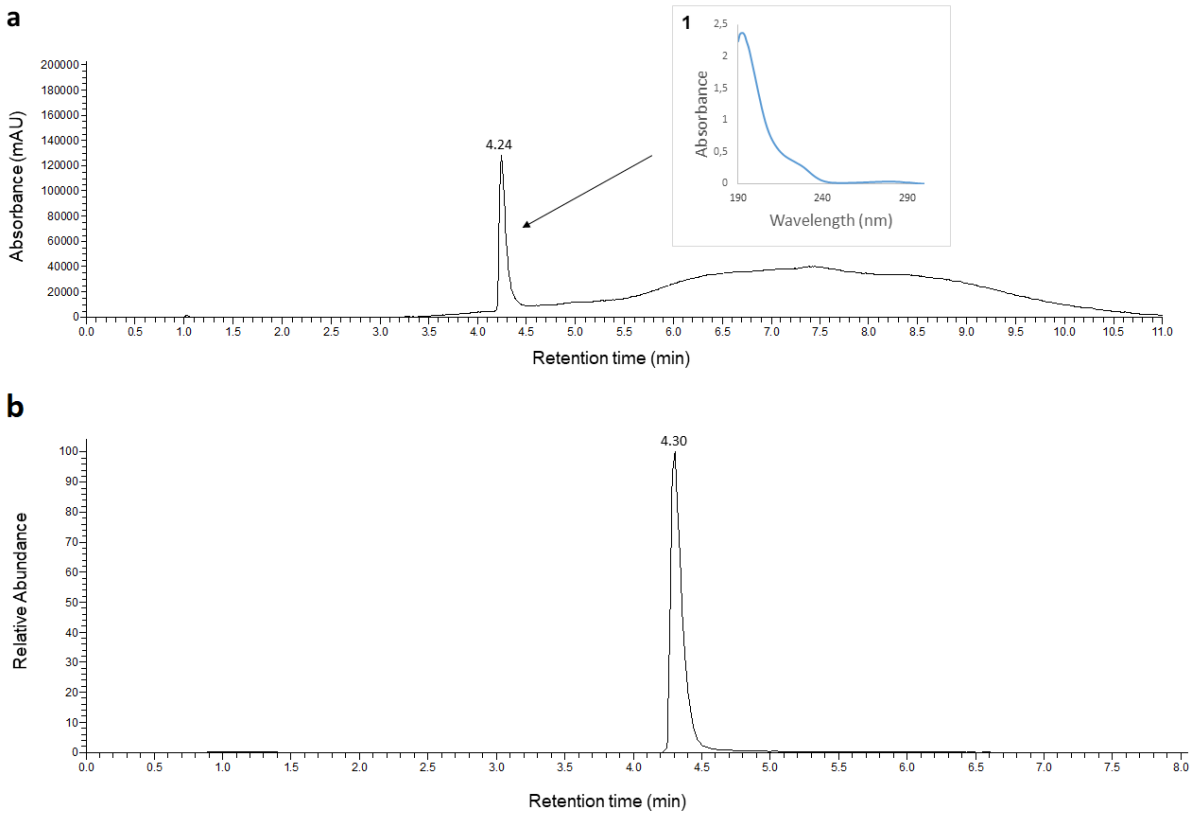

Fig. 1. UV chromatogram (a) and TIC (b) of standard solution of nivolumab at 25 µg/mL. UV absorption spectra of standard solution of nivolumab at 25 µg/mL D0 (a)1.

3.2. LC-MS nivolumab N-glycan-based isoform profile identification

The MS conditions applied in our previous work [31] proved to be useful here for the intact analysis of nivolumab and did not require any further adjustment. Fig. 1b shows a representative total ion chromatogram (TIC) of nivolumab standard solution (25 µg/mL), while Fig. 2 presents the MS results after deconvolution. N-terminal glutamate to pyroglutamate conversion was identified. Five N-glycoforms were identified, whose masses coincided with those previously published in nivolumab samples [42,43]. A2G0F/A2G0F was identified as the main glycoform, followed by A2G0F/A2G1F, A2G1F/A2G1F, A2G1F/A2G2F and A2G0F/A1G0F. This glycosylation pattern was identical in the different batches that were studied in this research and the same 5 Nglycoforms were detected. Table 1 shows the experimental masses obtained for each isoform and the glycoforms associated with their relative abundance (%) and error (ppm) for the control sample of nivolumab (25 µg/mL). Theoretical masses were calculated considering 2C-terminal lysine clipping, 2 N-terminal pyroglutamate formation and 16 disulphide bonds.

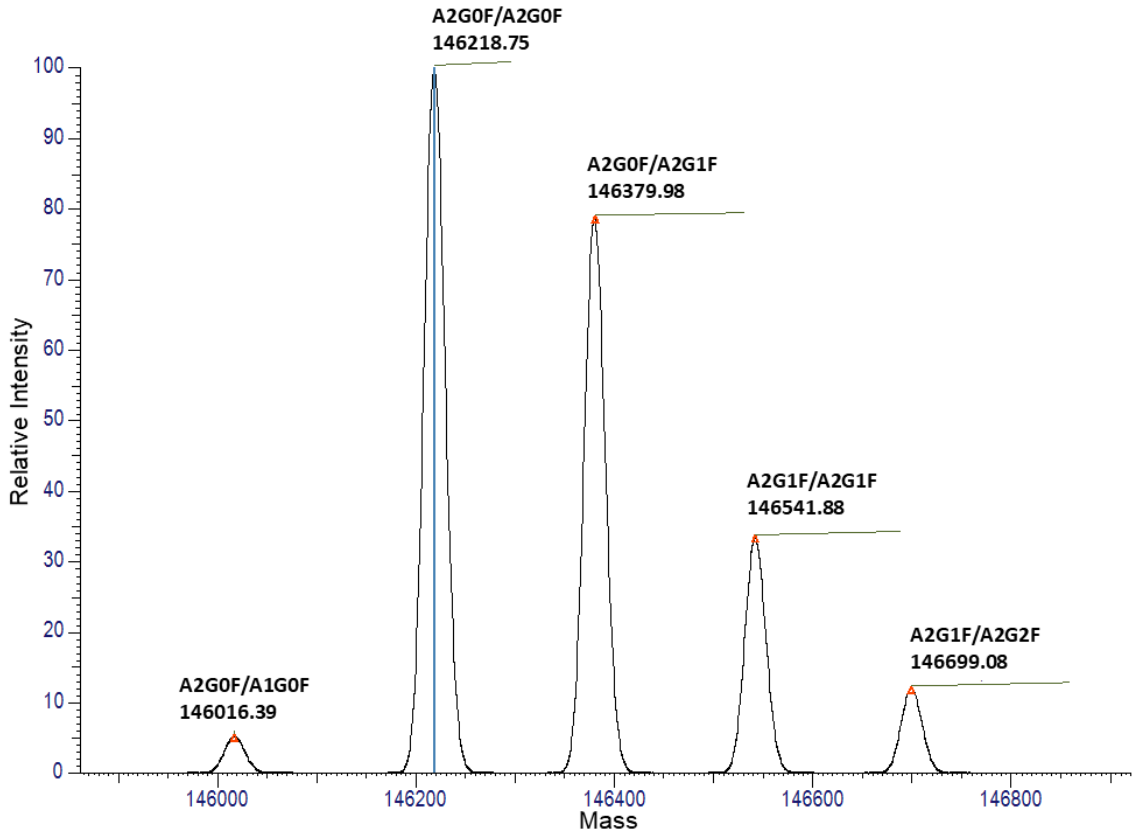

Fig. 2. Deconvoluted mass spectrum for nivolumab at 25 µg/mL showing the mass isoform profile and the N-glycoforms association obtained with the proposed method.

3.3. Validation of the analytical procedure for nivolumab quantification

The optimized procedure for RP chromatographic analysis described above was validated for nivolumab quantification purposes, using UV and MS signals to compare the figures of merit for the method when using one detector or the other. A review of the ICH Q2(R1) guideline is currently ongoing [44], which will define the common characteristic for the validation of procedures involving hyphenated techniques like LCMS. In the meantime, we followed above all the current ICH Q2(R1) [11]. However, given that none of the ICH guidelines provide acceptance criteria, we also followed the FDA recommendations for chromatographic methods and procedures [38] and the Hsu and Chien criteria [39].

Table 1
Experimental mass for the intact nivolumab in control and stressed samples. The relative abundances of *N*-glycoforms are also reported.

	Associated glycoforms	Experimental mass (Da)	Theoretical average mass (Da)	Mass difference (ppm)	Relative abundance (%)
Control	A2G0F/A1G0F	146016.4	146017.0	3.8	2.2
	A2G0F/A2G0F	146218.7	146220.2	10.0	43.6
	A2G0F/A2G1F	146380.0	146382.3	15.7	34.3
	A2G1F/A2G1F	146541.9	146544.4	17.3	14.6
	A2G1F/A2G2F	146699.1	146706.6	51.0	5.2
Temp 60 °C	A2G0F/A1G0F	146012.5	146017.0	30.3	2.0
	A2G0F/A2G0F	146217.3	146220.2	19.4	44.1
	A2G0F/A2G1F	146380.3	146382.3	13.7	34.0
	A2G1F/A2G1F	146540.7	146544.4	25.7	15.8
	A2G1F/A2G2F	146701.9	146706.6	31.8	4.0
NaCl	A2G0F/A1G0F	146013.6	146017.0	23.1	1.6
	A2G0F/A2G0F	146218.3	146220.2	12.9	44.0
	A2G0F/A2G1F	146379.9	146382.3	16.1	33.5
	A2G1F/A2G1F	146540.7	146544.4	25.4	15.8
	A2G1F/A2G2F	146697.0	146706.6	65.6	5.1
Light	Not identified	146239.4	–	–	46.5
	Not identified	146587.2	–	–	53.5

3.3.1. Linearity and detection and quantification limits

The results of the linearity study are shown in Table 2 for signals from UV and MS detectors. The coefficient of determination (R^2) was used to check the goodness of fit of the linear regression model.

If we consider the signals from the UV detector, a linear relationship can be observed over the 5 – 45 µg/mL nivolumab concentration range. This relationship was confirmed by the regression line established by the least squares method, with an R^2 value of 0.998, which indicates that the estimated regression line is a good fit for the experimental data. In addition, the intercept was not significant since the corresponding P-value was over 5 %. Linearity was also checked using the signals from the mass detector (total ions signals) for the same concentration range, i.e. 5 – 45 µg/mL (Table 2). In this case, results showed a slight decrease in the R2 (0.944). However, a matrix effect was detected due to the significant intercept value (p-value < 5 %). This indicates that the UV signal produced better results than the MS signal.

UV and MS detectors obtained similar results for DL and QL with slightly lower values for MS (Table 2).

Table 2. Analytical parameters of the UHPLC method using UV and (HESI/Orbitrap™) MS signals.

Parameter	Values from UV	Values from (HESI/Orbitrap™)MS
Intercept (*a*)	- 15,948	332,242,879
Slope (*b*)	24,198	83,190,184
Standard deviation of the intercept *s(a)*	8,161	137,211,598
Probability of significance of the intercept *P (%)*	6.64	2.62
Standard deviation of the slope *s(b)*	284.1	4,777,095
Coefficient of determination R^2	0.998	0.944
Linear range (µg/mL)	4.0-45.0	1.0-45.0
Quantification limit (µg/mL, estimated from SD(*a*))	4.0	1.0
Detection limit (µg/mL, estimated from SD(*a*))	2.0	0.2

3.3.2. Accuracy and precision

As stated in the ICH Q2(R1) guidelines [11], accuracy and precision were assessed across the linear range of the analytical procedure. The accuracy and precision results were expressed as recovery (%) and RSD (%), respectively. Both parameters were calculated by considering UV and MS signals separately. The results are shown in Table 3. Satisfactory

values were obtained for the UV signals, with recovery values close to 100 % for each concentration checked, so fulfilling the acceptance criteria (value within the 100 ± 3 % range). As regards precision, the criteria were not fulfilled for the lower concentration, with a RSD (%) > 5 %, but precision –both inter and intraday- increases in line with concentration, as expected. This means that for the target concentration (25 mg/mL), the analytical procedure fulfilled the criteria.

By contrast, the accuracy and precision results for the (HESI/Orbitrap™)MS signals were significantly worse across the linear range than those obtained for the UV signals (described above) and the criteria were not fulfilled. The recovery values were < 100%, and did not meet the criteria for any of the concentration levels checked. Intra- and interday precision results did not meet the selected criteria either, and in all cases the RSD (%) was over 5 %.

Table 3. Accuracy and precision from UHPLC using the-UV and (HESI/Orbitrap™)MS signals.

Analytical signal	Concentration (µg/mL)	Recovery (%)[a]	RSD (%)[b]	
			Intraday	Interday (6 days)
UV	5	99.18	8.07	10.60
	25	103.0	0.71	2.54
	45	100.18	1.35	2.53
(HESI/Orbitrap™)MS	5	52.34	50.0	41.03
	25	93.33	8.55	12.19
	45	93.25	5.70	6.75

[a] Recovery value based on three measurements.

[b] Relative standard deviation based on three measurements. Intraday means on the same day, whereas interday means on six different days.

3.3.3. Specificity

To evaluate the specificity of the proposed analytical procedure, forced degradation studies were performed according to the ICH Q2(R1) guidelines [11]. Another aim of these studies was to find out more about the possible degradation of nivolumab samples during real use in hospitals prior to administration to patients. With this in mind, in this study, we selected three stress factors that could potentially affect the stability of nivolumab when handled in hospitals. These are discussed below.

It is important to remember that slight physicochemical modifications, such as the presence of oligomers, will not be reflected in the chromatograms, unless UV-spectra were recorded to perform similarity analysis, as described in the literature [24–26]. The UV chromatograms recorded at three λ (214, 220 and 280 nm) in this study will not reflect these modifications. Nevertheless, a comparison between control and stressed samples was carried out in order to detect significant modifications, such as the breaking of the protein chains. As previously mentioned, three stresses were performed using Opdivo® samples to evaluate the specificity: thermal stress at 60 °C; high ionic strength, as the medical samples are diluted in 0.9 % NaCl for clinical administration; and light exposure due to the fact that therapeutic proteins are exposed to light during preparation for administration to the patient. In all cases, the UV chromatograms for the stressed and the control (fresh) samples of nivolumab were similar, in terms of both the profile and the area under the peaks. New chromatographic peaks were not detected in any of them and the main chromatographic peak appears at the same retention time in stressed and fresh samples (Fig. 3a), therefore indicating that none of the samples suffered protein breakdown.

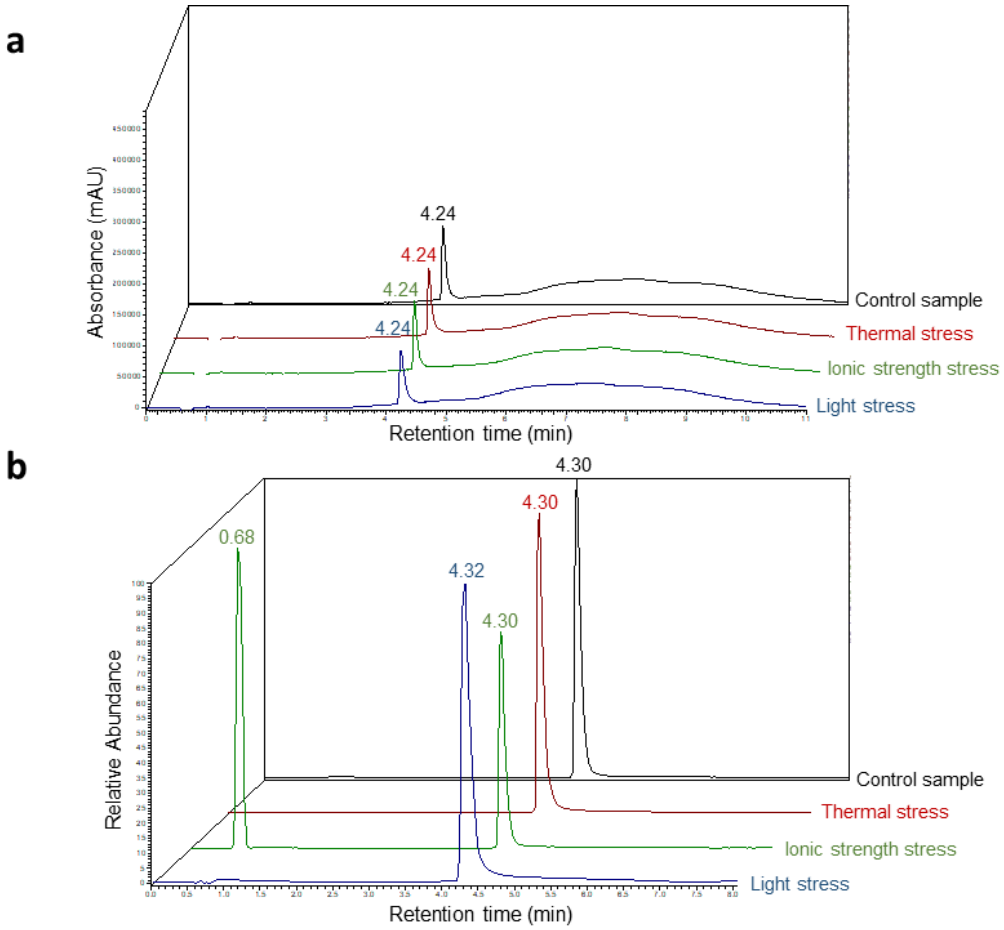

Fig. 3. Controlled degradation study of nivolumab 25 µg/mL using the (RP)UHPLC-UV-(HESI/Orbitrap™)MS method. Representative UV chromatogram (a) and TIC (b) of: control (fresh), thermal stress, ionic strength stress, and light stress samples. The chromatograms are displayed normalized from the main peak.

Consequently, specificity was assessed using the mass detector (MS results), which allows small physicochemical changes to be detected by evaluating the isoform profile. As regards the thermal stress at 60 °C, TIC chromatograms did not show any variation in the TIC chromatogram profiles for the stressed sample as compared to the control sample (Fig. 3b). Moreover, the MS isoform profile showed the same N-glycoforms in both the stressed and the control (fresh) samples (Fig. 4), indicating that there was no chemical degradation of nivolumab at this temperature. In the high ionic strength stress test, there was a decrease in the relative abundance of the TIC, which was attributed to the suppression of the mass signal due to the higher concentration of salt in the medium (Fig. 3b). We believe that the new peak detected at the front of this chromatogram (RT = 0.68 min) is an artefact, as its mass information was not related to nivolumab and it was not detected in the UV chromatogram. In this case, the MS isoform profile was similar in both stressed and control samples, and the same N-glycoforms were detected (Fig. 4). Finally, as regards light exposure stress, important modifications were detected by the mass analysis of the isoforms. The results showed that the molecular weight of the isoforms was different from that of the control samples, clearly indicating that chemical modifications had taken place (Fig. 4). An increase in the number of isoforms was also observed in the stressed sample, and the main isoform was different from that of the control (fresh) nivolumab sample. This shows that exposure to light caused important chemical modifications in the isoform profile of nivolumab, so indicating that it had suffered degradation. This highlights the need to use a high-resolution mass detector to detect such modifications, in that the isoforms promoted by light degradation were not chromatographically separated in RP mode, and they were not detected by changes in any of the three UV chromatograms registered at three different λ. Moreover, Fig. 4b shows that two original nivolumab isoforms remain after exposure to light as they are in the same mass range as the isoforms of the control sample. However, these two isoforms have different masses than the isoforms of fresh nivolumab, which means that no N-glycoforms can be attributed to these two masses. According to previous publications [16,45], when exposed to light, proteins can undergo photo-oxidation in residues such as tryptophan, tyrosine and phenylalanine. This suggests that the variation in the mass of the isoforms produced by light-stressed samples may be due to photooxidation of nivolumab. This is currently being investigated in our group using a bottom-up strategy (peptide mapping by LC-MS/MS).

After gathering together all the results of the degradation study to assess the specificity of the proposed (RP)UHPLC-UV-(HESI/Orbitrap™) MS method, these indicated that the degraded nivolumab could not be chromatographically separated. This means that degraded nivolumab cannot be differentiated from control nivolumab, as the elution time is similar for both degraded and non-degraded forms of this mAb (Fig. 3). Nevertheless, modifications in the isoforms were clearly detected by HRMS (Fig. 4). If we look at the results for each stress

test, the isoform profile for the thermal and high ionic strength tests remained unchanged compared to the deconvoluted mass spectrum for the control samples. However, the light exposure stress produced a different isoform profile, with a different total number of isoforms. Fig. 4a shows an increase in the number of isoforms with regard to control, thermal stressed and high ionic strength stressed samples, which means that light stress had a more noticeable effect on nivolumab than other stresses, which did not alter the chemical structure. Table 1 shows the masses obtained for the isoforms of the stressed and the control (fresh) samples of nivolumab and the associated N-glycoforms. It also includes the masses of the N-glycoforms and their relative abundance (%) and error (ppm). As occurred in previous research [24–26], although the proposed method was unable to chromatographically separate degraded nivolumab, it was capable of detecting and identifying, via HRMS, slight physicochemical modifications in the product. The method can therefore be considered as stability-indicating in nivolumab medicine samples, in which it can rigorously detect degradation.

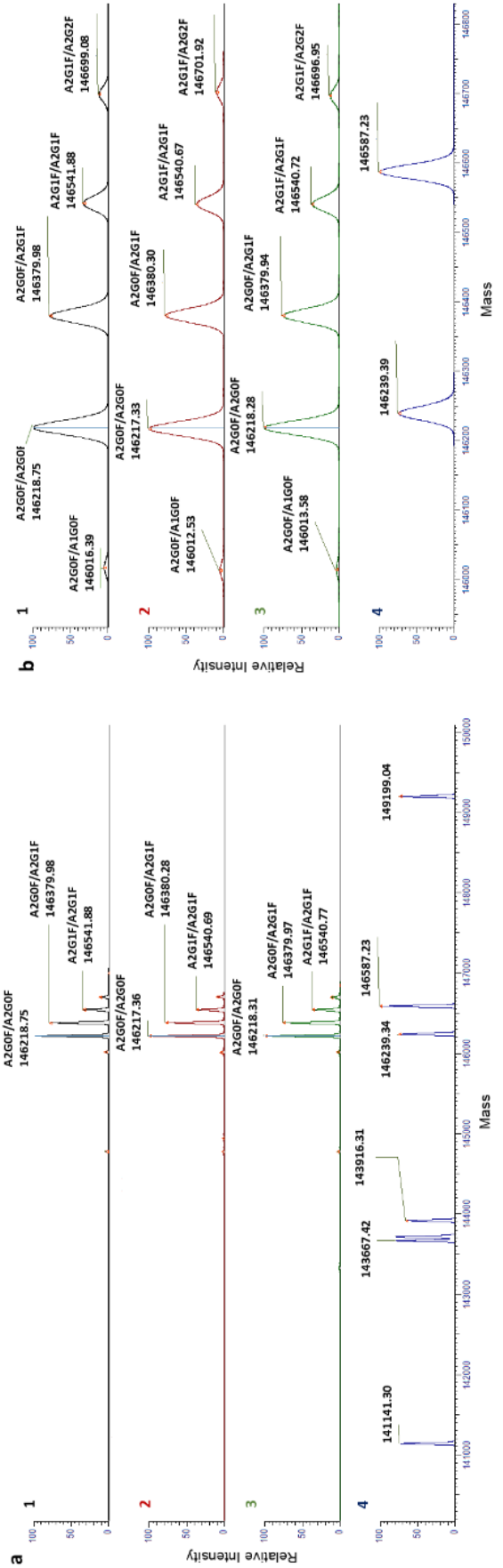

Fig. 4. Deconvoluted mass spectra for nivolumab 25 µg/mL showing the mass isoform profile with the associated N-glycoforms (a) and the corresponding expansion (b). Control (fresh) sample (1), thermal stress sample (2) ionic strength stress sample (3) and light stress sample (4).

3.3.4. Robustness test

The results of the study performed to assess the robustness of the method are summarized in Table 4. The retention time was most affected by small variations in the flow rate, and was only slightly altered by the changes in mobile phase composition and temperature. The same results were observed for both the UV and the HRMS detection techniques. This indicates that the flow rate was the most important factor influencing the robustness of the method.

The results set out in Table 4 indicate with regard to the UV signals that in all cases the N and k' values were within the FDA acceptance criteria (≥2000 and > 2.0, respectively). However, when the MS signals were used, k' met the acceptance criteria, but N did not. This shows that the method is more robust when using signals from the UV detector than when using MS signals.

Table 4. Results for the robustness of the method using UV and (HESI/Orbitrap™)MS signals. Control optimized parameters of the proposed method are shown in bold type.

Technique	Gradient variation (%)B	T (°C)	Flow (mL/min)	Retention time (min)	N[a]	k'[b]
UV	**80[c]**	**70[c]**	**0.3[c]**	**4.24[c]**	**2488,25[c]**	**5,42[c]**
	80	68	0.3	4.25	2229,94	5,44
	80	72	0.3	4.23	2979,05	5,41
	80	70	0.28	4.48	2621,44	5,40
	80	70	0.32	4.03	3089,83	5,30
	78	70	0.3	4.26	2653,81	5,44
	82	70	0.3	4.26	3007,28	5,44
(HESI/Orbitrap™)MS	**80[c]**	**70[c]**	**0.3[c]**	**4.30[c]**	**144,67[c]**	**6,68[c]**
	80	68	0.3	4.31	59,49	7,11
	80	72	0.3	4.28	28,14	9,17
	80	70	0.28	4.54	71,38	6,53
	80	70	0.32	4.07	60,10	15,28
	78	70	0.3	4.31	64,30	22,94
	82	70	0.3	4.31	48,72	29,79

[a] Theoretical plates.

[b] Capacity factor.

[c] Selected optimized conditions.

3.3.5. System suitability test

The results of the system suitability test are summarized in Table 5. This test was conducted using standard nivolumab samples at a concentration of 25 µg/mL. The mean values of N and k' were found to be within FDA acceptance criteria (≥ 2000 and > 2.0, respectively), with RSD values < 5 % when the UV signals were used [38,39]. However, the N values did not meet the acceptance criteria when the MS signals were used. Once again, from the chromatographic experimental point of view, the system suitability is greater when tested using the signal from the UV detector than when using the MS signal from the HRMS.

Table 5. Results for the system suitability of the method using UV and (HESI/Orbitrap™) MS signals.

Technique	Nivolumab standard sample	Retention time	N[a]	k'[b]
UV	25 µg /mL	4.24	2348,10	4,3
(HESI/Orbitrap™)MS	25 µg /mL	4.30	98,85	6,68

[a] Theoretical plates.

[b] Capacity factor.

3.4. Long-term stability of the medicine (Opdivo®) using UV detection

The results of the evaluation of the protein content in the daily surplus of the medicine Opdivo® stored for 15 days either at room temperature (20 °C) or refrigerated at 4 °C, both daylight protected, are shown in Fig. 5. After storage for 24 h at the two different storage conditions, nivolumab recovery values were > 90 % in both cases. After 15 days, nivolumab recovery values were > 80 % in both storage conditions (Table 1, supplementary material). In all the UV chromatograms registered, the nivolumab peak was detected at 4.24 ± 0.01 min and the shape remained unchanged for the two storage conditions (Fig. 1, supplementary material). On the basis of these UV detection results for the protein content in the medicine samples, the refrigerated samples could be considered stable for 15 days (recovery close to 90 %), while those stored at room temperature (20 °C) could be considered stable for 7 days. To evaluate possible modifications in the chemical structure of nivolumab, the MS isoform profile was analysed every day during the experimental period. Fig. 6 shows the variations in the isoform profile. In both storage conditions (4 °C and 20 °C), the three most abundant isoforms remain unchanged, while the other two (less abundant isoforms) were not always detected. This was attributed to the low intensity of these isoforms which were not always detectable by the mass spectrometer. Tables 2 and 3 of the supplementary material show the relative abundance (%) and error (ppm) of the associated glycoforms over the 15 days of the stability study for storage at 4 °C and 20 °C, respectively.

This long-term stability study was carried out, above all, for the purpose of applying and testing the stability-indicating method we had developed. Assessing the stability of nivolumab was only a secondary objective. This will be further assessed in greater depth in future stability studies using different techniques focused on different quality attributes of the medicine.

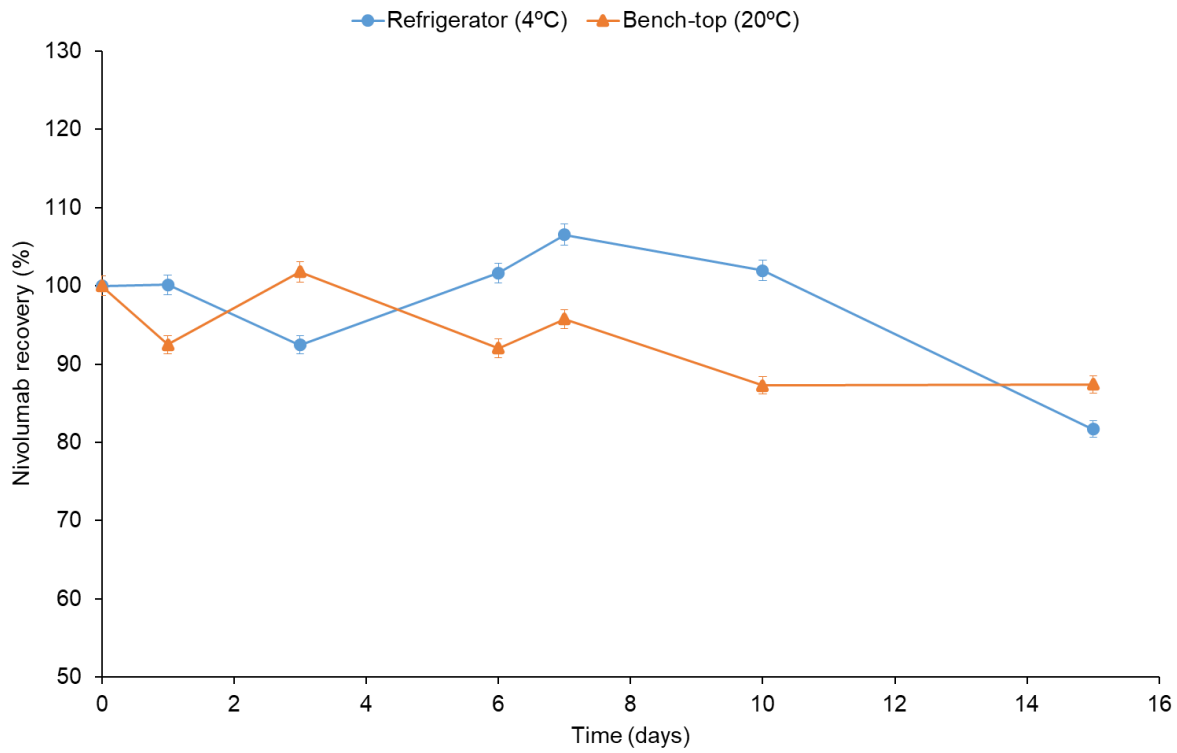

Fig. 5. Results of the stability study over time: protein content of the daily surplus of Opdivo® (nivolumab 10 mg/ml) solution during storage for 15 days under two different conditions: in a refrigerator at 4 °C (blue) and on the bench-top at 20 °C (orange). Nivolumab 25 µg/mL was the target concentration for (RP)UHPLC-UV-(HESI/Orbitrap™)MS method analysis.

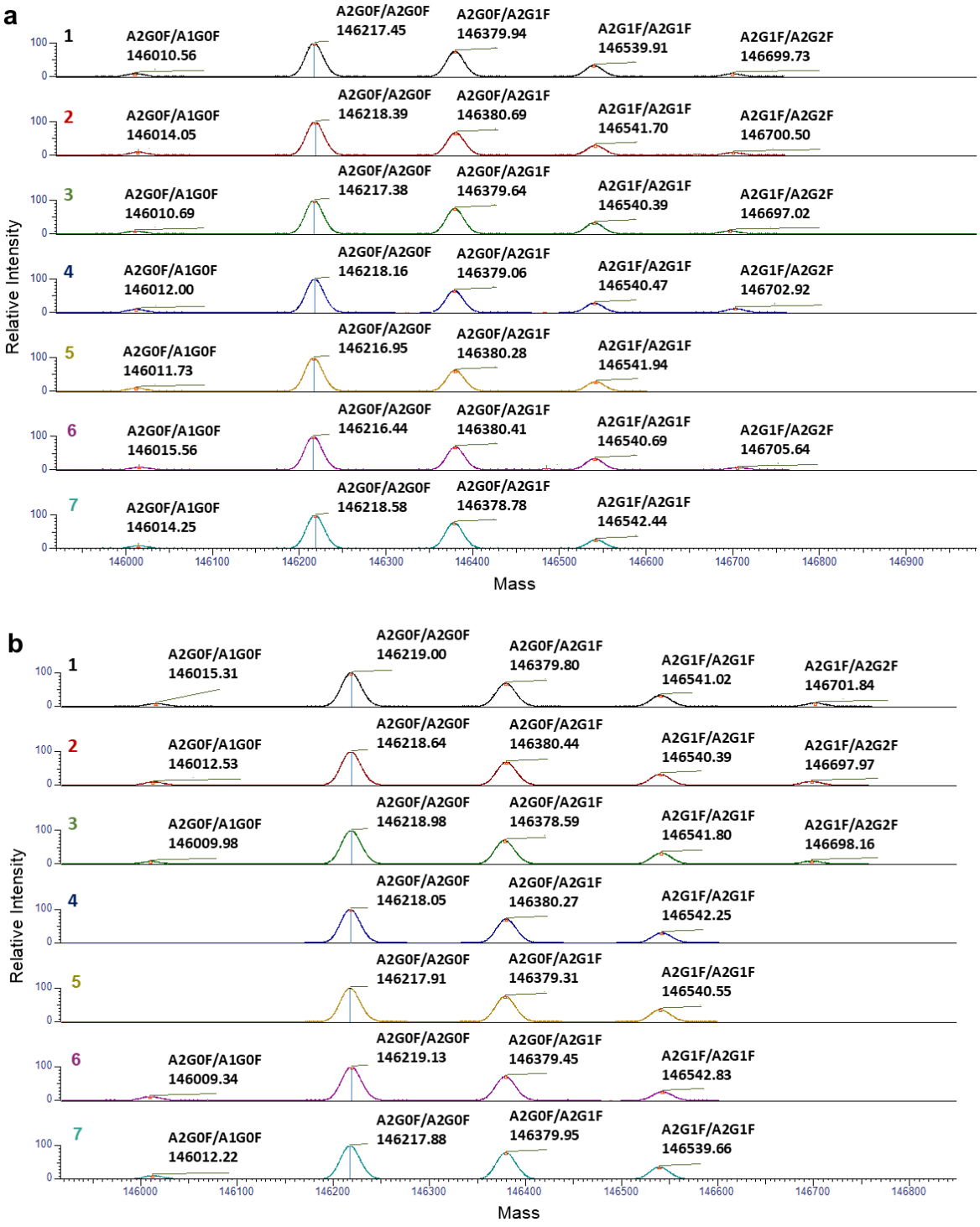

Fig. 6. Results of the stability study along time: Deconvoluted mass spectra (isoform profile including the associated N-glycoforms) resulted from the analysis of nivolumab in the daily surplus of the medicine Opdivo®. Two storage conditions: in a refrigerator at 4 °C (a) and on the bench-top at 20 °C (b). Checked days: Day 0 (1), day 1 (2), day 3 (3), day 6 (4), day 7 (5), day 10 (6), and day 15 (7).

4. Conclusions

For the first time, a (RP)UHPLC/UV-(HESI/Orbitrap™)MS method for nivolumab quantification (protein content) was successfully developed and validated as stability-indicating according to the ICH quality guideline Q2(R1), in that it was able to detect structural modifications in the degraded protein.

A comparative study of the figures of merit for the validated method using the UV and the (HESI/Orbitrap™)MS signals was conducted. Apart from the specificity and sensitivity parameters, all others worked better when using data from the UV signal. In the robustness and system suitability tests using the (HESI/Orbitrap™)MS signals, not all the acceptance criteria were met. Nevertheless, these signals played a crucial role in assuring method specificity in order to validate it as stability-indicating. This was achieved by identifying the molecular weight isoform profile of nivolumab. This provided information about structural characteristics (such as the N-glycosilation pattern or pyroglutamation identification). It also identified the main isoforms and detected any modifications due to protein degradation when they occurred. The method can therefore be classified as stability-indicating, according to the ICH Q2(R1).

The method was successfully applied to track the protein content in the daily surplus of the medicine Opdivo® (nivolumab 10 mg/mL) over the course of 15 days. This method complied with all the requirements to enable it to be used for the analysis of protein content, a critical quality factor in any quality control program in the pharmaceutical field.

CRediT authorship contribution statement

Anabel Torrente-López: Conceptualization, Validation, Formal analysis, Investigation, Writing – original draft, Visualization. **Jesús Hermosilla:** Conceptualization, Validation, Formal analysis, Investigation. **Raquel Pérez-Robles:** Writing – original draft, Supervision. **Antonio Salmerón-García:** Conceptualization, Formal analysis, Resources, Funding acquisition. **José Cabeza:** Formal analysis, Resources, Funding acquisition. **Natalia Navas:** Conceptualization, Methodology, Formal analysis, Writing – review & editing, Supervision, Funding acquisition, Project administration.

Declaration of Competing Interest

The authors declare that they have no known competing financial interests or personal relationships that could have appeared to influence the work reported in this paper.

Acknowledgements

Anabel Torrente-López is currently receiving a FPU predoctoral grant (ref.: FPU18/03131) from the Ministry of Universities, Spain. Jesús Hermosilla is currently benefiting from a research contract (P20_01029) from the Junta de Andalucía (Spain) and European Regional Development Funds. Raquel P´erez-Robles is currently granted a postdoctoral position from the Junta de Andalucía, Spain. This study was funded by Project P20-01029 (I + D + i - Junta de Andalucía, Spain) and by Project B-FQM-308-UGR20 (Universidad de Granada, Proyectos I + D + i del Programa Operativo FEDER Andalucía 2020) which means that it was also partially supported by European Regional Development Funds. Funding for open access charge: CBUA/Universidad de Granada.

Supplementary material

Table 1. Nivolumab recovery values of the stability study in two different conditions: refrigerator at 4 ºC and bench-top at 20ºC, both analysed by UHPLC-UV

Time (days)	Nivolumab recovery (%)	
	Refrigerator 4 ºC	Bench-top 20 ºC
0	100	100
1	100.15	92.49
3	92.47	101.80
6	101.63	92.04
7	106.53	95.75
10	101.95	87.28
15	81.70	87.41

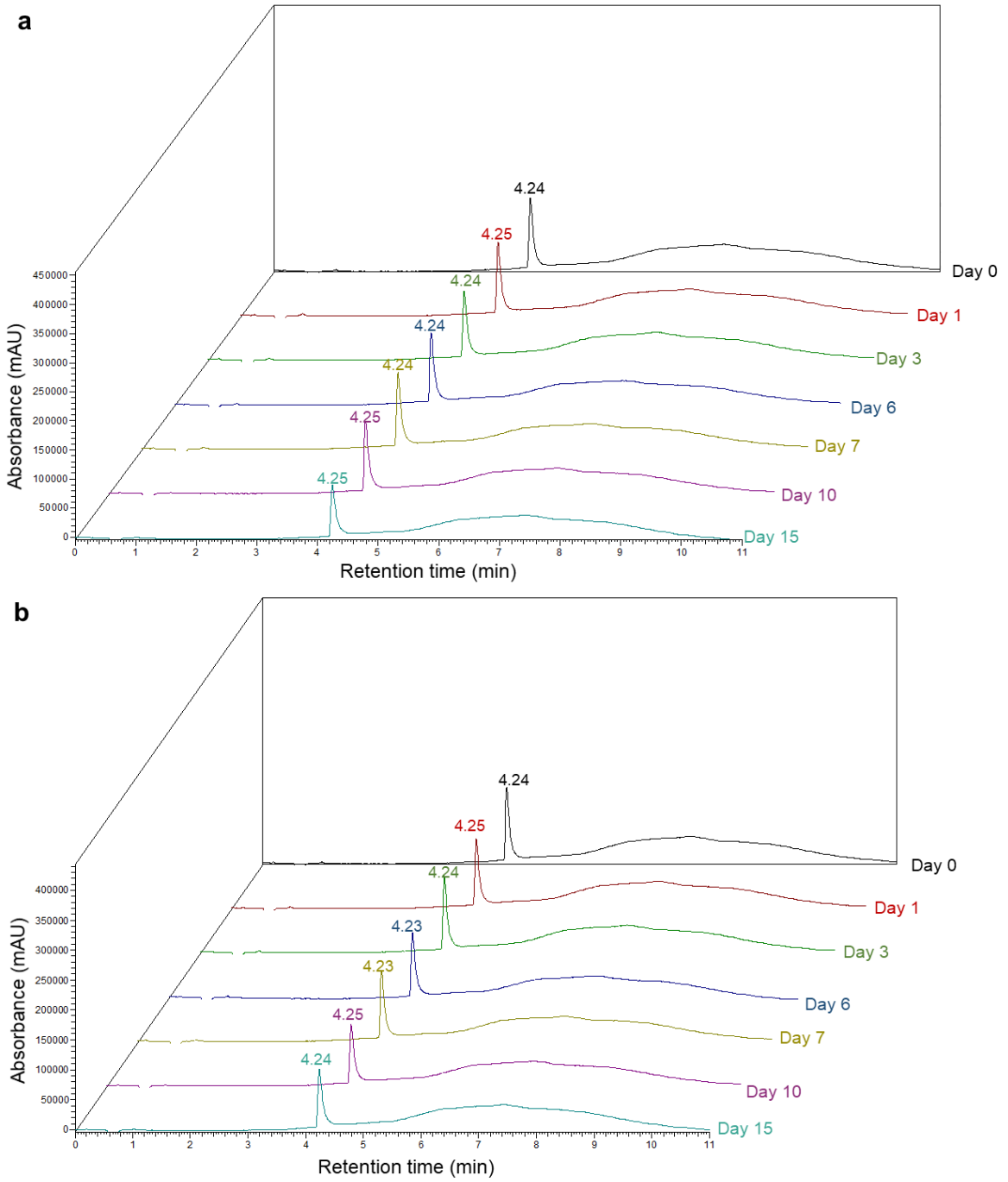

Fig. 1. Results of the stability study along time: representative UV chromatograms of the analysis of nivolumab (protein content) in daily surplus of the medicine Opdivo® stored in refrigerator at 4 °C (a) and in bench-top at 20 °C (b). Nivolumab 25 µg/mL was the target concertation for (RP)UHPLC-UV-(HESI/Orbitrap™)MS method analysis.

Table 2
Stability study of nivolumab 25 µg/mL stored in a refrigerator at 4 ºC. Experimental mass for the intact nivolumab in denatured conditions over 15 days. The relative abundances of N-glycoforms are also reported. Theoretical masses were calculated considering 2 C-term lysine clipping, 2 N-term pyroglutamate formation and 16 disulphide bonds

	Glycoforms associated	Experimental mass (Da)	Theoretical average mass (Da)	Mass difference (ppm)	Relative abundance (%)
Day 0	A2G0F/A1G0F	146010.6	146017.0	43.8	3.9
	A2G0F/A2G0F	146217.5	146220.2	18.5	45.0
	A2G0F/A2G1F	146379.9	146382.3	16.1	32.9
	A2G1F/A2G1F	146539.9	146544.4	30.9	14.3
	A2G1F/A2G2F	146699.7	146706.6	46.7	3.8
Day 1	A2G0F/A1G0F	146014.1	146017.0	19.9	4.4
	A2G0F/A2G0F	146218.4	146220.2	12.1	45.3
	A2G0F/A2G1F	146380.7	146382.3	11.0	31.9
	A2G1F/A2G1F	146541.7	146544.4	18.7	14.3
	A2G1F/A2G2F	146700.5	146706.6	41.4	4.1
Day 3	A2G0F/A1G0F	146010.7	146017.0	42.9	3.4
	A2G0F/A2G0F	146217.4	146220.2	19.0	44.4
	A2G0F/A2G1F	146379.6	146382.3	18.2	33.5

Table 2 (continuation)

	A2G1F/A2G1F	146540.4	146544.4	27.6	14.7
	A2G1F/A2G2F	146697.0	146706.6	65.2	3.9
Day 6	A2G0F/A1G0F	146012.0	146017.0	34.0	4.4
	A2G0F/A2G0F	146218.2	146220.2	13.7	47.3
	A2G0F/A2G1F	146379.1	146382.3	22.1	31.6
	A2G1F/A2G1F	146540.5	146544.4	27.1	11.5
	A2G1F/A2G2F	146702.9	146706.6	24.9	5.2
Day 7	A2G0F/A1G0F	146011.7	146017.0	35.8	3.8
	A2G0F/A2G0F	146217.0	146220.2	22.0	50.1
	A2G0F/A2G1F	146380.3	146382.3	13.8	31.7
	A2G1F/A2G1F	146541.9	146544.4	17.1	14.4
	A2G1F/A2G2F	-	-	-	-
Day 10	A2G0F/A1G0F	146015.6	146017.0	9.6	3.6
	A2G0F/A2G0F	146216.4	146220.2	25.4	46.2
	A2G0F/A2G1F	146380.4	146382.3	12.9	31.6
	A2G1F/A2G1F	146540.7	146544.4	25.6	15.5

Table 2 (continuation)

	A2G1F/A2G2F	146705.6	146706.6	6.4	3.0
Day 15	A2G0F/A1G0F	146014.3	146017.0	18.6	3.9
	A2G0F/A2G0F	146218.6	146220.2	10.8	46.5
	A2G0F/A2G1F	146378.8	146382.3	24.0	36.4
	A2G1F/A2G1F	146542.4	146544.4	13.6	13.1
	A2G1F/A2G2F	-	-	-	-

Table 3
Stability study of nivolumab 25 µg/mL stored in a refrigerator at 20 ºC. Experimental mass for the intact nivolumab in denatured conditions over 15 days. The relative abundances of N-glycoforms are also reported. Theoretical masses were calculated considering 2 C-term lysine clipping, 2 N-term pyroglutamate formation and 16 disulphide bonds

	Glycoforms associated	Experimental mass (Da)	Theoretical average mass (Da)	Mass difference (ppm)	Relative abundance (%)
Day 0	A2G0F/A1G0F	146015.3	146017.0	11.3	3.3
	A2G0F/A2G0F	146219.0	146220.2	7.9	46.1
	A2G0F/A2G1F	146379.8	146382.3	17.1	31.0
	A2G1F/A2G1F	146541.0	146544.4	23.3	15.2
	A2G1F/A2G2F	146701.8	146706.6	32.3	4.4
Day 1	A2G0F/A1G0F	146012.5	146017.0	30.3	4.2
	A2G0F/A2G0F	146218.6	146220.2	10.4	45.4
	A2G0F/A2G1F	146380.4	146382.3	12.7	31.0
	A2G1F/A2G1F	146540.4	146544.4	27.6	14.7
	A2G1F/A2G2F	146698.0	146706.6	58.7	4.7
Day 3	A2G0F/A1G0F	146010.0	146017.0	47.8	3.4
	A2G0F/A2G0F	146219.0	146220.2	8.1	45.8
	A2G0F/A2G1F	146378.6	146382.3	25.3	31.9

Table 3 (continuation)

	A2G1F/A2G1F	146541.8	146544.4	18.0	14.9
	A2G1F/A2G2F	146698.2	146706.6	57.4	4.0
Day 6	A2G0F/A1G0F	-	-	-	-
	A2G0F/A2G0F	146218.1	146220.2	14.4	49.8
	A2G0F/A2G1F	146380.3	146382.3	13.9	35.9
	A2G1F/A2G1F	146542.3	146544.4	14.9	14.3
	A2G1F/A2G2F	-	-	-	-
Day 7	A2G0F/A1G0F	-	-	-	-
	A2G0F/A2G0F	146217.9	146220.2	15.4	48.1
	A2G0F/A2G1F	146379.3	146382.3	20.4	35.4
	A2G1F/A2G1F	146540.6	146544.4	26.5	16.5
	A2G1F/A2G2F	-	-	-	-
Day 10	A2G0F/A1G0F	146009.3	146017.0	52.2	5.5
	A2G0F/A2G0F	146219.1	146220.2	7.0	48.3
	A2G0F/A2G1F	146379.5	146382.3	19.5	33.6
	A2G1F/A2G1F	146542.8	146544.4	11.0	12.5

Table 3 (continuation)

	A2G1F/A2G2F	-	-	-	-
Day 15	A2G0F/A1G0F	146012.2	146017.0	32.5	4.4
	A2G0F/A2G0F	146217.9	146220.2	15.6	44.9
	A2G0F/A2G1F	146380.0	146382.3	16.1	34.8
	A2G1F/A2G1F	146539.7	146544.4	32.6	15.9
	A2G1F/A2G2F	-	-	-	-

References

[1] European Medicines Agency. Nivolumab: Summary of Product Characteristics., https://www.ema.europa.eu/en/documents/product-information/opdivo-eparproduct-information_en.pdf (accessed July 12, 2021).

[2] L.A. Raedler, Opdivo (Nivolumab): Second PD-1 Inhibitor Receives FDA Approval for Unresectable or Metastatic Melanoma., Am. Heal. Drug Benefits. 8 (2015) 180–3. chrome-extension://dagcmkpagjlhakfdhnbomgmjdpkdklff/enhancedreader.html?pdf=https%3A%2F%2Fbrxt.mendeley.com%2Fdocument%2Fcontent%2F95d92e80-a042-3bff-a804-f61cdfb0d7a1 (accessed December 3, 2020).

[3] D. Kazandjian, D.L. Suzman, G. Blumenthal, S. Mushti, K. He, M. Libeg, P. Keegan, R. Pazdur, FDA Approval summary: nivolumab for the treatment of metastatic non-small cell lung cancer with progression on or after platinum-based chemotherapy, Oncologist. 21 (2016) 634–642, https://doi.org/10.1634/theoncologist.2015-0507.

[4] J.X. Xu, V.E. Maher, L. Zhang, S. Tang, R. Sridhara, A. Ibrahim, G. Kim, R. Pazdur, FDA approval summary: nivolumab in advanced renal cell carcinoma after antiangiogenic therapy and exploratory predictive biomarker analysis, Oncologist. 22 (2017) 311–317, https://doi.org/10.1634/theoncologist.2016-0476.

[5] Y.L. Kasamon, R.A. de Claro, Y. Wang, Y.L. Shen, A.T. Farrell, R. Pazdur, FDA approval summary: nivolumab for the treatment of relapsed or progressive classical hodgkin lymphoma, Oncologist. 22 (2017) 585–591, https://doi.org/10.1634/theoncologist.2017-0004.

[6] L. Wang, D. Zhao, K. Qin, F.U. Rehman, X. Zhang, Effect and biomarker of Nivolumab for non–small-cell lung cancer, Biomed. Pharmacother. 117 (2019), https://doi.org/10.1016/j.biopha.2019.109199.

[7] M.R. Nejadnik, T.W. Randolph, D.B. Volkin, C. Sch¨oneich, J.F. Carpenter, D.J.A. Crommelin, W. Jiskoot, Postproduction handling and administration of protein pharmaceuticals and potential instability issues, J. Pharm. Sci. 107 (2018) 2013–2019, https://doi.org/10.1016/j.xphs.2018.04.005.

[8] Y. Le Basle, P. Chennell, N. Tokhadze, A. Astier, V. Sautou, Physicochemical stability of monoclonal antibodies: A Review, J. Pharm. Sci. 109 (2020) 169–190, https://doi.org/10.1016/j.xphs.2019.08.009.

[9] ICH Secretariat (2005) International Conference on Harmonization (ICH) guideline ICH Q5E: Comparability of Biotechnological/Biological Products, 2005. http://www.emea.eu.int (accessed February 15, 2022).

[10] ICH Secretariat (1999) International Conference on Harmonization (ICH) guideline ICH Q6B: Specifications: Test Procedures and Acceptance Criteria for Biotechnological/Biological Products, 1999. http://www.emea.eu.int (accessed February 15, 2022).

[11] ICH Secretariat (2005) International Conference on Harmonization (ICH) guideline ICH Q2(R1): validation of analytical procedures: text and methodology., 2005.

[12] P. Bults, B. Spanov, O. Olaleye, N.C. van de Merbel, R. Bischoff, Intact protein bioanalysis by liquid chromatography – High-resolution mass spectrometry, J. Chromatogr. B Anal. Technol. Biomed Life Sci. (2019) 155–167, https://doi.org/10.1016/j.jchromb.2019.01.032.

[13] H. Zhou, Z. Ning, A.E. Starr, M. Abu-Farha, D. Figeys, Advancements in top-down proteomics, Anal. Chem. 84 (2012) 720–734, https://doi.org/10.1021/ac202882y.

[14] A. Goyon, V. D'Atri, B. Bobaly, E. Wagner-Rousset, A. Beck, S. Fekete, D. Guillarme, Protocols for the analytical characterization of therapeutic monoclonal antibodies. I – Non-denaturing chromatographic techniques, J. Chromatogr. B Anal. Technol. Biomed Life Sci. 1058 (2017) 73–84, https://doi.org/10.1016/j.jchromb.2017.05.010.

[15] V. D'Atri, A. Goyon, B. Bobaly, A. Beck, S. Fekete, D. Guillarme, Protocols for the analytical characterization of therapeutic monoclonal antibodies. III – Denaturing chromatographic techniques hyphenated to mass spectrometry, J. Chromatogr. B Anal. Technol. Biomed Life Sci. (2018) 95–106, https://doi.org/10.1016/j.jchromb.2018.08.013.

[16] J. Hernández-Jiménez, A. Salmerón-García, J. Cabeza, C. Vélez, L.F. Capitán-Vallvey, N. Navas, The effects of light-accelerated degradation on the aggregation of marketed therapeutic monoclonal antibodies evaluated by size-exclusion chromatography with diode array detection, J. Pharm. Sci. 105 (2016) 1405–1418,https://doi.org/10.1016/j.xphs.2016.01.012.

[17] M. Haberger, M. Leiss, A.K. Heidenreich, O. Pester, G. Hafenmair, M. Hook, L. Bonnington, H. Wegele, M. Haindl, D. Reusch, P. Bulau, Rapid characterization of biotherapeutic proteins by size-exclusion chromatography coupled to native mass spectrometry, MAbs. 8 (2016) 331–339, https://doi.org/10.1080/19420862.2015.1122150.

[18] J. Hermosilla, R. Sánchez-Martín, R. Pérez-Robles, A. Salmerón-García, S. Casares, J. Cabeza, L. Cuadros-Rodríguez, N. Navas, Comparative stability studies of different infliximab and biosimilar ct-p13 clinical solutions by combined use of physicochemical analytical techniques and enzyme-linked immunosorbent assay (ELISA), BioDrugs. 33 (2019) 193–205, https://doi.org/10.1007/s40259-019-00342-9.

[19] M. Tassi, J. De Vos, S. Chatterjee, F. Sobott, J. Bones, S. Eeltink, Advances in native high-performance liquid chromatography and intact mass spectrometry for the characterization of biopharmaceutical products, J. Sep. Sci. 41 (2018) 125–144, https://doi.org/10.1002/jssc.201700988.

[20] Y. Leblanc, C. Ramon, N. Bihoreau, G. Chevreux, Charge variants characterization of a monoclonal antibody by ion exchange chromatography coupled on-line to native mass spectrometry: Case study after a long-term storage at +5 ◦C, J. Chromatogr. B Anal. Technol. Biomed Life Sci. 1048 (2017) 130–139, https://doi.org/10.1016/j.jchromb.2017.02.017.

[21] F. Füssl, K. Cook, K. Scheffler, A. Farrell, S. Mittermayr, J. Bones, Charge variant analysis of monoclonal antibodies using direct coupled pH gradient cation exchange chromatography to high-resolution native mass spectrometry, Anal. Chem. 90 (2018) 4669–4676, https://doi.org/10.1021/acs.analchem.7b05241.

[22] Y. Yan, T. Xing, S. Wang, T.J. Daly, N. Li, Online coupling of analytical hydrophobic interaction chromatography with native mass spectrometry for the characterization of monoclonal antibodies and related products, J. Pharm. Biomed. Anal. 186 (2020), 113313, https://doi.org/10.1016/j.jpba.2020.113313.

[23] E. Farsang, D. Guillarme, J.L. Veuthey, A. Beck, M. Lauber, A. Schmudlach, S. Fekete, Coupling non-denaturing chromatography to mass spectrometry for the characterization of monoclonal antibodies and related products, J. Pharm. Biomed. Anal. 185 (2020), 113207, https://doi.org/10.1016/j.jpba.2020.113207.

[24] N. Navas, A. Herrera, A. Martínez-Ortega, A. Salmerón-García, J. Cabeza, L. Cuadros-Rodríguez, Quantification of an intact monoclonal antibody, rituximab, by (RP)HPLC/DAD in compliance with ICH guidelines, Anal. Bioanal. Chem. 405 (2013) 9351–9363, https://doi.org/10.1007/s00216-013-7368-1.

[25] A. Martínez-Ortega, A. Herrera, A. Salmerón-García, J. Cabeza, L. Cuadros-Rodríguez, N. Navas, Study and ICH validation of a reverse-phase liquid chromatographic method for the quantification of the intact monoclonal antibody cetuximab, J. Pharm. Anal. 6 (2016) 117–124, https://doi.org/10.1016/j.jpha.2015.11.007.

[26] A. Martínez-Ortega, A. Herrera, A. Salmerón-García, J. Cabeza, L. Cuadros-Rodríguez, N. Navas, Validated reverse phase HPLC diode array method for the quantification of intact bevacizumab, infliximab and trastuzumab for long-term stability study, Int. J. Biol. Macromol. 116 (2018) 993–1003, https://doi.org/10.1016/j.ijbiomac.2018.05.142.

[27] R. Pérez-Robles, L. Cuadros-Rodríguez, A. Salmerón-García, N. Navas, Development and validation of a (RP)UHPLC-UV-(HESI/Orbitrap)MS method for the identification and quantification of mixtures of intact therapeutical monoclonal antibodies using a monolithic column, J. Pharm. Biomed. Anal. 159 (2018) 437–448, https://doi.org/10.1016/j.jpba.2018.07.013.

[28] S. Fekete, D. Guillarme, Reversed-phase liquid chromatography for the analysis of therapeutic proteins and recombinant monoclonal antibodies, accessed December 2, 2020, LC GC Eur. 25 (2012) 540–550, https://www.chromatographyonline.com/view/reversed-phase-liquid-chromatography-analysis-therapeutic-proteins-and-recombinant-monoclonal-antibo.

[29] S. Fekete, S. Rudaz, J.L. Veuthey, D. Guillarme, Impact of mobile phase temperature on recovery and stability of monoclonal antibodies using recent reversed-phase stationary phases, J. Sep. Sci. 35 (2012) 3113–3123, https://doi.org/10.1002/jssc.201200297.

[30] W. Li, B. Yang, D. Zhou, J. Xu, W. Li, W.C. Suen, Identification and characterization of monoclonal antibody fragments cleaved at the complementarity determining region using orthogonal analytical methods, J. Chromatogr. B Anal. Technol. Biomed Life Sci. 1048 (2017) 121–129, https://doi.org/10.1016/j.jchromb.2017.02.019.

[31] S. Carillo, R. Pérez-Robles, C. Jakes, M. Ribeiro da Silva, S. Millán Martín, A. Farrell, N. Navas, J. Bones, Comparing different domains of analysis for the characterisation of N-glycans on monoclonal antibodies, J. Pharm. Anal. 10 (2020) 23–34, https://doi.org/10.1016/j.jpha.2019.11.008.

[32] A. Puszkiel, G. Noé, P. Boudou-Rouquette, C.-L. Cossec, J. Arrondeau, J.S. Giraud, A. Thomas-Schoemann, J. Alexandre, M. Vidal, F. Goldwasser, B. Blanchet, Development and validation of an ELISA method for the quantification of nivolumab in plasma from non-small-cell lung cancer patients, J. Pharm. Biomed. Anal. 139 (2017) 30–36, https://doi.org/10.1016/j.jpba.2017.02.041.

[33] E.A. Basak, A.J.M. Wijkhuijs, R.H.J. Mathijssen, S.L.W. Koolen, M.W.J. Schreurs, Development of an enzyme-linked immune sorbent assay to measure nivolumab and pembrolizumab serum concentrations, Ther. Drug Monit. 40 (2018) 596–601, https://doi.org/10.1097/FTD.0000000000000534.

[34] D. Pluim, W. Ros, M.T.J. van Bussel, D. Brandsma, J.H. Beijnen, J.H.M. Schellens, Enzyme linked immunosorbent assay for the quantification of nivolumab and pembrolizumab in human serum and cerebrospinal fluid, J. Pharm. Biomed. Anal. 164 (2019) 128–134, https://doi.org/10.1016/j.jpba.2018.10.025.

[35] K. Irie, A. Okada, Y. Yamasaki, C. Kokan, A. Hata, R. Kaji, K. Fukushima, N. Sugioka, Y. Okada, N. Katakami, S. Fukushima, An LC-MS/MS method for absolute quantification of nivolumab in human plasma: Application to clinical therapeutic drug monitoring, Ther. Drug Monit. 40 (2018) 716–724, https://doi.org/10.1097/FTD.0000000000000558.

[36] H.H. Chiu, H.W. Liao, Y.Y. Shao, Y.S. Lu, C.H. Lin, I.L. Tsai, C.H. Kuo, Development of a general method for quantifying IgG-based therapeutic monoclonal antibodies in human plasma using protein G purification coupled with a two internal standard calibration strategy using LC-MS/MS, Anal. Chim. Acta. 1019 (2018) 93–102, https://doi.org/10.1016/j.aca.2018.02.040.

[37] A. Millet, N. Khoudour, P. Bros, D. Lebert, G. Picard, C. Machon, F. Goldwasser, B. Blanchet, J. Guitton, Quantification of nivolumab in human plasma by LC-MS/HRMS and LC-MS/MS, comparison with ELISA, Talanta. (2020), 121889, https://doi.org/10.1016/j.talanta.2020.121889.

[38] Reviewer Guidance: Validation of Chromatographic Methods. Center for Drug Evaluation and Research, U.S. Food and Drug Administration (FDA)., 1994.

[39] M.W. Dong, HPLC and UHPLC for practicing scientists: Second edition, 2019. https://doi.org/10.1002/9781119313786.

[40] Nivolumab: Uses, Interactions, Mechanism of Action | DrugBank Online, (n.d.). https://go.drugbank.com/drugs/DB09035 (accessed February 7, 2022).

[41] T.M. Dillon, P.V. Bondarenko, D.S. Rehder, G.D. Pipes, G.R. Kleemann, M.S. Ricci, Optimization of a reversed-phase high-performance liquid chromatography/mass spectrometry method for characterizing recombinant antibody heterogeneity and stability, J. Chromatogr. A. 1120 (2006) 112–120, https://doi.org/10.1016/j.chroma.2006.01.016.

[42] J. Giorgetti, A. Beck, E. Leize-Wagner, Y.N. François, Combination of intact, middle-up and bottom-up levels to characterize 7 therapeutic monoclonal antibodies by capillary electrophoresis – Mass spectrometry, J. Pharm. Biomed. Anal. 182 (2020), 113107, https://doi.org/10.1016/j.jpba.2020.113107.

[43] J. Giorgetti, V. D'Atri, J. Canonge, A. Lechner, D. Guillarme, O. Colas, E. Wagner-Rousset, A. Beck, E. Leize-Wagner, Y.N. François, Monoclonal antibody Nglycosylation profiling using capillary electrophoresis – Mass spectrometry: Assessment and method validation, Talanta. 178 (2018) 530–537, https://doi.org/10.1016/j.talanta.2017.09.083.

[44] International Committee Harmonization, International Council for Harmonisation of Technical Requirements for Pharmaceuticals for Human Use. Final Concept Paper ICH Q14: Analytical Procedure Development and Revision of Q2(R1) Analytical Validation, 2018. http://www.ich.org (accessed February 7, 2022).

[45] B.A. Kerwin, R.L. Remmele, Protect from light: Photodegradation and protein biologics, J. Pharm. Sci. 96 (2007) 1468–1479, https://doi.org/10.1002/jps.20815.

CAPÍTULO 4

Comprehensive analysis of nivolumab, a therapeutic anti-PD-1 monoclonal antibody: impact of handling and stress

INTRODUCCIÓN AL CAPÍTULO 4

En el capítulo 4 se continua con los estudios analíticos del mAbs nivolumab, principio activo del medicamento Opdivo®, para llevar a cabo un análisis comprensivo del mismo. El objetivo principal de este estudio analítico fue evaluar el impacto de la manipulación hospitalaria sobre dicho medicamento y el riesgo asociado a la misma cuando hay acciones incorrectas involuntarias o cuando el medicamento se somete a condiciones estresantes no deseadas en hospitales. Con la finalidad de estudiar en profundidad las características fisicoquímicas y funcionales de nivolumab, se realizaron estudios de degradación forzada, los cuales simulan las condiciones extremas a las que el medicamento puede estar expuesto en hospitales. Para ello, muestras del medicamento Opdivo® fueron sometidas a: 40 °C durante 1 h, 60 °C durante 1 h, 1 ciclo de congelación/descongelación, 5 ciclos de congelación/descongelación, agitación a 300 rpm durante 24 h, exposición a la luz en una cámara de envejecimiento durante 24 h (ICH Q1B) y exposición a una alta concentración salina. La metodología aplicada se basó en el análisis de las muestras estresadas y comparación de los resultados con muestras control (no sometidas a degradación acelerada o estrés). Se emplearon diferentes metodologías analíticas desarrolladas *ad hoc* para analizar los diferentes CQAs fisicoquímicos, empleando diferentes técnicas analíticas: CD en el UV lejano para determinar la estructura secundaria de la proteína, IT-FS para analizar la estructura terciaria, DLS para el estudio del particulado, SE/UHPLC(UV)-[Native]MS para la determinación de oligómeros (mediante detección UV) y el perfil de isoformas (mediante detección por MS) (estrategia *top-down*); y se desarrolló y validó un método ELISA para el análisis de la actividad biológica (funcionalidad) mediante el estudio de la capacidad de unión de nivolumab con su diana terapéutica, el receptor PD-1. Los resultados indicaron que el estrés por luz fue el que mayor impacto tuvo sobre nivolumab, dado que condujo a la formación de dímeros no naturales y a una modificación del perfil de isoformas. Además, nivolumab mostró estabilidad hasta 60 °C (1 h). En cuanto a la funcionalidad, las muestras estresadas por luz y agitación fueron las que mostraron una mayor disminución de su capacidad de unión a PD-1, seguidas de las muestras sujetas a 5 ciclos de congelación/descongelación y fuerza iónica, mientras que el resto permanecieron estables. Como conclusiones de este trabajo se extrae que el medicamento Opdivo® debe ser manejado siempre protegido de la luz para evitar la degradación del mismo y prevenir, en la medida de lo posible, su agitación, con la finalidad de evitar una disminución de su actividad. De igual forma, se recomienda tener especial cuidado al preparar las diluciones de uso hospitalario de Opdivo® con NaCl, ya que una alta concentración de NaCl conlleva a modificaciones físicas

de la proteína. Y, por último, también se recomienda evitar la congelación del medicamento, dado que puede afectar a su capacidad de unión con su diana terapéutica.

SCIENTIFIC ARTICLE

Comprehensive Analysis of Nivolumab, A Therapeutic Anti-Pd-1 Monoclonal Antibody: Impact of Handling and Stress

Anabel Torrente-López[1], Jesús Hermosilla[1], Antonio Salmerón-García[2], José Cabeza[2] and Natalia Navas[1,*]

[1] Department of Analytical Chemistry, Science Faculty, Biohealth Research Institute (ibs.GRANADA), University of Granada, E-18071 Granada, Spain

[2] Department of Clinical Pharmacy, Biohealth Research Institute (ibs.GRANADA), San Cecilio University Hospital, E-18012 Granada, Spain

Pharmaceutics 14 (2022) 692

Accepted: 17 March 2022

DOI: 10.3390/pharmaceutics14040692

pharmaceutics

MDPI

Article

Comprehensive Analysis of Nivolumab, A Therapeutic Anti-Pd-1 Monoclonal Antibody: Impact of Handling and Stress

Anabel Torrente-López [1], Jesús Hermosilla [1], Antonio Salmerón-García [2], José Cabeza [2] and Natalia Navas [1,*]

[1] Department of Analytical Chemistry, Science Faculty, Biohealth Research Institute (ibs.GRANADA), University of Granada, E-18071 Granada, Spain; anabeltl@ugr.es (A.T.-L.); jesushf@ugr.es (J.H.)
[2] Department of Clinical Pharmacy, Biohealth Research Institute (ibs.GRANADA), San Cecilio University Hospital, E-18012 Granada, Spain; asalgar6@gmail.com (A.S.-G.); jose.cabeza.sspa@juntadeandalucia.es (J.C.)
* Correspondence: natalia@ugr.es; Tel.: +34-958-242-868; Fax: +34-958-243-328

Abstract

Nivolumab, formulated in the medicine Opdivo® (10 mg/mL), is a therapeutic monoclonal antibody (mAb) used in the treatment of different types of cancer. Currently, there is insufficient knowledge about the behaviour of this protein with regards to the risk associated with its routine handling or unintentional mishandling, or when subjected to stress conditions in hospitals. These conditions can be simulated in forced degradation studies, which provide an in-depth understanding of the biophysical and biochemical properties of mAbs. In this study, we carried out a physicochemical and functional characterisation of nivolumab, which was subjected to various stress conditions: heat, freeze/thaw cycles, agitation, light exposure and high hypertonic solution. We used a wide range of analytical techniques: Far-UV CD, IT-FS, DLS, SE/UHPLC(UV)-[Native]MS, and ELISA. The results show that exposure to light was the stress test with the greatest impact on the samples, revelling the formation of non-natural dimers and a different isoform profile. In addition, nivolumab (Opdivo®) demonstrated stability up to 60 °C (1 h). As regards functionality all the nivolumab (Opdivo®) stressed samples were found to be stable except for those subjected to light and agitation, and to a lesser extent, those subjected to FTC 5 and NaCl stresses.

Keywords

Nivolumab

Comprehensive analytical characterisation

Forced degradation

UHPLC-MS

Isoform profile

1. Introduction

Therapeutic monoclonal antibodies (mAbs) are a major class of biopharmaceuticals which have seen rapid growth in recent decades. They have an immunoglobulin (Ig) structure that is capable of specific binding to unique epitopes present in their target. As a consequence, mAbs have notably improved the treatment results for a wide variety of human-specific diseases such as cancer, autoimmune diseases, cardiovascular disorders, ophthalmic diseases, or asthma [1]. Most approved mAbs are selected from three human IgG isotypes (IgG1, IgG2, or IgG4), which are defined by the total number of disulphide bridges (16 for IgG1 and IgG4, and 18 for IgG2), disulphide bonds in the flexible hinge region (two for IgG1 and IgG4, and four for IgG2) and the different heavy-chain amino acid sequences. At present, the majority of mAbs that have been approved by the FDA and EMA are based on the IgG1 isotype, while IgG3-based therapeutics have received little attention for therapy development owing to their short half-life in the body, given that the clearance rate of IgG3 is significantly faster than that of other isotypes [2,3]. As for the IgG4 isotype, there has been a progressive increase in the number of IgG4-based therapeutics on the market and in clinical trials. This is thanks to the remarkable progress that biotechnological and pharmaceutical companies have made in developing more stabilised IgG4 formats, such as by introducing S228P point mutation in the core-hinge sequence of the mAb [2]. One of the therapeutic mAbs that is manufactured using hinge-stabilised engineering is nivolumab (Opdivo® from Bristol-Myers Squibb, Dublin, Ireland), a human IgG4 mAb, which binds to the programmed death-1 (PD-1) receptor and blocks its interaction with the ligands PD-L1 and PD-L2, according to the Summary of Product Characteristics for Opdivo® issued by the European Medicine Agency [4]. By blocking this pathway, nivolumab potentiates T-cell responses, including anti-tumour responses [5]. This is why this mAb is used, either by itself or in combination with another mAb, i.e., ipilimumab or cabozantinib, in cancer therapy. Opdivo® is indicated for the treatment of melanoma; non-small cell lung cancer (NSCLC); malignant pleural mesothelioma (MPM); renal cell carcinoma (RCC); and classical Hodgkin lymphoma (cHL), among other types of cancer. Nivolumab is produced in Chinese Hamster Ovary (CHO) cells using recombinant DNA technology and is presented as a concentrate for solution for infusion (sterile concentrate) at 10 mg/mL [4].

Like all mAbs, nivolumab consists of a large, highly complex molecule and is extremely sensitive to its environment [6]. Before administration to patients, mAbs may be subject to environmental stress conditions such as exposure to light, and mechanical or thermal stresses, among others [7,8]. These stresses can have a negative impact on the structure of the protein, leading to its chemical or physical degradation [9–12]. Routine handling prior to administration—e.g., for sample preparation—or inadvertent mishandling—e.g., incorrect storage—can expose mAbs to these environmental stress conditions, so giving rise to the

aforementioned forms of degradation [8]. These forms of degradation alter the quality of mAb-based products and can have a significant effect on their therapeutic efficacy, by limiting their bioactivity or increasing their immunogenicity [6,7]. One of the main concerns with therapeutic proteins is the increase of aggregation in clinical samples, a form of degradation that could modify the ability of the mAb to correctly interact with its specific target, and could lead to immunogenicity. Detecting degraded mAbs before administration to patients is therefore crucial for ensuring high quality, efficacy, and safety [7].

Forced degradation studies offer an opportunity to gain an in-depth understanding of the biophysical and biochemical properties of mAbs [13]. They can provide valuable information on the degradation pathways to which mAbs are exposed during handling in hospitals prior to administration. Usually, these studies involve subjecting a particular biopharmaceutical product to a range of relatively harsh experimental stress conditions for a short period of time. It is important to avoid applying both too much or too little stress. The information that forced degradation studies provide is very useful in support of real-time environmental conditions and when dealing with practical problems, such as when there is a break in the cold chain; when making pharmaceutical preparations prior to administration; or when deciding whether to use the surplus product from one treatment on another patient [13–16]. The forced degradation conditions employed in such studies typically include high temperature; freeze-thaw cycles; agitation; light; high ionic strength exposure, among others. These conditions are selected according to the probability that the medicine may be exposed to them during the different stages of handling these products in hospital. The most common degradation pathways are aggregation, fragmentation, deamidation and oxidation [13].

Forced degradation of nivolumab (Opdivo®)—as a representative example of an IgG4—[7] was conducted to evaluate the influence of degraded mAbs in a previously reported flow injection analysis (FIA) combined with UV spectroscopy and a statistical matching method [17] for the quality control of compounded mAbs in hospital. Surprisingly, when this FIA strategy was initially proposed, it was not validated by checking the specificity, although the method was proposed for mAb quantification. As a result, the stress study conducted later on nivolumab focused more on validating the FIA methodology applied in the hospital quality control process than on presenting a detailed study of the degradation of nivolumab. It did not assess, for example, the functionality of degraded nivolumab. Within the context of a long-term stability study, nivolumab was studied in its original vials after opening and handling in a normal saline bag for intravenous infusion [14]. Several physicochemical and functional properties of nivolumab were analysed. Although this research presented very valuable results, it did not focus on degradation studies, as its main objective was to study the stability of nivolumab over a period of more than 24 h, at different temperatures and after freeze/thaw cycles.

The aim of this research is therefore to carry out a comprehensive analytical characterisation and a forced degradation study of nivolumab (Opdivo® 10 mg/mL). For a proper characterisation of mAbs, complementary techniques must be used, including an appropriate set of physicochemical and functional tests. For this reason, we used a wide range of techniques to carry out this study, such as circular dichroism (CD) for the analysis of the secondary structure; fluorescence for the assessment of the tertiary structure; dynamic light scattering (DLS) to track particulate in the solutions; size-exclusion chromatography with UV detection (SE/UHPLC(UV)) to analyse oligomers; size-exclusion chromatography coupled to mass spectrometry (SE/UHPLC(UV)-MS(Orbitrap)) to determine the isoform profile including glycans; and an Enzyme-Linked Immunosorbent Assay (ELISA) to evaluate functionality by means of the specific bind nivolumab-PD1. To this end, forced degradation tests such as heating, freeze/thaw, agitation, light exposure and high ionic strength stresses were performed on samples of the medicine to evaluate degradation. These tests produced very interesting results that provide valuable new information about this biopharmaceutical, which could be useful for evaluating the potential consequences associated with its routine handling or unintentional mishandling in hospital.

2. Materials and Methods

2.1. Nivolumab Samples

Opdivo® vials (nivolumab 10 mg/mL, Bristol-Myers Squibb Pharma EEIG, Dublin, Ireland) were kindly supplied for this study by the Pharmacy Unit of the University Hospital “San Cecilio” (Granada, Spain). Hospital leftovers were used throughout the study and the analyses were performed immediately after opening the vial to ensure the stability indicated by the manufacturer [4]. The following batches were used during this study: ABJ9188; ABK3907; ABR9823; ABS8408; ABV0452; ABV2650; and ABW3154.

2.2. Forced Degradation (Stresses)

Forced degradation studies were carried out on the medicine Opdivo® by exposing the samples to each particular stress condition, always within the expiry date of the medicine once opened in order to avoid any degradation in nivolumab caused by the passage of time. Seven forced degradation conditions were tested: (i) exposure to a temperature of 40 °C for 1 h in a ThermoMixer® C thermoblock 1.5 mL (Eppendorf, Hamburg, Germany); (ii) exposure to a temperature of 60 °C for 1 h in a ThermoMixer® C thermoblock 1.5 mL (Eppendorf, Hamburg, Germany); (iii) one freeze–thaw cycle (room temperature of around 21/25 °C to – 20 °C) in a vertical Bosch freezer (GSE32420, Gerlingen, Germany); (iv) five freeze–thaw cycles (room temperature of around 21/25 °C to – 20 °C in a vertical Bosch freezer (GSE32420, Gerlingen,

Germany); (v) exposure to light irradiation (250 W/m2) for 24 h in an aging chamber (Solarbox 3000e RH, Cofomegra, Milan, Italy); (vi) agitation (300 rounds/min) for 24 h in a mechanical laboratory shaker (type 3006, Gesellschaft für Labortechnik, Burgwedel, Germany); and (vii) exposure to a hypertonic medium by diluting in 1.5 M NaCl at a final concentration of 2 mg/mL.

Control samples were used throughout the study (samples of the medicine Opdivo® 10 mg/mL not subjected to stress and analysed within the first 24 h after opening the medicine vial while ensuring no sample degradation). Both control samples and those subjected to stress were analysed at the concentration used in the medicine (10 mg/mL), in order to avoid alterations such as displacement of the aggregation equilibrium by dilution. In the CD study, the analysis required the dilution of the samples in reverse-osmosis-quality water (purified with a Milli-RO plus Milli-Q station from Merk Millipore, Darmstadt, Germany) at a concentration of 0.1 mg/mL to avoid detector saturation. The NaCl stressed sample and its corresponding control sample had to be analysed at 2 mg/mL since NaCl was added as a concentrated aqueous solution. All the stress tests were performed using 200 µL of the medicine (Opdivo® 10 mg/mL), except for the high ionic strength test, for which a smaller volume of medicine was used. This was because a certain volume of NaCl had to be added to the sample at the right concentration to prepare a final volume of 200 µL. The temperature stresses were performed in 1.5 mL Eppendorf tubes (Eppendorf, Hamburg, Germany); the FTCs, agitation and high ionic strength tests were carried out in 2 mL amber RAM vials with a 9 mm thread (Symta, Madrid, Spain); and the light stress was performed in 2 mL clear RAM vials with a 9 mm thread (Symta, Madrid, Spain).

2.3. Physicochemical Analytical Methods

2.3.1. Visual Inspections

A quick visual inspection was carried out each day, prior to experimentation, in order to check for evidence of formation of large aggregates, turbidity, suspended particles, colour changes, and gas formation. This inspection was conducted using the naked eye and carried out by three different analysts.

2.3.2. Far Ultraviolet (UV) Circular Dichroism (CD) Spectroscopy

CD spectroscopy in the far region was used to study conformational changes in the nivolumab's secondary structure over time. The experimental conditions were the same as those used in [18]. Opdivo® spectra were recorded using a JASCO J-815 spectropolarimeter (JASCO, Tokyo, Japan) equipped with a Peltier system for temperature control. Temperature was set at 20 °C for all measurements. The concentration of the solution samples to be analysed was optimized to 0.1 mg/mL of nivolumab. Spectra were acquired from 250 to 190 nm every 0.2 nm with a scan speed of 20 nm/min. The CD spectrum of NaCl stressed samples

was acquired from 250 to 200 nm due to the fact that the high salt concentration increased the voltage to over 700 V at a wavelength of less than 200 nm, and the voltage should be less than 700 V to obtain reliable data [19]. A total of five accumulations were averaged, with a bandwidth of 1 nm. A quartz cuvette with a path length of 1 mm was used. The first sample to be measured was the blank. The results for the blank were subtracted from all the samples so as to eliminate any possible interferences. Spectra Analysis software was used to apply the Means-Movement Smoothing to all the spectra. To determine the secondary structures, we used the Dichroweb website [20] and the most suitable algorithm and DataSet were CONTIN [21] and SP175 protein [22], respectively. A control sample was also subjected to a temperature ramp from 20 °C to 90 °C.

2.3.3. Intrinsic Tryptophan Fluorescence Spectroscopy (IT-FS)

Conformational changes in the tertiary structure of nivolumab can take place even if the secondary structure remains unchanged. When the tertiary structure undergoes conformational changes, some hydrophobic pockets can be exposed to the solvent, which encourages the formation of aggregates. A Cary Eclipse spectrofluorometer (Agilent, Santa Clara, CA, USA) equipped with a Peltier system for temperature control was used to carry out IT-F measurements. The experimental conditions were similar to those used in [18]. Emission spectra were recorded from 300 to 400 nm and the excitation wavelength was set at 298 nm. The samples were analysed at 10 mg/mL and the temperature was set at 20 °C. Excitation and emission slits were set to 2.5 nm and 5 nm, respectively. A total of five spectral accumulations were recorded for all measurements and the scan speed was set at 600 nm/min. The spectral centre of mass (C.M.) was considered as a mathematical representation of each spectrum, and was calculated using the following equation:

$$C.M.=\frac{\sum_i^n(\lambda i f i)}{\sum_i^n f i}$$

in which λi is the wavelength and fi the fluorescence intensity.

2.3.4. Dynamic Light Scattering (DLS)

A Zetasizer Nano-ZS90 Malvern (Malvern Instruments Ltd. Worcestershire, UK) was used to assess soluble particulates (from 1 to 10,000 nm) in Opdivo® (10 mg/mL nivolumab) samples. The experimental conditions were similar to those used in [18]. A 1 cm spectrophotometry disposable cuvette was used to obtain the measurements. The temperature was set at 20 °C. A minimum of 100 reads were recorded per measurement and the acquisition time was 5 s per read. The average hydrodynamic diameter (HD), polydispersity index (PDI), polydispersity (Pd, %) and volume size distribution of all the samples were studied.

2.3.5. Isoform Analysis by Size-Exclusion Ultra-High-Performance Liquid Chromatography (UHPLC) with UV-Visible Detection Coupled to (Native) Mass Spectrometry (SE/UHPLC-UV-[Native] MS) Using Volatile Salts

The analysis was performed by liquid chromatography using a Dionex UltiMate 3000 chromatograph (Thermo Scientific,Waltham, MA, USA), equipped with two ternary bombs; a degasser; an autosampler; a thermostatic column compartment; and a multiple wavelength detector (MWD-3000 Vis-UV detector). The chromatograph was coupled inline to a Q Exactive™ Plus Hybrid Quadrupole Orbitrap mass spectrometer (Thermo Scientific). The ionisation was performed using a heated electrospray ionisation (HESI) source. Chromatographic and MS conditions were similar to those used in [23]. A SEC columna 300 A, 2.7 µm, 4.6 × 300 mm (AdvanceBioSec, Agilent technologies, Santa Clara, CA, USA) was used and 8 µg of Opdivo® was injected into the column. The column temperature was set at 30 °C. This analysis was carried out under isocratic conditions of 100 mM ammonium acetate buffer (LC-MS purity grade, Sigma Aldrich, Madrid, Spain) prepared in reverse osmosis-quality water, at 0.3 mL/min for 20 min. The UV chromatograms were registered at different wavelengths, i.e., µ= 214 nm, µ = 220 nm and µ = 280 nm, using a bandwidth of 5 nm in all cases. The MS method was carried out in full positive polarity mode at a resolution of 17,500 (defined at m/z 200). The mass range was set at 2500–6000 m/z and the automatic gain control (AGC) target value was 3.0×10^6 with a maximum injection time of 200 ms and 10 microscans. In-source collision-induced dissociation (CID) was set to 100 eV. The MS instrumental parameters were set as follows: the sheath gas flow rate was 20 arbitrary units (AU); auxiliary gas flow rate was 5 AU; spray voltage was 3.6 kV; capillary temperature was 275 °C; probe heater temperature was 275 °C; and S-lens RF voltage was 100 V.

Native isoforms of the medicine and stressed samples were obtained by mass spectra deconvolution using BioPharma Finder™ software version 3.1 (Thermo Scientific) with ReSpect algorithms.

2.3.6. Aggregation Study by Size-Exclusion Ultra-High-Performance Liquid Chromatography (UHPLC) with UV-Visible Detection (SE/UHPLC-UV) Using Non-Volatile Salts

The aggregation study was conducted by liquid chromatography using the chromatograph (Dionex UltiMate 3000 chromatograph, Thermo Scientific) and SEC column (300 A, 2.7 µm, 4.6 × 300mm, AdvanceBioSec) described above. In this particular analysis, the chromatograph was used separately from the Q Exactive™ Plus Hybrid Quadrupole Orbitrap mass spectrometer. Therefore, the mobile phase was composed of non-volatile salts: 150 mM of phosphate buffer pH 7.0, which was prepared with monohydrate monobasic sodium phosphate (Panreac, Barcelona, Spain) and anhydrous disodium hydrogen phosphate (Panreac, Barcelona, Spain) in reverse-osmosis-quality water. The analysis was performed

under isocratic conditions for 18 min. The column temperature was set at 30 °C and 8 µg of sample (Opdivo®) were injected into the column at 0.3 mL/min. The UV chromatograms were registered at 214 nm, 220 nm and 280 nm, using a bandwidth of 5 nm in all cases.

The SEC column was calibrated to establish the relationship between the molecular weight and the retention time of nivolumab. The calibration kit (Agilent, Santa Clara, CA, USA) was composed of five proteins: thyroglobulin (670 kDa), ɣ-globulin (150 kDa), ovalbumin (45 kDa), myoglobin (17 kDa) and angiotensin II (1 kDa), although this last protein was not used in the calibration of the SEC column, due to its low molecular weight (M.W.). The experimental size exclusion column calibration model is M.W. = $1 \times 10^{8} e^{-0.828x}$; $R^2 = 0.9989$.

2.4. Functional-Based Method: Enzyme-Linked Immunosorbent Assay (ELISA)

In order to test the biological activity of nivolumab, we developed and optimised a new indirect, non-competitive ELISA method on the basis of the available bibliography [24–26] and of our previous research into other therapeutic mAbs [18,27,28]. The optimised method was as follows: firstly, 96-well Maxisorp immune plates were sensitised by adding 100 µL/well of 0.5 µg/mL Human PD-1 (CD279), FC Fusion (Sigma Aldrich, Madrid, Spain) diluted in 0.1Mcarbonate buffer solution pH 9.6 (prepared with sodium carbonate (Panreac, Spain) and sodium bicarbonate (Panreac, Spain)) and incubated overnight (18 h) at 4 °C. The plates were manually washed four times with 200 L/well of PBS-Tween 20 pH 7.4 containing 0.3% (v/v) Tween 20®. PBS was prepared using sodium chloride, potassium chloride, disodium phosphate monohydrate and potassium phosphate monobasic supplied by Panreac (Barcelona, Spain), while Tween 20 was supplied by Guinama (Valencia, Spain). The plates were then treated with 200 µL/well of the blocking buffer (PBS-Tween 20 pH 7.4 containing skimmed milk 2% (w/v)) for 2 h at 37 °C to eliminate nonspecific absorptions. After that they were washed four more times and filled with a 100 µL/well of nivolumab appropriately diluted in 0.1 M carbonate buffer (pH 9.6) at three concentrations: 5 ng/mL, 10 ng/mL and 25 ng/mL. The plates were incubated at 37 °C for 45 min in a universal digitronic precision oven P Selecta® (J.P. Selecta, s.a. Abrera, Barcelona, Spain), after which they were washed four times with PBS-Tween 20 and incubated again with 100 L/well of 1:1000 in PBS diluted anti-human IgG4-HRP (mouse anti-human IgG4 Fc antibody-HRP conjugate, Thermo Fisher, Landsmeer, the Netherlands) for 30 min at 37 °C. After being washed for four times, 100 L/well of the substrate solution (O-Phenylenediamine Dihydrochloride (OPD), Sigma Aldrich, Madrid, Spain) were added and incubated for 20 min at room temperature (around 25 °C) in darkness. Finally, 50 µL/well of 1M sulfuric acid solution was added to stop the reaction. Absorbance was recorded at 450 nm and 620 nm, and the analytical signal was the difference between the two absorbance values (NanoQuant Infinite 200 Pro, Tecan, Austria, GMBH).

This ELISA format allowed us to assess the specific interaction between nivolumab and its target, the PD-1 receptor. In this way, we were able to evaluate and quantify the biological activity of nivolumab after applying the stress factors indicated previously. To this end, the method was validated in terms of the calibration model, precision and accuracy.

The next stage was to investigate the standard calibration model using standard samples of nivolumab. In this case, fresh samples of the medicine Opdivo® (10 mg/mL nivolumab) were used as the standard due to the lack of any proper standard samples of nivolumab. The nivolumab concentrations checked to obtain the calibration model were 100, 50, 25, 10, 5, 1, and 0.5 ng/mL diluted in 0.1Mcarbonate buffer (pH 9.6). Each standard concentration was prepared and analysed in quintuplicate. From the graphical distribution results (absorbance vs. ng/mL nivolumab), the selected optimum concentrations for analysing nivolumab were 25, 10 and 5 ng/mL, as the corresponding response values were widely distributed within the permitted absorbance range, i.e., from 0 to 1. The Statgraphics Centurion 18 (Statgraphics Technologies, The Plains, VA, USA) software package was used for the statistical analysis of the calibration models. The coefficient of determination (R^2) and the lack-of-fit signification test were used to evaluate the best fit of these data to the different mathematical models. Once these concentrations were selected as representative of the calibration model, the precision and the accuracy of this ELISA method were evaluated according to the ICH recommendations Q2(R1) at these three concentrations [29]. The precision was checked as repeatability (intraday precision) and intermediate precision (interday precision; over three consecutive days). For the repeatability study, nine standard solutions were prepared within the same day and under the same experimental conditions: 3 samples at 5 ng/mL, 3 samples at 10 ng/mL and 3 samples at 25 ng/mL. Intermediate precision was assessed by analysing three standard solutions (5, 10 and 25 ng/mL of nivolumab) that were freshly prepared on three different days and under the same experimental conditions. Both repeatability and intermediate precision were determined as the relative standard deviation (RSD, %) of the concentrations calculated from the absorbance using the standard calibration curve. Accuracy was assessed by analysing three standard solutions of each concentration of nivolumab and determining the mean recovery percentage (R, %) for each concentration.

The functional study of the stressed samples was performed by simultaneously analysing control (fresh) and stressed nivolumab samples (both from Opdivo®) using the validated ELISA method. The results were then statistically compared (Student's t analysis with 95 % of confidence) to find out whether the ability of nivolumab to specifically bind to its target, the PD-1, had been altered in any way. To this end, the biological activity of each of the

stressed samples was compared with that of the control sample. The reported biological activity was the average of three replicates.

3. Results

3.1. Visual Inspections

All the samples remained clear after the different stress conditions considered in this study had been applied. This means that no precipitates or particulate matter could be detected with the naked eye, even in the samples exposed to 60 °C for one hour.

3.2. Far Ultraviolet (UV) Circular Dichroism (CD) Spectroscopy

The characteristic Far UV spectra of the nivolumab control and stressed samples are shown in Figure 1. The CD spectrum of the control sample was characterised by the wavelength of 209.7 ± 0.1 nm with ellipticity = 0, by the wavelength of the minimum at 218.0 ± 0.4 nm and by a shoulder at 228.7 ± 0.1 nm. As regards the stressed samples, the three aforementioned checkpoints were monitored in order to detect any changes in the secondary structures of nivolumab. The results obtained (Table 1) show that the characteristic wavelengths in the stressed samples remained unchanged with respect to the control sample, so indicating that the various stress tests we performed did not cause any changes in the secondary structure of nivolumab.

As expected, the secondary structure content showed a majority of β strands and random coil conformation after mathematical deconvolution of the CD spectra (Table 2). There were no significant changes when the stressed samples were compared to the control sample, as might be expected given the results of the CD spectra analysis. We were unable to assess the secondary structure content of the sample exposed to high ionic strength, because the high NaCl content of the solution meant that we had to record the spectra from 200 nm to 250 nm, an insufficient wavelength range for analysis by the selected algorithm and the protein dataset.

We also carried out a temperature ramp to check the thermal stability of nivolumab (0.1 mg/mL). The selected temperature range was from 20 °C (ambient conditions) to 90 °C (high stress conditions). The results indicated that the CD spectra remained unaltered up to 60 °C (Figure S1), so maintaining the values of the characteristic CD spectral parameters indicated above. By contrast, temperatures of over 60 °C caused significant spectral changes. On the basis of the results of the temperature ramp, we were able to select the most appropriate temperatures to carry out the thermal stress test. We therefore decided to subject nivolumab

to 40 °C, an easily reachable temperature in the summer in Spain, and 60 °C, the maximum temperature at which nivolumab remains unaltered, at least in terms of its secondary structure.

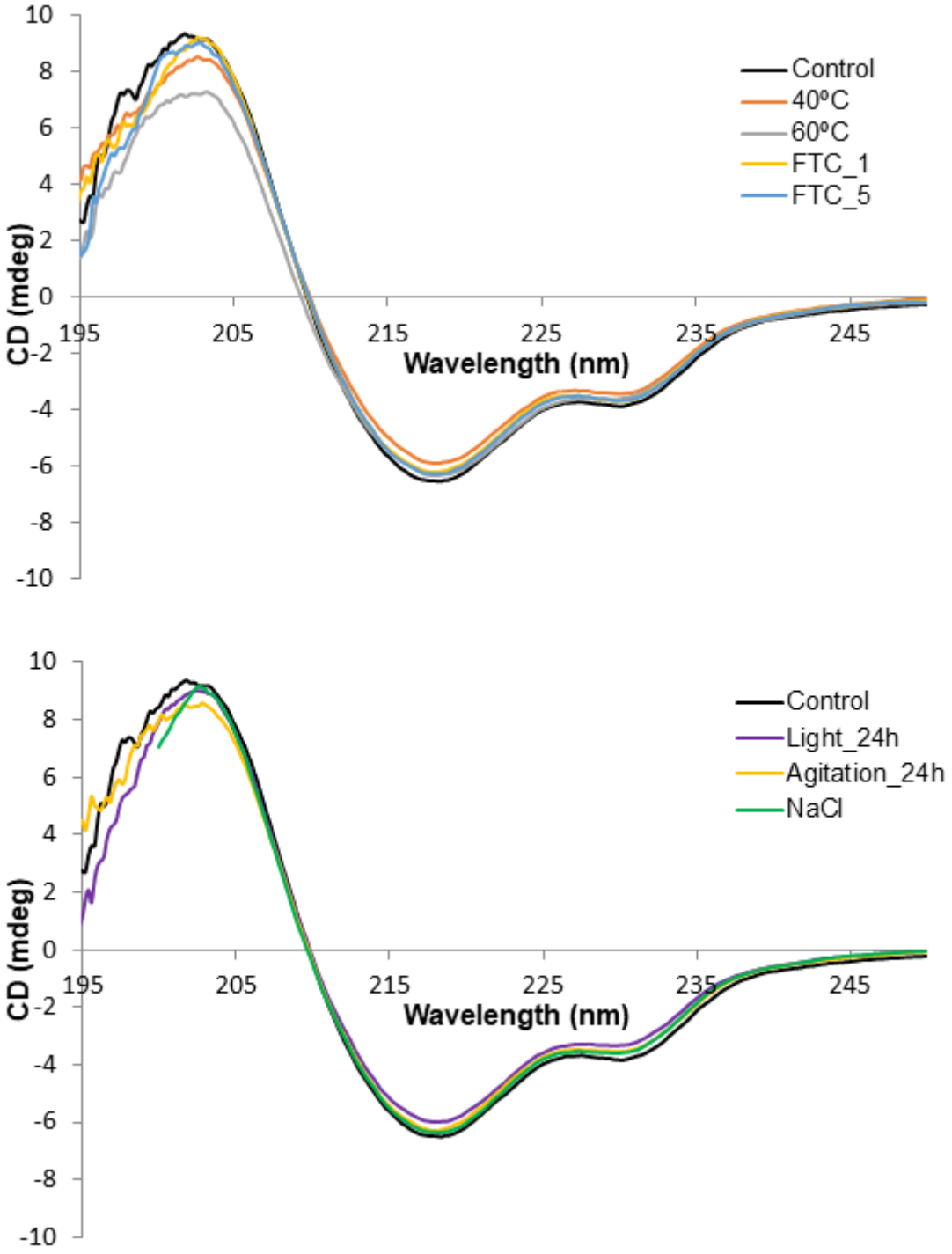

Figure 1. Far-UV CD spectra of all the stressed samples of nivolumab as compared with a control sample (black line).

Table 1. Secondary structures of nivolumab samples tracked by changes in the Far UV CD spectra.

Stress	Wavelength (nm) (Ellipticity = 0)	Minimum (nm)	Broad shoulder (nm)
Control	209.7 ± 0.1	218.0 ± 0.4	228.7 ± 0.1
40 ºC 1h	210	218.2	228.8
60 ºC 1h	209.4	218.2	228.6
FTC 1	209.8	217.8	228.8
FTC 5	209.9	218.2	228.4
Agitation 24h	209.8	217.8	228.4
Light stress 24h	209.8	218.2	228.8
NaCl	209.6	218.2	228.4

Table 2. Percentage estimation of the different secondary structures by Dichroweb from the Far UV CD spectra.

Stress	Helix 1	Helix 2	Strand 1	Strand 2	Turns	Unordered
Control	0	4.8	30.8	14.1	10.1	40.1
40 ºC 1h	0.1	4.8	31.6	14.2	10.2	39.1
60 ºC 1h	0	4.9	31.1	14.5	10.4	39.2
FTC 1	0	4.3	31.3	13.9	10.8	39.8
FTC 5	0.1	4.7	32.5	14.6	10.2	37.9
Agitation 24h	0	4.7	32.5	14.7	9.9	38.1
Light stress 24h	0.1	4.8	32.8	14.9	9.9	37.5
NaCl	-	-	-	-	-	-

3.3. IT-FS

Figure 2 shows the fluorescence spectra for the control and stressed samples of nivolumab. Most of the spectra are very similar in terms of both shape and intensity. The only spectrum to show different intensity was the one obtained after exposing the nivolumab sample to light, which showed decreasing intensity due to a decrease in the fluorescence signal of the tryptophan residues of nivolumab. This is probably due to degradation, as light stress is a well-known oxidising agent [30]. Tryptophan residues may be oxidised, so decreasing the intensity

of the IT-FS spectrum. This degradation could lead to differences in long-term stability, bioactivity and immunogenicity [31].

The spectra were used to calculate the C.M. value, a number used to characterise each sample in order to be able to detect any slight modifications in the tertiary structure of nivolumab more effectively. Slight modifications in the C.M. value with respect to the control samples indicate conformational changes in the spatial arrangement of the tryptophan residues; a shift to lower values indicates that the tryptophan residues are buried deep within the core of the protein, which has a more hydrophobic environment, while a shift to higher C.M. values indicates that the tryptophan residues are more exposed to the solvent, and therefore that the structure of the protein has unfolded to some extent [32]. Table 3 shows the C.M. values for the fluorescence spectra of control and stressed samples. No modifications were detected in the C.M values of the stressed samples as compared to the control. This indicates that the stress conditions tested using this technique did not cause any conformational changes in the tertiary structure of the protein.

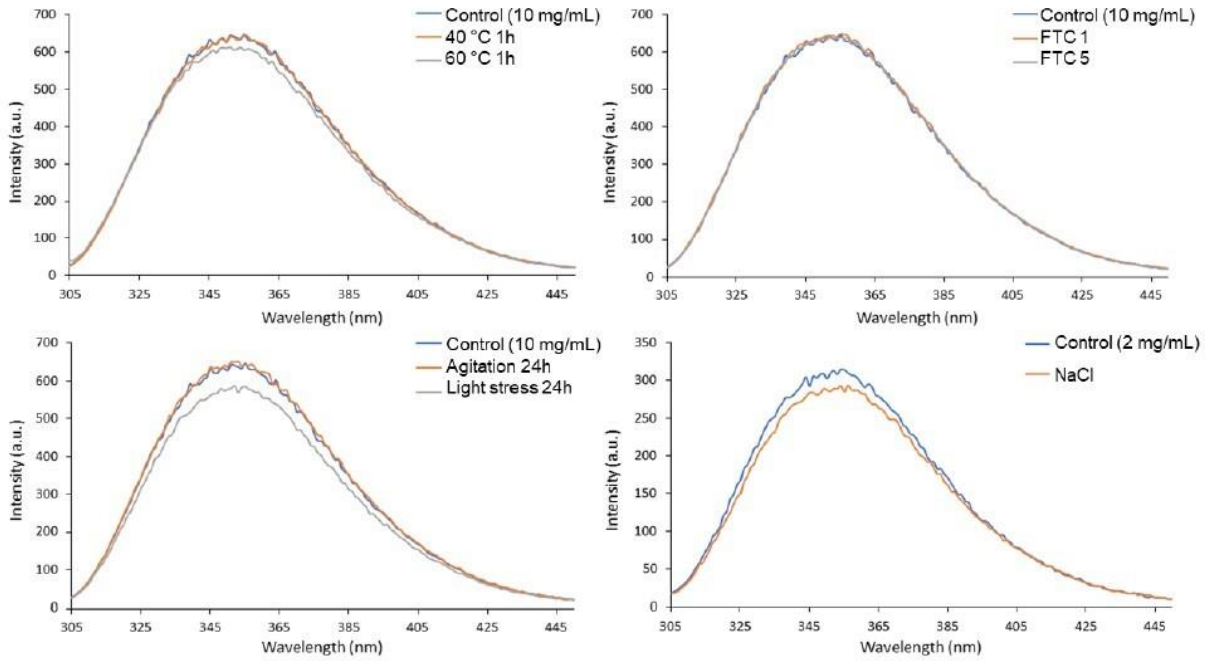

Figure 2. Nivolumab stress studies by IT-FS.

Table 3. Nivolumab tertiary structure assessed using the C.M. of the IT-FS spectrum.

Sample	Stress	Centre of Spectral Mass (C.M.) (Fluorescence Spectrum)
10 mg/mL	Control	361
	40 ºC 1 h	361
	60 ºC 1 h	361
	FTC 1	361
	FTC 5	361
	Agitation 24 h	361
	Light stress 24 h	361
2 mg/mL	Control	361
	NaCl	361

3.4. *DLS*

DLS results are shown in Table 4. Particulate size distributions by volume in the nivolumab (Opdivo®, 10 mg/mL) medicine and stressed samples are shown in Figure 3. Control samples (Opdivo®, 10 mg/mL nivolumab) showed a single population of particles attributed to the monomers of nivolumab with a hydrodynamic diameter (HD) of 9.7 × 3.2 nm and 9.3 × 3.2 nm for control 1 and control 2, respectively (two control samples were considered as the analyses were performed on different days). All the stressed samples remained unaltered, with no new particulate population detected up to 10 µm diameter size. All the samples had monomer populations of similar size, except for the one exposed to high temperature (60 °C, 1 h), which showed a slight increase in the HD. This could be attributed to increased hydration of the nivolumab monomers at this temperature, which was close to the temperature at which the secondary structure of nivolumab begins to degrade (as demonstrated above in the temperature ramp).

Table 4. Average hydrodynamic diameter (HD), polydispersity index (PDI) and polydispersity (%, Pd) of nivolumab sample solutions. Results that are different from the control appear in **bold**.

Sample	Stress	HD (nm)	PDI	Pd (%)
10 mg/mL	Control 1	9.7 ± 3.2	0.21	11.7
	40 ºC 1h	10.0 ± 3.1	0.22	9.5
	60 ºC 1h	**11.7 ± 5.8**	**0.32**	**60.7**
10 mg/mL	Control 2	9.3 ± 3.2	0.13	12.4
	FTC 1	9.1 ± 2.8	0.09	9.4
	FTC 5	9.4 ± 3.4	0.15	14.4
	Agitation 24h	9.8 ± 2.8	0.07	7.8
	Light stress 24h	9.4 ± 3.3	0.13	13.3
2 mg/mL	Control	9.4 ± 2.6	0.29	7.4
	NaCl	**13.9 ± 3.8**	**0.35**	6.9

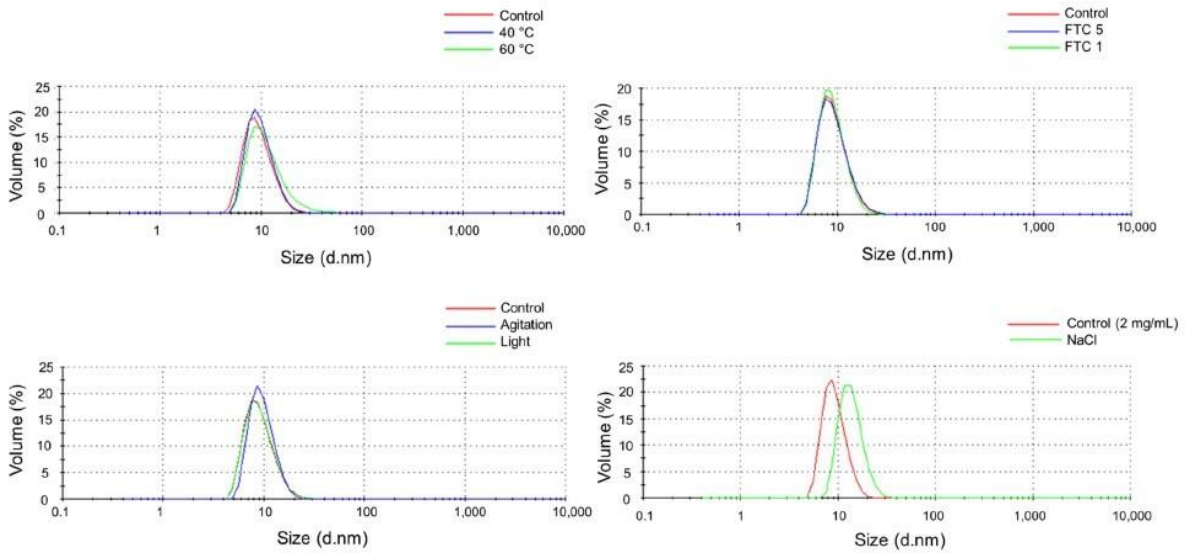

Figure 3. Particulate size distributions by volume in control and stressed samples of nivolumab.

The dilution required to subject nivolumab (Opdivo®, 10 mg/mL) to the stress of NaCl media (2 mg/mL) did not affect the single monomers' population detected in the medicine. The control sample prepared by diluting the medicine with water showed a single population with a HD of 9.4 ± 2.6 nm, which indicates that the HD was unaffected. In the nivolumab sample stressed with NaCl the HD increased to 13.9 ± 3.8 nm, which indicates that nivolumab may be slightly affected by exposure to a high ionic strength medium, and the electrostatic interaction between the surface of nivolumab and the electrolyte ions expands the volume of the protein.

This may be due to an increase in hydration on the surface of the protein, a result that coincides with the findings of previous research on mAbs [18].

We also assessed the polydispersity index (PDI) for each sample in order to corroborate that there was just one particulate population (i.e., monomers) in all the samples of nivolumab. PDI is a dimensionless parameter, which is scaled from 0 to 1, but is almost always greater than 0.05, which indicates highly monodisperse standards. It is generally accepted that a sample is highly monodisperse when the PDI value is ≤ 0.1 and moderately polydisperse when its value is between 0.1 and 0.4. Values above 0.7 indicate that the sample is probably not suitable for studying with the DLS technique as it has a very broad size distribution. As expected, given the standard deviation (SD) values for the HD, the PDI was around 0.1 and 0.2 for the majority of the samples, which confirmed that the solutions were moderately polydisperse. The samples exposed to 60 °C and NaCl showed a PDI of 0.32 and 0.35, respectively. These values indicate a higher degree of polydispersity, as also indicated by the SD values (5.8 and 3.8, respectively) of the HD in these samples.

The polydispersity (%, Pd) of the single population was calculated for each sample using the following equation:

$$Pd = \frac{(St.Dev)^2}{(Size)^2} * 100$$

where St.Dev is the SD (nm) of the population and Size (nm) is the mean size of the population. The Pd (%) measures the width of the assumed distribution. In terms of protein analysis, a Pd ≤ 20% indicates that the sample is monodisperse. In the DLS study, the results obtained by intensity were used to calculate the Pd (%) of each nivolumab sample (Table 4). All samples showed a polydispersity of less than 20%, except for the one subjected to the 60 °C stress test (60.7%). This indicates that this sample is polydisperse, as might be expected from the SD of the monomer population.

3.5. Isoform Analysis by SE/UHPLC(UV)-[Native]MS

The LC-MS method was used to identify the particular isoform profile of fresh and stressed nivolumab samples [23]. The use of volatile salts in the mobile phase (low ionic strength) was essential to enable the chromatographic system to be coupled directly to the mass detector. The nivolumab mass spectra profile was characterised under native conditions for all the samples. Nivolumab control samples showed three main isoforms, i.e., 146,215.4 (the most intense), 146,374.6 and 146,543.6 Da (the least intense). The first was assigned to the A2G0F/A2G0F glycoform, the second was assigned to the A2G0F/A2G1F and the third was assigned to the A2G1F/A2G1F (Figure 4a). These principal glycoforms were also identified in a parallel study of intact nivolumab under denatured conditions (manuscript in

preparation). This means that the main nivolumab isoforms have now been identified under both native and denatured LC-MS, so giving additional support to these findings.

Most of the isoform profiles for the stressed samples remained unchanged when compared to the control sample (Figure 4). The three main isoforms proposed for nivolumab in the control sample were exactly the same as those proposed in the stressed samples, so indicating that there were no significant chemical modifications in the main isoforms (Table 5). The only exception were the samples subjected to accelerated light degradation. In this case, in addition to the reduction in the number of isoforms detected, these isoforms had different masses (see Figure 4g), so indicating degradation of the protein. It is important to note that no isoform profile was obtained for the NaCl stress test. This was because the mass detector was unable to analyse the protein due to the excessive amount of salt used in this test. The N-glycan profiles for the control and stressed samples of nivolumab are presented in Table 5.

3.6. Aggregation Study by SE/UHPLC(UV)

Aggregation is one of the main indicators of protein degradation. In order to obtain the aggregates' profile of nivolumab, fresh and stressed samples were analysed by SE/UHPLC(UV) and their chromatographic profiles were compared in order to detect changes. The SE chromatogram for the control sample of nivolumab (fresh medicine 10 mg/mL) and the experimental size exclusion column calibration model are shown in Figures S2 and S3, respectively. In the SEC aggregation profile for the control sample, an important peak can be observed at 8.70 ± 0.01 min (99.6 ± 0.06% of the total area), which was assigned to nivolumab monomers. Just before the main peak there is a small peak eluting at 7.84 ± 0.02 min (0.4 ± 0.06% of the total area), which was assigned to the natural dimers present in the medicine. Assignment of the peaks was based on the indications of the specific chromatographic column and on the calibration of the column, performed using a commercial protein standard kit.

As regards the forced degradation study, Figure 5 shows the SE chromatograms resulting from the different stresses to which the nivolumab samples were exposed. The retention times and proportions of the peaks detected in their chromatographic profiles are presented in Table 6. No changes were detected in the SEC profile of the stressed samples of nivolumab and the relative proportions of monomers and dimers remained constant, except in the samples exposed to light (24 h) in which the dimers' peak was proportionally bigger. It was estimated that exposure to light stress caused 3% of the monomers to be transformed into dimers in 24 h (Table 6).

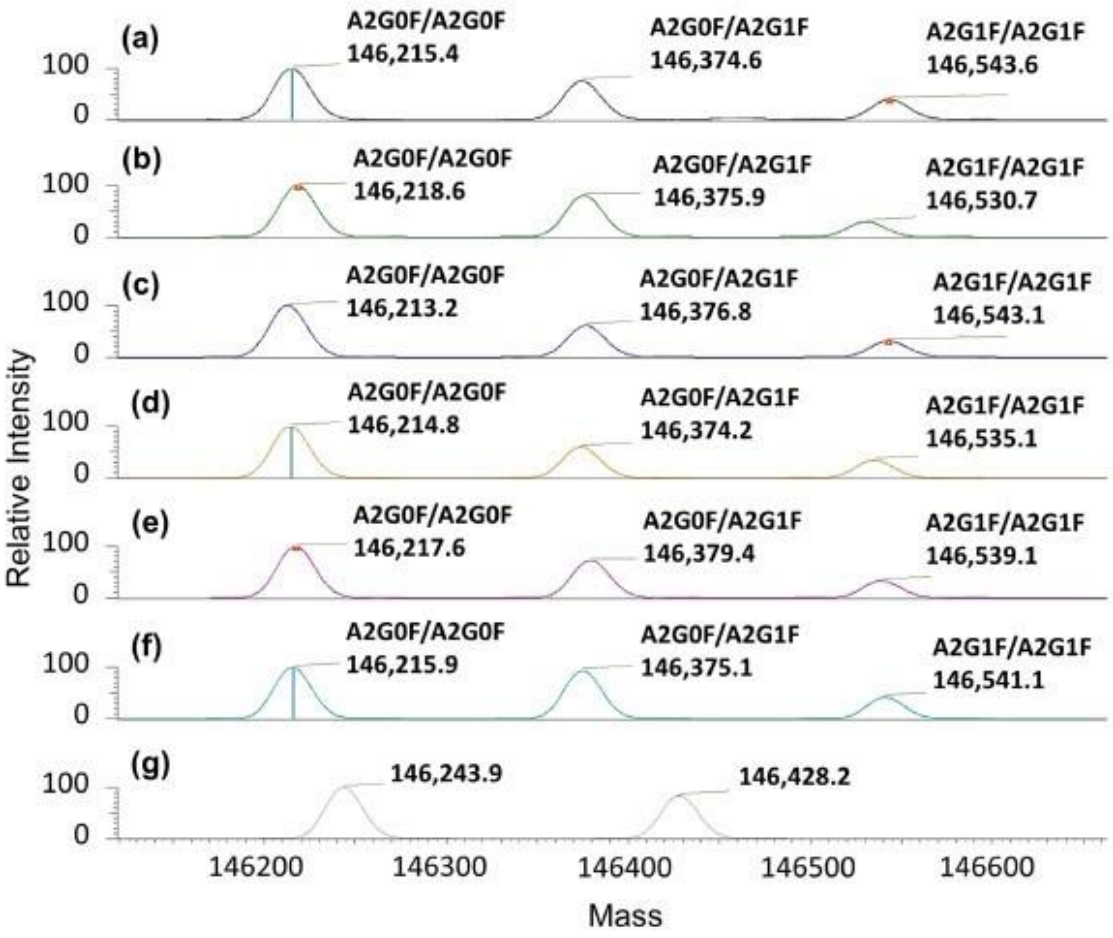

Figure 4. Deconvoluted mass spectra for nivolumab samples (10 mg/mL) showing the mass isoform profile with their proposed N-glycoforms: (a) fresh/control sample; (b) 40 °C/1 h exposure stress; (c) 60 °C/1 h exposure stress; (d) FTC 1; (e) FTC 5; (f) agitation stress; and (g) light stress.

Table 5. Experimental masses for intact nivolumab in native conditions for control and stressed samples. The relative abundances of N-glycoforms are also reported. Theoretical masses were calculated considering two C-term lysine clipping, two N-term pyroglutamate formation and 16 disulphide bonds.

	Glycoforms Associated	Experimental Mass (Da)	Theoretical Average Mass (Da)	Mass Difference (Da)	Mass Difference (ppm)	Relative Abundance (%)
Control	A2G0F/A2G0F	146,215.4	146,220.2	4.8	32.5	49.8
	A2G0F/A2G1F	146,374.6	146,382.3	7.7	52.3	36.7
	A2G1F/A2G1F	146,543.6	146,544.4	0.8	5.5	13.4
40 °C, 1 h	A2G0F/A2G0F	146,218.6	146,220.2	1.6	10.6	43.7
	A2G0F/A2G1F	146,375.9	146,382.3	6.4	43.7	40.1
	A2G1F/A2G1F	146,530.7	146,544.4	13.7	93.8	16.2
60 °C, 1 h	A2G0F/A2G0F	146,213.2	146,220.2	6.9	47.4	50.7
	A2G0F/A2G1F	146,376.8	146,382.3	5.5	37.4	33.6
	A2G1F/A2G1F	146,543.1	146,544.4	1.3	9.1	15.8
FTC 1	A2G0F/A2G0F	146,214,.8	146,220.2	5.4	37.0	51.0
	A2G0F/A2G1F	146,374.2	146,382.3	8.1	55.4	30.5
	A2G1F/A2G1F	146,535.1	146,544.4	9.4	63.8	18.4
FTC 5	A2G0F/A2G0F	146,217.6	146,220.2	2.6	17.8	49.9
	A2G0F/A2G1F	146,379.4	146,382.3	2.9	19.7	33.8
	A2G1F/A2G1F	146,539.1	146,544.4	5.3	36.2	16.4
Agitation 24 h	A2G0F/A2G0F	146,215.9	146,220.2	4.3	29.3	50.5
	A2G0F/A2G1F	146,375.1	146,382.3	7.2	49.3	31.0
	A2G1F/A2G1F	146,541.1	146,544.4	3.3	22.6	18.5
Light 24 h	Not identified	146,243.9	-	-	-	66.6
	Not identified	146,428.2	-	-	-	33.4

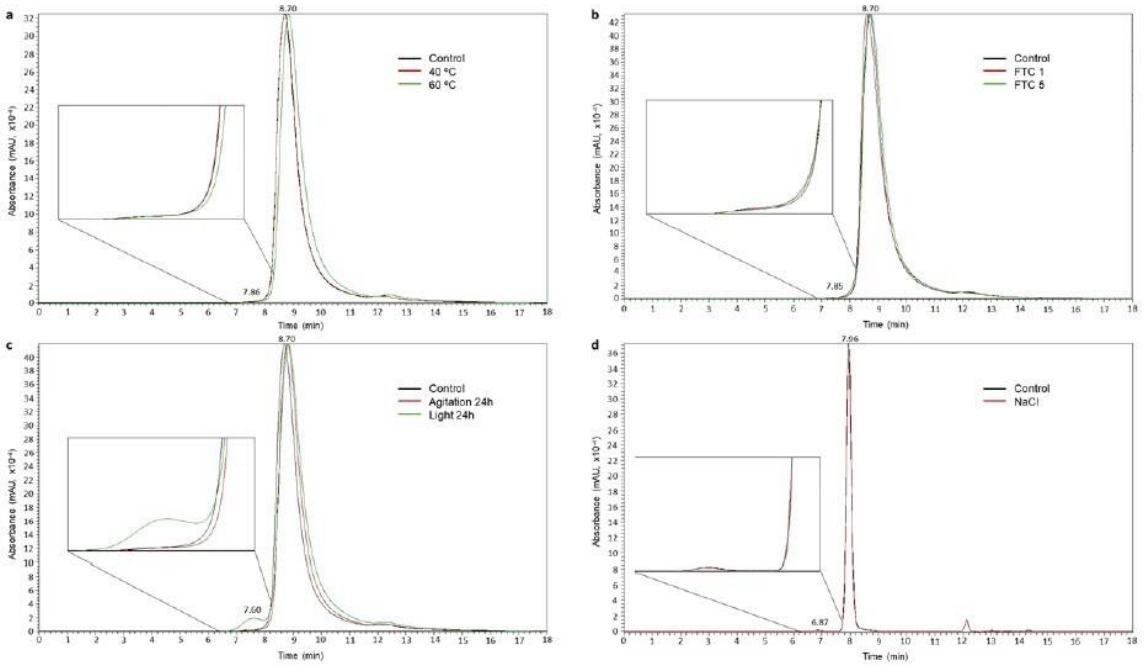

Figure 5. SE/UHPLC(UV) chromatograms for 10 mg/mL samples of nivolumab: (a) temperature stress; (b) FTC stress; (c) agitation and light stresses; and (d) ionic strength stress.

Table 6. Overall results for experimental retention time and relative proportions in the SEC analysis. Results that are significantly different from the control appear in **bold** type.

Stress	Monomer		Dimer	
	Retention time (min)	Proportion (%)	Retention time (min)	Proportion (%)
Control (10 mg/mL)	8.70	99.6	7.84	0.4
40 ºC 1h	8.71	99.6	7.84	0.4
60 ºC 1h	8.83	99.7	7.90	0.3
FTC 1	8.60	99.5	7.80	0.5
FTC 5	8.73	99.6	7.90	0.4
Agitation 24h	8.81	99.6	8.00	0.4
Light stress 24h	8.84	**96.6**	7.60	**3.4**
Control (2 mg/mL)	7.96	99.5	6.87	0.5
NaCl	7.95	99.8	6.83	0.2

During the course of the aggregation study, we had to replace the SEC column we were using with a new one. This change resulted in a modification of the chromatographic profiles as the new column showed higher peak resolution capability. In the chromatogram in Figure

5d, the chromatographic peaks for the control and NaCl stressed samples are thinner and the retention times are shorter than the chromatograms in the other panels (a, b and c), because the NaCl stress study was carried out using the new column. A non-assigned chromatographic peak was detected in all the SE chromatographic profiles at a retention time of 12.20 ± 0.02 min. However, this peak is not a sign of degradation as it was also detected in the control (fresh) medicine samples.

3.7. ELISA

The biological activity of nivolumab (antibody-antigen binding specificity) can be evaluated by ELISA-based binding assays. When exposed to stress, mAbs can undergo physicochemical modifications that may impair their effectiveness. The ELISA technique can be used to evaluate the impact of these modifications [27,28].

We developed a new ELISA method for this study. The first stage was therefore to validate the ELISA. The calibration model was established by selecting the mathematical function that best fits the experimental data (standard calibration curve in Figure S4). After reviewing various different mathematical models, a quadratic polynomial model was selected as the most suitable for calibration purposes, given its R2 (99.34%) and p-value (0.0252), which demonstrate, respectively, the goodness of fit and the significance of the selected mathematical model (Table 7).

Table 7. Characteristic parameters of the standard calibration curve (calibration model) and the figures of merit of the ELISA method.

Parameter	Value
Mathematical model fitted	Polynomial model
Function	$Y = -0.0002x^2 + 0.0322x + 0.0387$
s [a]	0.0000087
s [b]	0.0008737
s [c]	0.0121092
R^2 (%)	99.34
p-value	0.0252

[a] Standard deviation of the square concentration coefficient; [b] Standard deviation of the concentration coefficient; [c] Standard deviation of the constant for the polynomial function.

Other important aspects of validation include repeatability and intermediate precision, both expressed in terms of their RSD (%), as set out in Table 8. Accuracy, expressed as R

(%), is also presented in this table. For immunoassays, minimal acceptance limits of 20% are recommended, which means that the model fulfilled the precision criteria indicated for bioanalytical method validation [33,34]. The recovery values were between 92% and 106%, so demonstrating the high quality of the ELISA method we proposed for nivolumab, especially considering the huge variability inherent in immunoassay-based methods [28].

Table 8. Accuracy and precision of the ELISA.

Nivolumab concentration (ng/mL)	R (%) [a]	RSD (%) [b]	
		Intraday	Interday (3 days)
25	99.2	6.16	4.75
10	106	8.53	3.67
5	92	10.24	11.96

[a] Recovery value based on three determinations; [b] Relative standard deviation based on three determinations.

Once the ELISA had been fully validated, it was used to assess the biological activity of the stressed nivolumab samples. Figure 6 shows the results of the ELISA assays. Each stressed sample was analysed by obtaining the calibration graph, which was compared with the graph obtained in the analysis of the control (fresh) samples. In order to detect statistically significant differences, a Student's t analysis was carried out as a means of comparing the experimental data from control and stressed samples: in Figure 6 the results marked with asterisks are significantly different (one asterisk, p-value < 0.05) and very significantly different (two asterisks, p-value < 0.001) from the control. The results show that the samples of nivolumab subjected to heat (40 °C/1 h and 60 °C/1 h) retain their functionality as the control sample. The samples subjected to stress by agitation and light exposure showed a clear loss in PD-1 binding capacity, as revealed by the shift towards lower absorbance values of the graphical function for the stressed samples as compared to the graphical function for the control samples; a remaining PD-1 binding capacity of 80% (agitation) and 70% (light stress exposure) was estimated, after assuming a binding capacity of 100% in the control samples in each graph (Table 9). In the case of the samples subjected to FTC 1 and 5, results indicated a slight decrease in PD-1 binding capacity to PD-1 with respect of the control samples, estimating the remaining biological activity at around 90% for both samples. This is in line with the instruction in the Opdivo® technical reports about not freezing the medicine [4]. The ELISA assays also revealed two significant values (Figure 6) in the sample subjected to high ionic strength stress (NaCl). Therefore, the biological activity of the stressed sample differs from the control samples, with a remaining activity of around 90% (Table 9).

Table 9. Percentage estimation of the remaining activity in stressed nivolumab samples by ELISA.

Stress	Remaining activity (%)
40 ºC 1h	94.2 ± 4.2
60 ºC 1h	90.2 ± 4.3
FTC 1	88.5 ± 4.1
FTC 5	78.5 ± 4.6
Agitation 24 h	68.5 ± 4.8
Light 24 h	59.3 ± 8.7
NaCl	81.0 ± 12.7

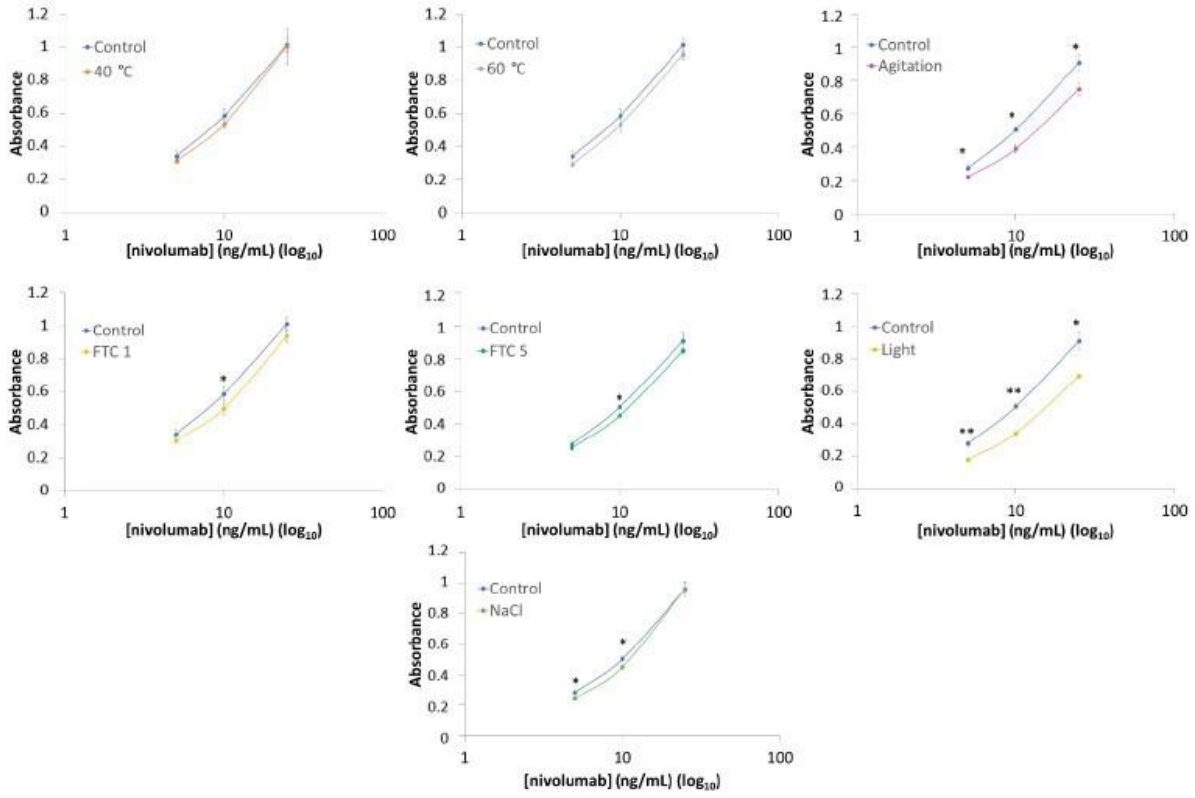

Figure 6. ELISA binding assay (5, 10 and 25 ng/mL) for the stressed samples as compared to a fresh (control) sample of nivolumab (*: *p*-value < 0.05; **: *p*-value < 0.001).

4. Discussion

Throughout this study, we used samples of nivolumab in its medicine formulation (Opdivo®, 10 mg/mL). We began by characterizing fresh control samples of nivolumab, which were then compared with stressed samples that had been subjected to a range of different stress conditions. The aim of these tests was to detect and identify possible changes in the medicine such as aggregation, denaturation or structural modifications, and the appearance of new particulates.

Results indicate that nivolumab medicine (Opdivo®, 10 mg/mL) is composed of monomers and natural dimers in relative proportions of 99.6% and 0.4%, respectively, as highlighted in the SEC profiles conducted on the batches (Table 6). The native LCMS(Orbitrap) isoform profile indicated three main glycoforms, which were assigned to A2G0F/A2G0F, A2G0F/A2G1F and A2G1F/A2G1F, in accordance with their particular masses (Figure 4 and Table 5). As regards the secondary structure of nivolumab derived from the CD spectrum, this consisted mainly of β-sheet (Table 2), as is normal in mAbs [18,27], and showed the characteristic spectral parameters: minimum at around 218.0 nm, shoulder at 228.7 nm and wavelength for ellipticity = 0 of around 209.7 nm. The tertiary structure, which was characterised by IT-FS, showed a centre of spectral mass (C.M.) of 361 nm (Table 3) for both the undiluted (10 mg/mL) and diluted (2 mg/mL) medicine. The DLS study indicated an HD of around 9.7 nm and 9.3 nm and a polydispersity of 11.7% and 12.4% for the undiluted nivolumab samples used as control, while the diluted medicine showed similar HD (9.4 nm) and polydispersity (7.4%) (Table 4). All these values are shared with other therapeutic mAbs [18,27].

The heat stress study was carried out by subjecting the medicine (Opdivo®, 10 mg/mL) to two different temperatures, 40 °C and 60 °C, for 1 h. In both cases, there were no significant changes in the medicine. SE/UHPLC(UV) analysis did not show any increase in the dimer population or the appearance of high molecular weight (HMW) aggregates (Figure 5). The lack of aggregation was also corroborated by DLS, which only detected one population of particulate, i.e., the monomers. However, in the sample subjected to 60 °C, there was an increase in HD (from 9.7 ± 3.2 nm in the control to 11.7 ± 5.8 nm in the stressed sample) and PDI (from 0.21 in the control to 0.32 in the stressed sample), which could be attributed to an increased hydration of the nivolumab monomers; this could be due to the fact that the heat stress temperature (60 °C) was very close to the temperature beyond which the secondary structure began to deteriorate (65 °C) (Table 4). In addition, CD and IT-FS did not detect any changes in the secondary and tertiary structures of the protein (Tables 1 and 2). For its part, the isoform profile was very stable and the glycoforms remained unaltered. The same glycoforms, with similar relative abundances, were identified in both the heat-stressed and

control samples of nivolumab (Figure 4 and Table 5). Moreover, ELISA assays demonstrated that subjecting nivolumab to 40 °C and 60 °C for 1 h did not affect its functionality, as measured in terms of its capacity to bind to its target (the PD-1) (Figure 6). Although previous researchers reported slight structural changes in IgG4 [35] and in nivolumab [7] when subjected to more aggressive heat stress, in this study we have demonstrated that nivolumab (Opdivo® 10 mg/mL) remains stable when subjected up to 60 °C for 1 h, and its binding capacity to PD-1 is unaffected.

It is well known that freeze/thaw cycles (FTC) can lead to protein aggregation, as they disturb the local structure on the surface of the residues of the protein, so giving rise to partial denaturation during freezing, which culminates in an aggregation process [36]. Nevertheless, no changes were noted in nivolumab in either FTC 1 or FTC 5. In both cases, the secondary and tertiary structures remained stable, as did the relative proportions of monomers and dimers. Moreover, DLS confirmed the absence of aggregates and the isoform profile remained unaltered. ELISA results showed that the nivolumab-PD-1 binding capacity decreased slightly to around 90% after one and five cycles. This means that this functional property is slightly affected by the freeze/thaw cycles, even though none of the physicochemical parameters that we studied indicated modifications in the medicine (Figure 6). As indicated earlier, this result is in line with the instruction in the technical report on Opdivo® [4] about not freezing this medicine.

Agitation for 24 h had no significant effects on the particulate in the nivolumab sample. SE/UHPLC(UV) demonstrated that there were no changes in the relative proportions of monomers and dimers, and DLS also confirmed that no new populations or aggregates appeared after application of this stress. In addition, the CD results showed a similar spectrum to the control sample, so indicating that the secondary structure remained unchanged. The same occurred with the tertiary structure, given that the IT-FS results for the stressed sample had a similar profile to the control, and their C.M. values were exactly the same. The isoform profile also remained unchanged, as revealed by the fact that the glycoforms assigned to the stressed sample matched those assigned to the control one. However, ELISA indicated a reduction in the capacity of nivolumab to bind to PD-1 (Figure 6 and Table 9), which could not be due to any structural modification, given the aforementioned results. However, it could be due to changes in the tertiary structure of nivolumab, given that the maximum emission of tryptophans in nivolumab is over 350 nm, which is a very high value, similar to that of the amino acid in aqueous solution [37]. This indicates that the tryptophans in nivolumab are close to a hydrophilic environment, and are therefore highly exposed to the solvent. As a result, IT-FS is unable to detect the structural changes that might lead to the loss of biological activity revealed

by ELISA. In the near future, we will be investigating these findings in much greater detail using peptide mapping analysis.

As regards the stress involving exposure to light for 24 h, non-natural aggregation was observed by SE/UHPLC(UV) (Figure 5). Previous research on other mAbs has shown that exposure to light induces aggregation [30,38], a finding that was also true for nivolumab medicine samples, in which the SE-chromatographic profile showed an increase in the peak for dimers, whose relative proportion was 3% higher than in the control sample (Table 6). Despite the increased proportion of dimers, CD assessment did not detect any changes in the secondary structure of nivolumab. As regards the tertiary structure of the protein, changes were detected, not in the C.M. (indicating no protein unfolding) of the IT-FS spectra, but in their intensity. This was probably due to the light-triggered oxidation of tryptophan residues. These changes may have caused the loss of biological activity, which could also have been induced by the aggregation of mAbs, as reported in previous research [39]. As expected, the nivolumab sample exposed to light showed a statistically highly significant decrease in the binding capacity of nivolumab to PD-1 (Figure 6), falling to around 70% of that of the control sample (Table 9). The isoforms profile was also very different because of the chemical changes (i.e., oxidations) caused by light exposure, which modified the molecular weight of nivolumab. This shows that the isoform profile was greatly affected by exposure to light despite being unaffected by the other forms of stress (Figure 4). Two new nivolumab isoforms were detected after the light exposure test with different masses compared to those detected in the control sample. No N-glycoforms could be attributed to these isoforms. All these results clearly indicated that exposure to light stress caused important degradation of nivolumab. These changes were probably due to the oxidative process to which the sample is exposed, as many previous publications suggest. We obtained similar results in a parallel study of nivolumab (manuscript in preparation).

As regards the stress by exposure to high ionic strength, the SE/UHPLC(UV) and DLS results indicated that no aggregation occurred, as monomers and dimers appeared in the same proportions as in the control sample and no HMW aggregates were detected, either by SEC or by DLS. Nevertheless, DLS results showed an increase in the HD value (from 9.4 ± 2.6 nm in the control to 13.9 ± 3.8 nm in the stressed sample) and in the PDI (from 0.29 in the control to 0.34 in the stressed sample). This was attributed to an increase in hydration, as indicated in Section 3.4 DLS (Table 4). CD results indicated that the secondary structure of nivolumab was not affected by this stress (Table 3). Despite all these results, ELISA indicated two significant values in Figure 6, referring that the binding capacity of nivolumab to the PD1 slightly (and significantly) decreased (around a 10%) with respect to the control samples. This could be due to the proposed increase in the hydration of the surface of the protein due to the increase in

ionic strength, which might affect the capacity of nivolumab to bind to PD-1, its therapeutic target. The changes detected by DLS may therefore contribute to this loss of biological activity.

4. Conclusions

Biopharmaceuticals can be exposed to a wide range of environmental stress conditions during routine handling in hospitals, as well as in previous stages such as research, development and manufacturing. The research findings presented in this paper focus above stresses to which nivolumab (Opdivo®) might be subject when handled in hospital prior to administration. To assess the impact of these stresses, various stress tests were performed. The results of these tests indicate that nivolumab is most affected by accelerated exposure to light. This is because light causes non-natural aggregation (dimerisation) of the protein and promotes oxidations (i.e., tryptophan residues). As a consequence of these chemical changes, it also alters the isoform profile. The results of the functional studies, which measured the capacity of nivolumab to bind to the PD-1 receptor, demonstrated that this capacity is substantially reduced when nivolumab is subject to stress by exposure to light. This means that it should be stored and handled away from the light so as to avoid degradation. On the other hand, nivolumab (Opdivo®) was found to remain highly stable when subjected to heat exposure for 1 h up to 60 °C, even though this was very close to the temperature at which nivolumab starts to deteriorate due to heat stress. As regards the agitation test, even though no significant conformational changes, aggregation or particulate were observed, the biological activity of nivolumab was affected, in that it caused a decrease in the ability of nivolumab to bind to the PD-1 receptor (estimated at around 20%). We therefore strongly recommend, as far as possible, to avoid shaking the medicine and its pharmaceutical preparations and to take great care during transport and handling. Caution must also be taken when diluting the medicine in NaCl, as physical modifications were detected when nivolumab was exposed to a highly hypertonic solution. We have also confirmed that freezing/thawing could affect the capacity of nivolumab to bind to PD-1, a finding that confirms the instruction in the Opdivo® technical report about not freezing the medicine. As expected, this research highlights the fragile nature of biopharmaceutics and, in particular, of nivolumab.

Author Contributions: A.T.-L.: Conceptualisation, Methodology, Validation, Formal analysis, Investigation, Writing—Original Draft, Visualisation; J.H.: Conceptualisation, Methodology, Investigation; A.S.-G.: Resources, Supervision, Project administration, Funding acquisition; J.C.: Resources, Supervision, Project administration, Funding acquisition; N.N.: Conceptualisation, Methodology, Resources, Writing—Review and Editing, Supervision, Project administration, Funding acquisition. All authors have read and agreed to the published version of the manuscript.

Funding: This study was partially funded by Project P20-01029 (I+D+i—Junta de Andalucía, Spain) and by Project B-FQM-308-UGR20 (Universidad de Granada, Proyectos I+D+i del Programa Operativo FEDER Andalucía 2020) which means that it was also partially supported by European Regional Development Funds.

Institutional Review Board Statement: Not applicable.

Acknowledgments: Anabel Torrente-López is currently receiving an FPU predoctoral grant (ref.: FPU18/03131) from the Ministry of Universities, Spain. Jesús Hermosilla is currently benefiting from a research contract (P20_01029) from the Junta de Andalucía (Spain) and European Regional Development Funds.

Conflicts of Interest: The authors declare no conflict of interest.

Supplementary material

Circular Dichroism

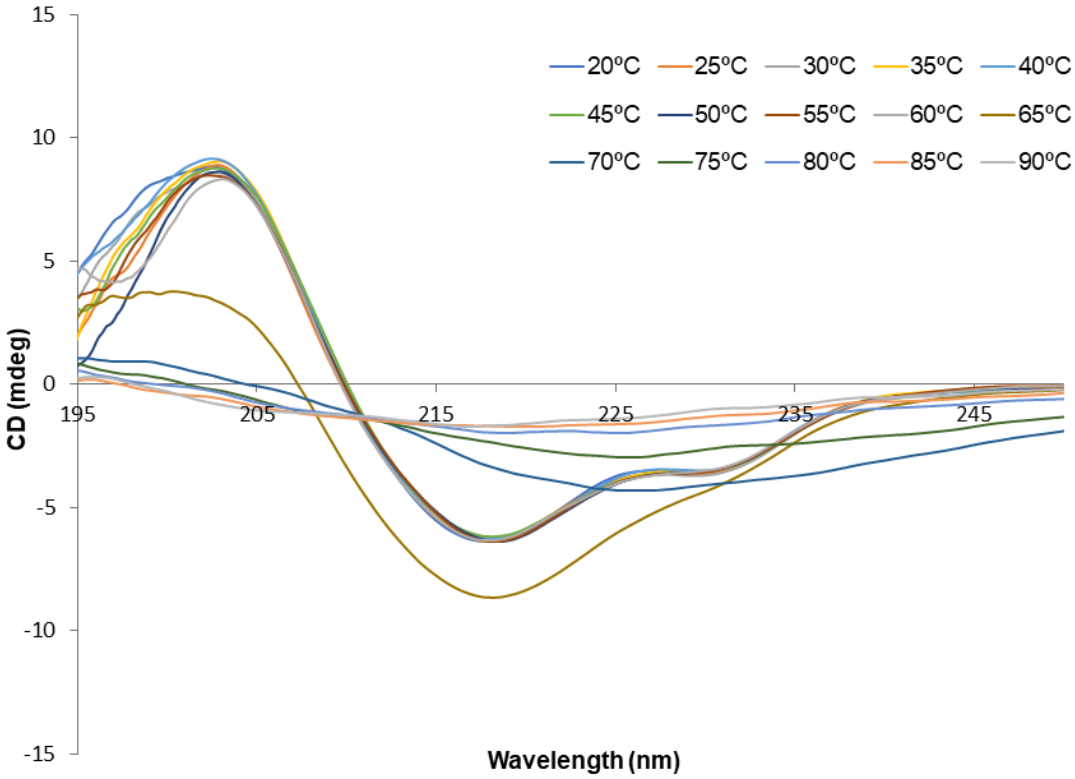

Figure S1. Resulting CD spectra of the temperature stability study by submitting nivolumab to a temperature ramp (from 20 °C to 90 °C).

Aggregation study by SE/UHPLC(UV)

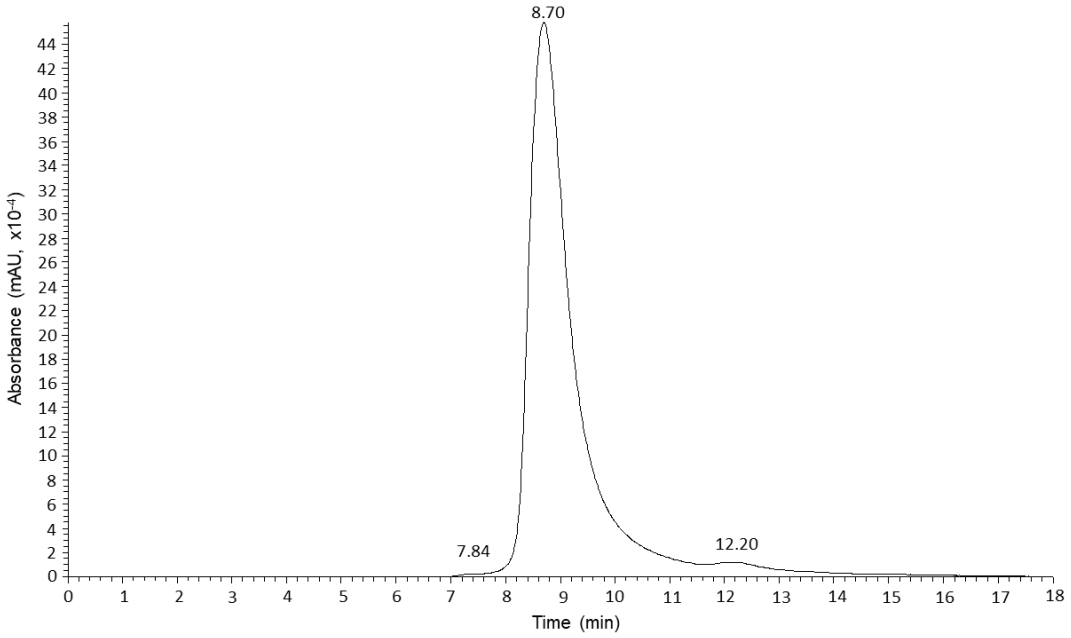

Figure S2. SE/UHPLC(UV) chromatogram for nivolumab fresh sample (Opdivo® 10 mg/mL).

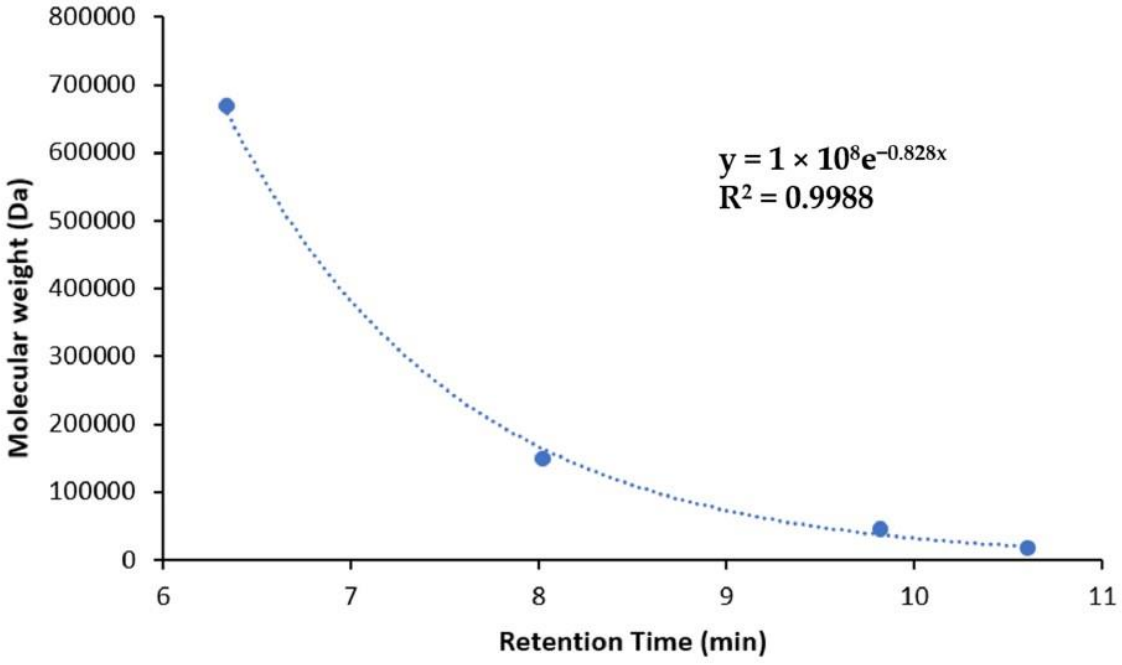

Figure S3. Experimental size exclusion column calibration model.

ELISA

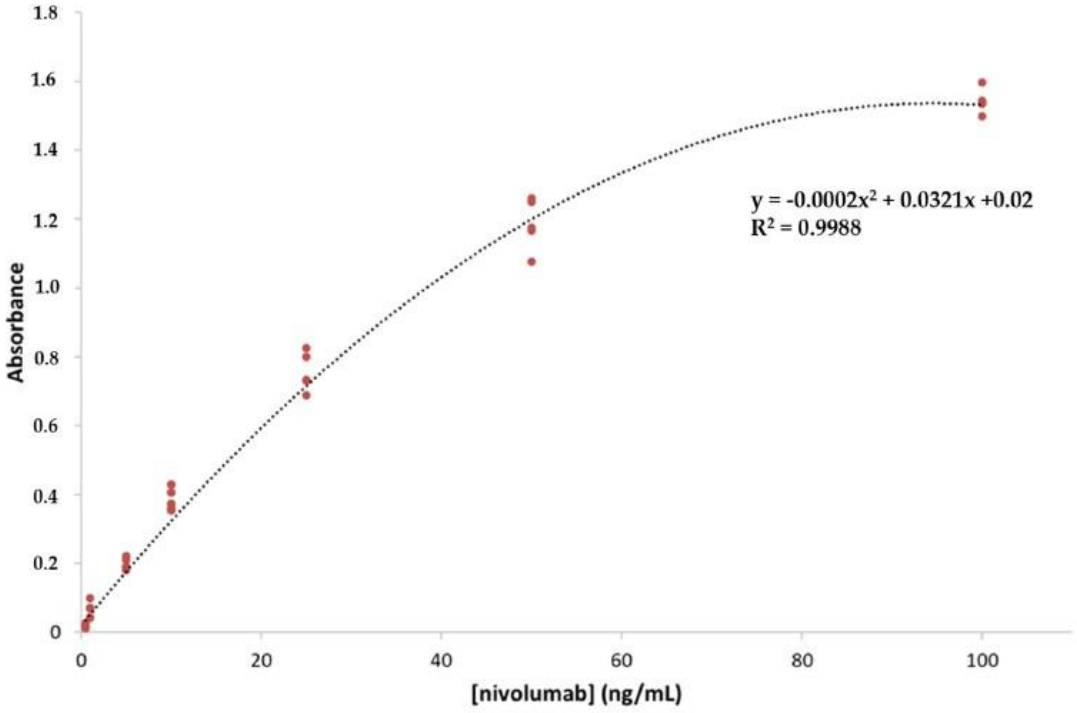

Figure S4. Standard calibration curve for the ELISA method.

References

1. Lu, R.-M.; Hwang, Y.-C.; Liu, I.-J.; Lee, C.-C.; Tsai, H.-Z.; Li, H.-J.; Wu, H.-C. Development of therapeutic antibodies for the treatment of diseases. J. Biomed. Sci. 2020, 27, 1. [CrossRef]

2. Hernandez-Alba, O.; Wagner-Rousset, E.; Beck, A.; Cianférani, S. Native Mass Spectrometry, Ion Mobility, and Collision-Induced Unfolding for Conformational Characterization of IgG4 Monoclonal Antibodies. Anal. Chem. 2018, 90, 8865–8872. [CrossRef] [PubMed]

3. Saito, S.; Namisaki, H.; Hiraishi, K.; Takahashi, N.; Iida, S. A stable engineered human IgG3 antibody with decreased aggregation during antibody expression and low pH stress. Protein Sci. 2019, 28, 900–909. [CrossRef] [PubMed]

4. European Medicines Agency. Nivolumab: Summary of Product Characteristics. (n.d.). Available online: https://www.ema.europa.eu/en/documents/product-information/opdivo-epar-product-information_en.pdf (accessed on 12 July 2021).

5. Shin, J.; Phelan, P.J.; Gjoerup, O.; Bachovchin, W.; Bullock, P.A. Characterization of a single chain variable fragment of nivolumab that targets PD-1 and blocks PD-L1 binding. Protein Expr. Purif. 2021, 177, 105766. [CrossRef] [PubMed]

6. Jaccoulet, E.; Daniel, T.; Dammak, D.; Prognon, P.; Caudron, E. Interest of flow injection spectrophotometry as an orthogonal method for analyzing biomolecule aggregates: Application to stressed monoclonal antibody study. Spectrochim. Acta Part A Mol. Biomol. Spectrosc. 2021, 251, 119436. [CrossRef]

7. Jaccoulet, E.; Daniel, T.; Prognon, P.; Caudron, E. Forced Degradation of Monoclonal Antibodies After Compounding: Impact on Routine Hospital Quality Control. J. Pharm. Sci. 2019, 108, 3252–3261. [CrossRef]

8. Nejadnik, M.R.; Randolph, T.W.; Volkin, D.B.; Schöneich, C.; Carpenter, J.F.; Crommelin, D.J.; Jiskoot,W. Postproduction Handling and Administration of Protein Pharmaceuticals and Potential Instability Issues. J. Pharm. Sci. 2018, 107, 2013–2019. [CrossRef]

9. Hawe, A.; Kasper, J.C.; Friess,W.; Jiskoot,W. Structural properties of monoclonal antibody aggregates induced by freeze–thawing and thermal stress. Eur. J. Pharm. Sci. 2009, 38, 79–87. [CrossRef]

10. Wang,W. Protein aggregation and its inhibition in biopharmaceutics. Int. J. Pharm. 2005, 289, 1–30. [CrossRef]

11. Luo, Q.; Joubert, M.K.; Stevenson, R.; Ketchem, R.R.; Narhi, L.O.; Wypych, J. Chemical Modifications in Therapeutic Protein Aggregates Generated under Different Stress Conditions. J. Biol. Chem. 2011, 286, 25134–25144. [CrossRef]

12. Joubert, M.K.; Luo, Q.; Nashed-Samuel, Y.; Wypych, J.; Narhi, L.O. Classification and Characterization of Therapeutic Antibody Aggregates. J. Biol. Chem. 2011, 286, 25118–25133. [CrossRef] [PubMed]

13. Nowak, C.; Cheung, J.K.; Dellatore, S.M.; Katiyar, A.; Bhat, R.; Sun, J.; Ponniah, G.; Neill, A.; Mason, B.; Beck, A.; et al. Forced degradation of recombinant monoclonal antibodies: A practical guide. mAbs 2017, 9, 1217–1230. [CrossRef]

14. Le Guyader, G.; Vieillard, V.; Mouraud, S.; Do, B.; Marabelle, A.; Paul, M. Stability of nivolumab in its original vials after opening and handing in normal saline bag for intravenous infusion. Eur. J. Cancer 2020, 135, 192–202. [CrossRef] [PubMed]

15. Bardin, C.; Astier, A.; Vulto, A.; Sewell, G.; Vigneron, J.; Trittler, R.; Daouphars, M.; Paul, M.; Trojniak, M.; Pinguet, F. Guidelines for the practical stability studies of anticancer drugs: A European consensus conference. Ann. Pharm. Françaises 2011, 69, 221–231. [CrossRef] [PubMed]

16. Tamizi, E.; Jouyban, A. Forced degradation studies of biopharmaceuticals: Selection of stress conditions. Eur. J. Pharm. Biopharm. 2016, 98, 26–46. [CrossRef] [PubMed]

17. Jaccoulet, E.; Schweitzer-Chaput, A.; Toussaint, B.; Prognon, P.; Caudron, E. Simple and ultra-fast recognition and quantitation of compounded monoclonal antibodies: Application to flow injection analysis combined to UV spectroscopy and matching method. Talanta 2018, 187, 279–286. [CrossRef] [PubMed]

18. Hermosilla, J.; Sánchez-Martín, R.; Pérez-Robles, R.; Salmerón-García, A.; Casares, S.; Cabeza, J.; Cuadros-Rodríguez, L.; Navas, N. Comparative Stability Studies of Different Infliximab and Biosimilar CT-P13 Clinical Solutions by Combined Use of Physicochemical Analytical Techniques and Enzyme-Linked Immunosorbent Assay (ELISA). BioDrugs 2019, 33, 193–205. [CrossRef]

19. Kelly, S.M.; Jess, T.J.; Price, N.C. How to study proteins by circular dichroism. Biochim. Biophys. Acta Proteins Proteom. 2005, 1751, 119–139. [CrossRef]

20. Whitmore, L.;Wallace, B.A. Protein secondary structure analyses from circular dichroism spectroscopy: Methods and reference databases. Biopolymers 2008, 89, 392–400. [CrossRef]

21. Provencher, S.W.; Gloeckner, J. Estimation of globular protein secondary structure from circular dichroism. Biochemistry 1981, 20, 33–37. [CrossRef]

22. Lees, J.G.; Miles, A.J.;Wien, F.;Wallace, B.A. A reference database for circular dichroism spectroscopy covering fold and secondary structure space. Bioinformatics 2006, 22, 1955–1962. [CrossRef] [PubMed]

23. Carillo, S.; Pérez-Robles, R.; Jakes, C.; da Silva, M.R.; Martín, S.M.; Farrell, A.; Navas, N.; Bones, J. Comparing different domains of analysis for the characterisation of N-glycans on monoclonal antibodies. J. Pharm. Anal. 2020, 10, 23–34. [CrossRef] [PubMed]

24. Pluim, D.; Ros,W.; van Bussel, M.T.; Brandsma, D.; Beijnen, J.H.; Schellens, J.H. Enzyme linked immunosorbent assay for the quantification of nivolumab and pembrolizumab in human serum and cerebrospinal fluid. J. Pharm. Biomed. Anal. 2019, 164, 128–134. [CrossRef] [PubMed]

25. Puszkiel, A.; Noé, G.; Boudou-Rouquette, P.; Cossec, C.L.; Arrondeau, J.; Giraud, J.-S.; Thomas-Schoemann, A.; Alexandre, J.; Vidal, M.; Goldwasser, F.; et al. Development and validation of an ELISA method for the quantification of nivolumab in plasma from non-small-cell lung cancer patients. J. Pharm. Biomed. Anal. 2017, 139, 30–36. [CrossRef]

26. Rattanapisit, K.; Phakham, T.; Buranapraditkun, S.; Siriwattananon, K.; Boonkrai, C.; Pisitkun, T.; Hirankarn, N.; Strasser, R.; Abe, Y.; Phoolcharoen, W. Structural and In Vitro Functional Analyses of Novel Plant-Produced Anti-Human PD1 Antibody. Sci. Rep. 2019, 9, 15205. [CrossRef]

27. Hermosilla, J.; Pérez-Robles, R.; Salmerón-García, A.; Casares, S.; Cabeza, J.; Bones, J.; Navas, N. Comprehensive biophysical and functional study of ziv-aflibercept: Characterization and forced degradation. Sci. Rep. 2020, 10, 2675. [CrossRef]

28. Suárez, I.; Salmerón-García, A.; Cabeza, J.; Capitán-Vallvey, L.F.; Navas, N. Development and use of specific ELISA methods for quantifying the biological activity of bevacizumab, cetuximab and trastuzumab in stability studies. J. Chromatogr. B 2016, 1032, 155–164. [CrossRef]

29. International Conference on Harmonisation (ICH) Guidelines ICH Q2 (R1), Validation of Analytical Procedures: Text and Methodology. 1995. Available online: http://www.emea.eu.int (accessed on 9 November 2021).

30. Hernández-Jiménez, J.; Salmerón-García, A.; Cabeza, J.; Vélez, C.; Capitán-Vallvey, L.F.; Navas, N. The Effects of Light-Accelerated Degradation on the Aggregation of Marketed Therapeutic Monoclonal Antibodies Evaluated by Size-Exclusion Chromatography with Diode Array Detection. J. Pharm. Sci. 2016, 105, 1405–1418. [CrossRef]

31. Kerwin, B.A.; Remmele, R.L. Protect from Light: Photodegradation and Protein Biologics. J. Pharm. Sci. 2007, 96, 1468–1479. [CrossRef]

32. Royer, C.A. Probing Protein Folding and Conformational Transitions with Fluorescence. Chem. Rev. 2006, 106, 1769–1784. [CrossRef]

33. Findlay, J.; Smith,W.; Lee, J.; Nordblom, G.; Das, I.; DeSilva, B.; Khan, M.; Bowsher, R. Validation of immunoassays for bioanalysis: A pharmaceutical industry perspective. J. Pharm. Biomed. Anal. 2000, 21, 1249–1273. [CrossRef]

34. DeSilva, B.; Smith, W.; Weiner, R.; Kelley, M.; Smolec, J.; Lee, B.; Khan, M.; Tacey, R.; Hill, H.; Celniker, A. Recommendations for the Bioanalytical Method Validation of Ligand-Binding Assays to Support Pharmacokinetic Assessments of Macromolecules. Pharm. Res. 2003, 20, 1885–1900. [CrossRef] [PubMed]

35. Kumru, O.; Liu, J.; Ji, J.A.; Cheng, W.; Wang, Y.J.; Wang, T.; Joshi, S.B.; Middaugh, C.R.; Volkin, D.B. Compatibility, Physical Stability, and Characterization of an IgG4 Monoclonal Antibody After Dilution into Different Intravenous Administration Bags. J. Pharm. Sci. 2012, 101, 3636–3650. [CrossRef] [PubMed]

36. Zhang, A.; Qi, W.; Singh, S.K.; Fernandez, E.J. A New Approach to Explore the Impact of Freeze-Thaw Cycling on Protein Structure: Hydrogen/Deuterium Exchange Mass Spectrometry (HX-MS). Pharm. Res. 2011, 28, 1179–1193. [CrossRef]

37. Hellmann, N.; Schneider, D. Hands On: Using Tryptophan Fluorescence Spectroscopy to Study Protein Structure. In Protein Supersecondary Stuctures. Methods and Protocols.; Humana Press Inc.: Totowa, NJ, USA, 2019; pp. 379–401. [CrossRef]

38. Hernández-Jiménez, J.; Martínez-Ortega, A.; Salmerón-García, A.; Cabeza, J.; Prados, J.C.; Ortíz, R.; Navas, N. Study of aggregation in therapeutic monoclonal antibodies subjected to stress and long-term stability tests by analyzing size exclusion liquid chromatographic profiles. Int. J. Biol. Macromol. 2018, 118, 511–524. [CrossRef]

39. Qi, P.; Volkin, D.B.; Zhao, H.; Nedved, M.L.; Hughes, R.; Bass, R.; Yi, S.C.; Panek, M.E.; Wang, D.; DalMonte, P.; et al. Characterization of the photodegradation of a human IgG1 monoclonal antibody formulated as a high-concentration liquid dosage form. J. Pharm. Sci. 2009, 98, 3117–3130. [CrossRef]

CAPÍTULO 5

Physicochemical and functional comprehensive analysis of pembrolizumab based on controlled degraded studies: impact on antigen-antibody binding

INTRODUCCIÓN AL CAPÍTULO 5

En el capítulo 5 se ha llevado a cabo un análisis comprensivo de pembrolizumab (Keytruda®), mAb de tipo IgG4, empleado para el tratamiento de distintos tipos de cáncer, perteneciente al grupo de puntos de control inmunitario. Al igual que en el capítulo anterior, el objetivo principal de este trabajo fue evaluar el impacto de la manipulación hospitalaria sobre la estabilidad de este medicamento. Para ello, muestras de Keytruda® fueron sometidas a diferentes condiciones de degradación acelerada y controlada: 40 °C durante 1 h, 60 °C durante 1 h, 1 ciclo de congelación/descongelación, 5 ciclos de congelación/descongelación, exposición a la luz en una cámara de envejecimiento durante 24 h, agitación fuerte durante 24 h, agitación suave durante 1 minuto y dilución en una disolución hipertónica de NaCl. De nuevo, con la finalidad de analizar las muestras estresadas y caracterizar el propio medicamento (muestras control), se llevó a cabo un amplio estudio en el que se desarrollaron *ad hoc* y validaron un conjunto de metodologías de análisis fisicoquímico y funcional, para llevar a cabo un análisis comprensivo de los CQAs. Se emplearon con tal fin las siguientes técnicas analíticas: para detectar la formación de particulado y agregación de bajo peso molecular (oligómeros) se emplearon las técnicas DLS y SE/UHPLC(UV); la estructura proteica secundaria y terciaria se estudiaron mediante CD e IT-FS, el perfil de isoformas del mAb se identificó y cuantificó por RP/UHPLC(UV)-MS (estrategia *top-down*) y para la identificación y cuantificación de PTMs presentes en la estructura química de pembrolizumab se empleó el análisis de digeridos enzimáticos mediante RP/UHPLC(UV)-MS/MS (estrategia *bottom up*); por último, la funcionalidad o actividad biológica de pembrolizumab fue evaluada mediante ELISA, por tanto, evaluando la capacidad de unión del mAb a su diana terapéutica, el receptor PD-1. Los resultados indicaron que la principal vía de degradación de pembrolizumab es la agregación. Esto se puso de manifiesto tras la exposición a la luz y a 60 °C (1 h), ya que ambos estreses mostraron la formación de dímeros no naturales y de agregados de alto peso molecular. El estrés por luz también reveló un perfil de isoformas distinto al de la muestra control (sin estresar) y un aumento de las oxidaciones. El estudio de funcionalidad reveló una disminución de la capacidad de unión de pembrolizumab a su diana terapéutica, el receptor PD-1, en todas las situaciones de estrés evaluadas. Aun así, la actividad biológica remanente permaneció elevada en todos los casos, siendo el estrés a 60 °C y la exposición a la luz los más afectados. Como conclusiones, se ha indicado que el medicamento Keytruda® debe manejarse siempre protegido de la luz, evitar someterlo a agitación durante su transporte o manipulación y evitar medios hipertónicos en las diluciones. Además, este trabajo destaca la sensibilidad de

pembrolizumab a la exposición a distintas condiciones ambientales estresantes, poniendo de manifiesto que, incluso si no se detectan cambios conformacionales, agregación o formación de particulado, puede ocurrir una disminución de su capacidad de unión a su diana terapéutica. Esto ocurre, por ejemplo, en el caso del estrés por congelación/descongelación (5 ciclos), por lo que también se recomienda no congelar el medicamento. A lo largo del estudio, se realiza también una comparación de los resultados obtenidos con los obtenidos en el capítulo anterior, es decir, se comparan los resultados de los dos medicamentos estudiados (Opdivo® y Keytruda®), ya que ambos están constituidos por mAbs de punto de control inmunitario IgG4 (nivolumab y pembrolizumab) cuya diana terapéutica es la misma proteína, el receptor PD-1.

SCIENTIFIC ARTICLE

Physicochemical and functional comprehensive analysis of pembrolizumab based on controlled degraded studies: impact on antigen-antibody binding

Anabel Torrente-López[1], Jesús Hermosilla[1], Antonio Salmerón-García[2], José Cabeza[2], Adolfina Ruiz-Martínez[3] and Natalia Navas[1,*]

[1] Department of Analytical Chemistry, Science Faculty, Biohealth Research Institute (ibs.GRANADA), University of Granada, E-18071 Granada, Spain

[2] Department of Clinical Pharmacy, Biohealth Research Institute (ibs.GRANADA), San Cecilio University Hospital, E-18012 Granada, Spain

[3] Department of Pharmacy and Pharmaceutical Technology, Pharmacy Faculty, University of Granada, E-18011 Granada, Spain

Submitted to a JCR-listed Scientific Journal

July 2023

Abstract

Monoclonal antibodies-based medicines are widely used in the treatment of different types of cancer. These medicines are very sensitive to the exposition to different environmental conditions and their manipulation in hospitals may affect their safety and efficacy. This is the case of pembrolizumab (Keytruda®, 25 mg/mL), for which there is not yet much information regarding its behaviour with respect to the risk associated with its routine handling or unintentional mishandling. Here we performed an extensive physicochemical and functional analysis of pembrolizumab including controlled degradation studies: samples of the medicine were subjected to heat, freeze/thaw, agitation, accelerated light exposure and high hypertonic solution. After that, the samples were analysed by a set of analytical techniques to evaluate critical quality attributes: Far-UV CD, IT-FS, DLS, RP/UHPLC(UV)-MS, SE/UHPLC(UV), RP/UHPLC(UV)-MS/MS and ELISA. The results provide an in-depth understanding of the biochemical and biophysical properties of pembrolizumab, showing that the medicine is affected by accelerated light exposure and temperature of 60°C, demonstrated by the detection of non-natural dimers and HMWS. Light exposure also revealed a different isoform profile and increased oxidations. Regarding functionality, all the stressors promoted a decrease in pembrolizumab capacity to bind to PD-1 receptor, although the biological activity remained still high for all of them, being 60 °C and accelerated light exposure the most affected.

Keywords

Comprehensive analytical characterisation

Forced degradation study

UHPLC-MS/MS peptide mapping

In-use stability

Pembrolizumab

1. Introduction

Today, monoclonal antibody-based therapeutics (mAbs) are highly successful biopharmaceuticals due to their broad therapeutic applications. These products are mainly used for the treatment of different types of cancer and immune disorders as well as in new emerging diseases such as the severe acute respiratory syndrome coronavirus 2 (SARS-CoV-2) [1,2].

Most approved mAbs by the FDA and the EMA are based on the IgG1 isotype. However, the IgG4-based therapeutics are progressively increasing in the pharmaceutical market given their ability to form different IgG4 formats, such as bispecific antibodies (bsAbs), which bring new features to them (e.g., bsAbs are able to bind to two different antigens). This ability is due to the characteristics of their primary structure, e.g., the flexibility of the hinge region (shorter than IgG1). Moreover, biopharmaceutical companies are working on developing more stabilised IgG4 mAbs by introducing mutations in the core-hinge sequence. Pembrolizumab is an example of such stabilisation, in which a S228P point mutation was introduced into the core-hinge sequence [3].

Pembrolizumab (Keytruda®) is a humanised mAb of the IgG4/kappa isotype which binds to the programmed cell death 1 (PD-1) receptor. It is designed to directly block the interaction between the PD-1 and its ligands, PD-L1 and PD-L2. The PD-1 pathway represents a major immune checkpoint, which can be activated by cells in the tumour microenvironment to overcome active T-cell immune surveillance. Thus, pembrolizumab, through the blockade of this pathway, enhances the functional activity of T cells to facilitate tumour regression [4,5].

MAb therapeutics usually require a compounding stage in hospitals before patient administration. This consists of a dilution of the marketed medicine that is usually available with a relatively high concentration (in solution or lyophilized powder). Even though compounding is carried out following good manufacturing practices, the protein may face different stresses along this process as well as during administration, handling or storage stages. In hospitals, mechanical and thermal stresses are the most likely to occur and the degradation pathways normally involve physical (i.e., unfolding or aggregate formation [6]) and chemical (i.e., covalent bond formation, oxidation or amino acid modification) degradation of the protein. These degradations may threaten the clinical benefits of the medicine as they alter the integrity of the mAb and this could affect the bioactivity or increase the risk of immunogenicity of the biopharmaceutical product. In addition, structural changes could affect the ability of the mAb to interact with its therapeutic target correctly. Therefore, the detection of degraded mAbs before patient administration is essential [7].

Moreover, mAbs can undergo different types of post-translational modifications (PTMs). The most common functional PTMs that can be found in recombinant mAbs include N- and C- terminal modifications and glycosylation, and also, non-functional but degraded PMT such as oxidation and deamidation as well as structural alterations, such as aggregation. All of them have important functional implications in therapeutic mAbs. These modifications have to be analyse as critical quality attributes (CQAs) as they alter the properties of these proteins [8,9] and they could have a significant impact on the efficacy and safety of the biopharmaceutical product [10,11].

Forced degradation studies are a valuable methodology for simulating accidental exposure of mAbs therapeutics to stressful conditions during their handling, storage and administration as they offer useful information about the possible degradation pathways that could potentially affect the safety and efficacy of the biopharmaceutical product. To perform these studies, we have to consider the most common instabilities of mAbs i.e., light exposure, agitation, thermal stress, etc. Along with stress type, the total time of stress exposure and the extent to which the drug product should be exposed to that stressful condition also need to be considered in order to achieve realistic degradation pathways [12]. Usually, these stresses are carried out at relatively harsh conditions within a short time period and they provide an in-depth understanding of the physicochemical properties of the mAb therapeutic [13,14]. In this way, forced degradation studies help in the identification of CQAs by studying the impact of PTMs on biological functions.

As a consequence of their structural complexity, the physicochemical characterisation of mAbs requires a wide variety of analytical techniques in order to analyse the different aspects of the protein structure [15,16]. For example, this is shown in a recent study carried out with pembrolizumab, in which several complementary analytical techniques were used to study the physicochemical stability and functional activity of pembrolizumab at 1 mg/mL at both refrigerated and room temperature conditions for 14 days [17]. However, scarce information was provided on any of the analytical methods used.

The purpose of the present research is to perform a comprehensive analytical characterisation and a forced degradation study of pembrolizumab (Keytruda®). To this end, several and complementary analytical techniques were used to carry out a proper physicochemical and functional characterisation of this mAb. The techniques used for this study include circular dichroism (CD) for the evaluation of the secondary structure; fluorescence for the analysis of the tertiary structure; dynamic light scattering (DLS) to study the particulate in the solutions of the samples; size-exclusion chromatography with UV detection (SE/UHPLC(UV)) to analyse oligomers; reverse phase chromatography coupled to mass spectrometry (RP/UHPLC(UV)-(HESI/Orbitrap)MS) to determine the isoform profile

including glycans; RP/UHPLC(UV)-(HESI/Orbitrap)MS/MS for peptide mapping analysis to determine PTMs; and an Enzyme-Linked Immunosorbent Assay (ELISA) to assess functionality by means of the specific binding of pembrolizumab to the PD-1 receptor. In this way, forced degradation tests were performed on samples of the medicine to assess degradation. These tests include heating, freeze/thaw cycles, agitation, light exposure, high ionic strength and guanidine exposure. All of them provide valuable new information about this protein for the evaluation of the potential consequences associated with its routine handling or unintentional mishandling in hospital.

2. Materials and methods

2.1. Pembrolizumab samples

Keytruda® leftover samples (pembrolizumab 25 mg/mL, Merck Sharp & Dohme B.V., Haarlem, Netherlands) were provided by the Pharmaceutical Unit of the University Hospital “San Cecilio” (Granada, Spain) and used over the course of the study. In order to ensure the stability indicated by the manufacturer, each analysis was performed with fresh samples i.e., immediately after opening the vials. These are the batches used throughout this study: W004254, W006628, W009988, W013760 and W027879.

2.2. Forced Degradation: Stresses

Samples of the medicine Keytruda® were exposed to different stress conditions in order to perform the forced degradation studies. These samples were always used within the expiry date of the medicine once opened to prevent any degradation in pembrolizumab caused by the passage of time. In this study, pembrolizumab was subjected to eight forced degradation conditions: (i) exposure to a temperature of 40 °C for 1 h in a ThermoMixer® C thermoblock 1.5 mL (Eppendorf, Hamburg, Germany); (ii) exposure to a temperature of 60 °C for 1 h in a ThermoMixer® C thermoblock 1.5 mL (Eppendorf, Hamburg, Germany); (iii) one freeze–thaw cycle (room temperature of around 21/25 °C to −20 °C) in a vertical Bosch freezer (GSE32420, Gerlingen, Germany); (iv) five freeze–thaw cycles (room temperature of around 21/25 °C to −20 °C in a vertical Bosch freezer (GSE32420, Gerlingen, Germany); (v) exposure to light irradiation (250 W/m2) for 24 h in an aging chamber (Solarbox 3000e RH, Cofomegra, Milan, Italy); (vi) agitation (300 rounds/min) for 24 h in a mechanical laboratory shaker (type 3006, Gesellschaft für Labortechnik, Burgwedel, Germany); (vii) exposure to a hypertonic medium by diluting in 1.5 M NaCl (Panreac, Barcelona, Spain) at a final concentration of 5 mg/mL; and (viii) exposure to denaturing conditions by diluting pembrolizumab in 8 M GndHCl (pH 8.5, Sigma-Aldrich, USA) at a final concentration of 5 mg/mL; this GndHCl medium was used as a

positive control for pembrolizumab degradation. Additionally, a gentle agitation stress was carried out to gain a deeper understanding of the extent to which the agitation can affect the stability of the medicine. For this reason, gentle agitation stress was only studied by those analytical techniques where changes in the 24-hour agitation stress were detected. Every stress test was performed using 200 µL of the medicine (Keytruda® 25 mg/mL). For the high ionic strength and denaturing tests, a smaller volume of the medicine was used since a certain volume of NaCl and GndHCl had to be added (as a concentrated aqueous solution) to the sample to prepare a final volume of 200 µL. Therefore, these samples were analysed at a final concentration of 5 mg/mL. The temperature stresses were performed in 1.5 mL Eppendorf tubes (Eppendorf, Hamburg, Germany); the FTCs, agitation, high ionic strength and denaturing tests were carried out in 2 mL amber RAM vials with a 9 mm thread (Symta, Madrid, Spain); and the light stress was performed in 2 mL clear RAM vials with a 9 mm thread (Symta, Madrid, Spain).

Control samples were used as reference samples throughout this study. These are samples not subjected to stress and analysed within the expiry date of the medicine once the vial is opened to ensure no sample degradation. Control samples and those subjected to stress conditions were analysed at the concentration of the medicine (25 mg/mL), i.e., without performing any dilution to avoid any alteration of the medicine. However, the CD study required working with diluted samples to avoid detector saturation. For that reason, the medicine was diluted in reverse-osmosis-quality water (purified with a Milli-RO plus Milli-Q station from Merk Millipore, Darmstadt, Germany) at a concentration of 0.1 mg/mL.

2.3. Physicochemical Analytical Methods

2.3.1. Visual Inspections

Visual inspections were carried out using the naked eye prior to experimentation in order to check for evidence of formation of large aggregates, turbidity, suspended particles, colour changes, and gas formation.

2.3.2. Far Ultraviolet (UV) Circular Dichroism Spectroscopy

The secondary structures of pembrolizumab were assessed by CD spectroscopy in the far-UV region (190-260 nm). The experimental conditions were similar as those used in [18], using a JASCO J-815 spectropolarimeter (JASCO, Tokyo, Japan) equipped with a Peltier system for temperature control that was maintained at 20 ºC for all the measurements. All control and stressed medicine (25 mg/mL) and diluted (5 mg/mL) samples were diluted in water to 0.1 mg/mL of pembrolizumab. The spectra were acquired from 260 to 190 nm every 0.2 nm with a scan speed of 50 nm/min. In the case of NaCl and GndHCl experiments, CD spectra were registered from 260 to 200 nm and from 260 to 205 nm respectively, due to the high ionic

content, and thus, the exponential increase of the voltage signal monitored in the HT channel. Each spectrum was the resultant of five accumulations, registered with a bandwidth of 1 nm. An absorption QS quartz macro cell 100-1-P-40 (Hellma Analytics, Munich, Germany) with an optical path length of 2 mm was used throughout the analyses. Before registering the spectra, the blank was first measured and subtracted. Spectra Manager software version 2 was used to apply the Savitzky-Golay Smoothing to all the spectra.

Several spectral features were monitored after stress testing: wavelength (nm) at ellipticity = 0, negative maximum (nm) and the broad shoulder (nm). Furthermore, to estimate the secondary structure content (%), the Dichroweb server was used, and the most suitable algorithm and DataSet used were those on which the normalised root mean square deviation (NRMSD) fit parameter was lower [19].

Additionally, to evaluate pembrolizumab thermal stability, a temperature ramp was applied to a fresh control sample (0.1 mg/mL) from 20 ºC to 90 ºC. For so, a single spectrum was acquired at intervals of 5 ºC, at a ramp rate of 5 ºC/min by Interval Data Analysis, with the same instrument parameters described above.

2.3.3. Intrinsic Tryptophan Fluorescence Spectroscopy

The tertiary structure of pembrolizumab medicine (25 mg/mL) and diluted (5 mg/mL) stressed and control samples was analysed by Intrinsic Tryptophan Fluorescence Spectroscopy (IT-FS). A Cary Eclipse spectrofluorometer (Agilent, Santa Clara, CA, USA) was used to carry out IT-F measurements. Fluorescence emission spectra were recorded from 300 nm to 450 nm by selectively exciting the tryptophan residues at 298 nm. These were registered at room temperature, setting excitation and emission slits to 5 nm and 5 nm respectively, and a total of three spectral accumulations were recorded for all measurements at a scan speed of 600 nm/min.

The spectral centre of mass (C.M.) was considered as a mathematical representation of each spectrum, and was calculated using the equation 1, from 300 nm to 450 nm:

(1) $$C.M. = \frac{\sum_i^n \lambda i * Fi}{\sum_i^n Fi}$$

Where λi is the wavelength associated with its fluorescence intensity Fi.

2.3.4. Dynamic Light Scattering

The particles size distribution of pembrolizumab medicine (25 mg/mL) and diluted (5 mg/mL) stressed and control samples from 1 nm to 10 µm was characterised by DLS. For this, the population's mean hydrodynamic diameter (D_h), polydispersity (Pd %) and the polydispersity index (PDI) were evaluated by photon correlation spectroscopy using a dynamic

light scatter (DLS, Zetasizer Nano ZS-90, Malvern Panalytical, Malvern, UK), equipped with a backscattered light detector, operating at 90º and 25 ºC. For this study, the temperature was set at 20 °C. The acquisition time was 5 s per read and the 100 reads were recorded per measurement. The results were calculated by the cumulants analysis using the Zetasizer Software 8.01 version (Malvern Panalytical, Malvern, UK). For all the measurements, low-volume quartz cuvettes (ZEN2112) for size and molecular weight measurements (Malvern Instrument, Malvern, UK) were used.

2.3.5. Isoform analysis by RP/UHPLC(UV)-(HESI/Orbitrap)MS

To determine the isoform profile of pembrolizumab medicine (Keytruda®), a denatured intact protein analysis was performed using reverse phase liquid chromatography and mass spectrometry. For this purpose, we used a Dionex UltiMate 3000 chromatograph (Thermo Scientific, Waltham, MA, USA), equipped with two ternary bombs, a degasser, an autosampler, a thermostatic column compartment, and a multiple wavelength detector (MWD-3000 Vis-UV detector). The chromatograph was coupled in-line to a Q-Exactive™ Plus Hybrid Quadrupole Orbitrap mass spectrometer (Thermo Scientific, Waltham, MA, USA). The ionisation was performed using a heated electrospray ionisation (HESI) source. Both chromatograph and mass spectrometer were operated using software programmes provided by Thermo Fisher Scientific. The chromatographic instrument was operated by Chromeleon™ 7 and Xcalibur™ 4.0 software and the mass spectrometer by Tune™ Software. Chromatographic and MS conditions were similar to those used in [20].

A MAbPac™ RP column, 4 µm, 2.1 mm × 50 mm (Thermo Fisher Scientific, P/N 088648) was used to carry out the chromatographic analysis of pembrolizumab. The column temperature was set at 70 °C and the mobile phase flow rate was 0.3 mL/min. The injection volume of pembrolizumab samples was 5 µL at a concentration of 100 ppm of pembrolizumab. Two mobile phases were used to carry out this analysis using a gradient mode: 0.1 % FA in deionised water (mobile phase A) and 0.1 % FA in ACN (mobile phase B). The gradient conditions were set as follows: 25 % B increased to 45 % B in 2.5 min, with a further increase to 80 % B in 0.5 min with a 2 min isocratic hold. Initial conditions were then restored in 0.2 min and maintained for a further 5.8 min to achieve column re-equilibration. Total run time for the analysis was 11 min. The chromatograms were recorded at three different wavelengths: 214 nm, 220 nm and 280 nm, with a reference wavelength of 350 ± 10 nm. To obtain the figures of merit used throughout this study, we used λ = 214 nm and the other two wavelengths were used just to corroborate the protein nature of the chromatographic peaks.

The MS analysis was performed using full positive polarity and protein mode. MS scan was set at a resolution of 17,500 (defined at m/z 200) with the mass range set to 1500–4500

m/z and an AGC target value of 3.0×10^6 with a maximum injection time of 100 ms and 10 microscans. In-source CID was set to 100 eV, spray voltage at 3.8 kV, sheath gas flow rate at 35 AU, auxiliary gas flow rate at 10 AU, capillary temperature at 275 °C, probe heater temperature at 175 °C and S-lens RF voltage at 80 V.

The mass spectra were deconvoluted using the BioPharma Finder™ software version 5.0 (Thermo Fisher Scientific) with ReSpect algorithms to obtain the N-glycan-based mass isoform profiles of pembrolizumab fresh and stressed samples. To perform the deconvolution, we used pembrolizumab sequence obtained from the DrugBank database [21], we also considered the fact that pembrolizumab has 16 disulphide bonds and two post-translational modifications (PTMs) commonly found in mAbs produced in CHO cell lines, such as pembrolizumab, were taken into account: 2 N-term pyroglutamate formation and 2 C-term lysine clipping.

2.3.6. Aggregation Study by SE/UHPLC(UV)

The aggregation study was performed by liquid chromatography using a Dionex UltiMate 3000 chromatograph (Thermo Scientific, Waltham, MA, USA), equipped with two ternary bombs; a degasser; an autosampler; a thermostatic column compartment; and a multiple wavelength detector (MWD-3000 Vis-UV detector). Chromatographic conditions were similar to those used in [18]. A SEC column of 300 A, 2.7 µm, 4.6 × 300 mm (AdvanceBioSec, Agilent technologies, Santa Clara, CA, USA) was used and 20 µg of Keytruda® was injected into the column. The column temperature was set at 30 °C. This analysis was carried out under isocratic conditions of 150 mM of phosphate buffer pH 7.0, which was prepared with monohydrate monobasic sodium phosphate (Panreac, Barcelona, Spain) and anhydrous disodium hydrogen phosphate (Panreac, Barcelona, Spain) in reverse-osmosis-quality water, at 0.3 mL/min for 18 min. The UV chromatograms were registered at different wavelengths, i.e., λ= 214 nm, λ= 220 nm and λ = 280 nm, using a bandwidth of 5 nm in all cases and a reference band at 360 ± 10 nm.

The calibration of the SEC column was carried out using a kit composed of five proteins (Agilent, Santa Clara, CA, USA): thyroglobulin (670 kDa), γ-globulin (150 kDa), ovalbumin (45 kDa), myoglobin (17 kDa) and angiotensin II (1 kDa), although this last protein was not used in the calibration of the SEC column, due to its low molecular weight (M.W.). This calibration was performed with the aim of establishing the relationship between the molecular weight and the retention time of pembrolizumab. The experimental size exclusion column calibration model is $M.W. = 1.65 \times 10^8 e^{-0.8688x}$; $R^2 = 0.9993$. However, pembrolizumab showed a lower M.W. than expected (around 64,100 Da), proving that its size is more compacted than it should be for its corresponding M.W, which is around 149,000 Da.

2.3.7. RP/UHPLC(UV)-(HESI/Orbitrap)MS/MS for peptide mapping analysis of digested mAb samples

In order to perform a peptide mapping analysis of pembrolizumab, a tryptic digestion was carried out using a SMART Digest™ kit (Thermo Fisher Scientific). For that, Keytruda® (25 mg/mL) samples were diluted in mili-Q water to 2 mg/mL. Reagents were prepared immediately before the digestion as follows: DL-dithiothreitol (DTT; Sigma-Aldrich, Wicklow, Ireland) reducing agent was dissolved in 50 mM NH_4HCO_3 (Bioultra, ≥ 99,5 %; Sigma-Aldrich, San Luis, USA) buffer (at pH 7,8 – 8) at 100 mM; iodoacetamide (IAA; Sigma-Aldrich, Wicklow, Ireland) alkylating agent was dissolved in 50 mM NH_4HCO_3 buffer at 100 mM and protected from light to prevent degradation; and trifluoroacetic acid (TFA; Scharlab S.L, Barcelona, Spain) was diluted in water to 10 % v/v.

The digestion of the protein follows the next steps. Firstly, Keytruda® 2 mg/mL was added to SMART Digest™ buffer and, subsequently, DTT 100 mM was added to perform disulphide bond reduction. The samples were incubated at 57 °C for 30 minutes. Then, alkylation was carried out with IAA 100 mM at 25 °C for 30 minutes in darkness. Hereafter, 5 µL of SMART Digest™ trypsin resin were added to digestion samples and they were incubated at 70 °C for 45 minutes with shaking at 1400 rpm. The reaction was stopped adding DTT 100 mM and TFA 10 % (v/v). Samples were centrifuged immediately after stopping the reaction at 13000 rpm for 10 minutes to recollect the tryptic peptides, which were monitored by LC-MS/MS analysis. The digestion was performed in Eppendorf 0,5 mL tubes. Incubations were carried out in a ThermoMixer® C thermoblock (Eppendorf, Hamburg, Germany), whereas the centrifugation was performed with a MIKRO 220R centrifuge (Hettich, Tuttlingen, Germany).

Analysis was performed using a Dionex UltiMate 3000 chromatograph (Thermo Scientific, Waltham, MA, USA) coupled in line to a Q-Exactive hybrid quadrupole-Orbitrap mass spectrometer (Thermo Scientific, Waltham, MA, USA). The chromatograph is equipped with two ternary bombs, a degasser, an auto-sampler, a thermostatted column compartment and a multiple-wavelength detector (MWD-3000 Vis-UV detector). For the separation of the peptides, we used the column Acclaim™ RSLC 120 C18, 120Å, 2,2µm, 2,1mm x 250mm (Thermo Scientific, product nº 074812). Column temperature and flow were set at 25 °C and 0.3 mL/min, respectively. A binary gradient was used to carry out the analysis, which consisted of 0.1 % (v/v) formic acid (Fisher Scientific, Geel, Belgium) in water (phase A) and 0.1 % (v/v) formic acid in acetonitrile (VWR International Eurolab S.L, Barcelona, Spain) (phase B). This gradient was initiated at 2 % B, which increased to 40 % B over 45 minutes, and then to 80 % B over one minute. Gradient was kept at 80 % B for 4 minutes, and then shifted to 2 % B over 0.5 minutes. Finally, 2 % B was kept for 5 minutes for column reconditioning.

The MS method consisted of full positive polarity MS scan at 70,000 resolution setting (at *m/z* 200) with AGC target value of 3.0×10^6 and the mass range set to 200-2,000 *m/z*. The maximum injection time was set at 200 msec and one microscan. In-source CID was set to 0 eV. MS^2 parameters were stablished as a resolution setting of 17,500 (at m/z 200), AGC target value of 1.0×10^5, maximum injection/ionization time of 200 msec and an isolation window set to 2.0 *m/z*.

PTMs identification and quantitation was performed using BioPharma Finder 5.0 software using Full MS and MS/MS data, a minimum confidence score of 95 %, a mass deviation of 5 ppm and up to 1 trypsin miscleavage.

2.3.8. Functional-Based Method: Enzyme-Linked Immunosorbent Assay (ELISA)

With the aim of testing the biological activity of pembrolizumab, we performed an indirect, non-competitive ELISA method following our previous developed and optimized method for nivolumab [18], given the similarity between these two IgG4 mAbs. This method was as follows: firstly, 96-well Maxisorp immune plates were sensitized by adding 100 µL/well of 0.5 µg/mL Human PD-1 (CD279), FC Fusion (Sigma Aldrich, Madrid, Spain) diluted in 0.1 M carbonate buffer solution pH 9.6 (prepared with sodium carbonate (Panreac, Spain) and sodium bicarbonate (Panreac, Spain)) and incubated overnight (18 h) at 4 °C. The plates were washed four times using an Intelispeed Washer IW-8 (Biosan SIA, Latvia) with 200 µL/well of PBS-Tween 20 pH 7.4 containing 0.3 % (v/v) Tween 20®. PBS was prepared using sodium chloride, potassium chloride, disodium phosphate monohydrate and potassium phosphate monobasic supplied by Panreac (Barcelona, Spain), while Tween 20 was supplied by Guinama (Valencia, Spain). The plates were then treated with 200 µL/well of the blocking buffer (PBS-Tween 20 pH 7.4 containing skimmed milk 2 % (w/v)) for 2 h at 37 °C to eliminate nonspecific absorptions. After that they were washed four more times and filled with a 100 µL/well of pembrolizumab appropriately diluted in 0.1 M carbonate buffer (pH 9.6) at three concentrations: 5 ng/mL, 10 ng/mL and 25 ng/mL. The plates were incubated at 37 °C for 45 min in a universal digitronic precision oven P Selecta® (J.P. Selecta, s.a. Abrera, Barcelona, Spain), after which they were washed four times with PBS-Tween 20 and incubated again with 100 µL/well of 1:1000 in PBS diluted anti-human IgG4-HRP (mouse anti-human IgG4 Fc antibody-HRP conjugate, Thermo Fisher, Landsmeer, the Netherlands) for 30 min at 37 °C. After being washed for four times, 100 µL/well of the substrate solution (O-Phenylenediamine Dihydrochloride (OPD), Sigma Aldrich, Madrid, Spain) were added and incubated for 20 min at room temperature (around 25 °C) in darkness. Finally, 50 µL/well of 1M sulfuric acid solution was added to stop the reaction. Absorbance was recorded at 450 nm and 620 nm, and the analytical signal was the difference between the two absorbance values (TECAN SUNRISE™

microplate absorbance reader for 96-well plates connected to the computer running XFluor4 software, Tecan, Austria, GMB).

The method was validated in terms of the calibration model, precision and accuracy. Therefore, this ELISA format allowed us to quantify and evaluate the biological activity of pembrolizumab by assessing the specific interaction between this mAb and the PD-1 receptor. Thus, the remaining biological activity of stressed samples of pembrolizumab could be analysed comparing them with the biological activity of the control samples.

The standard calibration model was investigated using fresh samples of the medicine Keytruda® (25 mg/mL pembrolizumab) as standard samples. This calibration model was obtained testing seven different concentration of pembrolizumab diluted in 0.1 M carbonate buffer (pH 9.6): 100, 50, 25, 10, 5, 1, and 0.5 ng/mL. Each standard concentration was prepared and analysed in quintuplicate. Considering the graphical distribution from this calibration model (absorbance vs. ng/mL pembrolizumab), three optimum concentrations of pembrolizumab were selected to perform the following analysis of this mAb: 25, 10 and 5 ng/mL. The statistical analysis of the calibration models was performed using the Statgraphics Centurion 18 (Statgraphics Technologies, The Plains, VA, USA) software package, and the coefficient of determination (R^2) and the lack-of-fit signification test were used to evaluate the best fit of these data to the different mathematical models. The precision and the accuracy were evaluated according to the ICH recommendations Q2(R1) at the three selected optimal concentrations of pembrolizumab [22]. This evaluation was performed in the same way as our previous study with nivolumab [18]. The precision was checked as repeatability and intermediate precision, i.e., intraday and interday precision (over three consecutive days), respectively. Repeatability was assessed by analysing nine standard solutions within the same day and under the same experimental conditions: 3 samples at 5 ng/mL, 3 samples at 10 ng/mL and 3 samples at 25 ng/mL. For the intermediate precision study, three standard solutions (5, 10 and 25 ng/mL of pembrolizumab) were freshly prepared on three different days and they were analysed under the same experimental conditions. Both repeatability and intermediate precision were assessed as the relative standard deviation (RSD, %) of the concentrations calculated from the absorbance using the standard calibration curve. Accuracy was determined by analysing three standard solutions of each concentration of pembrolizumab and determining the mean recovery percentage (R, %) for each concentration.

Once the ELISA method was validated, this was used to perform the functional study of pembrolizumab. To this end, the control (fresh) and stressed pembrolizumab samples (both from Keytruda®) were analysed simultaneously and compared afterwards to assess whether pembrolizumab was able to maintain its ability to specifically bind to its target (the PD-1 receptor) after applying the stress conditions. These results were statistically compared using

the *Student's t* analysis with 95 % of confidence and the biological activity of each stressed sample (considered as the average of three replicates) were then compared with that of the control sample.

3. Results

3.1. Visual Inspections

All the stressed samples showed no precipitations or particulate formation when they were checked with the naked eye. Therefore, all of them remained clear after being subjected to the different stress conditions considered in this study.

3.2. Far Ultraviolet (UV) Circular Dichroism Spectroscopy

Figure 1 illustrates the CD spectra of the stressed samples in comparison with their respective control. In Table 1, the main spectral features are included: wavelength (nm) at ellipticity 0, the negative maximum and the broad shoulder, while Table 2 shows the secondary structure content estimation (%).

The pembrolizumab control CD spectrum is characterised by a wavelength at ellipticity 0 of 209.0 ± 0.2 nm, a negative maximum at 218.0 ± 0.2 nm and a broad shoulder at 229.6 ± 1.0 nm: this spectrum corresponds to a structure with majority of β-sheet (48 %) and unordered (39 %) contents, with low turns and α-helix contents (10 % and 2 % respectively) (Table 2). These parameters remained unchanged in most of the stressed samples, indicating that pembrolizumab native secondary structure was conserved upon the different stress conditions.

The exception occurred with 60 °C and GndHCl stresses. In the case of 60 °C, the wavelength at ellipticity=0 and negative maximum changed significantly with respect to control (Table 1): the secondary structure content estimation indicated a slight increase in α-helix content and a decrease of β-sheets. In the GndHCl stress, the typical native β-sheet CD spectrum disappeared: no maximum at 202 nm, no negative maximum at 217 nm and no shoulder at 230 nm were observed; pembrolizumab secondary structure was lost under this condition as expected by the chaotropic nature of guanidine.

Regarding the thermal stability (Figure S1), pembrolizumab CD spectrum is maintained unaltered until 60 °C. From temperatures of 65 °C, the spectra changed significantly, indicating denaturation and loss of the native conformation.

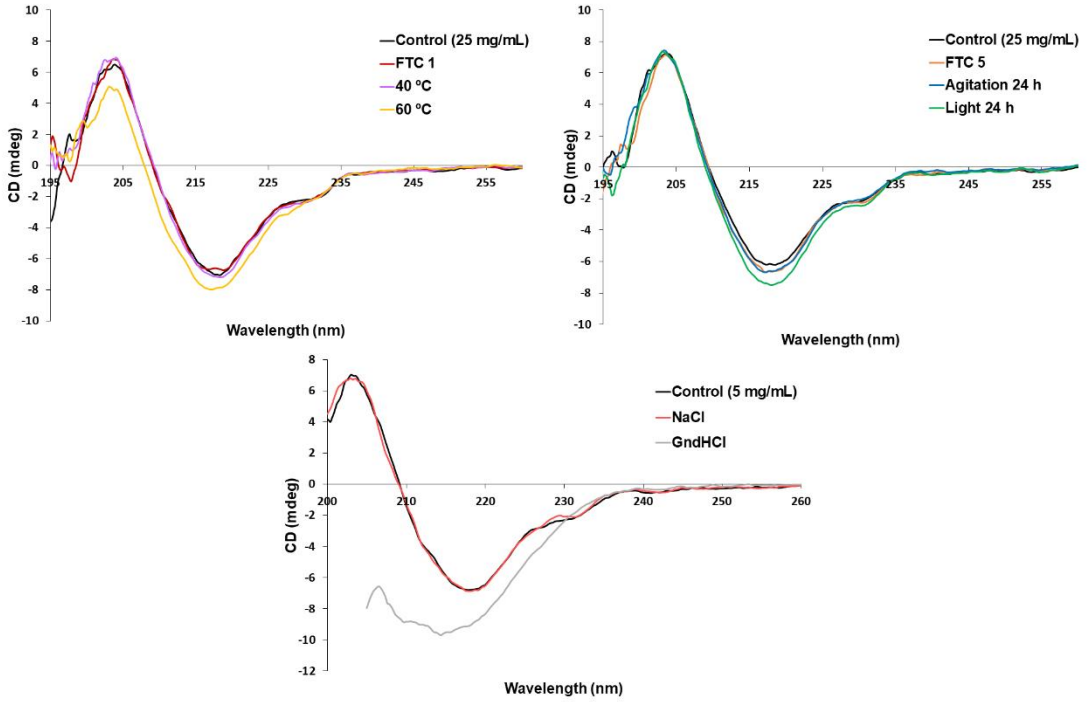

Figure 1. Far-UV CD spectra of pembrolizumab (25 mg/mL) stressed and control samples.

Table 1. Pembrolizumab (25 mg/mL) CD spectral features: control (mean ± standard deviation from 3 replicates) and stressed samples.

Stress	Wavelength (nm) (ellipticity = 0)	Negative maximum (nm)	Broad shoulder (nm)
Control 1	209.2 ± 0.2	218.0 ± 0.2	229.6 ± 1.0
40 ºC 1h	209.2	218.2	228.6
60 ºC 1h	**208.0**	**217.4**	**227.6**
FTC 1	209.2	218.2	228.8
FTC 5	209.4	218.0	229.4
Agitation 24h	209.4	217.6	229.8
Light stress 24h	209.0	218.0	229.8
NaCl	209.0	218.4	230.2
GndHCl	**-**	**214.5**	**240.8**

In bold type is highlighted those features that were significantly different to control values.

Table 2. Secondary structure content (%) estimation by Dichroweb server of pembrolizumab (25 mg/mL) stressed and control samples. Control is the mean ± standard deviation from 3 replicates. The analysis program and Dataset selected were CDSSTR and SP175t respectively.

Stress	Helix 1	Helix 2	Strand 1	Strand 2	Turns	Unordered
Control	0	2 ± 1	35 ± 1	14 ± 0	10 ± 1	38 ± 1
40 ºC 1h	0	2	35	14	10	39
60 ºC 1h	0	3	33	14	10	39
FTC 1	0	2	35	14	10	38
FTC 5	0	1	36	14	11	37
Agitation 24h	0	1	35	14	10	38
Light stress 24h	0	2	35	14	10	38
NaCl	-	-	-	-	-	-
GndHCl	-	-	-	-	-	-

In bold type is highlighted those percentages that were significantly different to control values.

3.3. *Intrinsic Tryptophan Fluorescence Spectroscopy (IT-FS)*

The IT-FS results are shown in Figure 2 and Table 3. Figure 2 shows the fluorescence emission spectra of the stressed and control pembrolizumab samples. Table 3 shows the spectral C.M. calculated by equation 1. Both pembrolizumab control medicine (25 mg/mL) and diluted (5 mg/mL) samples have a C.M. of 346 nm, which corresponds to an emission maximum of 335 nm approximately, indicating that Trp residues are located in the core of the macromolecule, highly excluded from the solvent [23]. This result is similar to the previously obtained with a similar protein (ziv-aflibercept) within our research group [24]. Most of the stress conditions tested here did not alter this parameter, except samples stressed by 60 ºC/1h and GndHCl (Table 3), in which red-shifts of their spectra emission maxima were observed: the C.M. increased to 349 nm and 367 nm respectively, indicating a partial and a total exposition of Trp residues to the polar solvent. It is noteworthy the increase in the fluorescence signal upon these stresses, unexpectedly when denaturation takes place [23].

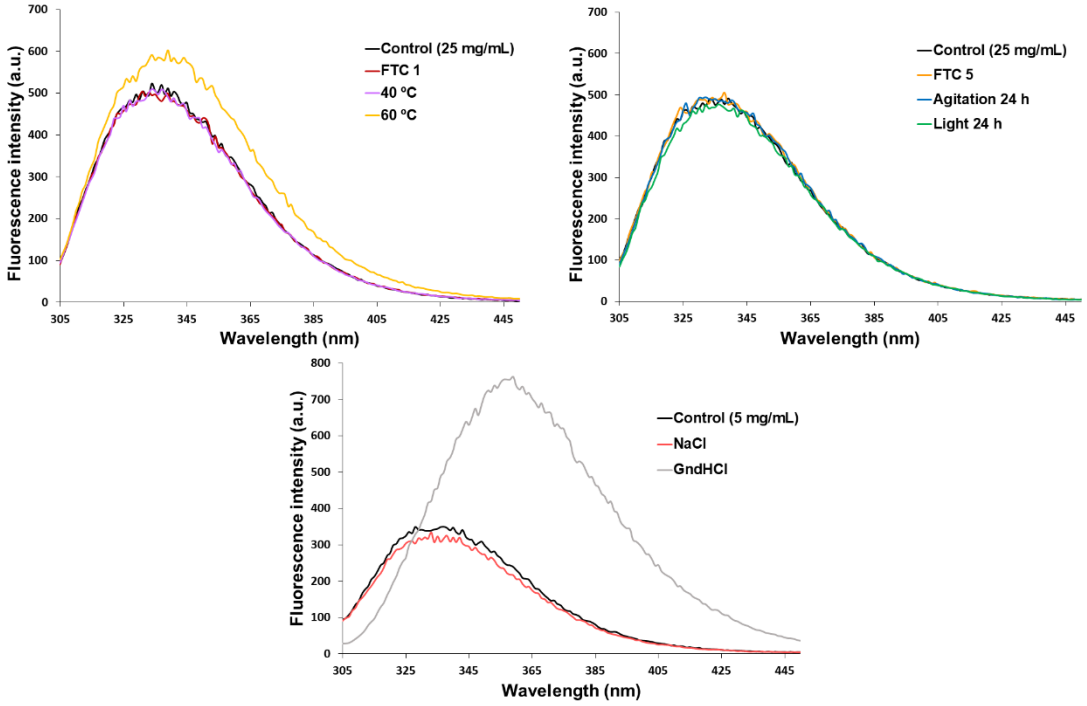

Figure 2. Intrinsic tryptophan fluorescence emission spectra of pembrolizumab medicine (25 mg/mL) and diluted (5 mg/mL) stressed and control samples.

Table 3. Calculated Centre of spectral Mass (C.M.) of pembrolizumab medicine (25 mg/mL) and diluted (5 mg/mL) stressed and control samples.

Sample	Stress	Centre of spectral mass (C.M.) of the fluorescence spectrum (nm)
25 mg/mL	Control	346
	40 ºC 1 h	346
	60 ºC 1 h	**349**
	FTC 1	346
	FTC 5	346
	Agitation 24 h	346
	Light stress 24 h	346
5 mg/mL	Control	346
	NaCl	346
	GndHCl	**367**

3.4. *Dynamic Light Scattering (DLS)*

Figure 3 shows the DLS results; the size distribution graphs of pembrolizumab medicine (25 mg/mL) and diluted samples (5 mg/mL) after stress testing are represented in comparison with their respective control. In addition, the main parameters assessed, that is, average D_h of the populations detected, polydispersity (Pd %) and PDI are included in Table 4.

The DLS control medicine sample (25 mg/mL), registered in duplicate, is characterised by a unique population with an average D_h of 9.6 ± 2.8 nm and 9.5 ± 2.8 nm respectively, both with PDI values of 0.08 and Pd (%) of 8 %. The control diluted sample (5 mg/mL) is also characterised by a unique population of 7.0 ± 2.1 nm, with a PDI of 0.07 and a Pd (%) of 8.5 %. These populations were highly monodispersed, associated with pembrolizumab monomers in solution.

After stressing the medicine samples (25 mg/mL), most of the parameters remained unchanged under most of the conditions tested except for the 60 ºC experiment; in this case, the D_h increased significantly from 9.6 nm to 10.7 nm. Similarly occurred to polydispersity parameters, PDI increased from 0.08 to 0.18 and the Pd (%) from 8 % to 22.8 %: this can be explained by a partial denaturation and starting aggregation of pembrolizumab.

In the case of diluted samples (5 mg/mL), the D_h increased significantly in the NaCl stressed sample: from 7.0 nm to 11.4 nm; in the case of GndHCl, the D_h increased significantly from 7 nm to 21.4 nm and the PDI value also increased significantly from 0.07 to 0.18. NaCl sample showed a bigger D_h, interpreted as a larger apparent hydrodynamic size, which is contribution of the molecule's hydration shell due to the salt ions. GndHCl stressed sample was characterised by a significantly bigger D_h, explained by a complete denaturation of pembrolizumab, which increases its real size, thus affecting its diffusion properties.

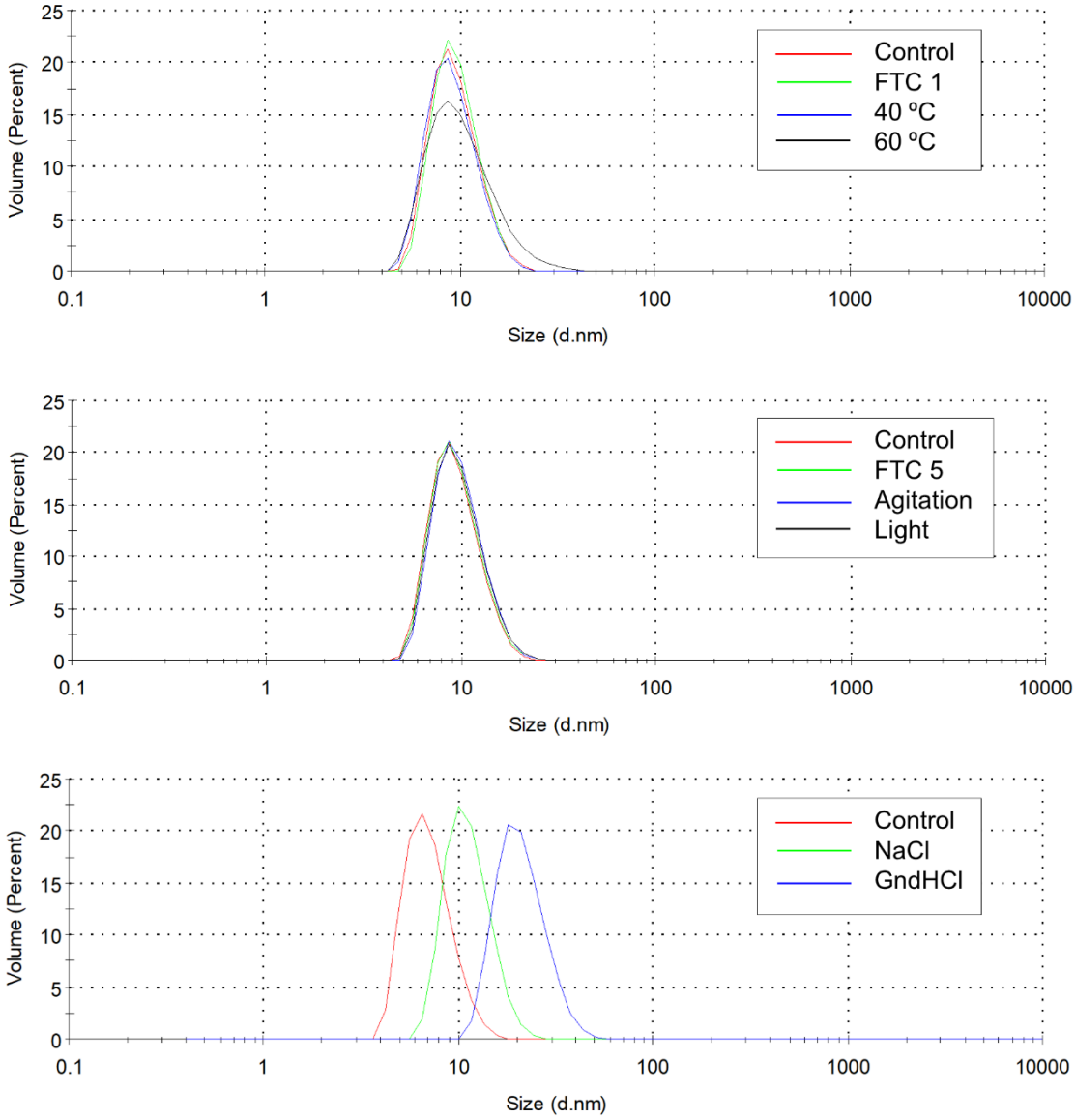

Figure 3. Size distribution graphs by volume of pembrolizumab medicine (25 mg/mL) and diluted (5 mg/mL) stressed and control samples.

Table 4. DLS parameters of pembrolizumab medicine (25 mg/mL) and diluted (5 mg/mL) stressed and control samples.

Sample	Stress	HD (nm)	PDI	Pd (%)
25 mg/mL	Control 1	9.6 ± 2.8	0.08	8.0
	40 ºC 1h	9.4 ± 2.8	0.08	8.4
	60 ºC 1h	**10.7 ± 4.6**	**0.18**	**22.8**
	FTC 1	9.7 ± 2.6	0.04	6.8
25 mg/mL	Control 2	9.5 ± 2.8	0.08	8.0
	FTC 5	9.6 ± 2.8	0.08	8.4
	Agitation 24h	9.9 ± 2.9	0.07	8.1
	Light stress 24h	9.8 ± 2.9	0.07	8.7
5 mg/mL	Control	7.0 ± 2.1	0.07	8.5
	NaCl	**11.4 ± 3.1**	**0.07**	**6.6**
	GndHCl	**21.4 ± 6.3**	**0.18**	**8.3**

In bold type is highlighted those parameters that were significantly different to control values.

3.5. Isoform analysis by RP/UHPLC(UV)-(HESI/Orbitrap)MS

The particular isoform profile of pembrolizumab fresh and stressed samples was identified using the LC-MS method described in the materials and methods section. The pembrolizumab mass spectra profile was characterised under denatured conditions for all the samples. Pembrolizumab control sample showed five main isoforms: A2G0F/A2G0F was identified as the main glycoform, followed by A2G0F/A2G1F, A2G1F/A2G1F and, in a smaller and similar proportion A2G0F/A1G0F and A2G0F/A2G0 (Figure 4).

Most of the stressed samples of pembrolizumab showed exactly the same isoform profile as the control sample, which indicates that the applied stresses did not provoke significant chemical modifications in the main isoforms proposed (Figure 4). However, the exposition of pembrolizumab to accelerated light degradation for 24 hours did cause modification on the isoform profile. In this case, as the only exception, there was a splitting of the three main isoforms (A2G0F/A2G0F, A2G0F/A2G1F and A2G1F/A2G1F) in which new masses slightly below and above the mass corresponding to the main isoforms proposed for the control sample were obtained (Figure 4).

Table 5 shows the experimental masses obtained for each isoform and the glycoforms associated with their relative abundance (%) and error (ppm) for the control and stressed samples of pembrolizumab. To calculate the theoretical masses, 2N-terminal pyroglutamate formation, 2C-terminal lysine clipping and 16 disulphide bonds were considered.

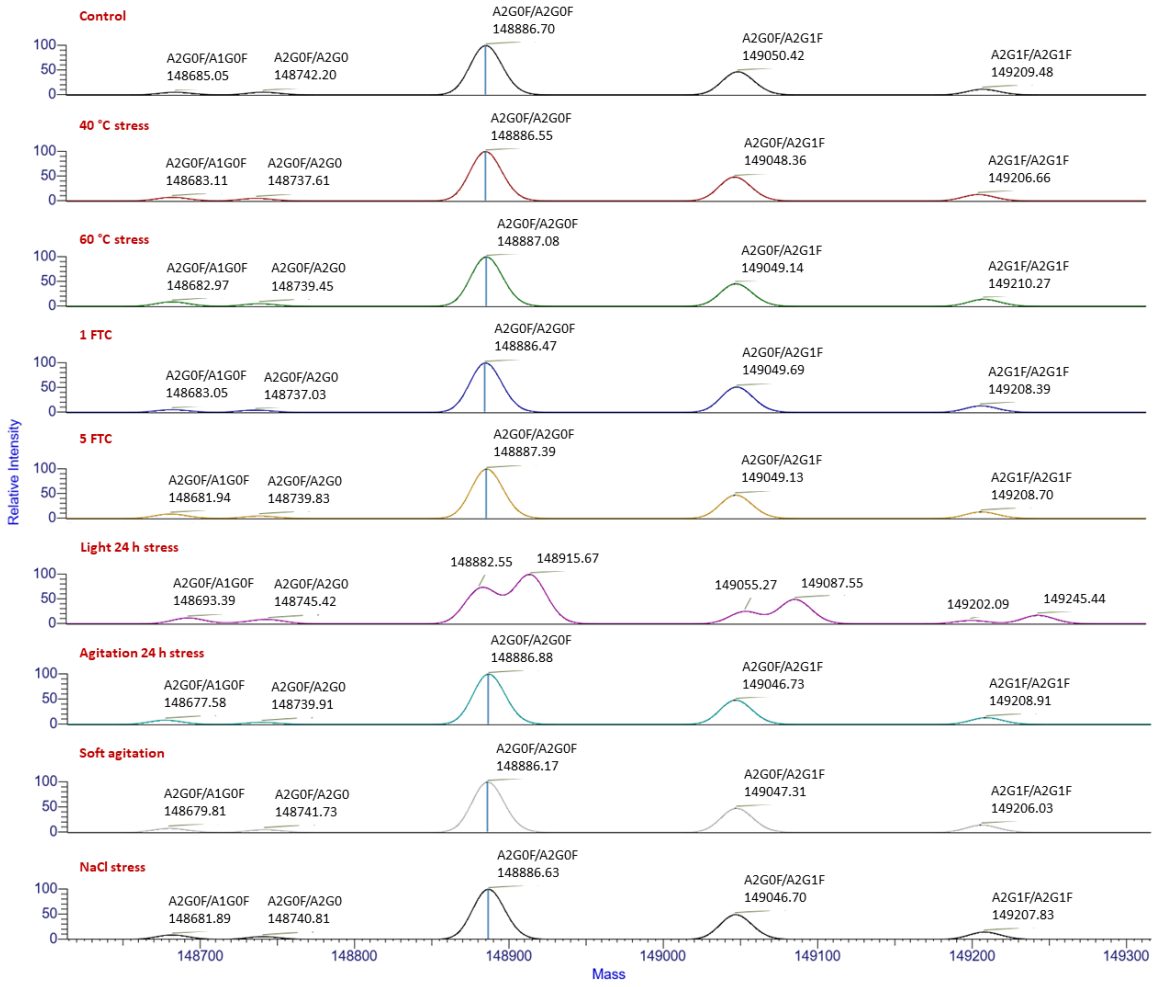

Figure 4. Deconvoluted mass spectra for pembrolizumab medicine samples (25 mg/mL) showing the mass isoform profile with their proposed N-glycoforms.

Table 5. Experimental masses and relative abundances of N-glycoforms for intact pembrolizumab in denatured conditions for control and stressed samples. Theoretical masses were calculated considering two C-term lysine clipping, two N-term pyroglutamate formation and 16 disulphide bonds.

	Glycoforms associated	Experimental mass (Da)	Theoretical average mass (Da)	Mass difference (Da)	Mass difference (ppm)	Relative abundance (%)
Control	A2G0F/A1G0F	148685.1	148684.1	-0.9	-6.4	3.0
	A2G0F/A2G0	148742.2	148741.2	-1.0	-7.0	3.1
	A2G0F/A2G0F	148886.7	148887.3	0.6	4.0	59.5
	A2G0F/A2G1F	149050.4	149049.4	-1.0	-6.6	27.7
	A2G1F/A2G1F	149209.5	149211.6	2.1	14.1	6.6
40 ºC, 1h	A2G0F/A1G0F	148683.1	148684.1	1.0	6.7	4.1
	A2G0F/A2G0	148737.6	148741.2	3.6	23.9	2.9
	A2G0F/A2G0F	148886.6	148887.3	0.8	5.0	57.7
	A2G0F/A2G1F	149048.4	149049.4	1.1	7.2	27.9
	A2G1F/A2G1F	149206.7	149211.6	4.9	33.0	7.4
60 ºC, 1h	A2G0F/A1G0F	148683.0	148684.1	1.1	7.6	5.1
	A2G0F/A2G0	148739.5	148741.2	1.7	11.5	2.9
	A2G0F/A2G0F	148887.1	148887.3	0.2	1.5	57.7
	A2G0F/A2G1F	149049.1	149049.4	0.3	2.0	26.3

Table 5 (continuation)

	A2G1F/A2G1F	149210.3	149211.6	1.3	8.8	8.0
FTC 1	A2G0F/A1G0F	148683.1	148684.1	1.1	7.1	3.0
	A2G0F/A2G0	148737.0	148741.2	4.1	27.8	2.6
	A2G0F/A2G0F	148886.5	148887.3	0.8	5.6	57.6
	A2G0F/A2G1F	149049.7	149049.4	-0.3	-1.7	29.4
	A2G1F/A2G1F	149208.4	149211.6	3.2	21.4	7.4
FTC 5	A2G0F/A1G0F	148681.9	148684.1	2.2	14.5	5.1
	A2G0F/A2G0	148739.8	148741.2	1.3	8.9	2.7
	A2G0F/A2G0F	148887.4	148887.3	-0.1	-0.6	57.5
	A2G0F/A2G1F	149049.1	149049.4	0.3	2.1	27.1
	A2G1F/A2G1F	149208.7	149211.6	2.9	19.3	7.5
Light 24h	A2G0F/A1G0F	148693.4	148684.1	-9.3	-62.5	4.2
	A2G0F/A2G0	148745.4	148741.2	-4.3	-28.6	2.9
	—	148882.6	—	—	—	22.8
	—	148915.7	—	—	—	35.0
	—	149055.3	—	—	—	9.0
	—	149087.6	—	—	—	17.7
	—	149202.1	—	—	—	2.3

Table 5 (continuation)

	—	149245.4	—	—	—	6.1
Agitation 24h	A2G0F/A1G0F	148677.6	148684.1	6.5	43.9	4.7
	A2G0F/A2G0	148739.9	148741.2	1.3	8.4	2.2
	A2G0F/A2G0F	148886.9	148887.3	0.4	2.8	57.7
	A2G0F/A2G1F	149046.7	149049.4	2.7	18.2	27.8
	A2G1F/A2G1F	149208.9	149211.6	2.7	17.9	7.6
Soft agitation	A2G0F/A1G0F	148679.81	148684.1	4.3	28.9	0.6
	A2G0F/A2G0	148741.73	148741.16	-0.6	-3.8	3.0
	A2G0F/A2G0F	148886.17	148887.3	1.1	7.6	59.7
	A2G0F/A2G1F	149047.31	149049.44	2.1	14.3	28.3
	A2G1F/A2G1F	149206.03	149211.58	5.6	37.2	8.4
NaCl	A2G0F/A1G0F	148681.89	148684.1	2.2	14.9	5.0
	A2G0F/A2G0	148740.81	148741.16	0.4	2.4	3.1
	A2G0F/A2G0F	148886.63	148887.3	0.7	4.5	56.1
	A2G0F/A2G1F	149046.7	149049.44	2.7	18.4	27.6
	A2G1F/A2G1F	149207.83	149211.58	3.8	25.1	8.2

3.6. Aggregation Study by SE/UHPLC(UV)

The chromatographic profiles of fresh and stressed samples of pembrolizumab were compared in order to detect changes in their aggregates' profile given that aggregation is an indicator of protein degradation. The control sample of pembrolizumab (fresh medicine 25 mg/mL) shows a main peak at 9.04 ± 0.02 min (95.0 ± 0.2 % of the total area) in its SE chromatogram (Figure S2). This main peak was assigned to pembrolizumab monomer while the small peak just before the main one, which elute at 8.63 ± 0.01 min (5.0 ± 0.2 % of the total area), was assigned to the natural dimers present in the medicine. The identification of the peaks was based on the indications of the chromatographic column used for this analysis, i.e., a specific column for mAbs aggregate analysis [25] (Figure S3).

Figure 5 shows the different SE chromatograms regarding the forced degradation study. Every chromatogram represents a comparison between pembrolizumab control sample and the different stresses to which pembrolizumab samples were exposed. Moreover, Table 6 presents the retention times and proportions of the peaks detected in the chromatograms of the different pembrolizumab samples. Observing these results, no changes were detected in the SEC profile for most of the stressed samples of pembrolizumab. However, in the samples exposed to 60 °C appeared a big new peak before the dimers, which was assigned to high molecular weight species (HMWS), and the samples exposed to light (24 h) showed an increase in the dimers' peak proportion and two new peaks were detected, also attributed to HMWS. Therefore, the monomer proportion for these two stressed samples was reduced given the appearance of new aggregate species.

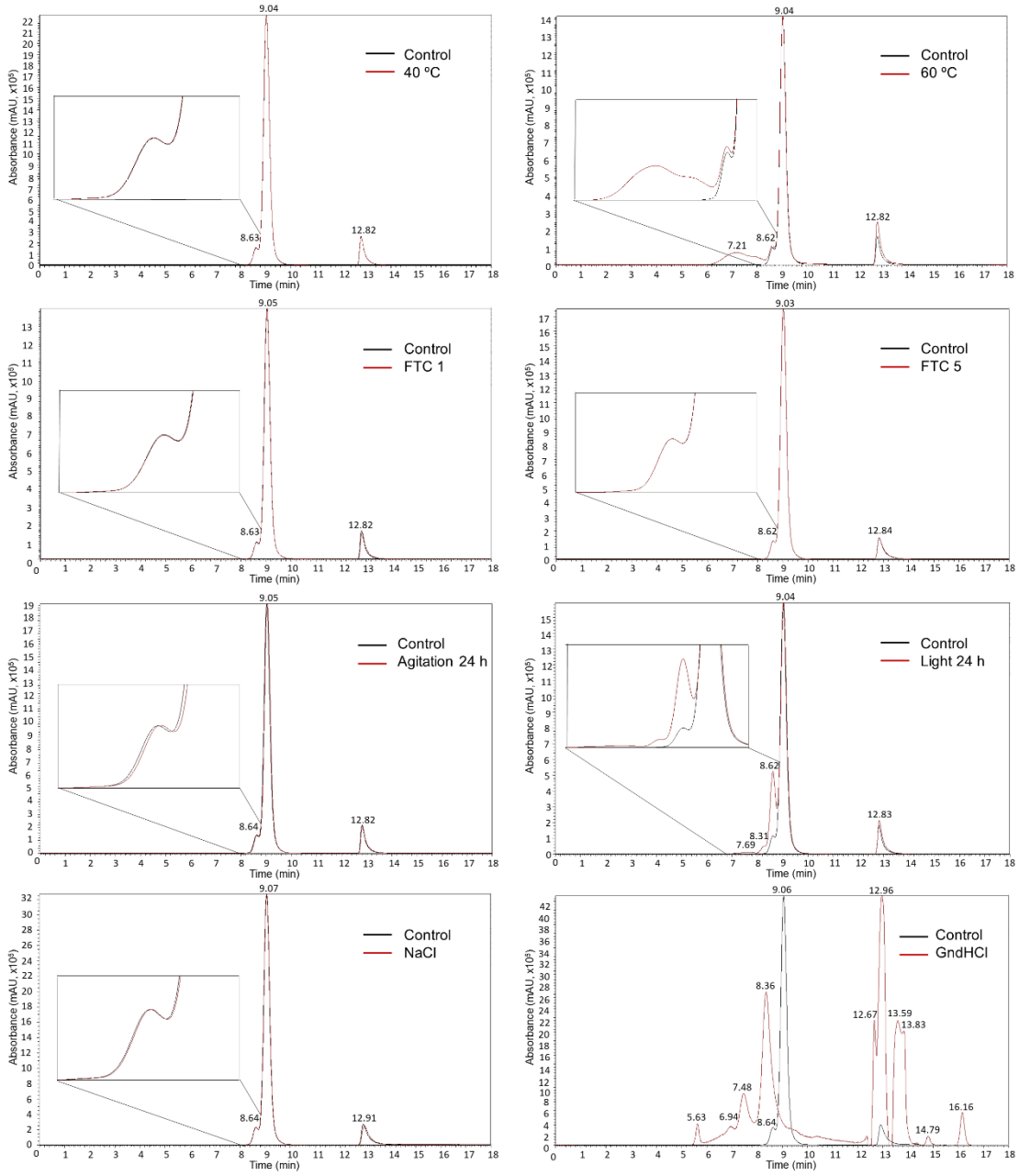

Figure 5. SE/UHPLC(UV) chromatograms for the different stressed samples of pembrolizumab (25 mg/mL) compared to the control sample (unstressed pembrolizumab).

Table 6. Overall results for experimental retention time and relative proportions of the control (mean ± standard deviation from 3 replicates) and stressed samples in the SEC analysis. Results that are significantly different from the control are indicated in bold type.

Stress	Monomer		Dimer		HMWS 1		HMWS 2	
	Retention time (min)	Proportion (%)	Retention time (min)	Proportion (%)	Retention time (min)	Proportion (%)	Retention time (min)	Proportion (%)
Control	9.04 ± 0.02	95.0 ± 0.2	8.63 ± 0.01	5.0 ± 0.2	-	-	-	-
40 ºC 1h	9.04	95.1	8.63	4.9	-	-	-	-
60 ºC 1h	9.04	**85.9**	8.62	5.2	**7.21**	**8.9**	-	-
FTC 1	9.05	95.2	8.63	4.8	-	-	-	-
FTC 5	9.03	95.0	8.62	5.0	-	-	-	-
Agitation 24h	9.05	94.8	8.64	5.2	-	-	-	-
Light stress 24h	9.04	**75.6**	8.62	**21.4**	**8.31**	**1.6**	**7.69**	**1.3**
NaCl	9.07	94.7	8.64	5.3	-	-	-	-
GndHCl	-	-	-	-	-	-	-	-

The chromatogram of the sample exposed to GndHCl shows a protein completely denatured given the denaturing capacity of this compound. For this reason, this stress was used as a control sample to test the ability of the technique to detect aggregates.

In all the SEC profiles a non-assigned chromatographic peak was detected at 12.87 ± 0.05 min. However, this peak was not considered a sign of protein degradation since it was also detected in the control (fresh medicine) samples, it was also invariant in all the samples, and even, a similar peak was also detected in similar experiments in others mAbs products, such as Opdivo® (nivolumab) [18].

3.7. Peptide mapping analysis by RP/UHPLC(UV)-(HESI/Orbitrap)MS/MS

Peptide mapping analysis is a comprehensive tool for protein characterisation which consists in performing a proteolysis of the biotherapeutic and a subsequent LC-MS/MS analysis of the peptides. Pembrolizumab control and stressed samples were subjected to the tryptic digestion described in the materials and methods section, allowing us to determine the PTMs present in pembrolizumab fresh (control) sample and the possible variations of these PTMs after subjecting the medicine to the different stresses considered along this study. The sequence coverage obtained after the deconvolution of the MS/MS data was 100 % (Figure S4).

In this work, we checked the most common PTMs in mAbs, i.e., pyroglutamate formation, deamidations, isomerisations and oxidations, as well as the N-glycan profile in pembrolizumab from medicine (Keytruda®) and stressed samples. For every PTM studied, the abundance (%) was calculated and the results of the stressed samples were compared to the control one. Peptide mapping analysis gives site-specific information of the detected PTMs, which allows us to specifically determine the implications of such modifications when variations occur due to a specific stress of the medicine compared to the control sample. In this case, all the samples (control and stressed) showed around 94 % of pyroglutamate formation (Figure S5) in N-terminal position, therefore, this PTM is characteristic of pembrolizumab and no derived from the stress applied.

Regarding deamidations, the most abundant deamidated positions detected were at positions N55 and N315, while Q6, Q41 and Q159 were also deamidated but in a lower abundance. As for isomerisations, there were only two positions affected, which were D126 and D401. However, in all these cases, abundances were lower than 2 %. It was therefore proposed that neither deamidation nor isomerisation was present in pembrolizumab in either control or stressed samples.

In terms of oxidation, it is a common modification at methionine and tryptophan residues, and the main oxidised position detected in pembrolizumab was M105 (around 30 %

of abundance), although there were less abundant oxidation positions such as W110, M252, M358 and M428, with abundances lower than 3 % (Figure 6A). For all these residues, a significant increase in abundance is observed when samples are subjected to light stress for 24 h, indicating that light exposure leads to increased oxidations in pembrolizumab. The detected high abundance of the oxidation in M105 could be attributed to the sample treatment required for the digestion procedure as this oxidation showed the same abundance for both control and stressed samples (except for light exposure stress, in which clearly increase this oxidation as the results of the stressor applied). Thus, the high abundance of oxidation at that position may not be attributed to stress exposure, apart from light-stressed sample, and this could indicate that M105 is easily oxidisable with respect to the other methionine residues. It is important to mention that M105 position is within the Complementary Determining Region (CDR) domain and it is involved in van der Waals contact with PD-1 receptor [26]. Therefore, an oxidation in that position could compromise the effective binding of pembrolizumab to PD-1, which is the case for samples subjected to light stress, as discussed in section 3.8.

The conserved N-glycosylation site of pembrolizumab is at position N297 of the heavy chain, showing the glycoforms A2G0F, A1G0F and A2G1F as the most abundant after peptide mapping analysis. A2G0, A1G1F, A1G0, A2G2F and M5 glycoforms were also found in lower abundance (Figure 6B). As expected, there was no variation in abundance between control and stressed samples for all glycoforms detected, and the unglycosylated pembrolizumab was around 0.8 % of abundance.

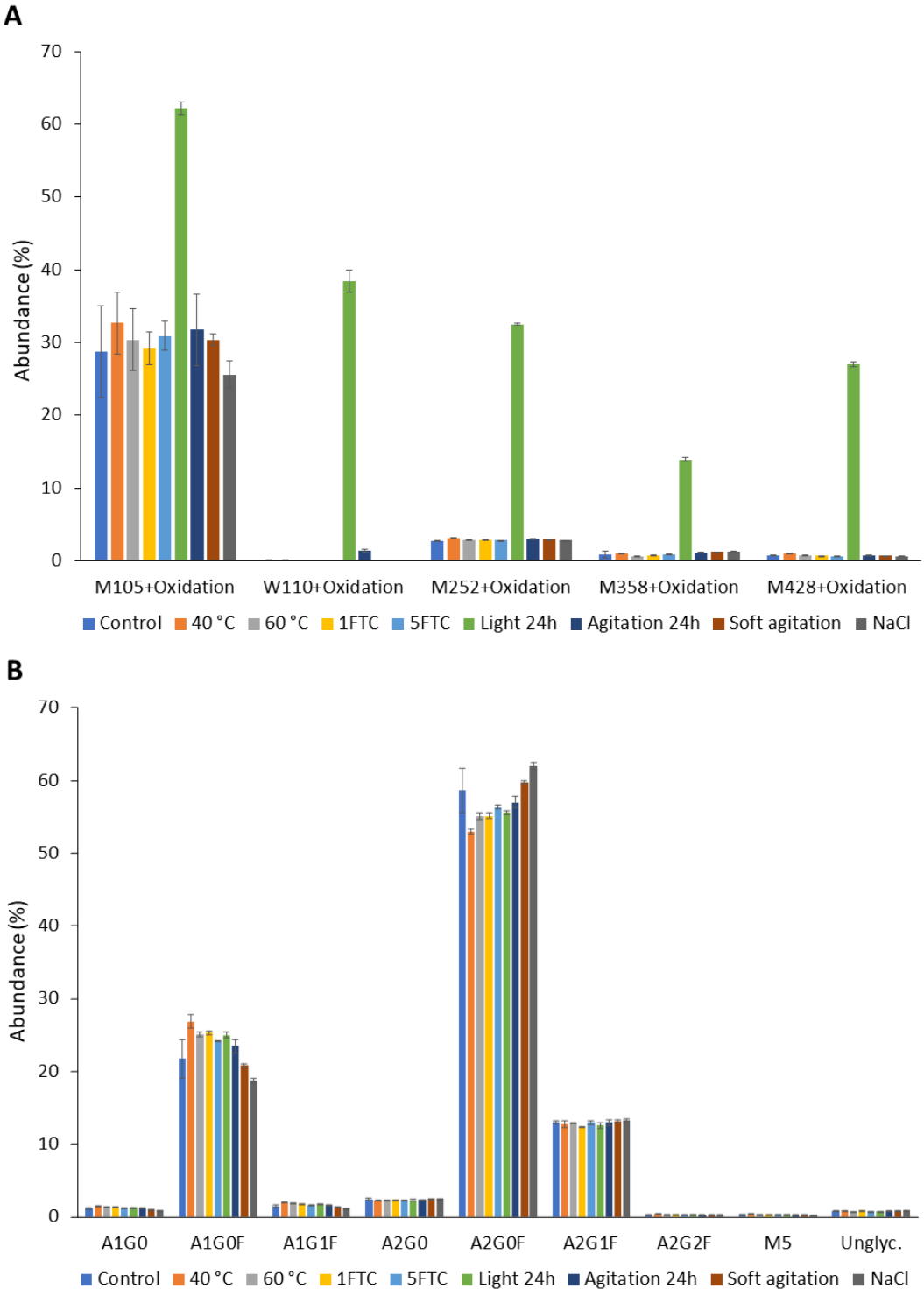

Figure 6. PMTs in pembrolizumab control and stressed samples: (A) oxidations; and (B) N-glycans.

It is also interesting to mention that peptide mapping results of pembrolizumab showed some similarities with the ones of nivolumab. Both are IgG4 mAbs and share similar positions

for the different amino acids, where we can also find similar PTMs at those positions. The manuscript with the results for peptide mapping of nivolumab is in preparation for submission for publication shortly, and will include a comparative discussion between these two IgG4 therapeutics.

3.8. ELISA

ELISA can be used to evaluate the impact of the physicochemical modifications that stress conditions may cause in mAbs functionality. These modifications can impair the effectiveness of these kind of medicines. By means of ELISA, the biological activity of pembrolizumab after its exposure to the different stresses considered in this study can be evaluated by measuring the antibody-antigen binding capacity.

For the study of pembrolizumab control and stressed samples, the first stage was to validate the ELISA method developed in previous studies [18] for testing pembrolizumab biological activity. The mathematical function that best fit the experimental data was selected as the calibration model (standard calibration curve in Figure S6). In this case, the most suitable mathematical model for calibration purposes was the double reciprocal since its R^2 (99.19) demonstrates the goodness of fit of this model (Table 7).

Table 7. Characteristic parameters of the standard calibration curve (calibration model) and the figures of merit of the ELISA method.

Parameter	**Value**
Mathematical model fitted	Double reciprocal
Function	Y = 1 / (0.4529 + 10.1256 / X)
s_a	0.0195
s_b	0.1912
R^2 (%)	99.19
P-value	0.7684

[a] Standard deviation of the intercept.

[b] Standard deviation of the slope.

For further validation of this method, repeatability and intermediate precision, both expressed as RSD (%), as well as accuracy, expressed as R (%), were studied (Table 8). It is important to consider that, for immunoassays, minimal acceptance limits of 20 % are recommended [27,28]. Therefore, this model fulfilled the precision criteria indicated for bioanalytical method validation. The recovery values were between 96 % and 101 %, which

indicates the high quality of this ELISA method, especially considering the huge variability inherent in immunoassays.

Table 8. Accuracy and precision of the ELISA method.

Pembrolizumab concentration (ng/mL)	R (%)[a]	RSD (%)[b]	
		Intraday	Interday (3 days)
25	96	2.38	7.39
10	99	4.08	10.98
5	101	8.03	14.46

[a] Recovery value based on three determinations;

[b] Relative standard deviation based on three determinations.

After the validation of the ELISA method proposed for pembrolizumab, it was used to evaluate the biological activity of the different stressed samples of this mAb. Figure 7 gathers the results of the ELISA assays. For the analysis of each stressed sample, the calibration graph was obtained and compared with the graph of the control (fresh) sample. A Student's *t* analysis was performed in order to detect statistically significant differences between the control and the stressed samples: in Figure X the results marked with asterisks are significantly different (one asterisk, p-value < 0.05) and very significantly different (two asterisks, p-value < 0.001) from the control.

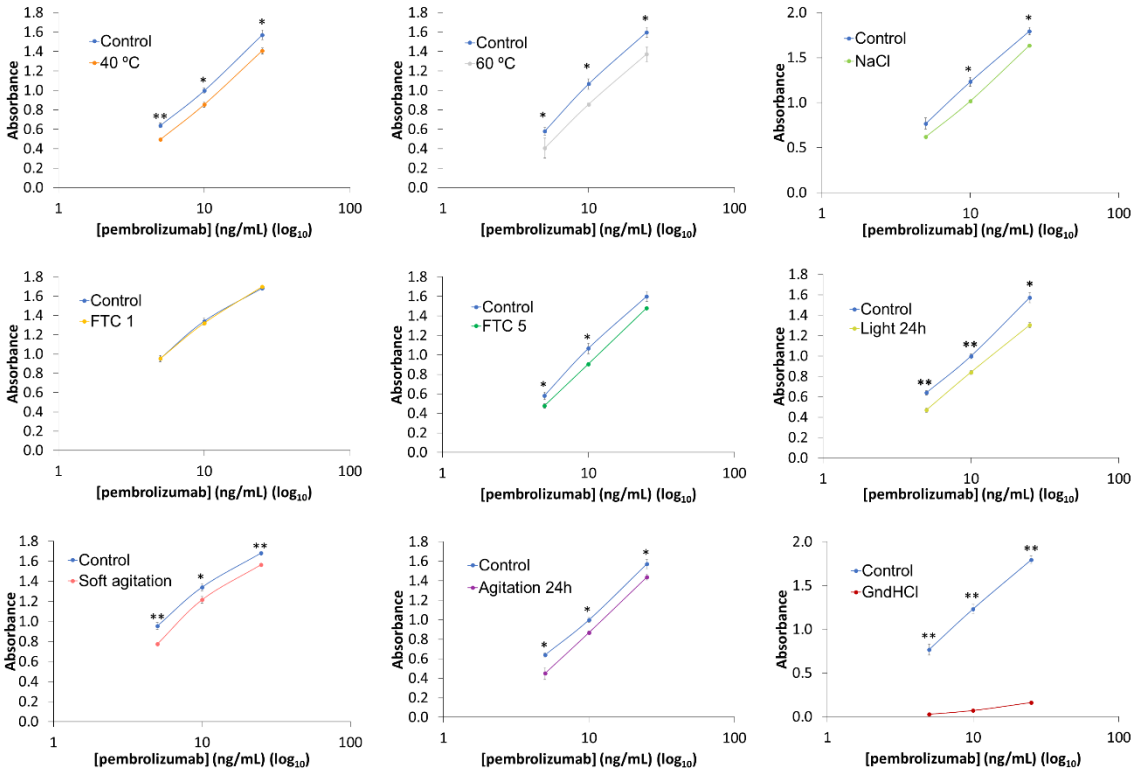

Figure 7. ELISA binding assay (5, 10 and 25 ng/mL) for the stressed samples as compared to a fresh (control) sample of pembrolizumab (*: *p*-value < 0.05; **: *p*-value < 0.001).

Results indicate that most of the applied stresses lead to a loss of the ability of pembrolizumab to bind to the PD-1 receptor, as most of them show a significant difference in absorbance values when comparing the graphical function of the stressed samples with that of the control sample. In the case of the samples stressed by light (24 h), soft agitation and GndHCl (positive control for protein denaturation) the difference in absorbance values is mostly highly significant. The only case where no change is observed between the stressed sample and the control sample is in the FTC1 stress. These results highlight the susceptibility of pembrolizumab to exposure to stressful conditions. Table 9 shows an estimation (in percentage) of the remaining activity in the stressed samples of pembrolizumab, considering a PD-1 binding capacity of 100 % for the control sample. We can observe that the highest loss of biological activity occurs in the GndHCl-stressed sample, as expected, followed by the sample stressed at 60 °C, light (24 h) and agitation (24 h) exposure, which show a loss of activity around 20 %.

Table 9. Percentage estimation of the remaining activity in stressed nivolumab samples by ELISA.

Stress	Remaining activity (%)
40 ºC 1h	84.1 ± 6.2
60 ºC 1h	78.8 ± 8.0
FTC 1	99.9 ± 1.2
FTC 5	86.6 ± 5.3
Soft agitation	88.3 ± 6.2
Agitation 24 h	82.9 ± 11.2
Light 24 h	80.2 ± 5.8
NaCl	84.8 ± 5.6
GndHCl	6.1 ± 2.7

4. Discussion

In this study, pembrolizumab fresh control samples were characterized in its medicine formulation (Keytruda®, 25 mg/mL) by different analytical techniques. This control samples were then compared to pembrolizumab stressed samples that had been subjected to a range of different stress conditions with the aim of detecting and identifying possible denaturation, aggregation or structural modifications of the medicine. Throughout this discussion, a comparison will also be made between the results obtained with pembrolizumab and those obtained with nivolumab (an IgG4 protein like pembrolizumab) in a similar work by the same authors [18].

Pembrolizumab medicine (Keytruda®, 25 mg/mL) secondary structure consists mainly of β-sheet (48 %) and unordered (39 %) contents (Table 2) as expected in mAbs [24,29], and its spectral parameters showed a negative maximum at 218 nm, shoulder at around 230 nm and wavelength at ellipticity 0 of around 209 nm. Pembrolizumab tertiary structure was characterised by IT-FS and it showed a C.M. of 346 nm (Table 3) either for the undiluted (25 mg/mL) or diluted (5 mg/mL) medicine, indicating Trp residues are buried into the protein structure, as expected. The DLS results indicated the existence of a single size population attributed to pembrolizumab monomers with a D_h of around 9.6 nm and a polydispersity of 8 % for the undiluted samples, while the diluted sample (5 mg/mL) showed a D_h of around 7.0 nm and a polydispersity of 8.5 % (Table 4). SEC profiles highlighted that pembrolizumab is

composed of monomers and natural dimers in relative proportions of around 95 % and 5 %, respectively (Table 6). The denatured LC-MS isoform profile indicated five main glycoforms, which were assigned to A2G0F/A2G0F, A2G0F/A2G1F, A2G1F/A2G1F, A2G0F/A1G0F and A2G0F/A2G0, in accordance with their particular masses (Figure 4 and Table 5). The most abundant glycoform corresponds to A2G0F/A2G0F, which was confirmed with the peptide mapping results given that A2G0F was found as the most abundant N-glycan present in pembrolizumab. Peptide mapping analysis also confirmed the presence of the other N-glycans detected by denatured intact analysis, i.e., A1G0F, A2G1F and A2G0, and some others in less abundancy, i.e., A1G1F, A1G0, A2G2F and M5. As for PTMs, pembrolizumab showed a very high percentage (around 94 % of abundance) of pyroglutamate formation and it also revealed positions more prone to suffer deamidations and/or oxidations (Figure 6).

The heat stress study was performed by subjecting pembrolizumab medicine (Keytruda®) to two different high temperatures for 1 h: 40 °C and 60 °C. For the samples stressed at 40 °C, there were no significant changes in the medicine given that all the analytical techniques employed to characterise this samples indicated similar results to the control samples. However, although no changes were observed, ELISA results showed a decrease in the PD-1 binding capacity of pembrolizumab (Figure 7) and a loss of activity of around 16 % (Table 9). Regarding the stress at 60 °C, more changes were detected. CD results revealed a significant change in the wavelength at ellipticity=0, negative maximum and shoulder with respect to control sample (Table 1) and a slight transformation of β-sheets to α-helix (Table 2). As for the tertiary structure, the Trp residues are more exposed to the polar solvent, which was indicated by a red shift of their spectra emission maxima (C.M. from 346 nm in the control sample to 349 nm in the stressed one (Table 3)). Also, there is an increase in the fluorescence intensity that could be attributed to an increase in the quantum yield as a consequence of the greater exposure of the Trp residues to the polar solvent (Figure 2). This aggregation is confirmed by DLS and SEC, where DLS showed a significant increase in the D_h (from 9.6 nm in the control to 10.7 nm in the stressed sample) and polydispersity (from 8 % to 22.8 %) (Table 4), and SEC revealed the detection of HMWS, confirming all this the presence of aggregates after the heat stress at 60 °C/1h (Figure 5). LC-MS showed a similar isoform profile to the control sample, with no new detected N-glycoforms. ELISA results indicate a significant loss of functionality, maintaining a remaining activity of around 79 % (Table 9), which undoubtedly can be attributed to the increase of aggregates. In the case of nivolumab, none of the heat stresses provoked either aggregate formation or loss of biological activity, showing that nivolumab has a better resistance to high temperatures [18].

Freeze/thaw cycles (FTC) may cause a partial denaturation of the protein given the disturbance of the local structure on the surface of this protein during freezing. Thus, this

disturbance can lead to protein aggregation [30]. However, no changes were detected in pembrolizumab in either FTC1 or FTC5 stresses. CD and IT-FS results showed no modifications in pembrolizumab secondary and tertiary structure. In the same way, DLS and SEC did not reveal any new populations or aggregation. Also, the isoform profile remained unchanged for both FTC stresses. Also, pembrolizumab-PD-1 binding capacity decreased to around 87 % for the FTC5 stress (Table 9). Although Keytruda® technical report indicates not to freeze the medicine [4], these results showed that nothing happened to the medicine with just one FTC while five cycles showed a loss of functionality, and this is in line with the instructions of the technical report. When comparing these results with the nivolumab study, we found that nivolumab binding capacity to PD-1 receptor was also affected by FTC, although, in this case, both 1 and 5 cycles showed a slight decrease in the binding capacity. Such decreases (around 90 %) were similar to the one obtained after subjecting pembrolizumab to 5 FTC. Also, similarly to pembrolizumab, there were no other physicochemical modifications in nivolumab after subjecting it to 1 and 5 FTC [18].

Agitation for 24 h had not significant effect on the physicochemical parameters studied since the secondary and tertiary structure remained unaltered compared to the control sample by means of the methodology applied. The CD spectrum and IT-FS profile are similar to the control sample and the C.M. values were exactly the same. Moreover, there were no new particulate in the stressed sample which was confirmed by DLS. SE/UHPLC(UV) demonstrated that the relative proportion of monomers and dimers remained unchanged, while RP/UHPLC(UV)-(HESI/Orbitrap)MS/MS showed the same isoform profile as the control sample. Nevertheless, ELISA indicated a loss of functionality with a reduction of around 17 % of its PD-1-binding capacity (Figure 7 and Table 9). This fact could not be explained by the physicochemical results obtained. Therefore, we decided to test if a soft agitation could also provoke a loss of functionality in pembrolizumab. ELISA results indicate that soft agitation of the medicine during 1 min can also lead to a reduction in the capacity of pembrolizumab to bind to PD-1 (Figure 7), which showed a remaining activity of around 88 % (Table 9). In a similar way, nivolumab did not show any physicochemical modification after exposure to agitation stress for 24 h, although it showed a reduction in its capacity to bind to PD-1 of around 20 % -very similar to pembrolizumab-. In this case, soft agitation was not necessary to be performed [18].

Regarding the accelerated light exposure stress for 24 h, there were no changes detected in the secondary and tertiary structure since CD and IT-FS showed similar results to the control sample. In a similar way, DLS did not show the appearance of new populations after the light exposure as the D_h and polydispersity had similar values to the control. Nevertheless, non-natural aggregation was observed by SE/UHPLC(UV) since HMWS were

clearly detected in the SEC profile of the stressed sample as well as an increase in the dimers' peak when compared to the control one. In Table 6 we can see a reduction in the monomers proportion (from 95 % in the control sample to 75.6 % in the light stressed one) while increasing the dimers proportion (from 5.0 % to 21.4 %) and the HMWS were detected as two new different populations. Although the proportion of the HMWS is very small, we can clearly see them in Figure 5, right before the dimers' peak. It is important to mention that this behaviour after light exposure is common in mAbs as indicated in previous works, which corroborate that this kind of stress induces aggregation in this type of proteins [18,31,32]. The aggregation of pembrolizumab may have affected its binding capacity to the PD-1 receptor. Moreover, light exposure induced oxidation in pembrolizumab samples as clearly revealed by LC-MS/MS peptide mapping analysis, where we identified significant increases in the abundance of oxidated residues, specifically at M105, W110, M252, M358 and M428 positions (Figure 6A). The high oxidation of M105 likely have affected the binding capacity of pembrolizumab to PD-1, as it is part of the pembrolizumab CDR. It is also interesting to mention that the isoform profile was different from that of the control sample as each of the three main glycoforms for the control sample, i.e., A2G0F/A2G0F, A2G0F/A2G1F and A2G1F/A2G1F, were split into two for the stressed sample, showing new masses (slightly above and below the mass corresponding to the control glycoforms) and no N-glycoforms could be attributed to these isoforms (Figure 4 and Table 5). This was attributed to chemical modifications on the protein part of pembrolizumab, such as the increase in oxidised amino acids, more than the chemical modifications on the N-glycan profile, which was corroborated unchanged by LC-MS/MS peptide mapping. ELISA results indicate a statistically highly significant decrease in the absorbance intensity compared to the control sample (Figure 7) and around a 20 % reduction of pembrolizumab biological activity (Table 9). As for nivolumab study, we also observed aggregate formation after light exposure for 24 h. However, nivolumab showed a different behaviour in the formation of the new aggregates as there was just an increase in the dimers proportion with the consequent reduction of monomers, while pembrolizumab showed the formation of dimers as well as two new populations of HMWS. Light exposure also provoked the modification of the isoform profile for both pembrolizumab and nivolumab, attributing this fact to chemical changes caused by light such as oxidation in the protein core. In addition, ELISA showed a loss of biological activity of around 30 % for nivolumab, which is even higher than that of pembrolizumab (20 %) [18].

The high ionic strength stress had no effect on the secondary structure of pembrolizumab as the CD spectrum showed a similar shape and spectral features to the control sample. The same occurred with the tertiary structure, which indicated exactly the same C.M. value as the control sample, although the fluorescence intensity was a bit lower than the

control one. This could be attributed to an increase in hydration due to the salt ions around the molecule, which may cause a decrease in the quantum yield of Trp residues. This increase in hydration is corroborated with the increase in the D_h that can be observed in the DLS results (Table 4). Despite this increase in the D_h, DLS size distribution graphs showed a single population which correspond to the monomers (Figure 3). Therefore, there is no aggregate formation in pembrolizumab samples after the exposition to high ionic strength stress, which was also corroborated by SE/UHPLC(UV) since the monomers and dimers proportions remained unaltered (Table 6). Also, the isoform profile remained unchanged compared to the control sample. However, the ELISA graphical function of the NaCl stressed sample revealed two concentration points with a significant loss of PD-1 binding capacity (Figure 7) and the biological activity dropped to around 85 % (Table 9). With regard to nivolumab, it also showed an increase in the HD value and a decrease in its binding capacity to the PD-1 receptor (of around 10 %), which could be also attributed to the proposed increase in hydration [18].

As expected, the most dramatic changes in the structural integrity of pembrolizumab were caused by the GndHCl stress. GndHCl is a strong denaturing chaotropic, selected in this study as a positive control for pembrolizumab degradation. This denaturing agent was already used in previous studies in our group with the same purpose [24]. Regarding the conformation of the protein, the secondary and tertiary structures were significantly altered. The three parameters studied by CD showed notable changes as well as the C.M. value, which highly increased regarding the control sample. As regards aggregation, an important increase was observed by DLS in the D_h (from 7 nm to 21.4 nm) and PDI (from 0.07 to 0.18) (Figure 3 and Table 4), suggesting a hard denaturation of the protein and an aggregate formation. This was corroborated by SE/UHPLC(UV), in which we can observe the detection of new HMWS. Apparently, the monomers are transformed into dimers and HMWS since, observing the chromatogram (Figure 5), the monomers peak disappears while increasing the dimers peak and three new peaks appear right before the dimers, indicating the formation of aggregates. In this chromatogram, we can also see some peaks after the dimers, which could correspond to fragments of the protein as a consequence of the chaotropic denaturation provoked by the GndHCl. Regarding the functionality study, ELISA results showed almost a complete loss of biological activity, retaining only a 6 % of its binding capacity to PD-1 (Table 9). However, this loss of functionality was expected given the strong denaturing capacity of the GndHCl, which could also promote degradation, even at low concentration, of PD-1 on the ELISA plate.

5. Conclusion

Routine handling in hospitals, as well as transportation, development and manufacturing of biopharmaceuticals can compromise their stability given that they may be exposed to a wide range of environmental stress conditions during these different stages before patient administration, affecting the safety and efficacy of the medicine. For this reason, the present work focuses on the study of the effects that hospital handling may have on pembrolizumab (Keytruda®, 25 mg/mL) physicochemical and functional characteristics. To assess the impact of stressful conditions on this medicine, various stress tests were carried out. Results indicate that accelerated light exposure is the most harmful environmental condition for pembrolizumab, as it causes non-natural aggregation (increase in dimers proportion and appearance of HMWS) as well as a promotion of oxidations. These chemical changes alter the isoform profile and lead to a reduction in the binding capacity of pembrolizumab to its therapeutic target, the PD-1 receptor. Given these results, it is very important to storage and handle pembrolizumab protected from light. Moreover, pembrolizumab is also affected by the exposition to high temperatures, especially to 60 °C, where we found HMWS after the analysis by SE/UHPLC(UV) and a loss of around 20 % of the biological activity tested by ELISA. However, the exposure to 40 °C did not cause aggregation although a slight loss (16 %) of its capacity to bind to PD-1 receptor was noted. Therefore, the exposition to high temperatures should be avoided while handling pembrolizumab in hospitals or during transportation to assure the safety and efficacy of the medicine. As for FTC1 and FTC5, even though no significant physicochemical modifications were observed, the biological activity of pembrolizumab after FTC5 stress was affected, showing a reduction in its binding capacity to PD-1. For this reason, pembrolizumab (Keytruda®, 25 mg/mL) should not be frozen as indicated in its technical report. In the same way, agitation stress showed no conformational changes, aggregation or particulate, but a loss of biological activity. This loss was also observed after subjecting pembrolizumab to a soft agitation, indicating that this protein is highly sensitive to agitation. Therefore, agitation should be avoided when handling Keytruda® (25 mg/mL) in hospitals. Caution must also be taken when preparing dilutions of the medicine in NaCl, as an increase in hydration of the molecule was observed by DLS after its exposure to a highly hypertonic solution, with a consequent reduction (15 %) in the binding capacity of pembrolizumab to the PD-1 receptor. It is important to highlight that all these experiments were conducted using open vials of Keytruda® (25 mg/mL). As expected, pembrolizumab, as a biopharmaceutical product, is highly sensitive to exposure to different environmental stress conditions, showing a particular sensitivity to lose some of its binding capacity to its therapeutic target measured by means of ELISA.

Acknowledgments

Anabel Torrente-López is currently receiving an FPU predoctoral grant (ref.: FPU18/03131) from the Ministry of Universities, Spain. Jesús Hermosilla, during the present work was benefiting from a research contract (ref. P20_01029) from the Junta de Andalucía (Spain) and European Regional Development Funds.

Funding

This study was funded by Project P20-01029 (I+D+I Research program from the Regional Government of the Andalucía, Spain) and by Project B-FQM-308-UGR20 (Universty of Granada, I+D+I proyects from the Operative Programme FEDER Andalucía 2020 which means that it was also partially supported by European Regional Development Funds.

Author Contributions

A.T.-L.: Conceptualisation, Methodology, Validation, Formal analysis, Investigation, Writing—Original Draft, Visualisation; J.H.: Conceptualisation, Methodology, Investigation; A.S.-G.: Resources, Supervision, Project administration, Funding acquisition; J.C.: Resources, Supervision, Project administration, Funding acquisition; A.R-M.: Writing—Review and Editing, Supervision; N.N.: Conceptualisation, Methodology, Resources, Writing—Review and Editing, Supervision, Project administration, Funding acquisition. All authors have read and agreed to the published version of the manuscript.

Supplementary data

Circular dichroism

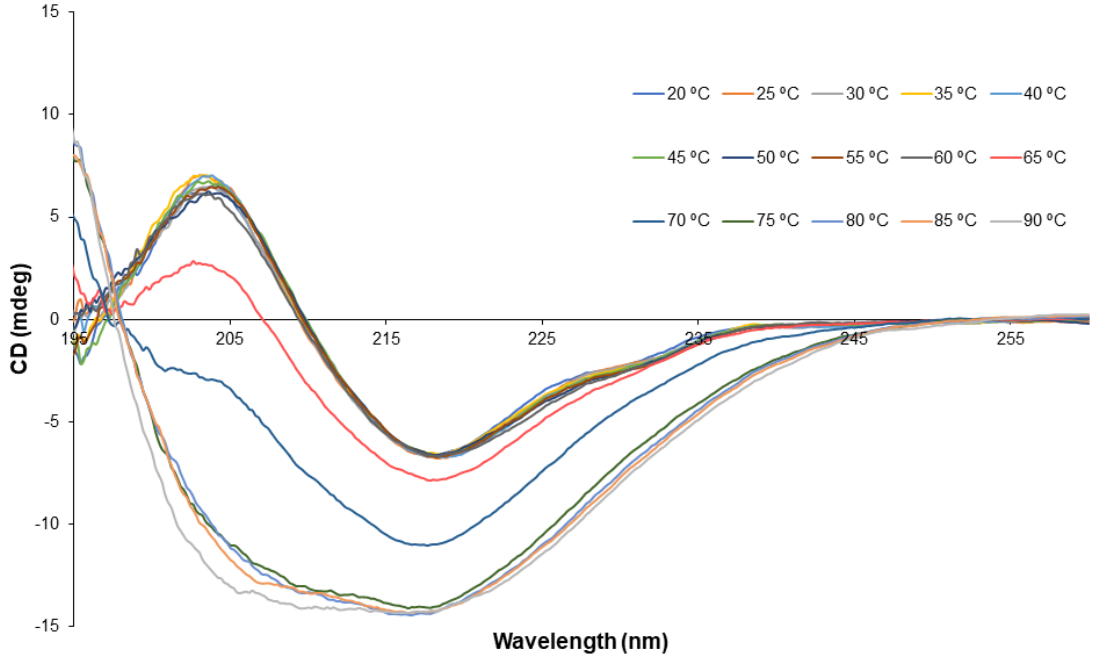

Figure S1. Pembrolizumab thermal stress ramp from 20 °C to 90 °C monitored by CD spectroscopy in the far-UV.

Aggregation study by SE/UHPLC(UV)

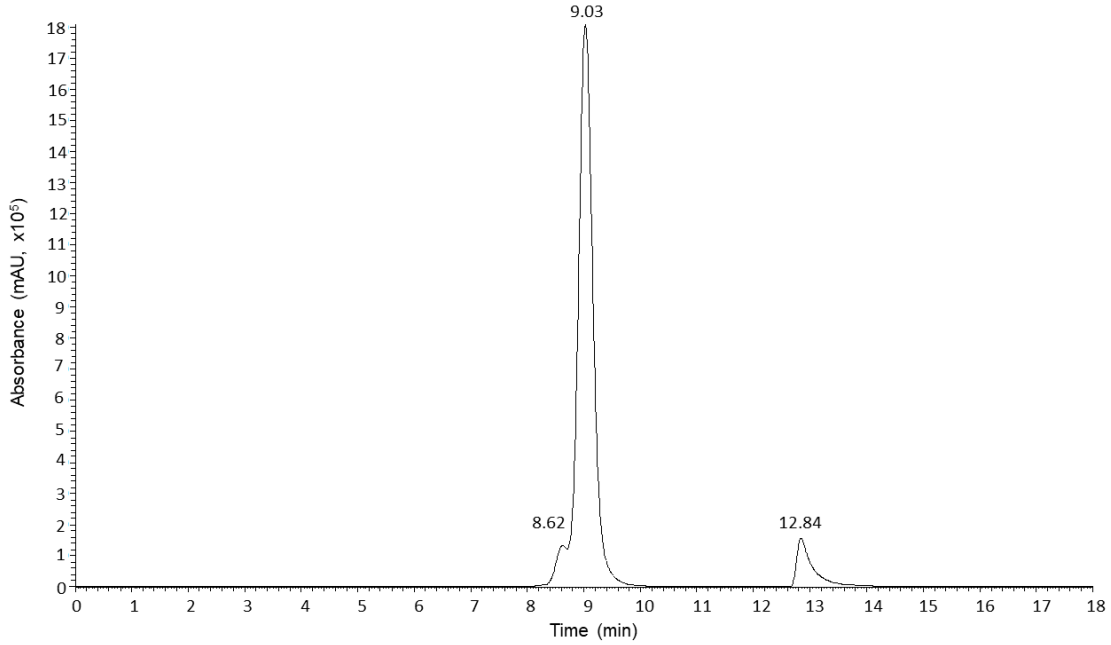

Figure S2. SE/UHPLC(UV) chromatogram for pembrolizumab fresh sample (Keytruda® 25 mg/mL)

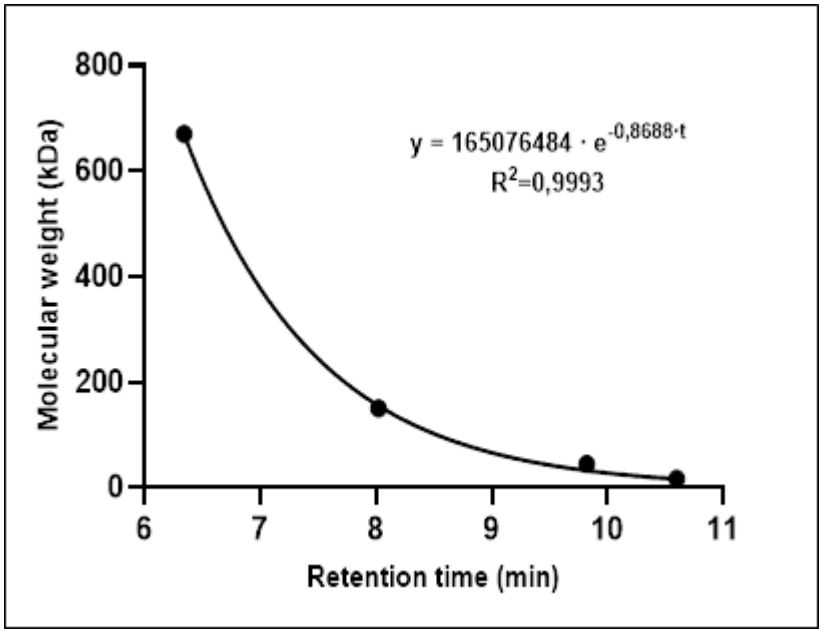

Figure S3. Experimental size exclusion column calibration model.

Peptide mapping

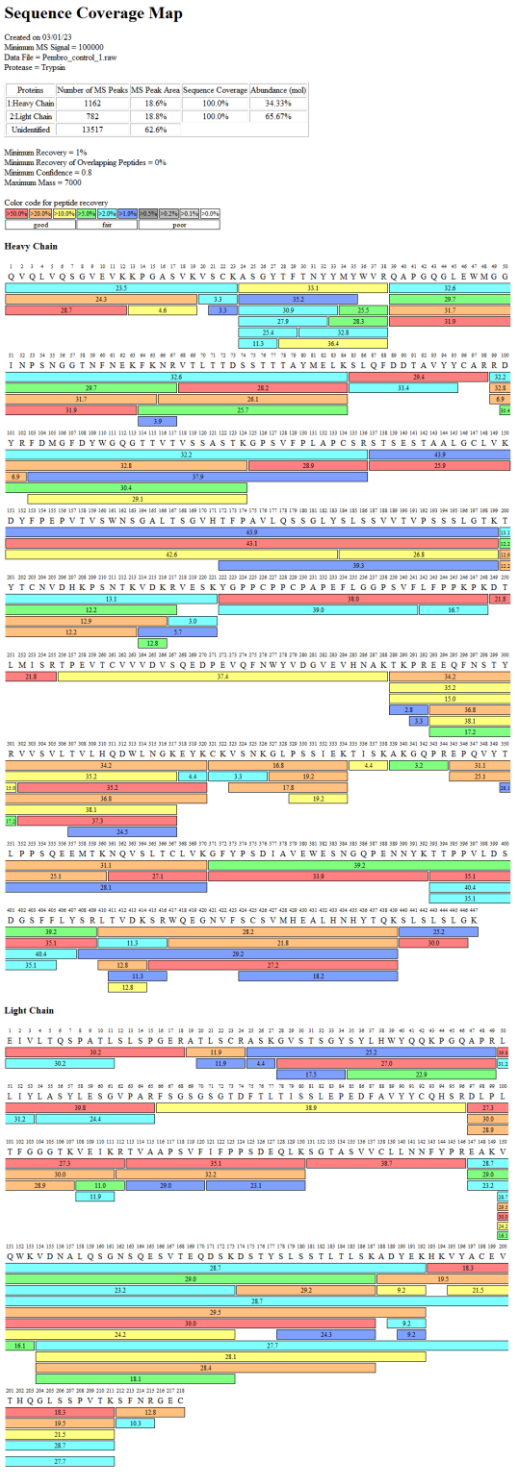

Figure S4. Sequence coverage map for peptide mapping analysis.

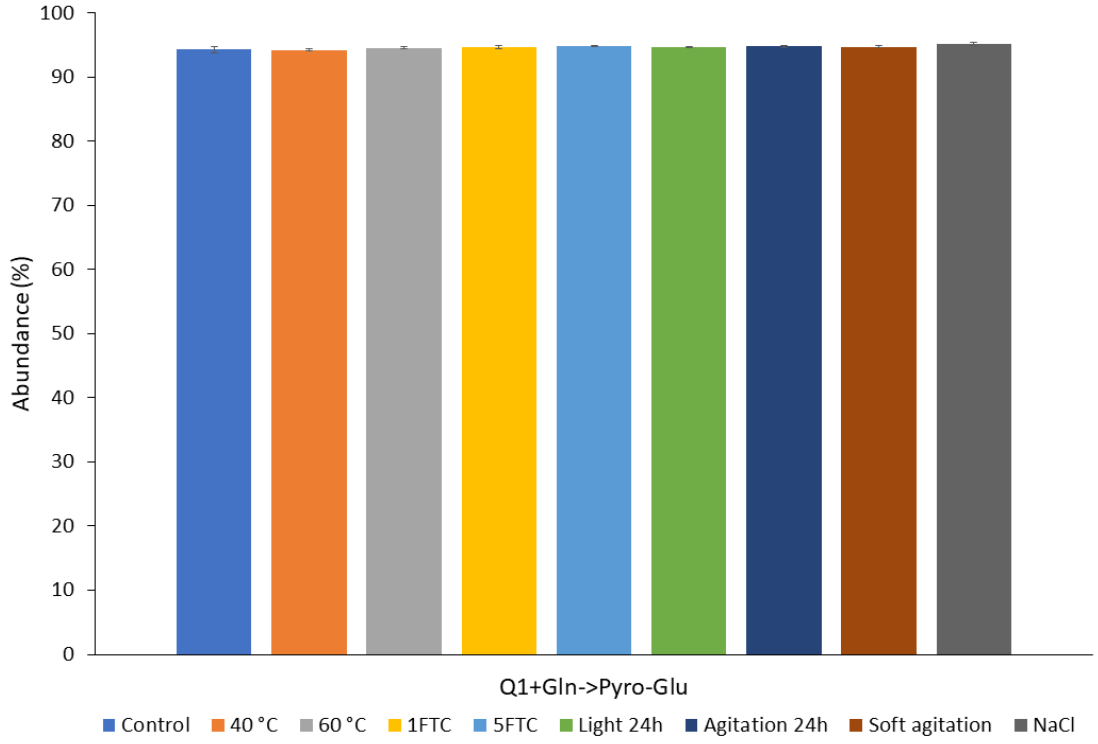

Figure S5. Pyroglutamate formation in pembrolizumab (25 mg/mL) control and stressed samples.

ELISA

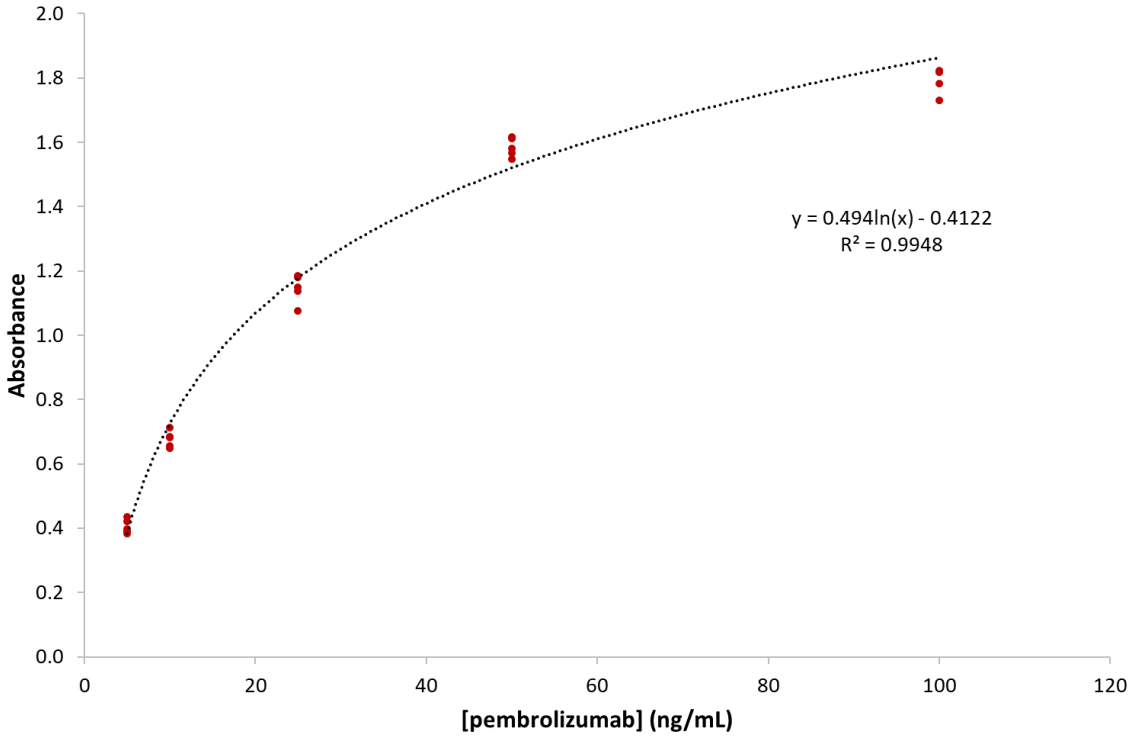

Figure S6. Standard calibration curve for the ELISA method.

References

[1] A. Torrente-López, J. Hermosilla, N. Navas, L. Cuadros-Rodríguez, J. Cabeza, A. Salmerón-García, The relevance of monoclonal antibodies in the treatment of COVID-19, Vaccines. 9 (2021) 1–17. https://doi.org/10.3390/vaccines9060557.

[2] H. Kaplon, J.M. Reichert, Antibodies to watch in 2021, MAbs. 13 (2021). https://doi.org/10.1080/19420862.2020.1860476.

[3] O. Hernandez-Alba, E. Wagner-Rousset, A. Beck, S. Cianférani, Native Mass Spectrometry, Ion Mobility, and Collision-Induced Unfolding for Conformational Characterization of IgG4 Monoclonal Antibodies, Anal. Chem. 90 (2018) 8865–8872. https://doi.org/10.1021/acs.analchem.8b00912.

[4] European Medicines Agency. Pembrolizumab: Summary of Product Characteristics., (n.d.).

[5] B. Hutchins, G.C. Starling, M.A. McCoy, D. Herzyk, F.M. Poulet, J. Dulos, L. Liu, S.P. Kang, L. Fayadat-Dilman, M. Hsieh, C.L. Andrews, G. Ayanoglu, C. Cullen, R. de Waal Malefyt, R.A. Kastelein, S. Le Saux, J. Lee, S. Li, D. Malashock, S. Sadekova, G. Soder, H. van Eenennaam, A. Willingham, Y. Yu, M. Streuli, G.J. Carven, A. van Elsas, Biophysical and immunological characterization and in vivo pharmacokinetics and toxicology in nonhuman primates of the anti-PD-1 antibody pembrolizumab, Mol. Cancer Ther. 19 (2020) 1298–1307. https://doi.org/10.1158/1535-7163.MCT-19-0774.

[6] R. Wälchli, P.J. Vermeire, J. Massant, P. Arosio, Accelerated Aggregation Studies of Monoclonal Antibodies: Considerations for Storage Stability, J. Pharm. Sci. 109 (2020) 595–602. https://doi.org/10.1016/j.xphs.2019.10.048.

[7] E. Jaccoulet, T. Daniel, P. Prognon, E. Caudron, Forced Degradation of Monoclonal Antibodies After Compounding: Impact on Routine Hospital Quality Control, J. Pharm. Sci. 108 (2019) 3252–3261. https://doi.org/10.1016/j.xphs.2019.06.004.

[8] A. Beck, E. Wagner-Rousset, D. Ayoub, A. Van Dorsselaer, S. Sanglier-Cianférani, Characterization of therapeutic antibodies and related products, Anal. Chem. 85 (2013) 715–736. https://doi.org/10.1021/ac3032355.

[9] N. Alt, T.Y. Zhang, P. Motchnik, R. Taticek, V. Quarmby, T. Schlothauer, H. Beck, T. Emrich, R.J. Harris, Determination of critical quality attributes for monoclonal antibodies using quality by design principles, Biologicals. 44 (2016) 291–305. https://doi.org/10.1016/j.biologicals.2016.06.005.

[10] A. Delobel, Glycosylation of Therapeutic Proteins: A Critical Quality Attribute, in: Methods Mol. Biol., 2021: pp. 1–21. https://doi.org/10.1007/978-1-0716-1241-5_1.

[11] A. Shrivastava, S. Joshi, A. Guttman, A.S. Rathore, N-Glycosylation of monoclonal antibody therapeutics: A comprehensive review on significance and characterization, Anal. Chim. Acta. 1209 (2022). https://doi.org/10.1016/j.aca.2022.339828.

[12] E. Tamizi, A. Jouyban, Forced degradation studies of biopharmaceuticals: Selection of stress conditions, Eur. J. Pharm. Biopharm. 98 (2016) 26–46. https://doi.org/10.1016/j.ejpb.2015.10.016.

[13] C. Nowak, J. K. Cheung, S. M. Dellatore, A. Katiyar, R. Bhat, J. Sun, G. Ponniah, A. Neill, B. Mason, A. Beck, H. Liu, Forced degradation of recombinant monoclonal antibodies: A practical guide, MAbs. 9 (2017) 1217–1230. https://doi.org/10.1080/19420862.2017.1368602.

[14] A. Hawe, M. Wiggenhorn, M. van de Weert, J.H.O. Garbe, H.C. Mahler, W. Jiskoot, Forced degradation of therapeutic proteins, J. Pharm. Sci. 101 (2012) 895–913. https://doi.org/10.1002/jps.22812.

[15] S. Fekete, D. Guillarme, P. Sandra, K. Sandra, Chromatographic, Electrophoretic, and Mass Spectrometric Methods for the Analytical Characterization of Protein Biopharmaceuticals, Anal. Chem. 88 (2016) 480–507. https://doi.org/10.1021/acs.analchem.5b04561.

[16] A. Beck, V. D'Atri, A. Ehkirch, S. Fekete, O. Hernandez-Alba, R. Gahoual, E. Leize-Wagner, Y. François, D. Guillarme, S. Cianférani, Cutting-edge multi-level analytical and structural characterization of antibody-drug conjugates: present and future, Expert Rev. Proteomics. 16 (2019) 337–362. https://doi.org/10.1080/14789450.2019.1578215.

[17] P. Sundaramurthi, S. Chadwick, C. Narasimhan, Physicochemical stability of pembrolizumab admixture solution in normal saline intravenous infusion bag, J. Oncol. Pharm. Pract. 26 (2020) 641–646. https://doi.org/10.1177/1078155219868516.

[18] A. Torrente-López, J. Hermosilla, A. Salmerón-García, J. Cabeza, N. Navas, Comprehensive Analysis of Nivolumab, A Therapeutic Anti-Pd-1 Monoclonal Antibody: Impact of Handling and Stress, Pharmaceutics. 14 (2022) 692. https://doi.org/10.3390/pharmaceutics14040692.

[19] A.J. Miles, S.G. Ramalli, B.A. Wallace, DichroWeb, a website for calculating protein secondary structure from circular dichroism spectroscopic data, Protein Sci. 31 (2022) 37–46. https://doi.org/10.1002/pro.4153.

[20] S. Carillo, R. Pérez-Robles, C. Jakes, M. Ribeiro da Silva, S. Millán Martín, A. Farrell, N. Navas, J. Bones, Comparing different domains of analysis for the characterisation of N-glycans on monoclonal antibodies, J. Pharm. Anal. 10 (2020) 23–34. https://doi.org/10.1016/j.jpha.2019.11.008.

[21] Pembrolizumab: Uses, Interactions, Mechanism of Action | DrugBank Online, (n.d.). https://go.drugbank.com/drugs/DB09037 (accessed April 4, 2023).

[22] ICH Secretariat (2005) International Conference on Harmonization (ICH) guideline ICH Q2(R1): validation of analytical procedures: text and methodology., 2005.

[23] C.A. Royer, Probing Protein Folding and Conformational Transitions with Fluorescence, Chem. Rev. 106 (2006) 1769–1784. https://doi.org/10.1021/cr0404390.

[24] J. Hermosilla, R. Pérez-Robles, A. Salmerón-García, S. Casares, J. Cabeza, J. Bones, N. Navas,

Comprehensive biophysical and functional study of ziv-aflibercept: characterization and forced degradation, Sci. Rep. 10 (2020) 1–13. https://doi.org/10.1038/s41598-020-59465-7.

[25] SEC chromatography column PL1580-5301 | Agilent, (n.d.). https://www.agilent.com/store/productDetail.jsp?catalogId=PL1580-5301 (accessed July 12, 2023).

[26] J.Y. Lee, H.T. Lee, W. Shin, J. Chae, J. Choi, S.H. Kim, H. Lim, T. Won Heo, K.Y. Park, Y.J. Lee, S.E. Ryu, J.Y. Son, J.U. Lee, Y.S. Heo, Structural basis of checkpoint blockade by monoclonal antibodies in cancer immunotherapy, Nat. Commun. 7 (2016) 1–10. https://doi.org/10.1038/ncomms13354.

[27] J.W.A. Findlay, W.C. Smith, J.W. Lee, G.D. Nordblom, I. Das, B.S. DeSilva, M.N. Khan, R.R. Bowsher, Validation of immunoassays for bioanalysis: a pharmaceutical industry perspective, J. Pharm. Biomed. Anal. 21 (2000) 1249–1273. https://doi.org/10.1016/S0731-7085(99)00244-7.

[28] B. DeSilva, W. Smith, R. Weiner, M. Kelley, J. Smolec, B. Lee, M. Khan, R. Tacey, H. Hill, A. Celniker, Recommendations for the Bioanalytical Method Validation of Ligand-Binding Assays to Support Pharmacokinetic Assessments of Macromolecules, Pharm. Res. 20 (2003) 1885–1900. https://doi.org/10.1023/B:PHAM.0000003390.51761.3d.

[29] J. Hermosilla, R. Sánchez-Martín, R. Pérez-Robles, A. Salmerón-García, S. Casares, J. Cabeza, L. Cuadros-Rodríguez, N. Navas, Comparative Stability Studies of Different Infliximab and Biosimilar CT-P13 Clinical Solutions by Combined Use of Physicochemical Analytical Techniques and Enzyme-Linked Immunosorbent Assay (ELISA), BioDrugs. 33 (2019) 193–205. https://doi.org/10.1007/s40259-019-00342-9.

[30] A. Zhang, W. Qi, S.K. Singh, E.J. Fernandez, A New Approach to Explore the Impact of Freeze-Thaw Cycling on Protein Structure: Hydrogen/Deuterium Exchange Mass Spectrometry (HX-MS), Pharm. Res. 28 (2011) 1179–1193. https://doi.org/10.1007/s11095-011-0383-z.

[31] J. Hernández-Jiménez, A. Salmerón-García, J. Cabeza, C. Vélez, L.F. Capitán-Vallvey, N. Navas, The Effects of Light-Accelerated Degradation on the Aggregation of Marketed Therapeutic Monoclonal Antibodies Evaluated by Size-Exclusion Chromatography with Diode Array Detection, J. Pharm. Sci. 105 (2016) 1405–1418. https://doi.org/10.1016/j.xphs.2016.01.012.

[32] J. Hernández-Jiménez, A. Martínez-Ortega, A. Salmerón-García, J. Cabeza, J.C. Prados, R. Ortíz, N. Navas, Study of aggregation in therapeutic monoclonal antibodies subjected to stress and long-term stability tests by analyzing size exclusion liquid chromatographic profiles, Int. J. Biol. Macromol. 118 (2018) 511–524. https://doi.org/10.1016/j.ijbiomac.2018.06.105.

SECCIÓN 3

Large number of different therapeutic monoclonal antibodies

CAPÍTULO 6

Optimization of the ReFOLD Assay for Protein Stability Prediction

INTRODUCCIÓN AL CAPÍTULO 6

El capítulo 6 recoge un estudio de predicción de la estabilidad a largo plazo de medicamentos basados en mAbs terapéuticos, el cual fue llevado a cabo en la empresa Coriolis Pharma Research GmbH (Múnich, Alemania). En concreto, el ensayo realizado es conocido como el "ensayo ReFOLD", un método isotérmico basado en la desnaturalización química de proteínas. Este ensayo consiste en la exposición del mAb en su fórmula final a un agente desnaturalizante (urea) que desplegará parcialmente la estructura proteica de la proteína y, seguidamente, se eliminará el desnaturalizante para que la proteína se vuelva a plegar. Esto dará lugar a varios intermediarios proteicos (plegados y desplegados) y la agregación de los mismos ocurrirá dependiendo de la naturaleza intrínseca de la proteína y de las condiciones de formulación del medicamento. Por ello se puede asumir que, si las condiciones de formulación evitan la agregación de la proteína parcialmente desplegada, estas condiciones también evitarán su agregación durante el almacenamiento a largo plazo. El ensayo ReFOLD se llevó a cabo en investigaciones previas en Coriolis Pharma a una concentración de urea de 10 M. Sin embargo, dicha concentración mostró efectos indeseados en varios de los productos farmacéuticos ensayados, tales como formación de cristales, precipitación o formación de gel, aspectos que impiden obtener la información deseada sobre la estabilidad. Por ello, el objetivo principal del estudio que aquí se presenta es optimizar el ensayo ReFOLD reduciendo la concentración de urea, con la finalidad de eliminar/reducir dichos efectos indeseados y permita evaluar la estabilidad de los diferentes mAbs. Es decir, es importante que la concentración reducida de urea aún siga permitiendo una clasificación de la estabilidad de los productos farmacéuticos ensayados. En este capítulo, se sometieron un total de diez productos farmacéuticos comercializados al ensayo ReFOLD, en los que cada mAb fue estudiado a tres concentraciones distintas: la concentración original, 20 mg/mL y 2 mg/mL. El ensayo fue realizado usando dos concentraciones distintas de urea: 6.5 M y 6 M. Las muestras fueron analizadas por (SE)HPLC/UV y los resultados fueron comparados con los resultados obtenidos en los experimentos anteriores usando urea 10 M. Además, en este capítulo también se llevó a cabo una optimización del método SEC que se empleó en los estudios anteriores, consiguiendo una reducción del tiempo total de análisis de las muestras. De forma general, los resultados mostraron que ambas concentraciones de urea fueron adecuadas para reducir los efectos indeseados que se encontraron con urea 10 M, pero seguían sin permitir una clasificación coherente de la estabilidad de los productos farmacéuticos evaluados. Por tanto, con la finalidad de identificar la concentración de urea más adecuada para realizar el

ensayo ReFOLD, la cual permita el mejor balance entre la reducción de los efectos indeseados y la clasificación de la estabilidad de los medicamentos, será necesario probar el ensayo en un mayor número de productos farmacéuticos cuyo principio activo sea mAb.

SCIENTIFIC RESEARCH

Optimization of the ReFOLD Assay for Protein Stability Prediction

Anabel Torrente-López[1], Constanze Helbig[2], Natalia Navas[1] and Andrea Hawe[2]

[1] Department of Analytical Chemistry, Science Faculty, Biohealth Research Institute (ibs.GRANADA), University of Granada, 18071 Granada, Spain; anabeltl@ugr.es; natalia@ugr.es

[2] Coriolis Pharma Research GmbH, Fraunhoferstraße 18B, 82152 Planegg, Munich, Germany; Constanze.Helbig@coriolis-pharma.com; Andrea.Hawe@coriolis-pharma.com

Abstract

Therapeutic proteins, such as monoclonal antibodies (mAbs), present great physicochemical complexity, which makes them highly susceptible to instability. Their manufacturing, transport, storage, and handling prior to administration to patients can compromise their stability. This can lead to structural modification and the presence of degradation products, which can compromise the efficacy and safety of the drug product. Physicochemical characterization of therapeutic proteins is essential to assess their stability, which also depends on the formulation. Among the various degradation mechanisms a protein can undergo, the formation of protein aggregates and particles is a particular concern because of the immunogenicity implications they may cause in the patient. The development of methods and strategies for the physicochemical characterization of proteins are necessary to control and assure the stability of the therapeutic protein solutions. Therefore, stability predictive methods are useful for an early selection of the most resistant formulation candidates in drug product development. In particular, this work aims at the optimization of the ReFOLD assay, an isothermal chemical denaturation-based method. Assay optimization was carried out by testing a total of ten marketed drug products (monoclonal antibodies, mAbs) at three different protein concentrations: the original concentration of the formulation, 20 mg/mL and 2 mg/mL. Two different urea concentrations (approximately 6 M and 6.5 M) were selected to run the assay considering the fact that urea concentration had to be reduced in comparison to the original urea concentration (10 M urea) used in previous experiments with the ReFOLD assay. The application of 10 M urea had resulted in undesired effects during the assay, such as gel formation or crystallization. The processed samples were analyzed by high performance size-exclusion chromatography (HP-SEC) and the results were compared with those obtained from previous studies at 10 M urea. In general, this study showed that both urea concentrations tested (~6 M and ~6.5 M) were adequate to reduce the undesired effects found with 10 M urea but they still did not allow for a consistent stability ranking of the drug product tested. This could be due to the fact that these urea concentrations did not cause sufficient unfolding of the proteins. Thus, this study revealed the difficulty of the complete removal of the undesired effects while maintaining an adequate stability ranking of the mAb products tested when reducing the urea concentration. With this in mind, future studies will be needed in order to identify the most adequate urea concentration to perform the ReFOLD assay, which provides the best balance between reducing undesired effects and establishing a stability ranking of the drug products.

Keywords

Biopharmaceutical formulations

Monoclonal antibodies

Stability-predictive method

ReFOLD assay

HP-SEC

1. Introduction

Biopharmaceuticals, such as therapeutic proteins and especially monoclonal antibodies (mAbs), remain a growing field in the pharmaceutical industry with numerous approved treatments and ongoing clinical trials [1].

Proteins are large molecules with an inherent physicochemical complexity. Such complex molecules are susceptible to instability through different degradation pathways that can be promoted by different stress conditions during production, shipping, storage and even handling prior and during administration to patients. The most important concern about protein instability is related to the formation of proteinaceous particles as a major risk factor for the immunogenicity of formulated therapeutics. Thus, stability studies are a crucial part of quality control of biopharmaceuticals [2,3].

Stability of biopharmaceuticals can be categorized in two groups: physical and chemical stability. Physical stability of biopharmaceuticals is related to preservation of higher order structure and can be impacted by different degradation events (i.e., unfolding, dissociation, adsorption to containers, aggregation and precipitation). Chemical stability is compromised by the formation and/or breakage of covalent bonds in the first order structure of proteins and can be triggered by different degradation pathways (i.e., oxidation, deamidation, hydrolysis, disulfide exchange, etc.) [2,4].

The stability of these therapeutic protein products depends on their formulation, i.e., pH, buffer type, ionic strength or protein concentration [5]. For example, buffers are an integral component of many protein formulations. They play a crucial role in the stability of these products as they regulate pH but they can also increase conformational stability of proteins either by ligand binding or by an excluded solute mechanism. Also, buffers can alter the colloidal stability of therapeutic proteins and modulate interfacial damage [6].

Stability predictive methods are also required for an early selection of the most resistant formulation candidates in drug product development [5,7]. Candidate formulations can be exposed to stress studies and the stability of the tested formulations can be further assessed by, for example, studying resistance to aggregate formation. Moreover, these studies are also used to optimize production and manufacturing conditions and to assess the storage stability and shelf-life of these products. In general, long-term and accelerated stability studies can be distinguished: long-term stability studies are performed under the recommended storage conditions for the DPs under evaluation, so they have the disadvantage of lasting up to several years, while short-term stability studies provide faster results by storing samples at elevated temperature to shorten the overall study time [8].

The ReFOLD assay is a potential method for the prediction of protein stability during long-term storage as it considers multiple biophysical parameters, such as protein-protein interactions, protein-excipient interactions and protein conformational stability [5]. Thus, the information provided by the ReFOLD assay may correlate with long-term stability of biotherapeutic proteins. Currently, different indicators of long-term stability are applied, such as the (apparent) protein melting temperature (T_m), the aggregation onset temperature (T_{agg}) or the Gibbs free energy of protein unfolding. However, all of them show some disadvantages when compared to the ReFOLD assay (e.g., T_m and T_{agg} show a very weak or no correlation with the aggregation behaviour of many therapeutic proteins, especially mAbs, during storage at 4 °C and 25 °C). In addition, some advantages of the ReFOLD assay compared with other long-term stability indicators are that it requires a low volume of sample and it achieves a high throughput [5,7].

In the ReFOLD assay the protein is exposed to a denaturant and subsequently to a denaturant-free formulation buffer. The denaturant will (partially) unfold the protein and denaturant removal will result in (re)folding of this protein, giving rise to various unfolding (refolding) protein intermediates. Aggregation of these intermediates will occur depending on the protein itself and the formulation conditions, such as buffer type or protein concentration. Therefore, the following assumptions are made: if the formulation conditions suppress aggregation of (partially) unfolded protein, these formulation conditions will also suppress aggregation during long-term storage of the tested drug product [5].

In detail, protein samples are exposed to microdialysis against a high concentration of urea (~10 M in the original approach) in the formulation buffer of the protein for 24 hours as a first step. After this microdialysis, the protein monomers are (partially to fully) unfolded and protein aggregation is suppressed by the high concentration of urea. As a second step, the samples are subjected to another microdialysis for 24 hours, but this time against the original formulation buffer without urea. As the concentration of urea is reduced during this second microdialysis, the protein monomers will be (re)folded and the formation of aggregates from various unfolded and partially (re)folded protein monomers will occur dependent on the formulation and the physical stability of the protein itself. Finally, the samples subjected to the ReFOLD assay, as well as the untreated control samples, are analyzed by size exclusion chromatography (SEC) and the Relative Monomer Yield (RMY) is calculated. The RMY determines the monomer recovery after the ReFOLD assay and is thus a measure for the protein's capability to fold back into the native state. For the calculation of the RMY, the following equation is used:

$$RMY = \frac{Area\ (Monomer\ Peak\ after\ ReFOLD)}{Area\ (Monomer\ Peak\ prior\ ReFOLD)}$$

This quotient can give a result between zero and one, where a value of zero indicates that there is no protein monomer recovery after performing the ReFOLD assay and a value of one represents a complete monomer recovery after the assay. Figure 1 shows a scheme of the procedure of the ReFOLD assay [5].

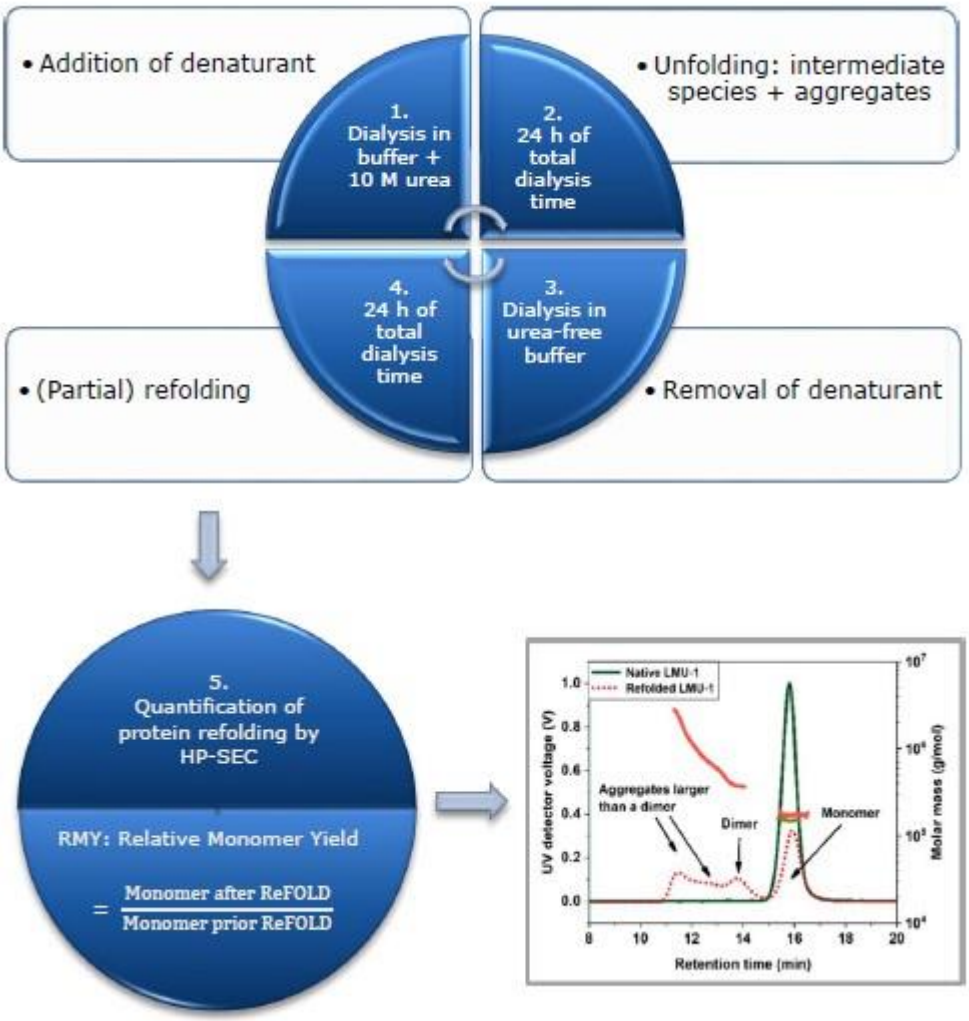

Figure 1. Working principle of the ReFOLD assay [9].

2. Aim

The ReFOLD assay was originally developed at a concentration of 10 M of urea (following indications from previous literature [5]), and has been further tested for eleven marketed mAb products in previous published and yet unpublished studies [9]. However, for eight out of eleven of the tested antibody drug products (DPs) undesired effects like gel formation, protein precipitation or urea crystallization were observed. Therefore, the main aim of the current research work was to optimize the ReFOLD assay conditions previously reported in the literature by reducing urea concentration. Importantly, while eliminating the above-mentioned undesired effects, applying the ReFOLD assay at a reduced urea concentration still had to allow for a stability ranking of the tested DPs.

To achieve the main aim, the following objectives had to be addressed:

- Testing of reduced urea concentrations to prevent gel formation, protein precipitation and urea crystallization
- Improve sample recovery from the microdialysis chamber (due to elimination of, e.g., gel formation)
- Compare RMYs at different urea concentrations to confirm stability ranking
- Identify other opportunities to improve the assay, such as an improvement in sample handling or the optimization of the SEC method

3. Materials and Methods

In this work, the ReFOLD assay was tested on a total of 10 marketed DPs, in two different stages. The DPs used for every stage are listed in Table 1 and Table 2, further details on their selection are provided in 3.1.

All DPs were tested at three different concentrations:

- Original concentration (in its marketed formulation)
- 20 mg/mL
- 2 mg /mL

Dilutions to 20 mg/mL and 2 mg/mL were prepared in the respective formulation buffer of each mAb product.

Table 1. DPs selected for the first stage.

DP	IgG subclass	Concentration [mg/mL]
mAb-1	IgG1	80
mAb-2	IgG1	25
mAb-3	IgG2	70
mAb-4	IgG1	50
mAb-5	IgG1	180

Table 2. DPs selected for the second stage.

DP	IgG subclass	Concentration [mg/mL]
mAb-6	IgG4	150
mAb-7	IgG2	140
mAb-8	IgG2	20
mAb-9	IgG2	140
mAb-10	IgG1	25

3.1. Materials: DP selection

For the selection of the DPs used in the first stage, we considered the undesired effects observed when performing the ReFOLD assay in previous studies with 10 M of urea. Table 3 summarizes all the mAb products used in previous assays and the observed undesired effects, such as crystal formation, precipitation and/or gel formation.

Table 3. Undesired effects observed during the ReFOLD assay with 10 M of urea. “X” indicates an observed undesired effect, “-” indicates that the effect was not observed.

Group	DP	Crystal formation	Turbidity / Precipitation	Gel formation
1	mAb-1	-	-	-
	mAb-6	-	-	-
	mAb-7	-	-	-
2	mAb-2	-	X	-
	mAb-8	-	X	-
	mAb-3	-	-	X
	mAb-11	-	X	-
	mAb-12	-	X	-
3	mAb-5	X	-	X
	mAb-9	X	-	X
	mAb-4	-	X	X

The DPs summarized in Table 3 were divided into three groups, depending on the number of undesired effects they showed:

- Group 1 corresponds to the most robust formulations, the ones that did not show any undesired effect.
- Group 2 consists of those DPs that showed exactly one undesired effect.
- Group 3 contains the most sensitive mAb products given that they showed at least two undesired effects.

We decided to select mAb-1, mAb-2, mAb-3, mAb-4 and mAb-5 as the most appropriate DPs for the first stage of the ReFOLD assay optimization as they were a good representation of the three different groups and they are also well distributed along the RMY range (from 0 to 1).

The DPs of the second stage were selected as new DPs to be tested with the ReFOLD assay to have a broader database of tested DPs.

3.2. Method: the ReFOLD assay

The practical procedure of the ReFOLD assay was carried out using microdialysis units, 3.5K MWCO (Catalogue number: 186000385C, Thermo Fisher Scientific, Massachusetts, USA) and deep 96-well plates, 2.2 mL volume (Catalogue number: 732-2892, Thermo Fisher Scientific, Massachusetts, USA).

As a preparatory step, the urea-supplemented buffers were made following these steps: the required amount of urea (Merck, Darmstadt, Germany) was weighed out in a Genius ME balance from Sartorius AG (Göttingen, Germany) and transferred into a 100 mL beaker. Then, 50 mL of formulation buffer were added to the beaker and the urea was dissolved with the help of a magnetic stirrer and a stirring plate for around 1 hour. Once the urea was completely dissolved, the urea-supplemented buffers were filtered using vacuum filtration with membrane filters of 0.22 µm pore size (PVDF Durapore®, Merck, Darmstadt, Germany). Following this procedure, we obtained urea-supplemented buffers at a final urea concentration of 5.93 M ± 0.11 M and 6.43 M ± 0.11 M. For the convenience of the reader, urea concentrations will be stated as rounded numbers, i.e., 6 M and 6.5 M, respectively, in the remaining text.

The ReFOLD assay was conducted as follows:

1. Dialysis against formulation buffer + urea: for each tested formulation, a microdialysis chamber was filled with 100 µL mAb formulation and placed in a well containing 1.5 mL of urea-supplemented formulation buffer under laminar air flow (LAF) conditions. The deep-well plate with all the samples was covered with Parafilm and aluminium foil to protect samples from light, and placed on top of an Eppendorf Thermomixer (Eppendorf, Hamburg, Germany) for agitation at 700 rpm. Buffer was exchanged with fresh buffer under LAF conditions after 4 h and 8 h.
2. The protein unfolding step was completed after 24 h of dialysis.
3. Dialysis against formulation buffer (without urea): the microdialysis chambers with the samples were placed in deep wells with 1.5 mL urea-free formulation buffer under LAF conditions and the agitation was continued at 700 rpm with the samples protected from light. A buffer exchange was performed after 4 h and 8 h.
4. The protein refolding step was completed after 24 h of dialysis.
5. Sample preparation for SEC analysis: the samples were removed from the microdialysis chambers and the protein concentration was adjusted to 1 mg/mL by gravimetric dilution in the urea-free formulation buffer. Samples were centrifuged at 10,000 g for 10 min at room temperature to remove insoluble aggregates.

6. Finally, the samples were analyzed by high performance size exclusion chromatography (HP-SEC) and the RMY was calculated for each sample.

For calculation of the RMY, the monomer peak area in the SEC chromatograms had to be quantified for the untreated mAb sample and the sample when processed in the ReFOLD assay.

3.3. Method: size exclusion chromatography (SEC)

A Dionex UltiMate 3000 system by Thermo Fisher Scientific (Massachusetts, USA) equipped with a TSKgel G3000SWxl, 7.8 ID x 300 mm, 5 µm column (Tosoh Bioscience, Tokyo, Japan) was used for SEC analysis. Table 4 displays a summary of the applied instrument settings. The mobile phase used was 100 mM sodium phosphate plus 200 mM L-arginine (pH 7.0). For the preparation of 1 L of this mobile phase, L-arginine (Merck, Darmstadt, Germany) and sodium dihydrogen phosphate monohydrate (Merck, Darmstadt, Germany) were weighed and transferred into a 1 L beaker. Then, they were dissolved in approximately 800 mL of mili-Q water using a magnetic stirrer. Once the reagents were dissolved, they were transferred into a 1 L volumetric flask in order to reach the final volume by adding water, and the solution was homogenized using a magnetic stirrer. The final pH of 7.0 was adjusted by titrating the buffer solution with ortho phosphoric acid 85% (Merck, Darmstadt, Germany) while homogenising with the help of a magnetic stirrer.

For RMY calculation, peak areas of the treated and untreated protein samples were determined with the help of Chromeleon 6.8 Chromatography Data System (CDS) software (Thermo Fisher Scientific, Massachusetts, USA).

Table 4. Selected parameters for SEC analysis.

Parameter	**Applied Setting**
Injection volume	50 µL
Flow rate	0.8 mL/min
Analysis time	22 min
Column temperature	25 °C
Detection wavelength	280 nm
Elution mode	Isocratic
Inject wash	Before injection Wash volume: 500.000 µL Wash speed: 32.000 µL/s Loop Wash Factor: 2.000
Temperature control of the sampler	6 °C

4. Results and Discussion

4.1. Optimization of the SEC method

The SEC method used in this work was developed in a previous study [9]. This method was now optimized by reducing the time of analysis per sample from 30 to 22 minutes and by setting the “inject wash” parameter to “before injection” instead of “before and after injection”. These two modifications resulted in a significant reduction in the total analysis time (e.g., when analyzing 54 samples the total analysis time had previously been around 30 hours and after optimization it was around 20 hours). At the same time, an appropriate chromatographic profile for the analyzed samples was maintained (Figure 2).

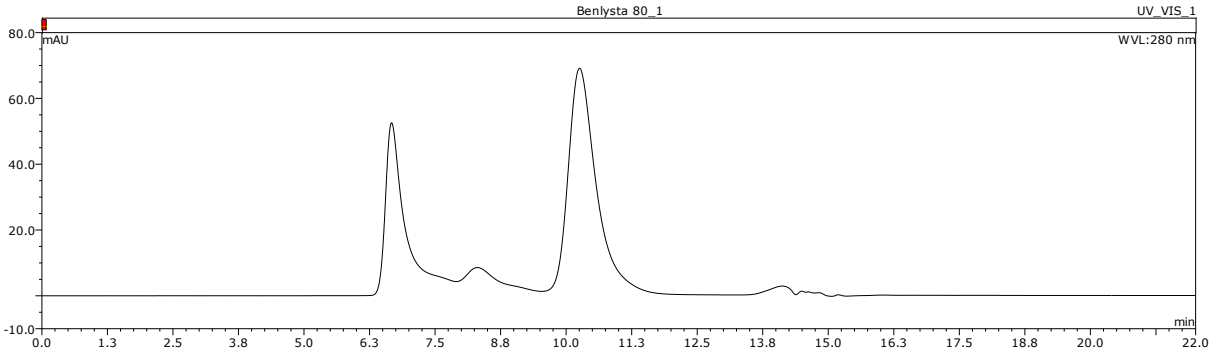

Figure 2. Example of a chromatographic profile obtained using the optimized SEC method. Sample: mAb-1 at original concentration after ReFOLD assay at 6 M urea.

4.2. Optimization of the ReFOLD assay

In this work, different experiments were performed to optimize the ReFOLD assay. Firstly, the mAb products of the first stage (Table 1) were subjected to the ReFOLD assay using reduced urea concentrations of 6 M and 6.5 M. The obtained results were compared to the results of previous assays using 10 M urea. The latter comparison considered the occurrence of undesired effects (e.g., protein precipitation), sample recovery from microdialysis chambers after refolding and trends in RMY when comparing multiple DPs. Given that 10 M urea showed a high incidence of undesired effects (eight out of eleven DPs, as indicated previously), we decided to reduce the urea concentration to find out whether these undesired effects can be prevented while still maintaining a stability ranking of the tested DPs. After a first assessment of the applicability of 6 M urea and 6.5 M urea in the assay, the ReFOLD assay was performed with the mAb products of the second stage to further increase the data base for conclusions on improved assay conditions. Again, using the two new urea

concentrations, the outcome was compared to the previous assay results obtained with 10 M urea.

4.2.1. First experiment: 6 M urea, first stage mAb products

The first experiment for optimization of the ReFOLD assay was performed using 6 M urea with the five mAb products of the first stage (Table 1). The results of the measurements are given in Figure 3.

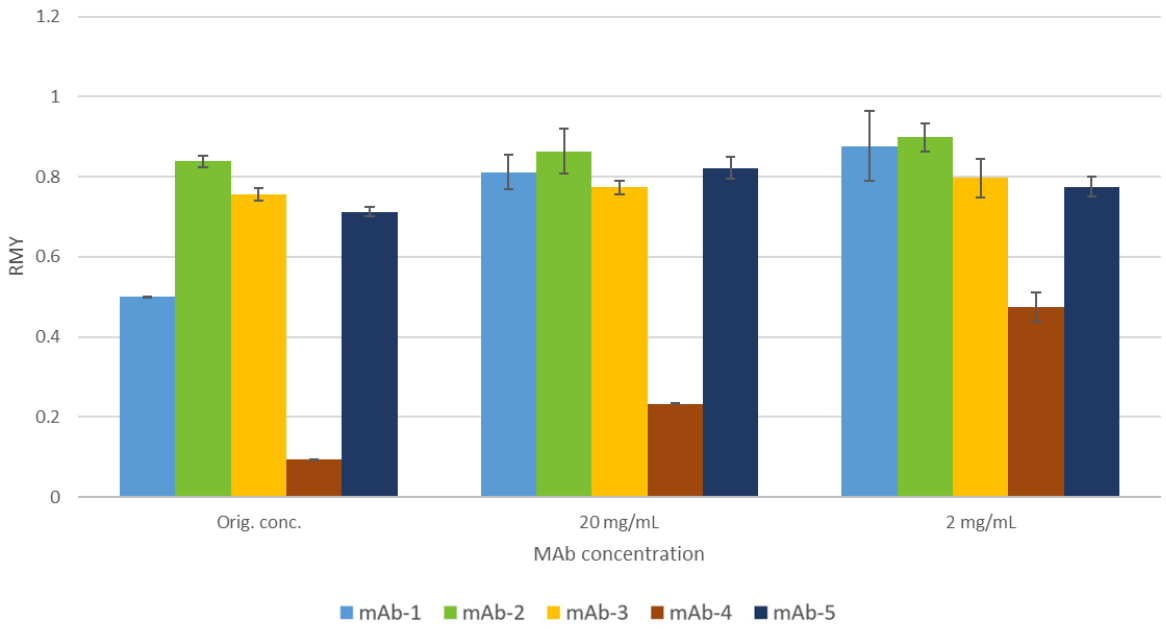

Figure 3. RMY values obtained in ReFOLD assays with 6 M urea for mAb products of the first stage.

For the RMYs obtained at 6 M urea we found a trend that had already been observed for the assay at 10 M urea (Figure 4) [9]: for decreasing mAb concentration (i.e., increasing dilution), the RMY values increased. This could be related to the likelihood of higher protein aggregate formation at higher concentrations, as aggregation is a concentration-dependent process [10]. However, for 6 M urea the ranking of the different DPs slightly changed with mAb concentration (Table 6, Appendix), which had not been observed for the ReFOLD assay at 10 M urea. For example, for 6 M urea, mAb-1 occupies position 4 for the RMY ranking at original concentration and position 1 for 20 mg/mL and 2 mg/mL. In contrast, for 10 M urea each studied mAb product occupies the same position in the RMY ranking for the three tested concentrations (e.g., mAb-1 occupies the first position for all the tested concentrations, while the second position is occupied by mAb-5). Thus, the reduced urea concentration of 6 M might not sufficiently unfold all mAbs at all concentrations. Nevertheless, the limited DP number

tested does not allow for a conclusion on whether the DP stability ranking when applying 10 M urea is generally the same across all mAb concentrations. It is also important to mention that at 6 M urea there is not much difference between the RMYs of each respective mAb at 20 mg/mL or 2 mg/mL (except for mAb-4, where we could observe that the RMY at 2 mg/mL is much higher that the RMY at 20 mg/mL), although for 10 M urea we could observe larger differences between the RMYs for these two mAb concentrations. This fact might be related to an insufficient urea concentration tested which did not allow to obtain significant differences between the RMY values.

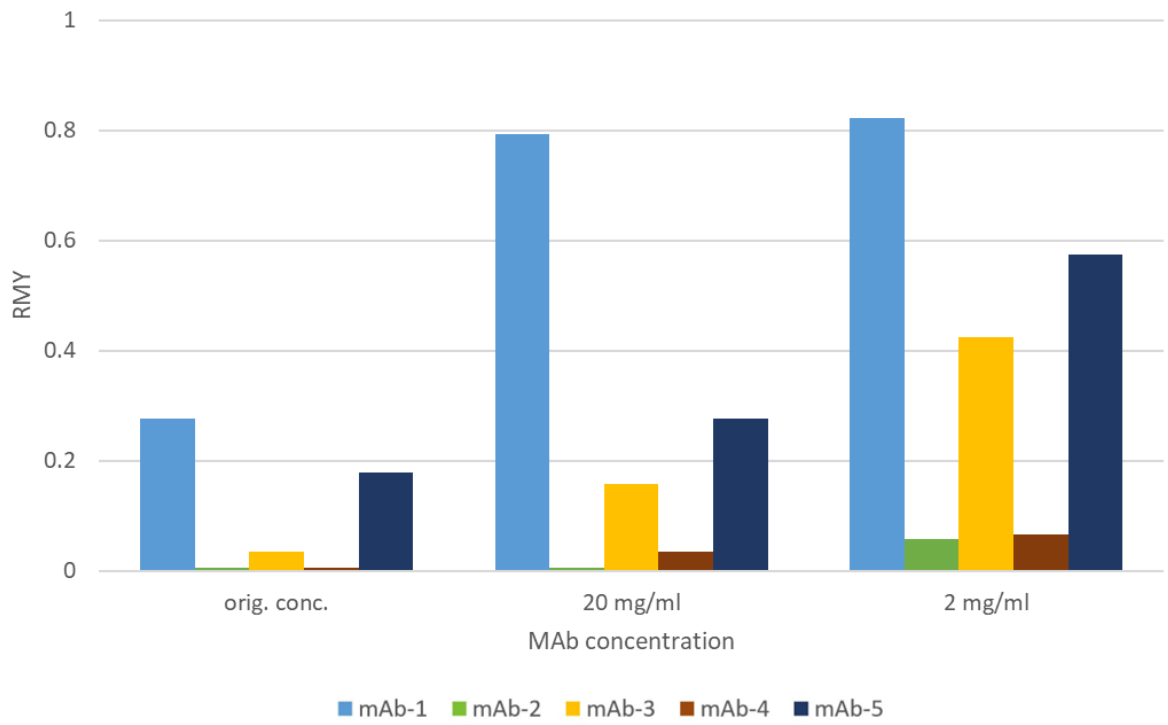

Figure 4. RMY values obtained in ReFOLD assays with 10 M urea for mAb products of the first stage.

In order to see if we could obtain a higher difference between the RMY values for the different mAb products at the same concentration, and considering that 6 M urea did not produce any of the previously described undesired effects, we decided to perform a second experiment with a higher urea concentration. The new urea concentration selected (6.5 M) should prevent undesired effects as much as possible while potentially generating a greater difference between the RMY values of the different DPs tested.

4.2.2. Second experiment: 6.5 M urea, first stage mAb products.

This second experiment for optimization of the ReFOLD assay was performed with the mAb products of the first stage and using 6.5 M of urea. The results of the ReFOLD assay are shown in Figure 5.

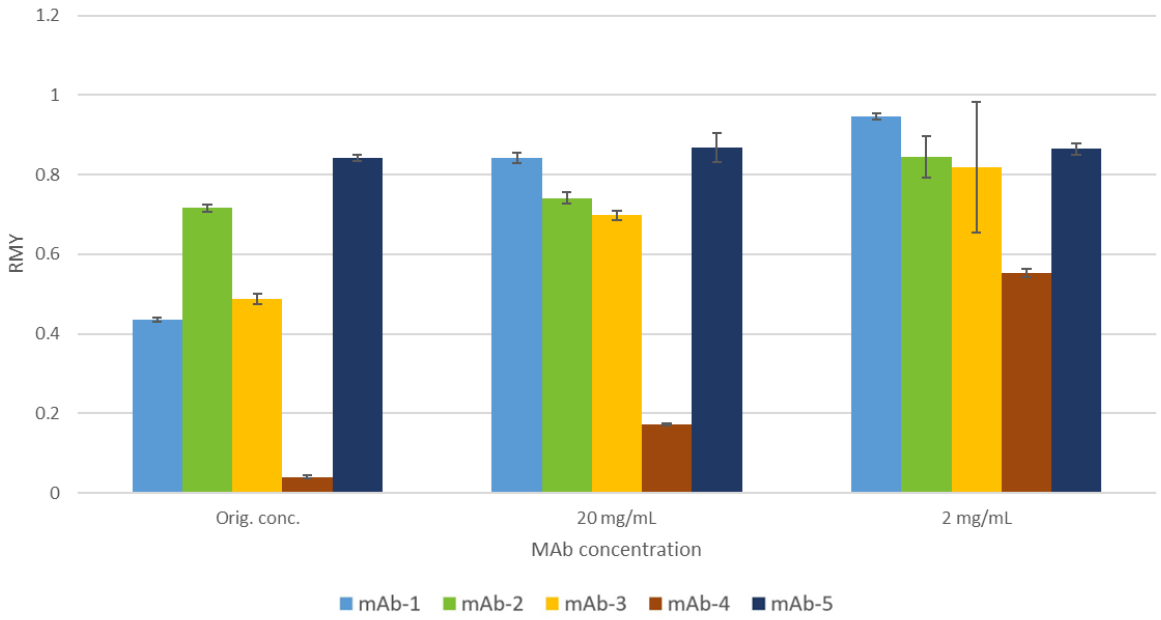

Figure 5. RMY values obtained in ReFOLD assays with 6.5 M urea for mAb products of the first stage.

The results of the ReFOLD assay at 6.5 M urea also showed an increase of the RMY values in higher diluted samples for each mAb product and a differing ranking for the different mAb products at original concentration, 20 mg/mL and 2 mg/mL (Table 6, Appendix). For example, mAb-1 occupies position 3 in the RMY order at the original concentration, but position 1 for 20 mg/mL and 2 mg/mL. In the case of 6.5 M urea, the RMYs exhibit similar separation of the different mAb products at each concentration to 6 M urea, i.e., for 6 M urea, mAb-1, mAb-2, mAb-3 and mAb-5 at 20 mg/mL and 2 mg/mL showed very similar RMY values, and the same occurred for 6.5 M urea However, when working at 6.5 M urea, mAb-4 showed turbidity at the original mAb concentration during the refolding step (Figure 6) and, although this did not affect the sample recovery from the microdialysis chamber, the RMY value is low (0.041), which demonstrates a clear loss of mAb, presumably due to aggregation. Nevertheless, the RMY value for mAb-4 at the original concentration when using 6 M urea is also low (0.093). Thus, even though mAb-4 did not show turbidity at 6 M urea, aggregation has occurred.

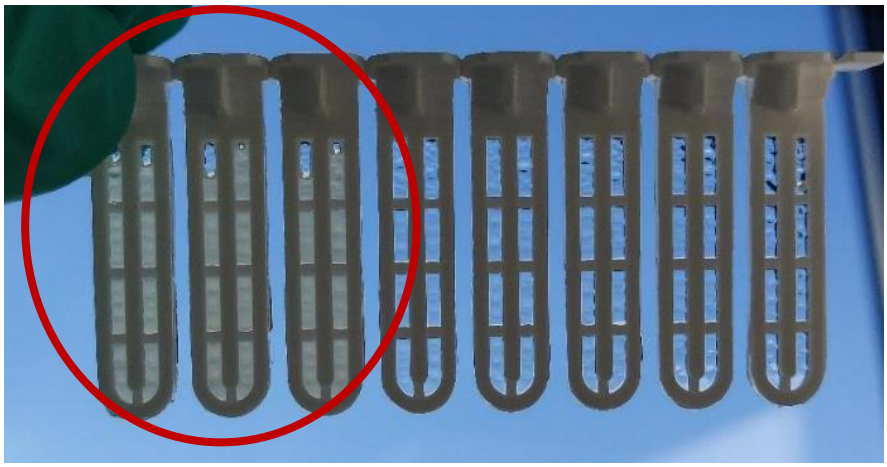

Figure 6. Microdialysis chambers filled with mAb-4. The three first chambers (red circle) correspond to mAb-4 samples at the original concentration after the ReFOLD assay with 6.5 M urea.

Evaluating the results of the first and second experiments, and comparing them with the results of previous ReFOLD assays with 10 M urea, we noticed that the RMYs at 6.5 M and 6 M urea are generally greater than at 10 M urea (see Figure 3, Figure 4 and Figure 5) [9]. For example, all tested concentrations for mAb-2 showed RMY values above 0.70 for 6 M and 6.5 M urea, while these values were less than 0.06 for 10 M urea. We also observed fewer undesired effects at 6.5 M and 6 M urea, as for 10 M urea eight out of eleven DPs showed undesired effects, but for 6.5 M there were just three out of ten DPs with undesired effects and for 6 M there were no undesired effects for any of the tested DPs. The RMY range is highly similar for both urea concentrations tested, although the differences between the mAb products are clearer at 6.5 M urea. Further, both urea concentrations (6 M, 6.5 M) did not show a consistent stability order of the tested DPs for the different mAb concentrations, except for mAb-4, which always occupies the last position. This could be related to an excessive decrease in urea concentration as for 10 M urea we could observe a stability ranking but not with the two new urea concentrations (Table 6, Appendix). Overall, at this stage of the research work 6 M and 6.5 M urea appeared to behave in a very similar way when performing the ReFOLD assay. However, both urea concentrations seemed to be insufficient for an adequate unfolding of the mAbs as none of them allow for a complete stability ranking of the mAb products tested.

4.2.3. Third experiment: 6.5 M and 6 M urea, second stage mAb products

This third experiment was carried out with the mAb products of the second stage (Table 2). At this point, 6.5 M was the more preferred urea concentration as it showed good results (the RMY values showed clearer separations than at 6 M urea and there was a clear reduction in undesired effects). However, we decided to test 6 M urea as well in case undesired effects

(like turbidity observed with mAb-4) would be observed with 6.5 M urea for the remaining DPs. It is also important to mention that 10 M urea results will not be discussed in this section as not all the mAbs of the second stage had been tested at 10 M urea.

Figure 7 shows the results of the ReFOLD assay with 6.5 M of urea, while Figure 8 shows the results with 6 M of urea. Note that the 6 M urea assay was conducted with just one replicate per concentration in order to save limited resources (particularly mAb DP material).

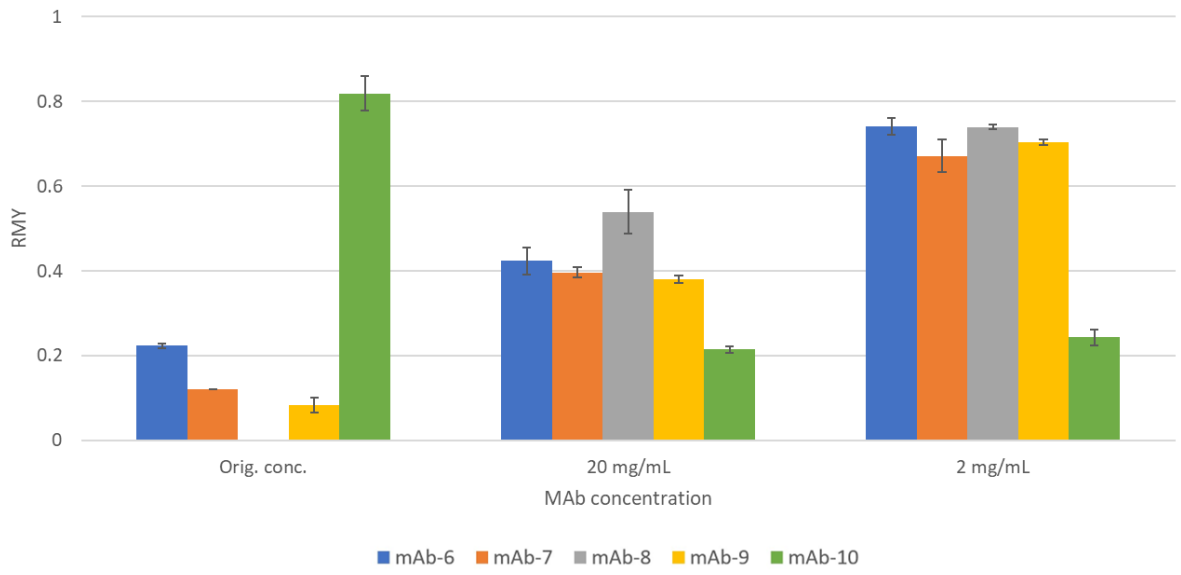

Figure 7. RMY values obtained in ReFOLD assays with 6.5 M urea for mAb products of the second stage.

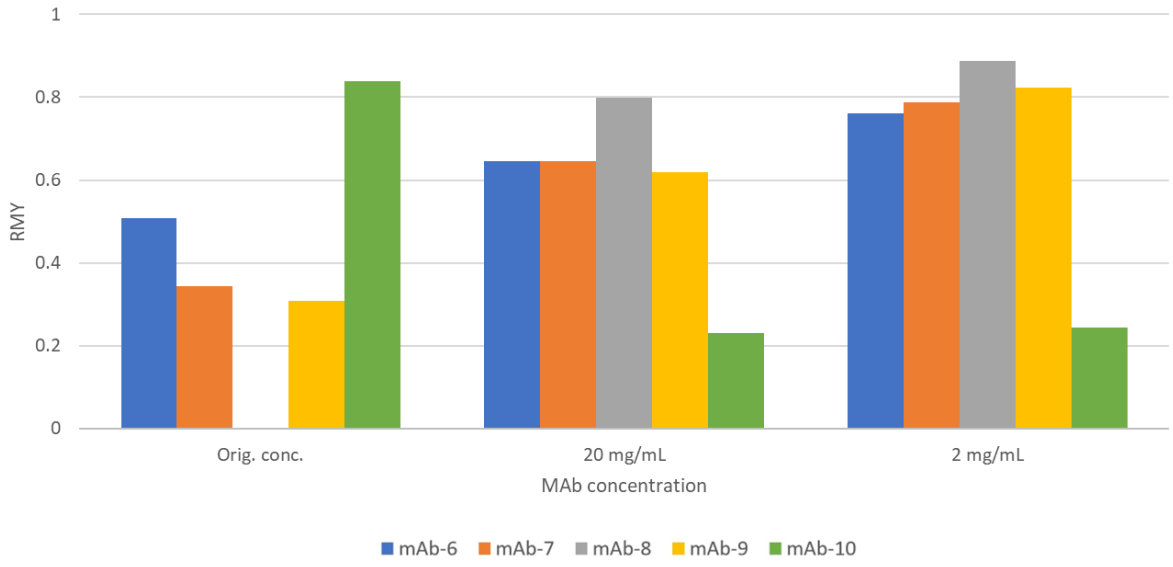

Figure 8. RMY values obtained in ReFOLD assays with 6 M urea for mAb products of the second stage.

For both urea concentrations tested, the trend in the increase of RMY values with decreasing protein concentration remained for all DPs, except for mAb-10, for which the RMY values decreased in higher diluted samples. Comparing 6 M and 6.5 M urea results (Table 7, Appendix), the stability ranking of the DPs at the original concentration was the same for both urea concentrations and the same occurred at 20 mg/mL and 2 mg/mL. We could also observe that the stability ranking for each mAb product was not consistent for each mAb concentration tested at either urea concentration The obtained RMY values were slightly higher at 6 M urea, and we found that there were larger differences between the RMYs of the different mAb products at a given concentration (e.g., 20 mg/mL) at 6.5 M urea.

However, mAb-7 and mAb-9 showed gel formation for the original concentration at 6.5 M urea. This was observed when the samples were recovered from the microdialysis chambers and let to sticking of the gel in the pipette tips (Figure 9). Importantly, the formed gels could not be well dissolved when diluting the samples to 1 mg/mL for subsequent SEC analysis (Figure 10). For 6 M urea, no undesired effects were encountered with any of the tested mAb products.

Figure 9. Gel stuck in the pipette tip.

Figure 10. Gel in suspension, not dissolved.

After performing the ReFOLD assay with the mAb products from both stages and the two new urea concentrations, the results showed that the strict reduction of the urea concentration, especially down to 6 M urea concentration, allowed the decrease of the undesired effects that were found in the experiments with 10 M urea. However, such a strict reduction of the urea concentration did not allow to obtain a consistent stability ranking for the tested DPs. Therefore, it is likely that the urea concentration cannot be reduced so much that all undesirable effects are avoided. Moreover, it is highly probable that the two new urea concentrations were not sufficient for a proper unfolding of the proteins. In the research carried out by Svilenov and Winter [5], they performed an experiment which showed that the unfolding of their tested protein was complete at 9.5 M urea. Thus, this study corroborates our hypothesis that 6 M and 6.5 M urea are insufficient to produce full unfolding of the tested proteins.

5. Summary, conclusions and outlook

Table 5 summarizes the findings made for the ReFOLD assay for each tested urea concentration.

As an overall conclusion, our findings indicate that there are no major differences between results obtained from the two new urea concentrations (6 and 6.5 M) tested in this study. Both urea concentrations improved sample recovery from the microdialysis chambers while still producing data that resolve differences in RMY for different concentrations of a single mAb and between DPs tested at the same concentration. We also identified 6 M as the more suitable urea concentration for the ReFOLD assay in order to completely avoid the undesired effects that were found in the original approach (10 M urea). However, 6 M urea did not allow for a consistent stability ranking of the DPs tested. Application of 6.5 M urea, resulted in undesired effects for some DPs tested (three out of ten) and still did not allow for a consistent stability ranking of the mAb products across the different mAb concentrations tested.

Therefore, the results of this study suggest that the two new urea concentrations used (6 M and 6.5 M) were too low to allow for a stability ranking of the mAb products tested. Thus, the achievement of the elimination of undesired effects together with the establishment of a stability ranking for the tested DPs seems incompatible.

For this reason, future studies with the ReFOLD assay will need to focus on testing further urea concentrations (between 6.5 M and 10 M) in order to find the best balance between the reduction of the undesired effects and a consistent stability ranking of the DPs. For that, it will also be necessary to test the assay on a larger number of mAb DPs in order to verify the broad applicability of the ReFOLD assay.

Table 5. Main findings for ReFOLD assays at each urea concentration.

Target under study	10 M Urea	6.5 M Urea	6 M Urea
Undesired effects	Eight out of eleven DPs tested showed gel formation, protein precipitation or urea crystallization	Reduced gel formation and protein precipitation, no urea crystallization: three out of ten DPs tested showed undesired effects	No gel formation, turbidity or crystallization for a total of ten DPs tested
Sample recovery from microdialysis chambers	Poor sample recovery for four DPs	Good sample recovery, except for two DPs	Good sample recovery for all DPs
Distribution along the RMY range	Widest distribution for the different mAb products at the same concentration	Narrower distribution for the different mAb products at the same concentration	Similar distribution for the different mAb products at the same concentration as for 6.5 M urea

6. References

[1] A. Roesch, S. Zölls, D. Stadler, C. Helbig, K. Wuchner, G. Kersten, A. Hawe, W. Jiskoot, T. Menzen, Particles in Biopharmaceutical Formulations, Part 2: An Update on Analytical Techniques and Applications for Therapeutic Proteins, Viruses, Vaccines and Cells, J. Pharm. Sci. 000 (2021). https://doi.org/10.1016/j.xphs.2021.12.011.

[2] E. Tamizi, A. Jouyban, Forced degradation studies of biopharmaceuticals: Selection of stress conditions, Eur. J. Pharm. Biopharm. 98 (2016) 26–46. https://doi.org/10.1016/j.ejpb.2015.10.016.

[3] A.L. Daugherty, R.J. Mrsny, Formulation and delivery issues for monoclonal antibody therapeutics, Adv. Drug Deliv. Rev. 58 (2006) 686–706. https://doi.org/10.1016/J.ADDR.2006.03.011.

[4] W. Wang, Instability, stabilization, and formulation of liquid protein pharmaceuticals, Int. J. Pharm. 185 (1999) 129–188. https://doi.org/10.1016/S0378-5173(99)00152-0.

[5] H. Svilenov, G. Winter, The ReFOLD assay for protein formulation studies and prediction of protein aggregation during long-term storage, Eur. J. Pharm. Biopharm. 137 (2019) 131–139. https://doi.org/10.1016/j.ejpb.2019.02.018.

[6] T.J. Zbacnik, R.E. Holcomb, D.S. Katayama, B.M. Murphy, R.W. Payne, R.C. Coccaro, G.J. Evans, J.E. Matsuura, C.S. Henry, M.C. Manning, Role of Buffers in Protein Formulations, J. Pharm. Sci. 106 (2017) 713–733. https://doi.org/10.1016/j.xphs.2016.11.014.

[7] H. Svilenov, L. Gentiluomo, W. Friess, D. Roessner, G. Winter, A New Approach to Study the Physical Stability of Monoclonal Antibody Formulations—Dilution From a Denaturant, J. Pharm. Sci. 107 (2018) 3007–3013. https://doi.org/10.1016/j.xphs.2018.08.004.

[8] P.J. Sinko, Chapter 14 Chemical kinetics and stability. Martin's Phycical Pharmacy And Pharmaceutical Sciences, in: Wolters Kluwer, L.W.& Wilkins (Eds.), 6th ed., 2011: pp. 318–355.

[9] S. Stein, Implementation of the ReFOLD assay for the stability assessment of therapeutic monoclonal antibodies, Martin-Luther-Universität Halle-Wittenberg, Department of Pharmacy, Chair of Pharmaceutical Technology, 2022.

[10] R. van der Kant, A.R. Karow-Zwick, J. Van Durme, M. Blech, R. Gallardo, D. Seeliger, K. Aßfalg, P. Baatsen, G. Compernolle, A. Gils, J.M. Studts, P. Schulz, P. Garidel, J. Schymkowitz, F. Rousseau, Prediction and Reduction of the Aggregation of Monoclonal Antibodies, J. Mol. Biol. 429 (2017) 1244–1261. https://doi.org/10.1016/J.JMB.2017.03.014.

7. Appendix

Table 6 and Table 7 contain the DP ranking in accordance to RMY for the tested DPs of the first and second stage, respectively, at each urea concentration. Table 7 does not include the results of 10 M urea, because not all the DPs of the second stage had been tested at 10 M urea.

Figure 11 and Figure 12 summarize the RMY values of the ten tested mAb products at 6.5 M and 6 M urea, respectively.

Table 6. RMY ranking for mAb DPs of the first stage.

RMY order (from highest to lowest RMY)	**10 M Urea**			**6.5 M Urea**			**6 M Urea**		
mAb concentration (mg/mL)	Orig.	20	2	Orig.	20	2	Orig.	20	2
1	mAb-1	mAb-1	mAb-1	mAb-5	mAb-1, mAb-2, mAb-3, mAb-5	mAb-1, mAb-2, mAb-3, mAb-5	mAb-2, mAb-3, mAb-5	mAb-1, mAb-2, mAb-3, mAb-5	mAb-1, mAb-2, mAb-3, mAb-5
2	mAb-5	mAb-5	mAb-5	mAb-2	-	-	-	-	-
3	mAb-3	mAb-3	mAb-3	mAb-1, mAb-3	-	-	-	-	-
4	-	mAb-4	-	-	-	-	mAb-1	-	-
5	mAb-2, mAb-4	mAb-2	mAb-2, mAb-4	mAb-4	mAb-4	mAb-4	mAb-4	mAb-4	mAb-4

Table 7. RMY ranking for mAb DPs of the second stage.

RMY order (from highest to lowest RMY)	**6.5 M Urea**			**6 M Urea**		
mAb concentration (mg/mL)	Orig.	20	2	Orig.	20	2
1	mAb-10	mAb-8	mAb-6, mAb-7, mAb-8, mAb-9	mAb-10	mAb-8	mAb-6, mAb-7, mAb-8, mAb-9
2	mAb-8	mAb-6, mAb-7, mAb-9	-	mAb-8	mAb-6, mAb-7, mAb-9	-
3	mAb-6	-	-	mAb-6	-	-
4	mAb-7, mAb-9	-	-	mAb-7, mAb-9	-	-
5	-	mAb-10	mAb-10	-	mAb-10	mAb-10

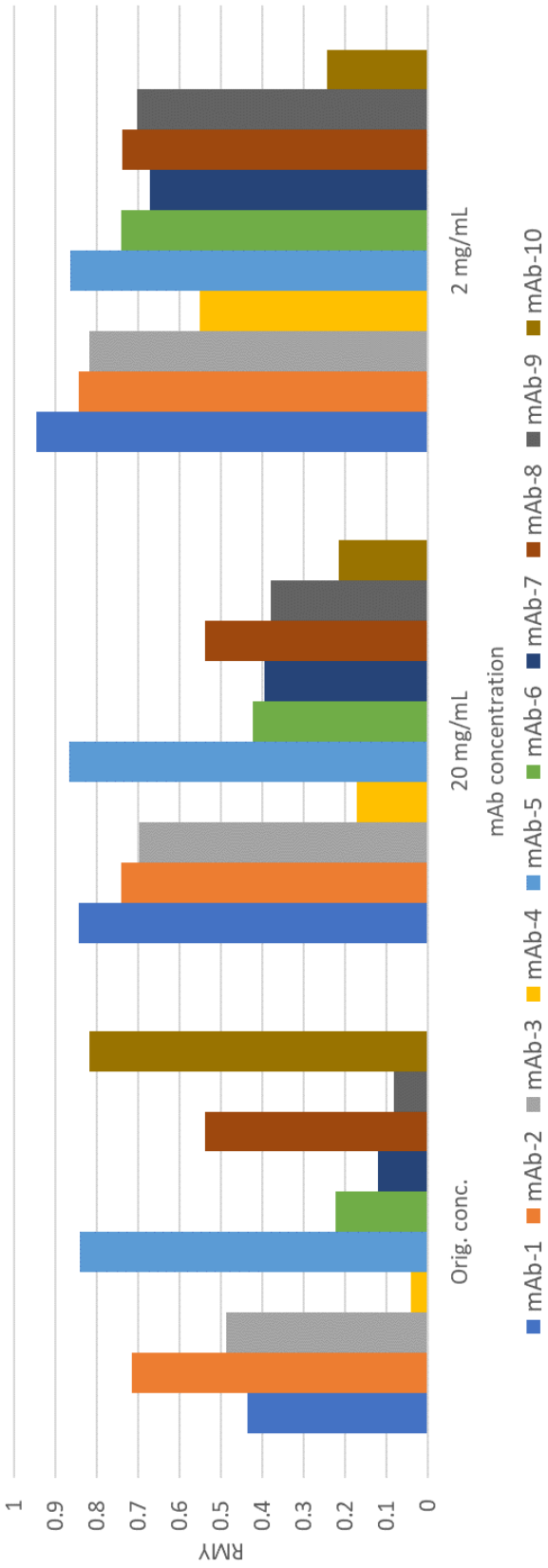

Figure 11. ReFOLD results of the ten tested mAb products at 6.5 M urea.

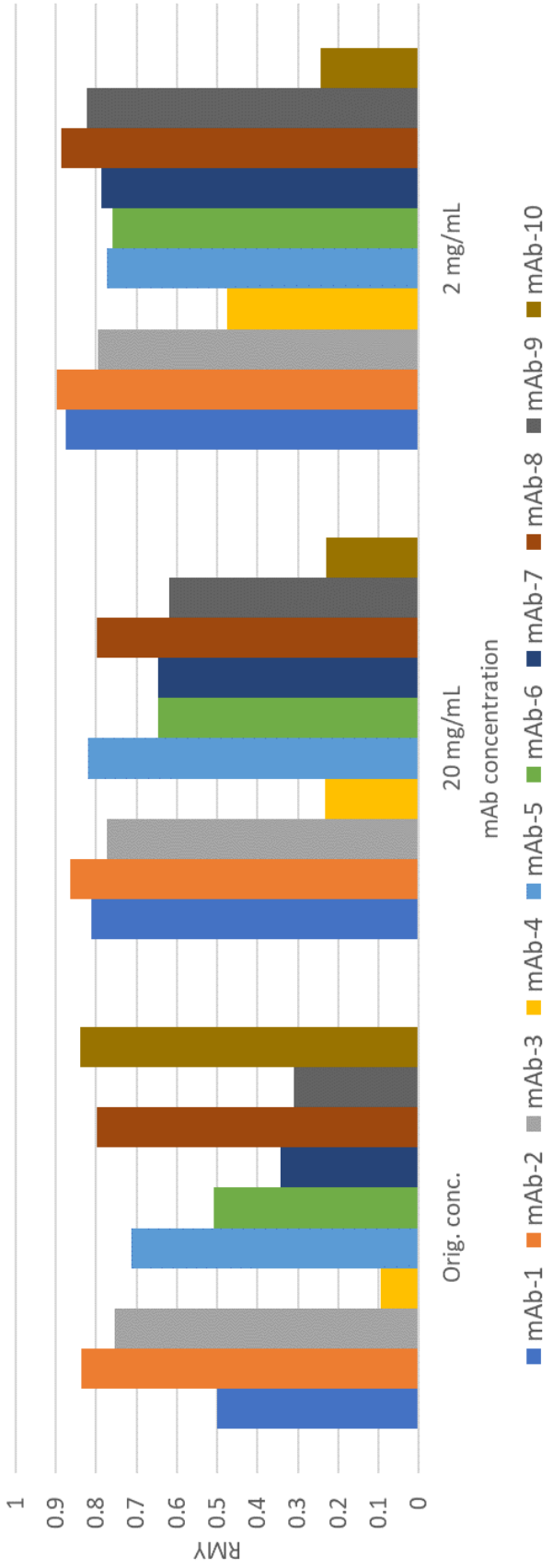

Figure 12. ReFOLD results of the ten tested mAb products at 6 M urea.

CONCLUSIONES FINALES/ FINAL CONCLUSIONS

CONCLUSIONES FINALES

A continuación, se exponen las conclusiones generales derivadas de los resultados recogidos en la presente Tesis Doctoral, ya que las conclusiones específicas de cada uno de los Capítulos han quedado recogidas en los mismos.

- La revisión bibliográfica de los mAbs utilizados en el tratamiento de la COVID-19 ha permitido obtener un mayor conocimiento acerca de los distintos tipos de mAbs que pueden ser utilizados en pacientes infectados por SARS-CoV-2. Esta revisión recoge dos grupos de mAbs terapéuticos: aquellos que bloquean un punto clave de la respuesta del sistema inmune de los pacientes infectados y aquellos que bloquean directamente la acción del virus. Al primer grupo pertenecen, por ejemplo, los inhibidores de la interleucina-6, mientras que el segundo grupo se conforma por diferentes subgrupos: mAbs aislados de pacientes infectados por SARS-CoV-2, mAbs capaces de neutralizar tanto al SARS-CoV como al SARS-CoV-2 y mAbs que han recibido una autorización de uso de emergencia (EUA). Con todo ello, se ha puesto de manifiesto la gran relevancia de los mAbs como agentes terapéuticos para el tratamiento de enfermedades emergentes, como es el caso de la COVID-19. También, ha supuesto un

FINAL CONCLUSIONS

The general conclusions derived from the results of this Doctoral Thesis are presented below, as the specific conclusions of each chapter have been included in them.

- The literature review of mAbs used in the treatment of COVID-19 has provided a better understanding of the different types of mAbs that can be used in patients infected with SARS-CoV-2. This review covers two groups of therapeutic mAbs: those that block a key point in the immune system response of infected patients and those that directly block the action of the virus. The first group includes, for example, interleukin-6 inhibitors, while the second group consists of different subgroups: mAbs isolated from SARS-CoV-2 infected patients, mAbs capable of neutralising both SARS-CoV and SARS-CoV-2, and mAbs that have received Emergency Use Authorisation (EUA). This has highlighted the great relevance of mAbs as therapeutic agents for the treatment of emerging diseases, such as COVID-19. It has also been an important starting point for training on the structure and functioning of this very important class of biopharmaceuticals with a major impact on the health field.

importante punto de partida como formación sobre la estructura y funcionamiento de esta importantísima clase de biofármacos de gran impacto en el ámbito de la salud.

- La caracterización analítica comprensiva de mAbs terapéuticos que se ha propuesto en esta Tesis Doctoral ha demostrado ser adecuada para llevar a cabo los estudios de estabilidad de los mismos en condiciones de uso hospitalario. Esto se debe a que el perfil de estabilidad propuesto permite evaluar con rigurosidad el conjunto de atributos críticos de la calidad mínimo indispensable para poder establecer conclusiones sobre dicha estabilidad.

- El perfil de estabilidad propuesto (conjunto de metodología analítica y funcional desarrollada y validada en esta Tesis) ha permitido determinar las estructuras de orden superior de los mAbs estudiados (estructuras secundarias y terciarias), el perfil de oligómeros, el particulado en disoluciones, el perfil de isoformas y variantes de carga, la identificación y cuantificación de PMTs, y la evaluación de la funcionalidad a través de la cuantificación de la actividad biológica.

- La metodología analítica puesta a punto y validada en esta Tesis Doctoral ha mostrado su utilidad para detectar rutas de degradación de los mAbs estudiados,

- The comprehensive analytical characterisation of therapeutic mAbs proposed in this Doctoral Thesis has proven to be suitable for carrying out stability studies of these mAbs under hospital use conditions. This is because the proposed stability profile allows a rigorous assessment of the minimum set of critical quality attributes required to draw conclusions on stability.
- The proposed stability profile (set of analytical and functional methodology developed and validated in this Thesis) has allowed the determination of the higher order structures of the mAbs studied (secondary and tertiary structures), the oligomer profile, the particulate in solutions, the profile of isoforms and charge variants, the identification and quantification of PMTs, and the assessment of functionality through the quantification of biological activity.
- The analytical methodology developed and validated in this Doctoral Thesis has shown its usefulness in detecting degradation routes of the studied mAbs, such as aggregations and chemical or structural modifications.
- The comprehensive analysis of the results obtained has made it possible to relate physical and chemical modifications with structural changes and loss of functionality in the studied

tales como agregaciones y modificaciones químicas o estructurales.

- El análisis comprensivo de los resultados obtenidos ha permitido relacionar modificaciones físicas y químicas con cambios estructurales y pérdidas de funcionalidad en los mAbs terapéuticos estudiados inhibidores de puntos de control inmunitario.

- Los estudios de estabilidad en condiciones de uso clínico de los medicamentos biotecnológicos estudiados han permitido resolver problemas reales en el ámbito hospitalario, demostrando así su gran utilidad.

- Los estudios de degradación acelerada, además de haber permitido la validación de los métodos propuestos en esta Tesis, muestran información sobre las posibles vías de degradación de los medicamentos estudiados, pudiendo determinar aquellos factores ambientales críticos a la hora de su manipulación.

- Desde el punto de vista de la estabilidad en condiciones de uso clínico, se ha comprobado que nivolumab y pembrolizumab, a pesar de que ambos son inmunoglobulinas del tipo 4 (IgG4) e inhibidores del receptor PD-1, no se comportan de la misma manera frente a las mismas potenciales vías de

therapeutic mAbs that inhibit immune checkpoints.

- The stability studies under clinical use conditions of the studied biotechnological medicines have made it possible to solve real problems in the hospital setting, thus demonstrating their great usefulness.

- The accelerated degradation studies, in addition to having allowed the validation of the methods proposed in this Thesis, provide information on the possible degradation pathways of the studied medicines, making it possible to determine those environmental factors that are critical when handling them.
- In terms of stability under clinical use conditions, nivolumab and pembrolizumab, although both are immunoglobulin type 4 (IgG4) and PD-1 receptor inhibitors, have been shown not to behave in the same way against the same potential degradation pathways. Overall, pembrolizumab has been shown to be less stable as it is affected by a greater number of stressful conditions to which it has been exposed.

- The ReFOLD assay has been shown to be suitable for predicting the long-term

degradación. De forma general, pembrolizumab ha demostrado ser menos estable ya que se ve afectado por un mayor número de condiciones estresantes a las que ha sido expuesto.

- Se ha demostrado que el ensayo ReFOLD es adecuado para la predicción de la estabilidad a largo plazo de medicamentos basados en mAbs. Sin embargo, se ha comprobado la dificultad de conseguir un balance adecuado entre la reducción de los efectos indeseados encontrados en ensayos previos y la clasificación de la estabilidad de los productos farmacéuticos ensayados. Con la finalidad de encontrar la concentración de urea que permita el mejor balance entre ambos aspectos, será necesario realizar el ensayo en un mayor número de productos farmacéuticos basados en mAbs.

- La información que deriva de los 5 trabajos experimentales recogidos en esta Tesis Doctoral pone de manifiesto la necesidad de implementar y seguir desarrollando metodologías analíticas robustas que permitan determinar características estructurales y de estabilidad de moléculas complejas, como son los mAbs, a pesar de la complejidad inherente de estos biofármacos y de sus formulaciones medicamentosas.

stability of mAbs-based drug products. However, it has proven difficult to achieve an adequate balance between reducing the undesired effects found in previous assays and ranking the stability of the tested pharmaceuticals. In order to find the urea concentration that allows the best balance between both aspects, it will be necessary to test a larger number of mAbs-based pharmaceuticals.

- The information derived from the 5 experimental studies collected in this Doctoral Thesis highlights the need to implement and further develop robust analytical methodologies to determine structural and stability characteristics of complex molecules, such as mAbs, despite the inherent complexity of these biopharmaceuticals and their medicinal product formulations.

PERSPECTIVAS FUTURAS / FUTURE PROSPECTS

PERSPECTIVAS FUTURAS

La investigación realizada en esta Tesis Doctoral se engloba dentro de los proyectos **FIS PI17-00547** ("Estudios de estabilidad en el tiempo de sobrantes de medicamentos biotecnológicos –anticuerpos monoclonales y proteínas de fusión–. Estudios conformacionales comprensivos", FEDER/Ministerio de Ciencia e Innovación-Instituto de Salud Carlos III, Fondos de Investigación en Salud), **P20-01029** y **B-FQM-308-UGR20** ("Estabilidad de anticuerpos monoclonales terapéuticos antineoplásicos en condiciones de uso clínico: evaluación de parámetros fisicoquímicos y funcionalidad biológica en el tiempo y durante su manipulación y administración. Potenciales fuentes de inestabilidad", FEDER/Junta de Andalucía-Consejería de Transformación Económica, Industria, Conocimiento y Universidades). En estos proyectos se contemplan estudios de estabilidad de proteínas terapéuticas, como los anticuerpos monoclonales, en ámbito hospitalario, para resolver problemas relacionados con ellos, desde su manipulación hasta la evaluación en la reutilización de los sobrantes, dado el altísimo coste de los tratamientos con este tipo de medicamentos. Por tanto, el trabajo experimental desarrollado en esta Tesis Doctoral ha supuesto un avance de dichos proyectos. Sin embargo, es necesario seguir investigando en la misma línea con el

FUTURE PROSPECTS

The research carried out in this Doctoral Thesis is included in the projects **FIS PI17-00547** ("Studies of stability over time of biotechnological drug leftovers -monoclonal antibodies and fusion proteins-. Comprehensive conformational studies", FEDER/Ministerio de Ciencia e Innovación-Instituto de Salud Carlos III, Fondos de Investigación en Salud), **P20-01029** and **B-FQM-308-UGR20** ("Stability of therapeutic antineoplastic monoclonal antibodies under clinical use conditions: evaluation of physicochemical parameters and biological functionality over time and during their handling and administration. Potential sources of instability", FEDER/Junta de Andalucía-Consejería de Transformación Económica, Industria, Conocimiento y Universidades). These projects include stability studies of therapeutic proteins in hospital settings, such as monoclonal antibodies. Their aim is to solve problems related to these proteins, from their handling to the evaluation of the reuse of leftovers, given the very high cost of treatments with this type of medicines. Therefore, the experimental work carried out in this Doctoral Thesis has been a step forward in these projects. However, it is necessary to continue research along the same lines in order to give continuity to the research carried out so far.

objetivo de continuar la investigación completada hasta el momento.

Como primer paso, se plantea la continuación de los estudios con pembrolizumab. Hasta el momento, como parte de los estudios realizados en la presente Tesis Doctoral, se ha realizado la caracterización fisicoquímica y funcional de dicha proteína en su medicamento comercial innovador Keytruda®, en su concentración original de 25 mg/mL. Sin embargo, Keytruda® (25 mg/mL) es un medicamento concentrado para solución para perfusión, es decir, no se emplea directamente, sino que este debe de ser manipulado para preparar las diluciones de uso clínico a concentraciones que pueden variar de 1 a 10 mg/mL. Con el trabajo realizado hasta el momento, no se han estudiado y caracterizado las diluciones de uso clínico, por lo que el objetivo de los futuros estudios con pembrolizumab es estudiar la estabilidad en condiciones de uso hospitalario de las diluciones de uso clínico del anticuerpo monoclonal pembrolizumab (Keytruda®), tanto en aspectos relacionados con su manejo en la práctica diaria como con la estabilidad de sus sobrantes en el tiempo.

Por otro lado, esta Tesis Doctoral recoge los estudios de caracterización fisicoquímica y funcional, además del análisis comprensivo de sus resultados, de dos mAbs terapéuticos inhibidores de puntos de control inmunitario: nivolumab y pembrolizumab. Sin embargo, estos no son los únicos inhibidores de puntos de control inmunitario que existen.

The first step is to continue studies with pembrolizumab. So far, as part of the studies carried out in this Doctoral Thesis, the physicochemical and functional characterisation of this protein has been carried out in its innovative commercial medicine Keytruda®, in its original concentration of 25 mg/mL. However, Keytruda® (25 mg/mL) is a concentrated medicine for solution for infusion, i.e., it is not used directly, but must be manipulated to prepare dilutions for clinical use at concentrations that can vary from 1 to 10 mg/mL. With the work carried out to date, the dilutions for clinical use have not been studied and characterised. Therefore, the aim of future studies is to assess the stability under hospital conditions of the dilutions for clinical use of the monoclonal antibody pembrolizumab (Keytruda®), both in aspects related to its handling in daily practice and the stability of its leftovers over time.

Moreover, this Doctoral Thesis includes physicochemical and functional characterisation studies, as well as a comprehensive analysis of the results, of two therapeutic mAbs that inhibit immune checkpoints: nivolumab and pembrolizumab. However, these are not the only immune checkpoint inhibitors available. Ipilimumab (Yervoy®) is another mAb that belongs to this group, which is in very advanced stages of characterisation in the research group in which this Thesis has been performed. For its

Ipilimumab (Yervoy®) es otro mAb que pertenece a este grupo, el cual se encuentra en fases muy avanzadas de su caracterización en el grupo de investigación en el que se ha desarrollado esta Tesis. Para su caracterización se están siguiendo estrategias analíticas similares a las desarrolladas para los estudios llevados a cabo con nivolumab y pembrolizumab, adaptándolas a las particularidades específicas de ipilimumab. Con ello, se pone de manifiesto que la metodología y técnicas analíticas que han sido desarrolladas y optimizadas para el análisis comprensivo de los mAbs terapéuticos incluidos en esta tesis son estrategias útiles que pueden seguir siendo aplicadas en futuros estudios con mAbs.

characterisation, analytical strategies similar to those developed for the studies carried out with nivolumab and pembrolizumab are being followed, adapting them to the specific characteristics of ipilimumab. This shows that the methodology and analytical techniques that have been developed and optimised for the comprehensive analysis of the therapeutic mAbs included in this Thesis are useful strategies that can be further applied in future studies with mAbs.